DISSERTATION

Titel der Dissertation

The Role of Tristetraprolin in Inflammation and Disease

angestrebter akademischer Grad

Doktor der Naturwissenschaften (Dr. rer.nat.)

Verfasser:	Franz Kratochvill
Matrikel-Nummer:	0100040
Dissertationsgebiet:	Molekulare Biologie
Betreuer:	Univ.-Prof. Dr. Pavel Kovarik

Wien, am 1. Februar 2010

Table of Contents

1. ZUSAMMENFASSUNG

Um menschliche Krankheiten besser verstehen zu können, ist eine genaue Analyse der Genexpression in gesunden und kranken Zellen notwendig. Obwohl der Transkription von Genen traditionell eine wichtige Rolle beigemessen wird, zeigen aktuelle Studien, dass auch Reifung, Transport, Stabilität und Translation der transkribierten mRNA wichtige Faktoren darstellen, welche in der Zelle streng kontrolliert werden. Die Stabilität vieler mRNAs wird von Sequenzen bestimmt, die sich im nicht translatierten 3' Bereich befinden und die Bindung bestimmter Proteine und/oder miRNAs ermöglichen. Eines dieser Proteine ist Tristetraprolin, kurz TTP. TTP erkennt und bindet RNA-Sequenzen, die reich an A- und U-Nukleotiden sind und führt mithilfe anderer Faktoren, die TTP als Plattform nutzen, zum raschen Abbau der mRNA.

Viele Gene, wie beispielsweise TNFα und Interleukin-1β, deren mRNA-Stabilität auf diese Weise von TTP kontrolliert wird, spielen eine wichtige Rolle in der Immunabwehr. In Mäusen führt daher der systemische Verlust des TTP-Gens bzw. das daraus resultierende Ungleichgewicht im Immunsystem zur Entwicklung diverser Pathologien wie Dermatitis und Rheumatoider Arthritis. Diese lassen sich auf eine erhöhte TNFα mRNA-Stabilität zurückführen. Um die Funktion von TTP in diversen Krankheiten genauer erforschen zu können, wurde im Zuge dieser Arbeit eine Maus generiert, deren TTP-Gen nun zelltypspezifisch deletiert werden kann. Unterbindet man die TTP-Expression dieser Mäuse in myeloiden Zellen, so entwickeln sich diese Tiere vorerst normal. Versetzt man ihnen allerdings einen endotoxischen Schock, so sterben sie schneller, was darauf hinweist, dass myeloides TTP eine wichtige Rolle bei der Kontrolle der Immunantwort während einer akuten Entzündung spielt. Wir konnten weiters zeigen, dass TTP die Stabilität vieler mRNAs steuert, die während einer Entzündung produziert werden. Viele TTP-Funktionen wiederum werden durch die p38 MAP-Kinase kontrolliert. Diese Kinase erhöht einerseits die TTP-Expression

und stabilisiert das TTP-Protein, blockiert andererseits aber auch den mRNA-Abbau durch TTP. Damit wird sichergestellt, dass am Beginn einer Entzündung, wenn also die p38 MAP-Kinase aktiv ist, nur wenige mRNAs in TTP-abhängiger Weise abgebaut werden. Im späteren Verlauf reduziert sich die p38 MAP-Kinase-Aktivität allerdings zusehends, wodurch sich der TTP-abhängige Abbau vieler mRNAs verstärkt. In dieser Phase wird die Stabilität von mehr als einem Drittel aller instabilen mRNAs, deren Expression durch die Entzündung aktiviert wurde, durch TTP reguliert. Drei dieser Gene (Interleukin-6, Interleukin-1α und Cxcl2) wurden für detailliertere Untersuchungen ausgewählt und erwiesen sich als echte TTP-Targets.

Zusätzlich identifizierten wir Interleukin-10 als einen weiteren Faktor, der den TTP-abhängigen mRNA Abbau kontrolliert. Interleukin-10 wird erst im späteren Verlauf einer Entzündungsreaktion produziert und erhöht dann die TTP-Expression. Zusätzlich blockiert Interleukin-10 mit der Zeit immer mehr die p38 MAP-Kinase und steigert so die Aktivität von TTP. Befindet sich die Entzündung in der Auflösung, so führt letztlich der völlige Einbruch der p38 MAP-Kinase-Aktivität zu einem raschen Abbau von TTP, womit der Ausgangzustand wiederhergestellt ist.

Diese Doktorarbeit beschreibt einen regulatorischen Kreislauf, der den Abbau von bis zu einem Drittel aller instabilen mRNAs kontrolliert, die während einer Entzündung induziert werden. Ein wichtiges Element in diesem Kreislauf ist TTP, da es die Akkumulation für die Entzündung wichtiger mRNAs zu Beginn zulässt, im späteren Verlauf diese aber rasch aus dem System entfernt. Daher spielt TTP eine wichtige Rolle für den Erhalt des immunologischen Gleichgewichts.

2. SUMMARY

Uncovering control of gene expression in healthy and abnormal cells is of uppermost importance for the understanding of human pathologies. While a lot of attention has been paid to the gene expression control at the transcriptional level, in recent years even more studies focused on mRNA maturation, transport, stability and translation. mRNA stability and translation are critically regulated by cis-acting sequences located in the 3' untranslated region (3' UTR) that act by recruiting various RNA-binding proteins (RBPs) and/or miRNAs. Tristetraprolin (TTP), a well known RBP, binds to AU-rich elements (AREs) within the 3' UTR thereby causing a rapid degradation of the targeted mRNA by facilitating the assembly of enzymes for decapping, deadenylation as well as 5´-to-3´ and 3´-to-5´ exonucleases.

Animal models as well as *in vitro* studies revealed a profound role of TTP in controlling immune homeostasis by regulating mRNA stability of inflammatory mediators such as TNFα and interleukin-1β (IL-1 β). Conventional TTP knockout mice develop severe inflammatory pathologies like rheumatoid arthritis and dermatitis that were linked to increased *Tnf* mRNA stability. Because of the very poor health and infertility of these animals, the precise function of TTP in animal models for inflammatory diseases could not be addressed. Thus, one project of this PhD thesis was to generate and characterize mice with a conditional TTP ablation. Animals deleted for TTP in myeloid cells appear healthy but are more susceptible to LPS-driven endotoxic shock, pointing out the so far unrecognized importance of myeloid-specific TTP in limiting the acute inflammatory response. Detailed analysis revealed that TTP is a critical player in a relay of negative feedback mechanisms that regulates the removal of a large proportion of unstable mRNAs produced upon inflammation. This feedback employs as a second factor the p38 MAPK, that influences TTP function in multiple ways: i) it induces TTP transcription and stabilizes TTP protein against degradation; ii) it inhibits the mRNA-destabilizing function of TTP by phosphorylation. When p38 MAPK activity is high immediately after LPS stimulation, only few mRNAs can be targeted by TTP for degradation.

However, as p38 MAPK activity gradually decreases at later stages of the inflammatory response, the TTP-mediated mRNA decay becomes more apparent. Microarray analysis revealed that at low p38 MAPK activity, more than one third of inflammation-induced unstable mRNAs are degraded in a TTP-dependent fashion. For the three candidate targets *IL-6*, *IL-1α* and *Cxcl2*, a set of additional experiments provided the evidence that they were true TTP targets. We furthermore show that the TTP-dependent mRNA decay was increased in part by IL-10. IL-10, that is produced later during inflammation, boosts TTP function both by enhancing TTP transcription and by increasing TTP mRNA-destabilizing activity through the inhibition of p38 MAPK. The complete drop of p38 MAPK activity during the resolution phase of inflammation ultimately leads to the degradation of TTP, resulting in reversion into the original state.

This study describes a regulatory circuit that controls the timely removal of one third of unstable inflammation induced mRNAs. A critical component of this circuit is the mRNA-destabilizing protein TTP whose function is regulated such that it allows a high accumulation of the early phase inflammatory mRNAs and their efficient removal during the later phase of the inflammatory response when these mRNAs are no longer needed. Thus, by controlling mRNA stability TTP fundamentally contributes to immune homeostasis.

3. Introduction

3.1 Transcriptional and Posttranscriptional Regulatory Networks

In eukaryotes, posttranscriptional mechanisms controlling various aspects in the life of an mRNA are known to be important regulators of gene expression. In this respect, RNA binding proteins (RBPs) have proven to be of critical importance. RBPs regulate RNA maturation, transport, stability and translational efficiency contributing to cellular homeostasis and gene expression dynamics [1]. Several new studies indicate that global changes in RNA stability are of particular importance during inflammatory responses [2].

Inflammation induced by pathogens as well as by sterile stimuli (e.g. TNFα, IL-1) trigger a massive reprogramming of gene expression [3]. Interestingly, the immediately activated genes generate mRNAs that display high and quick induction followed by a rapid decline. The mRNAs in this set of genes are very unstable and are enriched in AU-rich elements (AREs) in the 3' untranslated region (3' UTR) [2]. AREs have been known for a long time to control mRNA stability, therefore providing a link between the expression pattern seen and mRNA stability [4]. Regulatory circuits controlling globally gene expression at the level of transcription have been recently described [5]. However, networks regulating global mRNA stability both in time and quality during the cellular response to external stimuli are still elusive. They are likely to be dependent on RNA stabilizing and destabilizing proteins as well as miRNAs.

3.2 Posttranscriptional Gene Regulation by Tristetraprolin (TTP)

Tristetraprolin (TTP) is a Cys-Cys-Cys-His (CCCH) type tandem zinc-finger protein encoded by the gene *zfp36*. TTP was cloned independently by several groups as an immediate early

gene induced by insulin, phorbol ester and serum [6-8]. Almost 10 years ago the Blackshear laboratory described TTP as protein that binds to *Tnf* and *GM-Csf* mRNA and causes rapid deadenylation and mRNA decay [9, 10]. The tandem zinc-fingers responsible for RNA-binding in the center of the protein are flanked by three proline-rich regions reflected by the name TTP [11]. The N- or C-terminal domains of TTP provide a platform for several effector-proteins like enzymes involved in decapping and deadenylation as well as exonucleases [12, 13]. Up to now, TTP was shown to regulate mRNA stability of various transcripts in several cell-types (reviewed in [14]).

3.2.1 AU-rich elements (AREs)

TTP has been first described to directly bind to AU-rich elements (AREs) of mRNAs leading to rapid mRNA decay [9]. AREs are sequence elements rich in adenosine and uridine bases located in the 3' UTR of mRNAs. Based on the number and distribution of the core ARE pentamer AUUUA, generally three classes have been defined. Class I AREs contain several dispersed copies of AUUUA often found in a uridine-rich environment. Class II AREs have at least two overlapping UUAUUUAWW nonamers whereas Class III AREs are less well defined as uridine-rich regions containing no AUUUA pentamer [15]. Structural properties keeping AREs in a single- or double-stranded conformation have been described to be of importance for some ARE-binding proteins as HuR. In this study, oligonucleotides were designed that can turn a double-stranded ARE sequence into a single-stranded conformation. Subsequent HuR binding assays revealed that HuR preferentially associates with the single-stranded RNA form [16].

AREs have been found in as much as 4000 human mRNAs, representing 5-8% of human genes when searching for a 13 bp pattern of WWWU(AUUUA)UUUW with one mismatch allowed in the pentamer flanking region [17]. Between mouse and human approximately 25 % of the ARE clusters (as defined previously in [18]) of orthologous genes show significant

differences [19]. This means that there is a profound variation of the ARE pattern between species.

First evidence for a functional role of AREs in mRNA degradation was provided by cloning of the ARE sequence of the *GM-Csf* into an otherwise stable *globin* mRNA, causing rapid mRNA degradation [4]. To date, AREs have been implicated in posttranscriptional gene regulation by regulating mRNA decay through various mechanisms and/or by affecting translational efficiency. They are therefore predominantly found in genes that need to be in precise control of expression like many cytokines and growth factors [20].

3.2.2 TTP binding sites

TTP was initially shown to directly interact by its zinc finger domains with a stretch of several AUUUA sequences within the ARE located in the 3' UTR of *Tnf* [9]. Further studies using RNA SELEX revealed a preference for the extended UUAUUUAUU sequence rather than the simple AUUUA form [21]. However the TTP zinc finger domain has been shown to have an optimal affinity for a binding site consisting of two adenosine residues located 3-6 bases apart within a uridine-rich region [22]. Although AREs have been shown in numerous studies to be the main site for TTP binding, recent work suggests that also messages devoid of any ARE can be targeted by TTP [23, 24].

3.2.3 TTP targets

Upon binding, TTP was described to mediate deadenylation of *Tnf* and *GM-Csf* mRNA leading to rapid degradation [9, 10]. Since then, other targets have been found in various cell systems to be directly or indirectly targeted for degradation by TTP. For instance, in T lymphocytes TTP is induced upon TCR and CD28 co-receptor stimulation leading to increased *IL-2* and *IFNγ* mRNA decay [25, 26]. Various other cytokine mRNAs as *Cxcl1, IL-1β, IL-10* and *IL-3* have been shown to be targeted for degradation by TTP [27-31]. In

addition also *zfp36* mRNA*,* encoding TTP protein, has been suggested to be targeted by TTP forming an autoregulatory loop [32].

The human *inducible NO synthase* (*iNOS*) mRNA becomes destabilized in DLD-1 cells upon inhibition of p38 MAPK signaling which is consistent with a TTP-mediated decay. For this reason, *iNOS* was tested for direct interaction with TTP. However, coimmunoprecipitation studies revealed that TTP does not directly bind *iNOS* mRNA. Instead TTP interacts with yet another RNA binding protein KSRP that can bind to *iNOS* mRNA. KSRP mediates mRNA decay by attracting the exosome. TTP was therefore proposed to stabilize *iNOS* mRNA by capturing the KSRP-exosome complex [33].

A study comparing the mRNA decay-rate of Wt and TTP-deficient fibroblast by microarray analysis could define a set of 250 mRNAs stabilized in the TTP-deficient background. Although 8 of them were further tested by Northern blotting, only *Ier3* mRNA was characterized in detail to be a true TTP-target [24]. Two more global screens in dendritic cells and macrophages using RNA immunoprecipitation suggested a number of so far unknown TTP-targets [23, 27]. However, mRNAs identified by global screens as putative TTP-targets (e.g. *IL-6, IL-12* and *Cxcl2* [34, 35]) cannot be considered as true TTP-targets unless further tested, in order to reveal whether a message is directly bound by TTP and regulated at the level of mRNA decay.

3.2.4 TTP-mediated control of mRNA stability

TTP is transiently expressed in response to many stimuli e.g. LPS, TNFα, IL-4, TGFβ, glucocorticoids and interferons and then rapidly shuttles to the cytoplasm [36-41]. TTP was initially described to lead to rapid deadenylation and mRNA decay by recruiting poly(A) RNase [42]. However, recent studies indicate, that TTP is in a complex with 3'-5' exonucleases (e.g. CCR4), 5'-3' exonucleases (e.g. Xrn1), decapping enzyme as Dcp1 as well as with exosomal components. These data suggest a function for TTP as molecular link

between ARE-containing mRNAs and different mRNA decay machineries leading to 3' to 5' as well as 5' to 3' degradation (figure 1) [12, 43, 44].
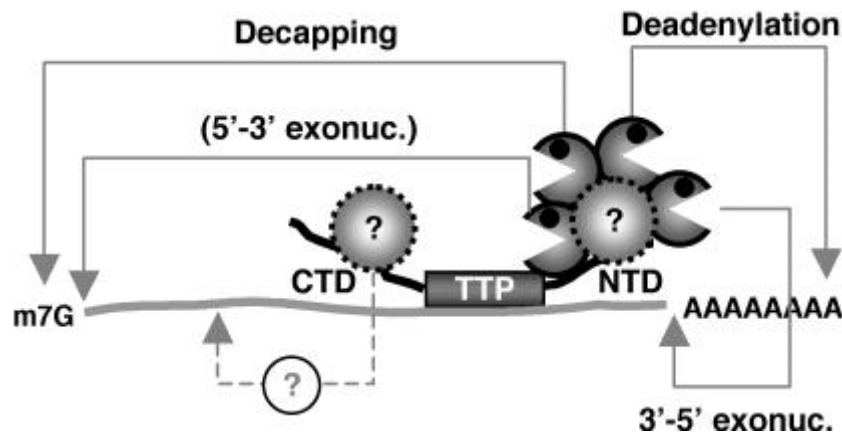

Figure 1: TTP by its N- and C-terminal domain (NTD, CTD) recruits different decay enzymes to targeted mRNAs providing a binding-platform for rapid degradation (figure from reference [12]).

In addition to the classical decay-pathways, also proteasome dependent mechanisms seem to be involved in TTP function. Therefore proteasome inhibition results in an impaired TTP function as shown recently [45].

In response to certain stressors, TTP can associate with cytoplasmic foci called stress granules (SGs) [46]. SGs are distinct sites within the cytoplasm of mammalian cells, forming upon eukaryotic initiation factor 2α phosphorylation during cellular stress [47]. These foci store untranslated mRNAs for reuse or transport to yet other cytoplasmic structure called GW bodies/processing bodies (PBs), where mRNAs are decapped and degraded [48]. TTP has been shown to promote the association between SGs and PBs therefore contributing to PB-dependent mRNA degradation. The current model assumes that during certain stress

conditions, mRNAs get released from polysomes and are delivered to SG where they are remodelled or sorted for degradation by PB in a TTP-dependent way [49].

3.2.5   Involvement of TTP in microRNA-dependent mRNA degradation

Beside the regulation of mRNA decay via cis-acting sequences in the 3´UTR, noncoding RNAs and microRNAs (miRNAs) have been extensively studied to influence RNA degradation and translation [50, 51]. Recent studies indicated that a specific miRNA, miR16, containing a UAAAUAUU sequence, is required for ARE-mediated mRNA turnover. This mRNA degradation is ARE and TTP-dependent. TTP interacts through association with Ago/eiF2C family members with the aforementioned miRNA facilitating ARE-mediated mRNA decay [52].

3.2.6 Functions of TTP not linked to mRNA decay

Aside its function in regulating mRNA stability, TTP has recently been shown to play a role in NF-κB signaling. TTP expression as well as NF-κB signaling are activated upon TNFα stimulation. However, TTP impairs the nuclear import of the NF-κB transcription factor unit p65 thereby blocking specific ARE-less NF-κB target genes independently of its function in mRNA degradation. This finding adds yet another level of possible regulation of gene expression by TTP during cellular stress [53, 54].

3.3 Posttranscriptional Regulation of TTP

3.3.1 p38 MAPK

Since the p38 Mitogen-activated protein kinase (MAPK) plays a fundamental role in the regulation of TTP, the general features of MAPK signaling are described in this paragraph. MAPKs are conserved serine/threonine protein kinases of cytoplasmic and nuclear targets

activated through phosphorylation by upstream MAPK kinases (MAP2K). The three known MAPK pathways, the Jun N-terminal kinase (JNK), the p38 MAPK and the extracellular signal-regulated kinase (ERK) pathway convert extracellular stimuli into a wide range of different responses. JNK and p38 MAPK pathway are also called stress kinase pathways as they are predominantly activated by environmental stress and pro-inflammatory cytokines thereby playing a key role during inflammation (figure 2) [55, 56].

Among the four p38 MAPK family members (p38α, p38β, p38γ and p38δ), p38α has been most extensively studied and appears to be the most widely expressed isoform [57]. Depending on the cell type, p38 MAPK is activated by a broad range of stress stimuli like LPS, hypoxia, toxins, UV radiation and pro-inflammatory cytokines such as IL-1 [58]. p38 MAPK then either activates MAPK-activated protein kinases (MKs) or directly phosphorylates sequence-specific transcription factors, transcriptional co-regulators and factors controlling mRNA stability and translation explaining the wide range of p38 MAPK-regulated biological processes (e.g. proliferation, survival, differentiation, inflammation and cancer) [55, 59]. Among the MKs activated by p38 MAPK are MK2, MK3, mitogen- and stress-activated kinase 1 and 2 (MSK1, MSK2), MAPK-interacting kinase 1 and 2 (MNK1, MNK2) and p38 regulated/activated kinase (PRAK) [59-61].

In macrophages, p38 MAPK is activated by TLRs and regulates the expression of a broad set of pro-inflammatory mediators (e.g. TNFα, IL-1 and IL-6) by both transcriptional and posttranscriptional mechanisms [57]. p38 MAPK has been proposed to affect specifically the stability of ARE-containing mRNAs such as *IL-3*, *IL-6* and *IL-8* by regulating TTP [62, 63]. However, besides a profound contribution for the onset of inflammation, p38 MAPK is also known to induce anti-inflammatory gene expression [61]. Activation of p38 MAPK and its downstream kinases MSK1 and MSK2 by LPS leads to increased IL-10 and dual-specific phosphatase-1 (DUSP1) expression. IL-10 and IL-10-induced DUSP1 have been demonstrated to inhibit p38 MAPK signaling therefore creating a negative feedback loop that limits the inflammatory response [64-66].
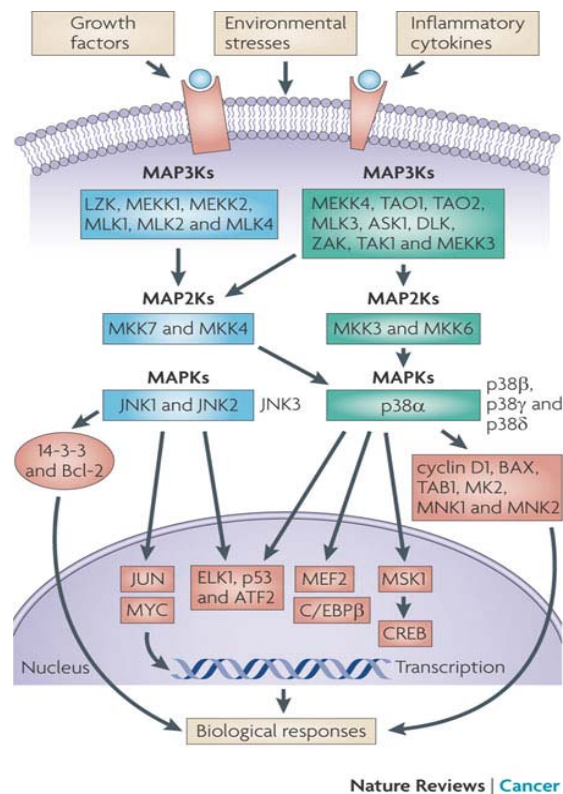
Figure 2: Stress-activated JNK and p38 MAPK pathways are activated by a wide range of environmental stresses. Upstream activators (e.g. MAP3Ks and MAP2Ks family members) and downstream targets (e.g. transcription factors and other effectors) of p38 MAPKs and JNKs are depicted (figure from reference [55]).

3.3.2 Transcriptional and posttranscriptional control of TTP

TTP was discovered as an immediate early gene because its mRNA is rapidly induced after serum stimulation in fibroblast. In macrophages, TTP mRNA is induced after LPS stimulation in a p38 MAPK dependent way and disappears to baseline within a few hours [39, 67]. In contrast to the labile mRNA, TTP protein appears stable after LPS treatment and gets slowly phosphorylated at different sites as shown by several studies [68-70]. p38 MAPK and its downstream kinase MAPKAP kinase-2 (MK2) can directly phosphorylate TTP [71-73]. Phosphorylation by MK2 of serines 52 and 178 leads to the exclusion of TTP from SGs by the assembly of 14-3-3:TTP complexes [46]. In association with 14-3-3, TTP is resistant to protein phosphatase 2a (PP2A)-dependent dephosphorylation and appears to be impaired in

promoting mRNA decay [46, 73] (figure 3). However, phosphorylated TTP is more stable as indicated by experiments using the specific p38α and p38β MAPK inhibitor SB203580. Thus, inhibition of p38 MAPK results in rapid dephosphorylation of TTP, relocalization from the cytoplasm to the nucleus and proteasomal degradation [70]. TTP is suggested to be stored and stalled by phosphorylation in a less active state till mRNA degradation of distinct messages is needed [70, 74]. p38 MAPK mediated regulation of TTP therefore happens at many levels, controlling TTP transcription as well as subcellular localization, protein stability and TTP activity [23, 33, 41, 48].
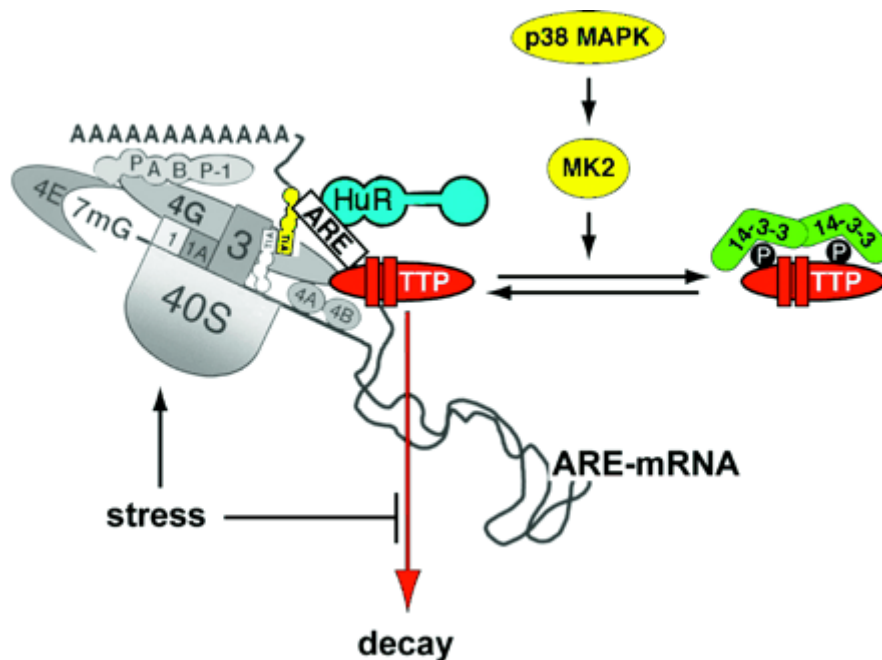
Figure 3: Inhibition of TTP-mediated mRNA decay by p38 MAPK phosphorylation and subsequent 14-3-3:TTP complex formation during stress (figure from reference [75]).

3.4 Role of TTP in Inflammation and Disease

TTP-deficient mice appear normal at birth but soon develop a complex phenotype. One to eight weeks after birth their weight gain rate starts to decrease followed by cachexia. In addition the animals develop multiple signs of inflammation as dermatitis, arthritis and conjunctivitis. Also several abnormalities of the hematopoietic system were detected like thymic hypoplasia and splenomegaly with a marked increase in myeloid cells especially in the bone marrow. However, treatment with TNFα antibody did prevent almost all aspects of the TTP-deficiency phenotype tested pointing out an important role of TTP in regulating *Tnf* mRNA stability [76]. Consecutive bone marrow transplantation experiments using bone marrow from TTP-deficient animals could mimic the phenotype seen in TTP-deficient mice. However, as the phenotype developed after a long latent period, the authors suggested that not lymphocyte progenitors but rather slowly reconstituting cells as cells of the monocyte/macrophage linage are responsible for the phenotype seen in these animals [77].

In human, TTP gene polymorphism analysis revealed up to 35 SNPs with a potential role in rheumatoid arthritis patients as well as other diseases [78, 79].

As pathologically stable transcripts are known to play a role in cancer development, reduced TTP levels have been associated with increased tumor incidents and progression. In this context, TTP has been shown to control mRNA stability of *Cox-2*, *IL-8*, *IL-3* and *VEGF* mRNA in different cancer models [80-83].

3.5 Interleukin-10 Signaling

mRNA stability is a major determinant for the expression of inflammatory molecules [2]. In this context, ARE-mediated mRNA decay by ARE-binding proteins like TTP and AUF1 is known to be important for limiting the inflammatory response providing a new strong anti-inflammatory mechanism [76, 84]. One of the most potent anti-inflammatory pathways is the interleukin-10 (IL-10) signaling cascade. Interestingly, the effectors of this pathway are largely unknown. IL-10 has been known for a long time to play a pivotal role as a potent anti-inflammatory cytokine, although its expression is induced by signaling pathways predominately driving inflammation as p38 MAPK pathway [65, 85]. IL-10 affects inflammation at the transcriptional as well as at the posttranscriptional level.

The pleiotropic IL-10 family of cytokines includes IL-19, IL-20, IL22, IL-24, IL-26, IL-28 and IL29, all sharing genetic similarities and affecting a broad range of biological functions [86]. IL-10 is produced by many cell types as various T-cell types, B-cells, monocytes and macrophages as well as granulocytes [87-91]. Binding of IL-10 to a complex of two IL-10 receptor 1 (IL-10R1) and two IL-10 receptor 2 (IL-10R2) molecules on most cells activates downstream Janus tyrosine kinases JAK1 and Tyk2. These kinases phosphorylate the cytoplasmic tails of the receptors recruiting STAT3 molecules. Activated STAT3 homodimers translocate subsequently to the nucleus and bind to STAT-binding sites on various promoters (figure 4) [85, 92]. We and others could demonstrate that IL-10 signaling plays a major role by controlling p38 MAPK induced inflammation. IL-10 drives expression of DUSP1 at later stages during the inflammatory response leading to gradually inactivation of p38 MAPK [64]. As a consequence, TTP gets rapidly dephosphorylated thereby increasing TTP activity [30].

IL-6 also signals via STAT3, though IL-6 signaling does not reproduce the anti-inflammatory properties of IL-10. This difference has been attributed to STAT3 driven SOCS3 expression. SOCS3 can bind and therefore inactivate the gp130 subunit of the IL-6 receptor, but not the IL-10 receptor. This means that IL-10 signaling allows a prolonged STAT3 activation

necessary for DUSP1 activation and down-regulation of p38 MAPK signaling [64, 93-95]. As a part of this PhD thesis it could be shown that the IL-10-dependent inhibition of p38 MAPK causes dephosphorylation of TTP thereby increasing the TTP-mediated mRNA degradation of the pro-inflammatory cytokines TNFα and IL-1α. These results established TTP as one of the effector molecules of IL-10 signaling (see Schaljo B. and Kratochvill F. et al. figure 3A and 5C in [30]).
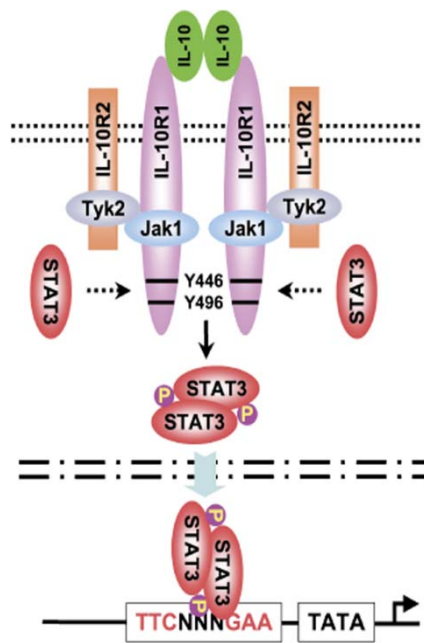
Figure 4: IL-10 signals via Jak1/Tyk2-STAT3 pathway (figure from reference [85]).

3.6 Other ARE Binding Factors

TTP remains the best described ARE-binding protein. However, several other proteins can bind to AREs in the 3' UTR of mRNAs controlling many features in the lifecycle of a nascent RNA. These proteins have been implicated in modulating not only mRNA stability, but also translational efficiency, transport and localization. As most of these proteins can target many RNAs in the cell, ARE-binding proteins are assumed to be main contributors in the global regulation of gene expression [96].

3.6.1 TIS11 family

The mammalian TIS11 family consist of the 4 members TTP (synonyms: TIS11, ZFP36, Nup475, GOS24), TIS11b (synonyms: Berg36, ERF-1, ZFP36L1, BRF-1), TIS11d (synonyms: ZFP36L2, ERF-2, BRF-2) and Zfp36l3 which is solely expressed in mouse placenta and the only TIS11 member not containing a functional nuclear export signal [14, 97, 98]. In other organisms TIS11 homologues have been identified as well. DTIS11 in Drosophila for instance, shares 90% sequence identity with murine TIS11b and TIS11d [99]. In Saccharomyces cerevisiae two members of the CCCH zing finger protein family, Cth1 and Cth2, have been cloned [100]. These two proteins degrade a battery of message involved in Fe-dependent metabolism [101, 102].

All TIS11 proteins and homologues have been described to be involved in mRNA degradation and bind to targeted transcripts by a conserved CCCH-type tandem zinc finger domain (figure 5) [14]. These domains are highly conserved within the murine TIS11 family so that most authors have made the assumption that the RNA binding affinity of the 3 murine TIS11 proteins is very similar [98].
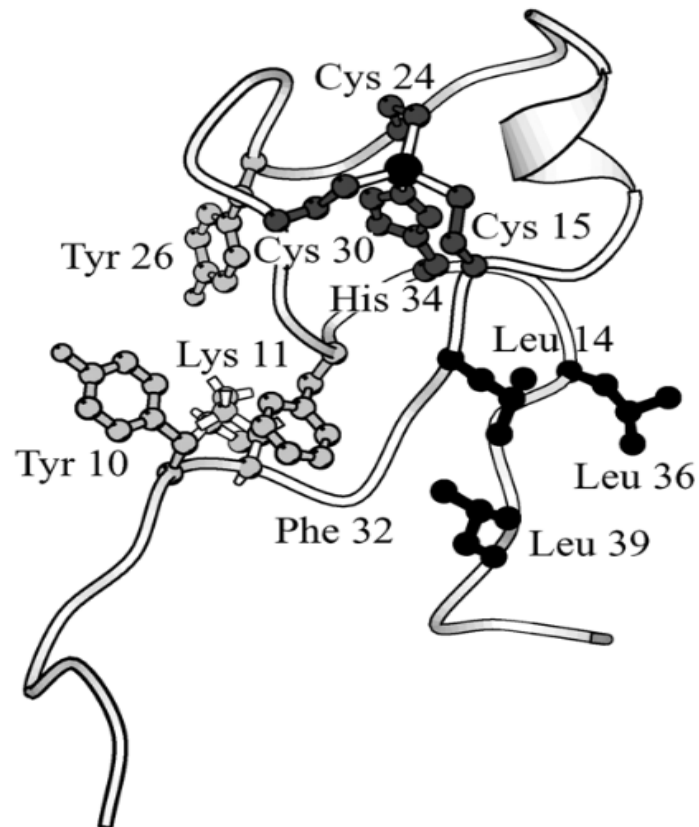
Figure 5: Ribbon diagram showing the first zinc-binding domain of TTP determined by multidimensional nuclear magnetic resonance spectroscopy. The metal binding site is depicted in dark grey and the leucine-rich core in black (figure from reference [103]).

Although these proteins are related and share common targets, they have distinct physiological roles. In contrast to the phenotype seen in the TTP knockout mouse described above, mice ablated for TIS11d die within 2 weeks of birth by developing intestinal and other hemorrhage. Further analysis revealed defective hematopoiesis and a role for TIS11d in hematopoietic stem and progenitor cell development [104]. Deletion of the third family member, TIS11b, results in abnormal placentation and early fetal death suggesting a developmental defect [105].

A possible explanation for the non-redundant role of the 3 TIS11 family members *in vivo* is provided by the finding that these proteins show major differences in the steady state protein levels in different cells and tissues as well as different expression-patterns in response to

stimulation or during developmental processes. *TTP* mRNA for example appears to be expressed at a similar level in human monocytes as *TIS11b* and *TIS11d*. However *TTP* is much higher induced in response to external stimuli like LPS. Therefore TTP is supposed to contribute to a larger extent to the regulation of mRNA stability during inflammation in these cells, accounting for almost 70 % of all TIS11 transcripts after LPS treatment [98].

3.6.2 AUF1

AUF1 (AU-binding factor 1), also known as hnRNPD (heterogeneous nuclear ribonucleoprotein D), comprises four protein isoforms (p37, p40, p42 and p45) generated by alternative splicing [106]. Every isoform contains two RNA recognition motifs through which they bind to AREs within selected mRNA targets. AUF1 was originally found to promote mRNA decay [107, 108], though it was also shown to stabilize transcripts as well as to promote translation [109, 110]. The broad spectrum of AUF1 targets, ranging from immune factors as *Tnf*, *IL-6* and *IL-1β* to genes affecting differentiation and carcinogenesis like *Cox-2* and *cyclin D1*, suggests a role of general importance of AUF1 in the cell [109, 111-114]. AUF1 knockout mice show a normal development, but appear to be more susceptible to LPS driven endotoxic shock due to an overproduction of IL-1β and TNFα [84]. Notably, while TTP knockout mice spontaneously develop various signs of inflammation due to an elevated TNFα level [76], loss AUF1 cannot recapitulate any of these syndromes [84]. This suggests that AUF1 and TTP have different properties in ARE-mediated mRNA decay. AUF1 executes *Tnf* mRNA degradation only upon activation of pro-inflammatory cytokines such as during LPS-challenge [84]. TTP in contrast was thought to control *Tnf* mRNA degradation independently of an inflammatory stimulus in the mouse, providing an explanation for the various syndromes of spontaneous inflammation developed in the conventional TTP knockout mouse [76]. However, as TTP expression is rapidly and transiently induced in macrophages in response to LPS, it is likely that TTP plays a role during acute forms of stress as well [39]. Accordingly, LPS stimulated TTP-/- macrophages produce higher levels

of proinflammatory cytokines as TNFα [77]. The role of TTP in acute inflammation has been confirmed in this PhD thesis by examining LPS-induced endotoxic shock in myeloid-specific TTP deletion.

3.6.3 Hu proteins

The Elav or Hu protein family, named after the Drosophila ortholog ELAV (embryonic lethal-abnormal vision) and their appearance as tumor-specific antigens in paraneoplastic neurological disorders in man, comprises the ubiquitous expressed HuR and the neuronal members of the family HuB, HuC and HuD. While HuB, HuC and HuD play important roles in neuronal differentiation and plasticity, the function of HuR is more related to cellular stress responses [115-119]. HuR binds to labile mRNAs bearing AU- or U-rich motifs in the 3' UTR increasing their stability or modifying translational efficiency [16, 120, 121]. Among the messages targeted by HuR are genes important in cell cycle control and proliferation as *cyclin A* and *c-fos* [122, 123] as well as mediators of carcinogenesis and inflammation like *VEGF*, *Cox-2* and *Tnf* [124]. Since HuR shares many mRNA targets with TTP, it has been proposed to counteract TTP-mediated mRNA degradation. Indeed, in various types of tumors HuR levels are elevated whereas those of TTP are reduced [82, 125, 126]. In normal colon tissue for instance, low HuR and higher TTP levels can be observed. However, in most adenomas and adenocarcinomas HuR expression is elevated and TTP expression is lost [82].

Recent HuR knockout studies in mice revealed, that global deletion leads to embryonic death around midgestion as a consequence of an impaired development of the extraembryonic placenta. Postnatal deletion of HuR leads to atrophy of hematopoietic organs, loss of intestinal villi and obstructive enterocolitis as a consequence of increase apoptosis of progenitor cell in the bone marrow, thymus and intestine depicting a role of HuR during development [127, 128].

3.6.4 KH-type splicing regulatory protein

The ARE-binding protein KSRP (KH-type splicing regulatory protein, also known as KHSRP) is known to regulate mRNA stability of several targets as *c-fos*, *iNOS*, *parathyroid hormone* (*Pth*), *Tnf*, *IL-2* and *IL-8* in a phosphorylation-dependent manner by recruiting mRNAs to the exosome and poly(A) ribonuclease (PARN) [129-134]. It has been demonstrated that KSRP undergoes p38 MAPK dependent phosphorylation during muscle differentiation which leads to impaired target-mRNA binding similar to TTP [134]. TTP is able to bind to KSRP thereby impairing KSRP mediated mRNA degradation of *iNOS* as described [33]. Recent studies implicated a role for KSRP in the biogenesis of a subset of miRNAs. In doing so, KSRP binds as a component of the Dicer complex to the terminal loop of miRNA precursors promoting their maturation [135, 136].

3.6.5 TIA-1 and TIAR

TIA-1 and its homologue TIAR are closely related ARE-binding proteins. Both bind with 3 conserved RNA recognition motifs (RRM) domains with high affinity to uridine-rich domains [137]. TIA1 knockout macrophages produce elevated levels of TNFα protein, although *Tnf* mRNA levels and transcript stability is not affected. Accordingly, TIA-1 deficiency leads to increased association with polysomes establishing TIA-1 as a silencer of translation [138]. Along its role in translation, TIA-1 and TIAR have been described to regulate splicing as well as the transport of untranslated mRNAs to SGs adding yet another function for RBPs [47, 139, 140].

3.6.6 NF90

The RNA-binding protein nuclear factor 90 (NF90), also known as NFAR (nuclear factor associated dsRNA), binds to and regulates the stability, transport and translation of several targeted mRNAs. As binding site, a 25 to 30 nucleotide long RNA signature motif rich in

adenines and uridines has been elucidated [141, 142]. The gene that encodes NF90 can, by alternative splicing, give rise to yet another protein called NF110. However, so far NF110 has not been studied in detail [143]. In addition to mRNA regulation, NF90 has been shown to bind to the *IL-2* promoter in T-cells controlling *IL-2* transcription. Hence, T-cell specific NF90 ablation in mice leads to impaired *IL-2* transcription and mRNA stabilization [144]. As NF90 has been also implicated in binding double-stranded RNA, it is supposed to be involved in the response to viral infections [144-147].

4. Aims

The precise regulation of gene expression is critical for the response to external stimuli as seen during inflammation. Besides control at the transcriptional level, posttranscriptional mechanisms have been shown to be of key importance. Herein mRNA stability enables the cell to induce a robust expression of selected transcripts upon transcriptional induction by impairing mRNA degradation. On the other hand, when transcription ceases a mechanism must be in place that rapidly removes transcripts from the system when they are no longer needed. Since TTP represents an mRNA-destabilizing factor that plays an important role in the removal of several inflammatory mRNAs it was decided to investigate its contribution to the global regulation of mRNA decay and to immune homeostasis. The aims of the PhD thesis were:

1) Contribution of TTP to global mRNA decay and elucidation of the regulatory circuits involved therein

One aim of this thesis was to globally identify mRNAs targeted by TTP for degradation during inflammation. In addition, it should be examined how the quality and quantity of the TTP-dependent mRNA decay is regulated in time during inflammatory response. Herein, the function of p38 MAPK and IL-10, the key pro- and anti-inflammatory molecules, respectively, should be investigated.

2) Studies of the role of TTP in inflammatory models using conditional deletion of TTP in mice

As the biological role of TTP-dependent mRNA degradation in diseases is only poorly understood, we aimed to establish a mouse line conditionally deleted for *zfp36*, the gene coding for TTP. This knockout mouse should then be used to elucidate the role of TTP in different animal models for inflammation-related human diseases.

5. MATERIALS AND METHODS

5.1 Cytokines, Reagents and Antibodies

p38 MAPK antibody was purchased from Santa Cruz (Santa Cruz, CA, USA). Rabbit antibody to TTP was obtained by immunizing rabbits with 44 C-terminal amino acids of murine TTP fused to GST. LPS from *Escherichia Coli* 055:B5 (Sigma-Aldrich, USA) was used at a concentration of 10 ng/ml for cell culture or 62.5 mg/kg for *in vivo* LPS challenge. Actinomycin D (act D) and SB203580 (all Sigma) were used at a concentration of 5 µg/ml and 4 µM, respectively.

5.2 Mammalian Cell Culture

5.2.1 Cell lines

Murine embryonic fibroblasts were grown in DMEM supplemented with 10 % FCS. Abelson-transformed B-cell clones were grown in complete RPMI medium (RPMI (PAA, Germany), 10 % FCS and 5 µM β-mercaptoethanol).

5.2.2 Primary cells

Primary macrophages, isolated from bone marrow of tibia and femur, were cultured in L cell-derived CSF-1 as previously shown [148]. Mice were housed in specific pathogen-free conditions and were 6-10 weeks of age at the time of bone marrow preparation. Conventional TTP-deficient mice (TTP-/-) were on C57Bl/6 background. Conditional TTP knockout mice (TTP^{fl}) and conditional knockin mice overexpressing TTP (Col1$^{tm1(TTP)}$; hereafter referred to as TTP^{high}) were on 129/OlaHsd C57Bl/6 mixed or C57Bl/6 background as specified in each experiment. TTP^{fl} LysMCre mice and TTP^{high} LysMCre mice were

obtained by crossing TTP[fl] and TTP[high] mice with the knockin LysMCre mouse line B6.129P2-Lyzs[tml(cre)lfo] (Jackson Laboratories Bar Harbor, Main, USA) on C57Bl/6 background. Mouse experiments were performed according to the national law.

5.2.3 Abelson-transformation and colony formation assay

For the preparation of Abelson-transformed B-cell progenitors, bone marrow from Wt or TTP-/- mice (C57Bl/6) was infected for 1 hour with viral supernatant derived from A010 cells supplemented with IL-7 (10 ng/ml) and polybrene (10 µg/ml) or left uninfected (mock). A010 cells produce an ectopic replication-deficient form of the Abelson virus described previously [149]. Cells were then maintained in complete RPMI medium supplemented with IL-7 for 15-20 hours. Thereafter cells were maintained in complete RPMI medium to generate growth factor independent cell lines or were plated in cytokine-free methylcellulose at a density of 2.5 x 10^5 cells/ml in 35-mm dishes for 6-12 days in order to calculate cloning efficiency by counting colonies.

5.3 Construction of Targeting Vector and Generation of Conditional TTP Knockout Mice

For conditional ablation of *zfp36* (encoding TTP), we created a deletion construct containing exon 2 of *zfp36* (the larger of the two *zfp36* exons) flanked by *LoxP* sites in front of an also *LoxP* site flanked neomycin (Neo) cassette. Therefore exon 2 was PCR amplified as well as a 1 kb region 3' downstream and a 5 kb region 5' upstream of exon 2 allowing homologous integration on the TTP locus. As template for the PCR reactions we purchased a Bac clone from Geneservice (BioCat GmbH, www.geneservice.co.uk), containing the genomic TTP

locus. The PCR products for exon 2, the 3' down- and the 5' upstream sequence of exon 2 were created using the following primers (respective restriction sites are underlined):

For exon 2 with the inclusion of SalI and XbaI restriction sites:

Exon 2 fw (SalI): 5'- ATC CTT <u>GTC GAC</u> TCC TCT CAG AGC CTC CAG T -3'
Exon 2 rv (XbaI): 5'- TGG ACC <u>TCT AGA</u> TCA CTC AGA GAC AGA GAT AC -3'

For the 3' downstream region with the inclusion of NotI and ClaI restriction sites:

3' region fw (NotI): 5'- GGA CGA <u>GCG GCC GC</u>C AAG TGC CTA CCT ACC CAG -3'
3' region rv (ClaI): 5'- GAG TTC <u>ATC GAT</u> GAA ACA TCC CGT TCC TGC C -3'

The primer set for the 5' upstream region was designed to create XhoI and HindIII sites at the end of the PCR fragment:

5' region fw (XhoI): 5'- A**CG TCT C**<u>CT CGA G</u>GC CAG CCA AAG TGG CTT AT -3'
5' region rv (HindIII): 5'- A**CG TCT C**<u>AA GCT T</u>AC AGG GTT CGG TTA GGC CA -3'

As there are also XhoI and HindIII sites located inside the 5' upstream region, the flanking XhoI and HindIII sites were created using the restriction enzyme Esp3I. This enzyme cuts one nucleotide on the leading and five nucleotides on the lagging strand downstream of a distinct recognition site (highlighted in bold).

The resulting products were inserted into the SalI/XbaI, NotI/ClaI and XhoI/HindIII restriction sites of the vector pEasy Flox (Addgene, Cambridge, USA; figure 6) respectively, creating the targeting vector depicted in figure 9A.
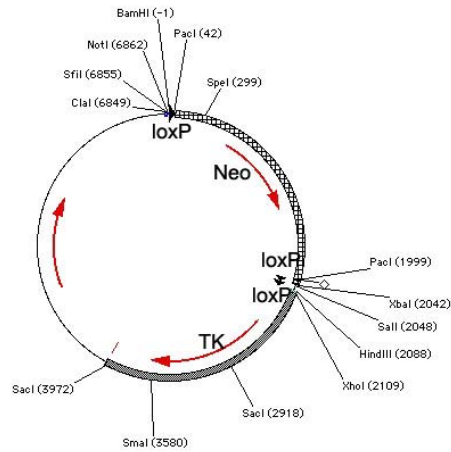
Figure 6: pEasy Flox; TK, thymidine kinase; Neo, neomycin.

The final vector was sequenced by Eurofins MWG Operon (Germany). Then the vector was linearized by ClaI digestion and electroporated into 129/OlaHsd embryonic stem cells (ES cells) using an Amaxa Nucleofector Kit according to the manufacturers protocol. Single cell clones were selected for Neo resistance and then isolated for further cultivation on 96-well plates. Clones were lysed for 1 hour at 60°C in Kawasaki-buffer (20 mM TrisHCl pH 8.3, 25 mM KCl, 1.5 mM $MgCl_2$ and 0.5 % Tween) supplemented with proteinase K (2 µg/ml), subsequently incubated at 95°C for 30 minutes and used for screening the chromosomal DNA for homologous integration of the targeting construct by PCR. For this purpose the following primers were used:

P1: 5'- TGT GAC TCG AAG AGA CCC TAA C -3'

P2: 5'- CAG GGT TCA GAG TCC CCT AG -3'

P3: 5'- ACC TGC GTG CAA TCC ATC TTG -3'

This primer set result in a 1.4 kb product in the Wt-allele and a 1.7 kb fragment when the vector has integrated by homologous recombination.

Before blastocyst injection, the Neo cassette was excised by transiently transfecting targeted ES cells with a Cre recombinase expressing construct. Loss of the Neo cassette but not exon 2 was monitored by PCR using the following primers:

P4: 5'- ATC TAG CTG ATC CAT ACT GGG -3'
P5: 5'- AGG TTC TCC CTG GAG TTT GTG TGA -3'

These primers amplified a 1.1 kb fragment in the Wt and a 1.2 kb fragment in the targeted allele when the Neo cassette was excised properly. Subsequent genotyping of conditional TTP knockout animals was done using the same primers.

Two positive clones were injected into C57Bl/6 blastocysts and used to generate chimeric mice. Male chimeric mice were mated to C57Bl/6 females and heterozygote offspring were further backcrossed with C57Bl6 to get C57Bl6 background using speed congenics.

5.4 Construction of Targeting Vector and Generation of Conditional TTP Knockin Mice

For conditional overexpression of TTP, cDNA of murine TTP was amplified by PCR using the following primers carrying AscI restriction sites (AscI sites are underlined):

TTP^{high} fw: 5'- TTA CTG TGG GC GCG CCC GGT CTC TTC ACC AAG GC -3'

TTP^{high} rv: 5'- TGC AAG CGG CGC GCC ATC TAG CTG ATC CAT ACT GG -3'

The resulting product was cloned into the AscI site of a modified pBR322 vector kindly provided by Dr. Robert Eferl. The construct is designed so that TTP is under the control of the human UbiC promoter (ubiquitin C promoter was shown to confer ubiquitous expression in transgenic mice [150]) with a floxed Neo+transcriptional STOP cassette inserted between the UbiC promoter and the cDNA of TTP. The transcriptional STOP cassette consists out of

three SV-40 poly-A sites and efficiently impairs read-through from the UbiC promoter. In addition, an enhanced cyan fluorescent protein (ECFP) is located after the TTP cDNA on the same transcript whose translation is driven by an IRES. Regions homologous to the collagen locus are located at both sides of the construct allowing homologue recombination to this site.

The vector was linearized by NotI digestion and electroporated into 129/OlaHsd embryonic stem cells using an Amaxa Nucleofector Kit according to the manufacturer's protocol. Single cell clones were selected for Neo resistance, isolated for further cultivation on 96-well plates and chromosomal DNA was screened by PCR for homologous integration as described before using the following primers:

P6: 5'- CCC CCT GAA CCT GAA ACA TA -3'

P7: 5'- ACG GGG AGA CAC ATT TCA AG -3'

P8: 5'-GCC ATC CCA ACA ATA CAT CAC A -3'

The primers result in a 1.6 kb fragment for the Wt and a 1.9 kb fragment for the correctly inserted construct.

Two positive clones were injected into C57Bl/6 blastocysts and used to generate chimeric mice. Male chimeric mice were mated to C57Bl/6 females and heterozygote offspring were further crossed to C57Bl/6 mice to obtain C57Bl/6 background using speed congenics as before.

5.5   RNA Analysis

5.5.1 RNA purification

Total RNA was isolated using Trizol LS reagent (Invitrogen) according to the manufacturer's instruction. RNA was quantified using Nanodrop (Peqlab) and visualized by gel electrophoresis before subsequent cDNA preparation or Microarray analysis.

5.5.2 Quantitative RT-PCR

For quantitative RT-PCR (qRT-PCR), total RNA was reverse transcribed using Mu-MLV reverse transcriptase (Fermentas) according to the manufacturer's protocol. qRT-PCR was then performed detecting the fluorescent dye SYBR Green (Molecular Probes) using a Master Cycler (Eppendorf). For *Dusp1* and *Bcl3* qRT-PCR we used the primer sets QT00288638 and QT01164611 from Qiagen (Duesseldorf, DE), respectively. For the PCR amplification of *TTP* mRNA as well as the housekeeping gene *HPRT* for normalization the following primers were used:

For *TTP*:

TTP forward: 5'- CTC TGC CAT CTA CGA GAG CC - 3'

TTP reverse: 5'- GAT GGA GTC CGA GTT TAT GTT CC- 3'

For *HPRT*:

HPRT forward: 5'- GGA TTT GAA TCA CGT TTG TGT CAT - 3'

HPRT forward: 5'- ACA CCT GCT AAT TTT ACT GGC AA - 3'

5.6 Protein Analysis

5.6.1 ELISA

For Enzyme-linked immunosorbent assay (ELISA), primary macrophages were seeded the day before ($2x10^6$ cells per 6 cm dish). Supernatant of LPS stimulated cells was collected and diluted 1:5 in reagent diluent. TNFα was then assayed using DuoSET ELISA kits (R&D Systems, Minneapolis, MN).

5.6.2 Western Blot

Western blot analysis was performed as described [151] using whole cell lysates from $2x10^6$ cells seeded on 6 cm plates the day before. Cells were treated as indicated and assayed using fluorophore-linked secondary antibodies (Molecular Probes-Invitrogen (Lofer, Austria) and Rockland (Gilbertsville, PA)) and an Odyssey infrared imaging system (LI-COR Bioscience, Lincoln, NE).

5.7 Animal models

5.7.1 LPS-induced shock model

LPS challenge was performed with age-matched (8 weeks) mouse groups for Wt (comprising Wt or TTP$^{fl/fl}$, n=10) and TTP$^{fl/fl}$ LysMCre mice (n=12) on a mixed background. LPS at a concentration of 62.5 mg/kg body weight dissolved in 0.9% NaCl was injected intraperitoneally and mice were monitored for time of death to calculate a Kaplan-Meier blot. All animal experiments were carried out in accordance with protocols approved by the Austrian Laws (GZ68.205/67-BrGZ/2003) and European Directives.

5.7.2 B-cell lymphoma formation

$2x10^6$ cells of Abelson-transformed Wt or TTP-/- B-cell lines (CD19^{+}/CD43^{+}/B220^{+}) were injected subcutaneously into the hind leg of age-matched C57Bl/6 mice (8 weeks). At the time of injection, cells were grown for at least a week in growth factor-free medium. Tumors were isolated 10 days later to determine tumor size and weight. Transformed B-cell lines from bone marrow of 3 individual Wt and 4 TTP-/- mice were injected into 4 animals each.

6.   RESULTS

In this thesis the regulation and function of TTP in inflammation and cancer development *in vitro* and *in vivo* will be addressed in the following four topics:

i) The role of TTP as an effector of the IL-10-mediated anti-inflammatory response in LPS-treated macrophages published by Schaljo B. et al. 2009 (Schaljo B. and Kratochvill F. contributed equally to this work) [30]. My contribution to this study was to show that IL-10 signaling leads to decreased TTP phosphorylation and subsequent increased TTP binding and decay of *Tnf* and *IL-1α* mRNA.

ii) The qualitative and temporal regulation of mRNA decay during inflammation by TTP and p38 MAPK (Kratochvill F. et al., manuscript submitted).
In this study we revealed a TTP and p38 MAPK dependent negative feedback loop that governs the mRNA decay of a broad set of inflammation induced genes.

iii) The generation of conventional TTP knockout as well as knockin mice and the role of myeloid TTP in an animal model of acute inflammation.
In order to dissect the role of TTP in various disease models we created a conditional TTP knockout mouse and confirmed its utility in a model of endotoxic shock.

iv) The role of TTP in *v-abl* induced B-cell lymphoma formation.
We investigated the contribution of TTP in *v-abl* induce transformation of murine bone marrow into growth factor independent cell lines and subsequent tumor formation *in vivo*.

6.1 Publication: Tristetraprolin is Required for Full Anti-inflammatory Response of Murine Macrophages to IL-10

Tristetraprolin Is Required for Full Anti-Inflammatory Response of Murine Macrophages to IL-10[1]

Barbara Schaljo,[2] * Franz Kratochvill,[2] * Nina Gratz,* Iwona Sadzak,* Ines Sauer,* Michael Hammer,[l#] Claus Vogl,[†] Birgit Strobl,[†‡] Mathias Müller,[†‡] Perry J. Blackshear,[§] Valeria Poli,[¶] Roland Lang,[l#] Peter J. Murray, and Pavel Kovarik[3] ***

IL-10 is essential for inhibiting chronic and acute inflammation by decreasing the amounts of proinflammatory cytokines made by activated macrophages. IL-10 controls proinflammatory cytokine and chemokine production indirectly via the transcription factor Stat3. One of the most physiologically significant IL-10 targets is TNF-a, a potent proinflammatory mediator that is the target for multiple anti-TNF-a clinical strategies in Crohn's disease and rheumatoid arthritis. The anti-inflammatory effects of IL-10 seem to be mediated by several incompletely understood transcriptional and posttranscriptional mechanisms. In this study, we show that in LPS-activated bone marrow-derived murine macrophages, IL-10 reduces the mRNA and protein levels of TNF-a and IL-1a in part through the RNA destabilizing factor tristetraprolin (TTP). TTP is known for its central role in destabilizing mRNA molecules containing class II AU-rich elements in 3' untranslated regions. We found that IL-10 initiates a Stat3-dependent increase of TTP expression accompanied by a delayed decrease of p38 MAPK activity. The reduction of p38 MAPK activity releases TTP from the p38 MAPK-mediated inhibition, thereby resulting in diminished mRNA and protein levels of proinflammatory cytokines. These findings establish that TTP is required for full responses of bone marrow-derived murine macrophages to IL-10. *The Journal of Immunology,* **2009, 183: 0000 –0000.**

O ne of the key players in immune homeostasis is IL-10, a cytokine that was discovered 18 years ago as a T cell-secreted factor that inhibited cytokine production by Th1 cells (1). Over the years, it became clear that IL-10 is produced by many cell types including T and B cells, macrophages, dendritic cells, mast cells, keratinocytes, or epithelial cells (2). It is generally considered that the main biological function of IL-10 is to limit or shut down inflammatory responses. This notion is supported by the phenotype of IL-10-deficient mice that develop severe inflammatory bowel disease due to spontaneous chronic inflammation and are susceptible to endotoxin treatment because of acute overpro

*Max F. Perutz Laboratories, Department of Microbiology and Immunobiology, University of Vienna, Vienna, Austria; [†]Institute of Animal Breeding and Genetics, University of Veterinary Medicine Vienna and [‡]University Center Biomodels Austria GmbH, University of Veterinary Medicine Vienna, Vienna, Austria; [§]Laboratory of Neurobiology, National Institute of Environmental Health Science, Research Triangle Park, NC 27709; [¶]Department of Genetics, Biology and Biochemistry, Molecular Biology Center, University of Turin, Turin, Italy; [l]Institute of Medical Microbiology, Immunology and Hygiene, Technical University Munich, Munich, Germany; [#]Institute of Microbiology, Immunology and Hygiene, University Hospital Erlangen, Erlangen, Germany; and **Departments of Infectious Diseases and Immunology, St. Jude Children's Research Hospital, Memphis, TN 38105

[2] B.S. and F.K. contributed equally to this work.

[3] Address correspondence and reprint requests to Dr. Pavel Kovarik, Max F. Perutz Laboratories, Department of Microbiology and Immunobiology, University of Vienna, Dr. Bohr-Gasse 9, A-1030 Vienna, Austria. E-mail address: pavel.kovarik@ univie.ac.at

duction of proinflammatory cytokines (3, 4). Many of these phenotypes can be recapitulated by T cell-specific deletion of the IL-10 gene, indicating that T cell-derived IL-10 is primarily responsible for chronic inflammation (5). Under conditions of acute inflammation, the main source of IL-10 are macrophages and dendritic cells (6). On the cellular level, IL-10 inhibits production of proinflammatory cytokines and regulates differentiation and proliferation of various immune cells. These effects depend entirely on the activation of the transcription factor Stat3 by IL-10 (7–11). The events downstream of Stat3 activation that mediate the antiinflammatory functions of IL-10 remain an area of active research. It is becoming increasingly clear that multiple mechanisms mediate the IL-10 function. On the one hand, IL-10 inhibits transcription of a subset of proinflammatory genes (12, 13). In a mouse model lacking 3' untranslated regions (UTR)[4] in the *Tnf* gene, the transcriptional mechanism was found to play a major role in IL-10 responses (13). On the other hand, IL-10 was also reported to act

posttranscriptionally by increasing the rate of mRNA decay of inflammatory cytokines such as TNF-a or by inhibiting translation (12, 14, 15). The posttranscriptional regulation depends on 3' UTR containing AU-rich elements (AREs) (16). However, far less is known about the IL-10-regulated effector genes that control the anti-inflammatory response. Several candidates have been described, but so far none have been shown to account for the majority of the anti-inflammatory effects (17). IL-10 was also demonstrated to up-regulate the dual-specificity phosphatase 1 (DUSP1) in LPS-stimulated macrophages. causing a more rapid inactivation of p38 MAPK (18). The reduction of p38 MAPK activity may lead to a decreased stability of ARE-containing mRNAs and/or reduced transcription by transcription factors that depend on p38 MAPK. Recently, the transcriptional repressor ETV3 and

the corepressor SBNO2 were characterized as IL-10/Stat3-induced genes that may contribute to the anti-inflammatory IL-10 effects (19). An important aspect of the above-mentioned studies that remains to be resolved is how IL-10 inhibits specifically only a subset of inflammatory genes. These studies indicate that yet unknown IL-10/Stat3 target genes need to be discovered to complement the current knowledge about the anti-inflammatory effects of IL-10.

In this study, we demonstrate that IL-10-mediated reduction of TNF-a and IL-1a production by LPS-treated mouse bone marrowderived macrophages (BMDMs) is less efficient in cells lacking the RNA-destabilizing factor tristetraprolin (TTP). TTP is known to bind and destabilize mRNAs of several proinflammatory cytokines (e.g., TNF-a) containing class II AREs in their 3' UTRs (20). TTP facilitates degradation of the bound mRNA by initiating the assembly of RNA decay machinery (21, 22). The RNA degradation activity of TTP is negatively regulated by p38 MAPK-dependent signaling (23–25). Mice lacking TTP (encoded by the *Zfp36* gene) develop multiple chronic inflammatory syndromes ranging from arthritis to cachexia to dermatitis that can all be relieved by reduction of TNF-a levels (26). By comparing LPS-treated wildtype and TTP-deficient BMDMs, we show that IL-10 accelerates, in a TTP-dependent way, the decay of TNF-a mRNA, resulting in a reduction of secreted TNF-a. Furthermore, IL-10 increases TTP expression in LPS-treated wild-type (WT) but not Stat3-deficient BMDMs. However, we show that the increased TTP levels are not sufficient to mediate the IL-10 effects. Instead, the IL-10-mediated reduction of p38 MAPK activity in LPS-treated BMDMs that is known to be caused by up-regulation of the p38 MAPK phosphatase DUSP1 (18) is required to act in concert with TTP to reduce mRNA levels of proinflammatory cytokines such as TNF-a and IL-1a. We propose that the sustained activation of Stat3 by IL-10 causes both an increased TTP expression and a reduction in p38 MAPK activity. The combination of these effects results in a reduction of mRNA stability and attenuation of cytokine production.

Materials and Methods
Reagents

Stat3, p38 MAPK, and DUSP1 (sc-1102) Abs were from Santa Cruz Bio-technology, the ERK Ab was from BD Transduction Laboratories, and the phosphotyrosine-Stat3 Ab (pY-Stat3) was from Cell Signaling and New England Biolabs. Rabbit Ab to TTP was obtained by immunizing rabbits with 44 C-terminal amino acids of TTP fused to GST. IL-10 and IL-6 (Sigma-Aldrich) were used at a concentration of 10 ng/ml, LPS from *Salmonella minnesota* (Alexis) was used at a concentration of 5–10 ng/ml, and anisomycin and actinomycin D (both Sigma-Aldrich) were used at a concentration of 100 ng/ml and 5 /g/ml, respectively. SB203580 (SB; Sigma-Aldrich) was dissolved in DMSO and used at final concentration 4 /M. ATP (1 /M; Sigma-Aldrich) was added 1 h before collecting the samples.

Cell culture

Primary macrophages were grown in L cell-derived CSF-1 as previously described (27). *Zfp36*-/- and Dusp1-/- mice (26) were on the C57BL/6 background. The *Zfp36* gene encodes TTP, which is the better known name and therefore is used throughout. For experiments with cells derived from TTP-/- and TTP+/+ mice, littermates originating from the TTP+/- colony were used. The LysMcre-Stat3fl/fl mice were obtained by crossing Stat3fl/fl mice (28) with LysMcre, strain B6.129P2-Lyzstm1(cre)llo (The Jackson Laboratory), all on the C57BL/6 background. Mice, 8–12 wk old at the time of bone marrow collection, were housed under specific pathogen-free conditions. Mouse experiments were conducted in compliance with national laws. Mouse macrophage line RAW 264.7 was grown in DMEM supplemented with 10% FCS.

Inducible expression of TTP

The open reading frame of the mouse TTP was PCR-amplified from cDNA. The PCR was used to add Flag tag DYKDDDDK at the C terminus. The TTP-Flag fragment was cloned into the pGL2-basic (Promega) containing a tetracycline-responsive element (TRE) in the promoter. The resulting plasmid pTRE-TTPfl was transfected into HeLa-Tet-off cells (BD Clontech) using nucleofection (Amaxa). After transfection, the cells were incubated overnight in medium with (no TTP expression) or without (TTP expression) tetracycline (1 /g/ml).

ELISA

For ELISA, BMDMs were seeded the day before use at 2×10^5 cells/well in a 24-well plate. Supernatants were diluted 1/8 in DMEM (for TNF-a)or 1/2 (for IL-1a) and cytokines were assayed using ELISA kits (R&D Systems) according to the manufacturer's instructions.

Quantitative Western blot

After treatment, whole cell extracts were prepared and assayed by Western blotting as described elsewhere (29). Detection and quantitation of signals were performed using the infrared imaging system Odyssey (LI-COR Biosciences).

Quantitation of gene expression by quantitative RT-PCR (qRT-PCR)

Total RNA was isolated using TRIzol reagent (Invitrogen). Reverse transcription was performed with Moloney murine leukemia virus reverse transcriptase (Fermentas). The following primers were used: for HPRT, the housekeeping gene used for normalization, HPRT forward (fwd) 5'-GG ATTTGAATCACGTTTGTGTCAT-3' and HPRT reverse (rev) 5'-ACAC CTGCTAATTTTACTGGCAA-3'; for TTP, TTP fwd 5'-CTCTGCCATC TACGAGAGCC-3' and TTP rev 5'-GATGGAGTCCGAGTTTATGTTC C-3'; for TNF-a, TNF-a fwd 5'-CAAAATTCGAGTGACAAGCCTG-3' and TNF-a rev 5'-GAGATCCATGCCGTTGGC-3'; for suppressor of cytokine signaling (SOCS) 3, SOCS3 fwd 5'-GCTCCAAAAGCGAGTACC AGC-3' and SOCS3 rev 5'-AGTAGAATCCGCTCTCCTGCAG-3'; and for TTP primary transcript, TTPpt fwd 5'-GACTGGCAAGCTCGTGAA GT-3', pt-TTP-rev 5'-CAGTCAGGCGAGAGGTGA-3'. For determination of mRNA decay by qRT-PCR, the primers TNF-a fwd 5'-TTCTGT CTACTGAACTTCGGGGTGATCGGTCC-3' and TNF-a rev 5'-GTAT GAGATAGCAAATCGGCTGACGGTGTGGG-3' and for IL-1a, the primer set QT00113505 from Qiagen was used. Amplification of DNA was monitored by SYBR Green (Molecular Probes (30).

RNA EMSA

To prepare extracts, cells were washed with cold PBS and lysed in buffer containing 10 mM Tris-HCl (pH 7.5), 50 mM NaCl, 30 mM NaPPi,50mM NaF, 2 mM EDTA, 1% Triton X-100, and a protease inhibitor mixture (Roche). Extracts were cleared by centrifugation at 15,000 rpm. Twelve-microliter cell extracts (30 /g of protein) from RAW 264.7 cells or 5-/l cell extracts (15 /g of protein) from pTRE-TTPfl-transfected HeLa-Tet-off cells were incubated with 0.5 /l of poly(U) RNA (100 ng/l), 0.5 /lof Cy5.5-labeled TNF-a ARE (1 pmol//l), 1 /l of RiboLock RNase Inhibitor (Fermentas), and 2.5 /lof5x Gelshift buffer (200 mM KCl, 5 mM MgCl$_2$, 0.5 mM EGTA, 2.5 mM DTT, 100 mM HEPES-KOH (pH 7.9), and glycerin 50% (v/v)) for 20 min at room temperature. For supershift assays, 0.5 /l of TTP antiserum was added. Samples were then separated on a 6% polyacrylamide gel. The Cy5.5 signal was detected and quantified using the infrared imaging system Odyssey (LI-COR Biosciences). Poly(U) RNA and Cy5.5'-labeled TNF-a ARE RNA were purchased from Microsynth. The sequence for Cy5.5'-labeled TNF-a ARE was as follows: 5'-AUUAUUUAUUAUUUAUUUAUUAUUUA-3'.

Statistical analysis

Data from independent experiments were analyzed using univariate linear regression models and the SPSS program. For qRT-PCR normalized copy numbers and for ELISA pg/ml were log-transformed. Residuals were plotted, visually inspected, and tested for normality. Design matrices were specified such that the coefficients for the relevant comparisons could be calculated, e.g., between the baseline and induced states and between genotypes. Only the significance levels are reported.

Results
IL-10 increases TTP expression in LPS-treated macrophages in a Stat3-dependent manner

TTP expression has been reported to be controlled by the transcription factors Stat1 (in response to IFNs) and Stat6 (in response to IL-4) (27, 31). Affymetrix analysis revealed that LPS-induced TTP expression is further enhanced by IL-10 (data not shown) at
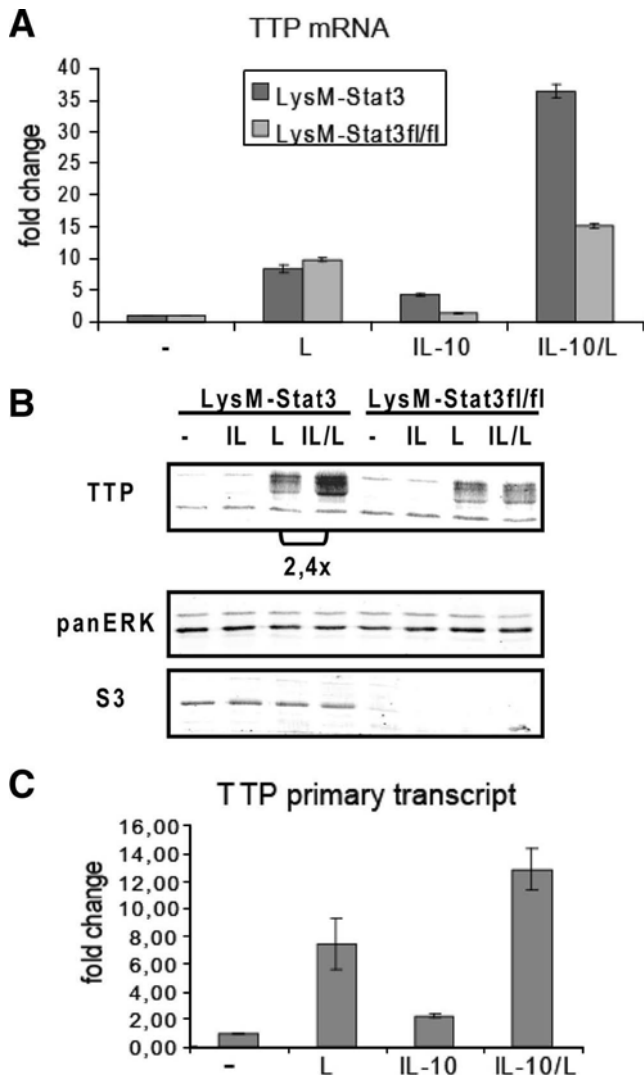
FIGURE 1. IL-10-mediated increase of TTP expression in LPS-treated macrophages depends on Stat3. *A*, BMDMs from LysMcre-Stat3 (LysM-Stat3) and LysMcre-Stat3^{fl/fl} (LysM-Stat3fl/fl) mice were treated for 1 h with LPS (L), IL-10, or both (IL-10/L). Induction of TTP mRNA was quantified using qRT-PCR. Bars indicate SDs, $n = 3$. *B*, BMDMs from LysMcre-Stat3 (LysM-Stat3) and LysMcre-Stat3^{fl/fl} (LysM-Stat3fl/fl) animals were left untreated or treated with IL-10 (IL), LPS (L), or both (IL/L) for 3 h. TTP protein levels were analyzed by Western blotting of cell extracts using TTP Ab. TTP appears in multiple bands representing phosphorylated forms. Blot was reprobed with Stat3 Ab to control for Stat3 deletion in LysMcre-Stat3^{fl/fl} cells and panERK Ab for loading control. Differences in TTP levels (normalized to panERK and quantitated using infrared imaging system Odyssey) in cells treated with IL-10/LPS compared with LPS alone are indicated. *C*, BMDM (WT) were stimulated for 30 min with LPS (L), IL-10, or both (IL-10/L), total RNA was isolated, DNase treated, and the amount of primary transcript was determined by qRT-PCR. Bars indicate SDs, $n = 3$.

30 min after treatment of Il10^{-/-} BMDMs with IL-10 and LPS, suggesting that TTP may represent a Stat3 target gene involved in the anti-inflammatory responses to IL-10. To examine the effect of IL-10 on TTP expression in more detail, we investigated TTP gene expression in BMDMs conditionally deleted for Stat3 (LysMcreStat3^{fl/fl}) and control LysMcre-Stat3 cells. LysMcre is known to delete loxP-flanked alleles in macrophage and

neutrophil lineages with >90% efficiency (7). Treatment of BMDMs with IL-10 and LPS caused a 2-to 3-fold increase in TTP mRNA (Fig. 1*A*) and protein levels (Fig. 1*B*) compared with LPS treatment alone. The IL-10-mediated increase in TTP expression required Stat3 since in LysMcre-Stat3^{fl/fl} cells the TTP levels remained unchanged upon IL-10 treatment. The expression of Stat3 was reduced by >90% in LysMcre-Stat3^{fl/fl} cells (Fig. 1*B*), thereby confirming the deletion efficiency by LysMcre. Analysis of TTP primary transcripts by PCR (Fig. 1*C*) and nuclear run-on assays (data not shown) revealed that the IL-10-mediated induction of TTP was caused by increased transcription.

These findings document that IL-10-activated Stat3 increases expression of TTP in LPS-stimulated macrophages. IL-10 alone only weakly increased TTP transcription, and this induction was not sufficient to generate detectable levels of TTP protein. This way of regulation resembles that of IFN-induced TTP expression, which was shown to be activated by IFNs and the IFN-activated Stat1 only if p38 MAPK signaling (by e.g., LPS) is stimulated in parallel (27). p38 MAPK is known to increase by yet unclear mechanisms the transcriptional activity of several Stat members (32–34).

TTP is required for full inhibitory effect of IL-10 on TNF-a and IL-1a production

To test whether TTP was an effector of the IL-10 anti-inflammatory responses, we measured the amount of secreted TNF-a by ELISA in BMDMs from TTP^{-/-} and control WT littermates that were treated with LPS with or without pretreatment with IL-10. We measured TNF-a production at 6, 8, and 10 h after LPS stimulation. After 10 h, TNF-a was diminished by IL-10 to

◆20% in control cells, whereas in TTP^{-/-} cells only a reduction to 60% was achieved (Fig. 2*A*). Similar results were obtained if cells were treated simultaneously with LPS and IL-10 (Fig. 2*B*), although the contribution of TTP to the IL-10 response was higher in the pretreatment protocol (Fig. 2A). These data show that TTP contributes to IL-10-mediated inhibition of TNF-a cytokine production.

To investigate whether the incomplete IL-10-mediated inhibition of TNF-a production in TTP^{-/-} BMDMs resulted from differences in mRNA amounts or in mRNA decay, we analyzed the amounts of TNF-a mRNA in LPS-stimulated TTP^{-/-} and control BMDMs with or without pretreatment with IL-10. In WT cells, IL-10 caused a reduction of TNF-a mRNA to 40% of the amount present in cells treated with LPS alone, whereas in TTP^{-/-} cells IL-10 caused a reduction to only 80% of the level in cells treated with LPS alone (Fig. 2*C*). In these experiments, TNF-a mRNA was measured after 2 h of LPS treatment since the amount of TNF-a mRNA peaks at this time point (Ref. 13 and data not shown). To further illustrate the role of TTP in IL-10-mediated decrease of TNF-a mRNA, we analyzed the rate of TNF-a mRNA decay in LPS-stimulated TTP^{-/-} and WT BMDMs with or without IL-10 pretreatment. Transcription was stopped after 3 h of LPS stimulation by addition of actinomycin D, and the degradation of TNF-a mRNA was followed in 15-min intervals for a total of 45 min after imposing the transcriptional stop (Fig. 3*A*). In LPS-treated control BMDMs, the decay rate of TNF-a mRNA was increased 2.5-fold by IL-10 treatment (half-life $t_{1/2}$ without IL-10 = 32 min; $t_{1/2}$ with IL-10 = 13 min). In LPS-treated TTP^{-/-} BM-DMs, the residual TNF-a mRNA decayed with a 2.5-fold longer half-life ($t_{[1/2]} = 82$ min) compared with WT. This difference is similar to the one reported previously (35). Importantly, IL-10 treatment of LPS-stimulated

TTP* cells did not increase the decay rate and the remnant mRNA levels were comparable to those in cells treated with LPS alone. LPS-stimulated macrophages produced endogenous IL-10 that is known to mask to some extent the effect of added IL-10 (see Ref. 18). Since TTP was recently

FIGURE 2. TTP is required for full IL-10-mediated inhibition of TNF-a

A Reduction of TNFa cytokine by IL-10 (o/n)

B Reduction of TNFa cytokine by IL-10

C Reduction of TNFa mRNA by IL-10
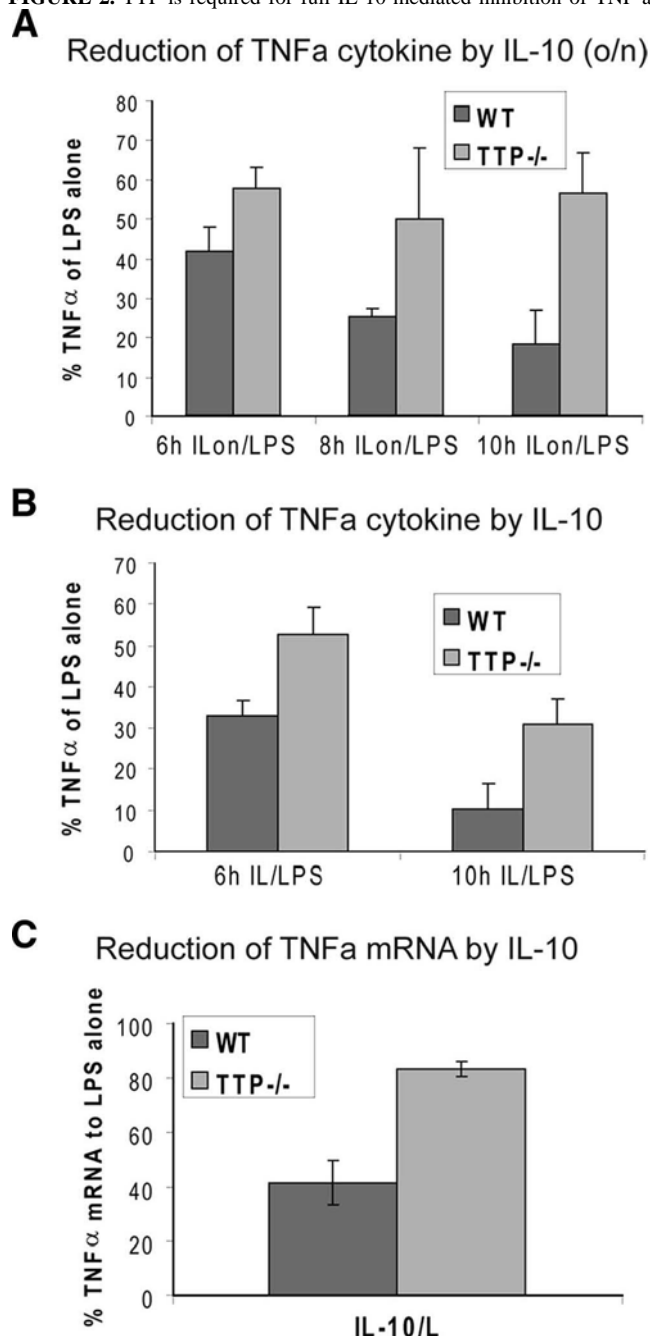
production. *A*, Reduction of LPS-induced TNF-a cytokine production in cells pretreated with IL-10. BMDMs from WT and TTP^{-/-} mice were treated with LPS or pretreated overnight (o/n) with IL-10 followed by stimulation with LPS (ILon/LPS) for indicated time points. Supernatants were collected and analyzed for TNF-a cytokine levels by ELISA. Reduction of TNF-a cytokine levels by IL-10 pretreatment (IL-10 o/n) relative (in percent) to LPS-alone treatment (100%) is depicted. SDs (*n* = 4) are indicated. *B*, Effect of simultaneous treatment with IL-10 and LPS on TNF-a cytokine production performed as described in *A*. Relative amounts of TNF-a cytokine secreted by LPS-treated WT and TTP^{-/-} BMDMs compared with cells simultaneously treated with IL-10/LPS are shown. SDs (*n* = 3) are indicated. *C*, Reduction of LPS-induced TNF-a mRNA in cells pretreated with IL-10. WT-BMDMs and TTP-deficient BMDMs (TTP^{-/-}) were treated 2 h with LPS or pretreated overnight with IL-10 followed by LPS addition (IL-10/L) and analyzed for expression of TNF-a by qRT-PCR, normalized to HPRT mRNA. Shown is the reduction of

TNF-a mRNA levels after IL-10/LPS treatment in relation to the sample treated with LPS alone. SDs (*n* = 3) are indicated.

shown to target IL-10 mRNA for degradation (36), we asked whether TTP^{-/-} BMDMs produce more IL-10 after stimulation with LPS. Cytokine measurement revealed that TTP-deficient cells secrete 2-to 3-fold more IL-10 than the WT cells (supplemental Fig. S1[5]). To assess the contribution of endogenous IL-10 to the IL-10-mediated TNF-a mRNA decay, we compared the TNF-a mRNA levels and decay rates in IL-10^{-/-} and WT cells. IL-10^{-/-} BMDMs expressed 2-fold more TNF-a than WT cells (Fig. 3*B*). Importantly, the reduction of TNF-a mRNA by exogenous IL-10 was more pronounced in IL-10^{-/-} cells compared with WT cells. The decay rate of TNF-a mRNA was not affected by IL-10 treatment of WT cells stimulated for 1 or 2 h with LPS (Fig. 3*C*). However, IL-10 accelerated the decay rate in IL-10^{-/-} cells treated for 2 h with LPS, but not for 1 h (Fig. 3*D*). Therefore, endogenous IL-10 can mask to a certain extent the effect of exogenous IL-10 on the mRNA decay. In addition, the IL-10-mediated increase in mRNA decay rate becomes more apparent at later time points of LPS treatment, consistent with the need for new protein synthesis (e.g., TTP). Note that the duration of LPS treatment in Fig. 3*A* was 3 h and that the differences in IL-10-imposed inhibition of TNF-a production in TTP^{-/-} vs WT cells increased with time of LPS treatment (Fig. 2, *A* and *B*).

To further substantiate the role of TTP in the anti-inflammatory effects of IL-10, we measured the IL-10-mediated reduction of IL-1a protein and mRNA in TTP^{-/-} and WT cells (Fig. 3, *E* and *F*). Efficient LPS-stimulated production of IL-1a, a known IL-10 target (13), depends on a second stimulus, such as ATP, that activates the IL-1-processing function of the inflammasome (37). Although IL-1a is not a direct substrate of caspase 1, production of mature IL-1a has been shown to be inflammasome/caspase 1 dependent (37). BMDMs from WT and TTP^{-/-} animals were stimulated with LPS (10 h) and ATP (1 h before the collection of supernatants) in the presence or absence of IL-10. IL-10 caused a decrease of IL-1a protein to 20% of LPS plus ATP-treated WT cells, whereas in TTP^{-/-} cells the IL-1a production was reduced only to 60% of the LPS plus ATP-treated samples (Fig. 3*E*). Similar differences between WT and TTP^{-/-} cells were determined also for the IL-10-mediated decrease in IL-1a mRNA (Fig. 3*F*).

To rule out that the absence of TTP affected activation of Stat3 by IL-10 that might result in reduced IL-10 responsiveness of TTP^{-/-} cells, the IL-10-induced tyrosine phosphorylation of Stat3 was determined in LPS-stimulated TTP^{-/-} and WT BMDMs in the presence or absence of IL-10. The level of tyrosine-phosphorylated Stat3 was under all conditions comparable in both genotypes (supplemental Fig. S2*A*). In addition, the stimulatory effect of LPS was similar in TTP^{-/-} and WT cells as judged by the activation of p38 MAPK (supplemental Fig. S2*B*). Thus, a different activation of the critical proinflammatory (p38 MAPK) and anti-inflammatory (Stat3) components in the WT and TTP^{-/-} cells could be excluded as a reason for the observed differences in IL-10 responses.

These data establish that TTP plays an important role in IL-10-mediated down-regulation of two critical inflammatory cytokines (TNF-a and IL-1a).

TTP function in IL-10 responses depends on IL-10-mediated reduction of p38 MAPK activity at later phase of inflammation

45

IL-10 and IL-6 are both known to activate Stat3 yet only IL-10 exhibits anti-inflammatory properties (38–40). To examine whether and to what extent IL-6 was able to stimulate TTP expression, BMDMs were treated with LPS with or without IL-6.

[5]The online version of this article contains supplemental material.
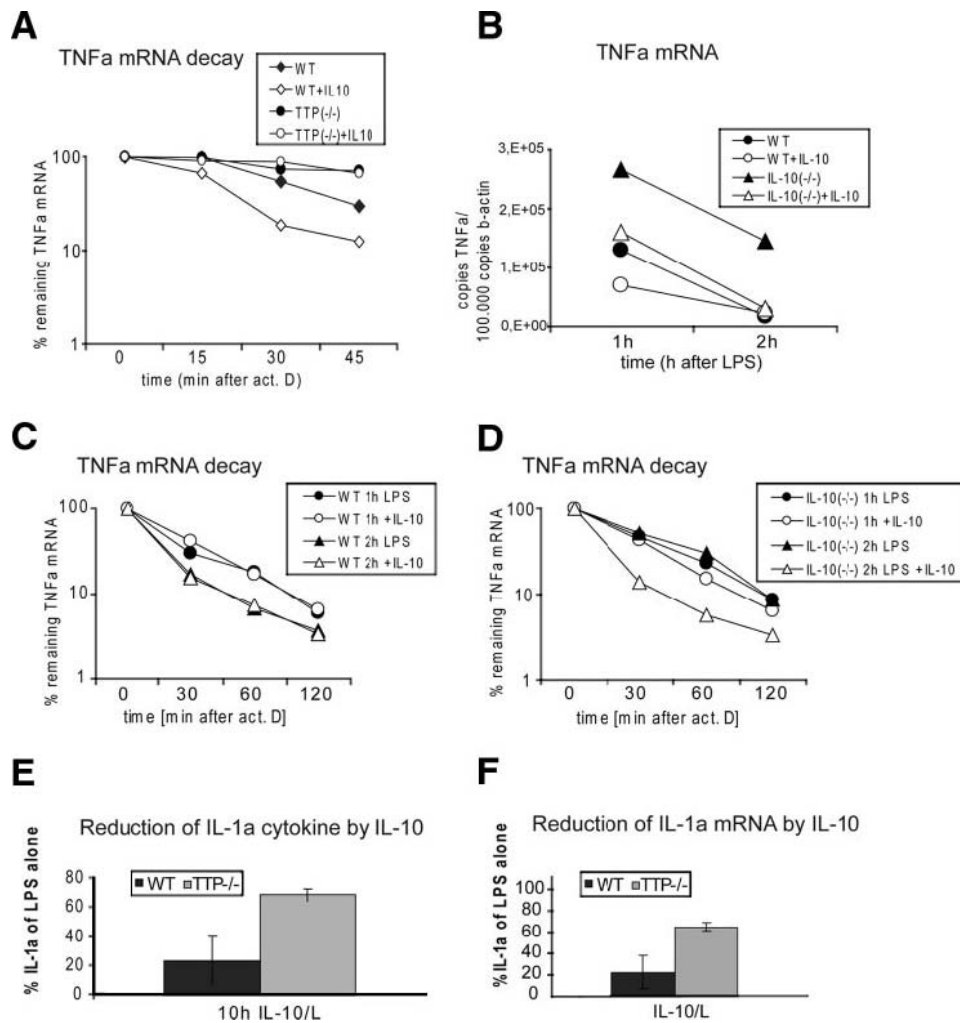
FIGURE 3. TTP is required for IL-10-mediated acceleration of TNF-a mRNA decay and for full IL-10-dependent reduction of IL-1a. *A*, IL-10-induced changes in decay of TNF-a mRNA. WT-BMDMs and TTP-deficient BMDMs (TTP[*]) were pretreated with IL-10 overnight and stimulated for 3 h with LPS followed by addition of actinomycin D (act D; 5 /g/ml) to stop transcription. After the indicated time points, TNF-a mRNA was quantified using qRT-PCR. Values were normalized against the housekeeping gene HPRT. Remnant TNF-a mRNA in percentage of the amount at the time point 0 of actinomycin D treatment is depicted. SDs ($n = 3$) are indicated. *B*, Effects of endogenous IL-10 on TNF-a mRNA induction in LPS-or LPS/IL-10-treated BMDMs. BMDMs derived from WT or IL-10[*] animals were treated for 1 or 2 h with LPS in the presence or absence of IL-10. The amount of TNF-a mRNA in these cells was determined by qRT-PCR. *C* and *D*, TNF-a mRNA decay in WT (*C*) and IL-10[*] (*D*) BMDMs. BMDMs were treated for 1 or 2 h with LPS in the presence or absence of IL-10. Thereafter, the transcription was stopped by actinomycin D and the remaining TNF-a mRNA was determined at the indicated times by qRT-PCR. Remnant TNF-a mRNA in percentage of the amount at the time point 0 of actinomycin D treatment is depicted. *E*, Reduction of IL-1a cytokine by IL-10. BMDMs from WT and TTP[*] mice were treated with LPS for 10 h in the presence or absence of IL-10. ATP was added 1 h before the collection of supernatants. Supernatants were collected and analyzed for IL-1a cytokine levels by ELISA. Reduction of IL-1a cytokine levels by IL-10 pretreatment relative (in percent) to LPS alone treatment (100%) is depicted. SDs are indicated, $n = 3$. *F*, Reduction of IL-1a mRNA by IL-10. BMDMs from WT and TTP[*] mice were treated with LPS for2hinthe presence or absence of IL-10. IL-1a expression was analyzed by qRT-PCR. Reduction of IL-1a mRNA by IL-10 treatment relative (in percent) to LPS alone treatment (100%) is depicted.

Interestingly, IL-6 was able to increase TTP expression in LPStreated macrophages almost to the same extent as IL-10 (Fig. 4*A*). Yet, consistent with the known properties of IL-6, IL-6 was not able to inhibit TNF-a (Fig. 4*B*) and IL-1a (Fig. 4*C*) in either WT or TTP[*] BMDMs. These data also implicate that the up-regulation of TTP expression by IL-10 cannot solely explain the role of TTP in the anti-inflammatory effects of this cytokine. We speculated that the role of TTP in IL-10 responses might be explained by an IL-10-dependent increase in TTP activity. TTP function is known to be negatively regulated by p38 MAPK and its downstream kinase MK2 (41). IL-10 has been reported to modestly inhibit p38 MAPK in the later phases of LPS treatment (18). The reduction of p38 MAPK activity is caused by the IL-10-mediated up-regulation of the dual-specificity phosphatase DUSP1 (Ref. 18 and Fig. 4*F*). We reasoned that such a reduction in p38 MAPK could relieve the p38 MAPK-dependent inhibition of TTP, thereby increasing the ability of TTP to down-regulate its target mRNAs. To investigate whether IL-6 was also able to reduce p38 MAPK activity, BMDMs were stimulated with LPS alone or along with either IL-10 or IL-6 and p38 MAPK activity was monitored after 2, 4, and 6 h. Treatment of LPS-stimulated cells with IL-10 caused a modest (3-fold) but consistent inhibition of p38 MAPK at 2, 4, and 6 h compared with the samples treated with LPS alone (Fig. 4*D*). To better document the IL-10 effect on p38 MAPK phosphorylation, the complete time course of IL-6-and IL-10-treated samples was run on a single gel

(supplemental Fig. S3*A*). The LPS-induced activation of p38 MAPK at an early time point (30 min) was not affected by IL-10 cotreatment (Fig. 4*E*). Importantly,

FIGURE 4. Effects of IL-6 on TTP expression, TNF-a and IL-1a production, and p38 MAPK activation in LPS-treated BMDMs. *A*, IL-6 and IL-10 increase
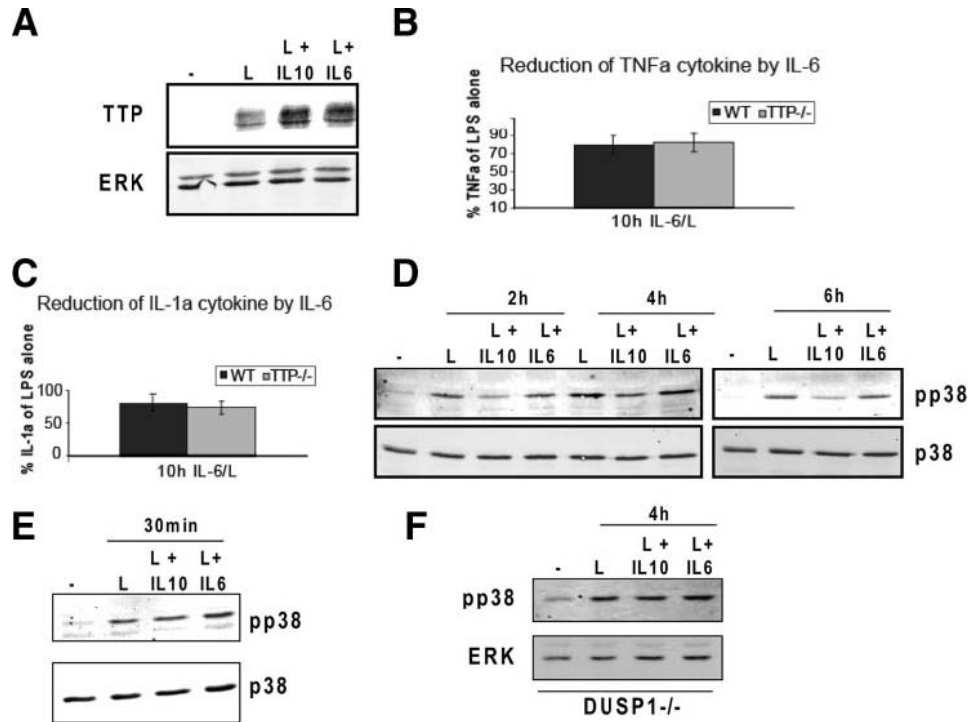
TTP expression to similar levels in LPS-treated BMDMs. BMDMs were stimulated for 2 h with LPS alone or along with IL-10 or IL-6, and whole cell extracts were prepared. Expression of TTP was analyzed by Western blotting. panERK Ab was used for loading control. *B* and *C*, IL-6 does not reduce TNF-a production (*B*) or IL-1a (*C*) production in LPS-treated TTP$^{-/-}$ and control WT BMDMs. WT and TTP$^{-/-}$ BMDMs were stimulated for 10 h with LPS with or without cotreatment with IL-6. Amounts of TNF-a and IL-1a in supernatants were determined by ELISA. SDs of three representative experiments ($n = 3$) are indicated. *D*, IL-10 but not IL-6 decreases p38 MAPK activity in LPS-treated BMDMs. Whole cell extracts of BMDMs treated for 2, 4, and 6 h with LPS alone or cotreated with IL-10 or IL-6 were analyzed for activation of p38 MAPK by Western blotting using Ab to activated p38 MAPK (pp38). Ab to total p38 MAPK (p38) was used for loading control. *E*, p38 MAPK is not inhibited by IL-10 or IL-6 after 30 min of treatment. BMDMs were treated for 30 min with LPS with or without cotreatment with IL-10 or IL-6. p38 MAPK activation was determined as in *D*. *F*, IL-10 no longer reduces p38 MAPK phosphorylation in DUSP1$^{-/-}$ BMDMs. DUSP1$^{-/-}$ BMDMs were treated for 4 h with LPS alone, LPS + IL-10 or LPS + IL-6, and the activation of p38 MAPK was examined as in *D*. Figures are representative of at least three experiments.

p38 MAPK activity was not reduced by treatment with IL-6 at any time point examined (Fig. 4, *D* and E, and supplemental Fig. S3*A*). These findings are in agreement with the induction of mRNA for the MAPK phosphatase DUSP1 by IL-10 but not IL-6 in LPStreated macrophages (18). To further support the role of DUSP1 in the IL-10-mediated effect on p38 MAPK activity, we examined p38 MAPK phosphorylation in DUSP1$^{-/-}$ BMDMs treated with LPS alone or along with either IL-10 or IL-6 for 4 h. In DUSP1$^{-/-}$ cells, IL-10 was no longer able to reduce p38 MAPK phosphorylation after treatment (Fig. 4*F*). Consistent with the IL-10-mediated decrease in p38 MAPK phosphorylation, at the 4 h-time point, the induction of DUSP1 by IL-10 plus LPS compared with LPS alone was more apparent than after a shorter treatment (1 h; supplemental Fig. S3*B*). The different effect of IL-10 and IL-6 on p38 MAPK is in agreement with the anti-inflammatory properties that are exhibited by IL-10 but not IL-6. The difference between IL-10 and IL-6 with regard to their anti-inflammatory properties has been attributed to SOCS3 that, as part of the negative feedback loop, binds to the gp130 subunit of the IL-6 receptor but not to the IL-10 receptor (38 –40). Thus, SOCS3, a Stat3 target gene, is able to inhibit signaling elicited by IL-6 but not by IL-10. Consequently, IL-10 induces a prolonged Stat3 activation, whereas IL-6-mediated Stat3 activation is rapidly shut down. Consistently, in LPS-treated BMDMs IL-10 and IL-6 caused a comparable Stat3 activation after 30 min of cytokine treatment, whereas after 2 h Stat3 remained active only in cells stimulated with IL-10 but not IL-6 (supplemental Fig. 3*C*). These data suggest that a sustained Stat3 activation is needed for inhibition of p38 MAPK.

Although p38 MAPK is needed for TTP expression and protein stability (24, 25, 42), the kinase negatively regulates TTP activity at least at two levels. First, phosphorylation of TTP at Ser^{52} and Ser^{178} by MAPK-activated protein kinase kinase 2 (MK2), a kinase downstream of p38 MAPK, provides binding sites for 14-3-3 proteins that reduce the destabilizing activity of TTP (23, 43). Second, phosphorylation of TTP by MK2 was reported to negatively regulate its binding to AREs (25). To show that the IL-10-mediated decrease in p38 MAPK activity was able to change TTP properties in terms of its phosphorylation and binding to AREs, we analyzed the mobility of TTP in SDS-PAGE and binding of TTP to AREs in EMSA experiments. TTP appears in SDS-PAGE in the form of multiple bands that reflect various degree of predominantly p38 MAPK-dependent phosphorylation (24). To demonstrate p38 MAPK effects on TTP phosphorylation and binding to AREs, we first used an inducible expression of TTP in HeLa-Tet-off cells. This system allows manipulation of p38 MAPK activity without affecting the transcription of the TTP gene that is known to require p38 MAPK activity (27, 42). Stimulation of HeLa-Tet-off cells expressing TTP (i.e., without tetracycline) with anisomycin (a p38 MAPK agonist (44)) resulted in a more pronounced appearance of a slower migrating hyperphosphorylated TTP band, whereas the p38 MAPK inhibitor SB reduced the amount of the hyperphosphorylated TTP and also the total TTP level due to TTP protein destabilization (Fig. 5*A*). The analysis of

FIGURE 5. IL-10 reduces TTP phosphorylation and increases in vitro binding of TTP to ARE. *A* and *B*, HeLa-Tet-off cells were transiently transfected with
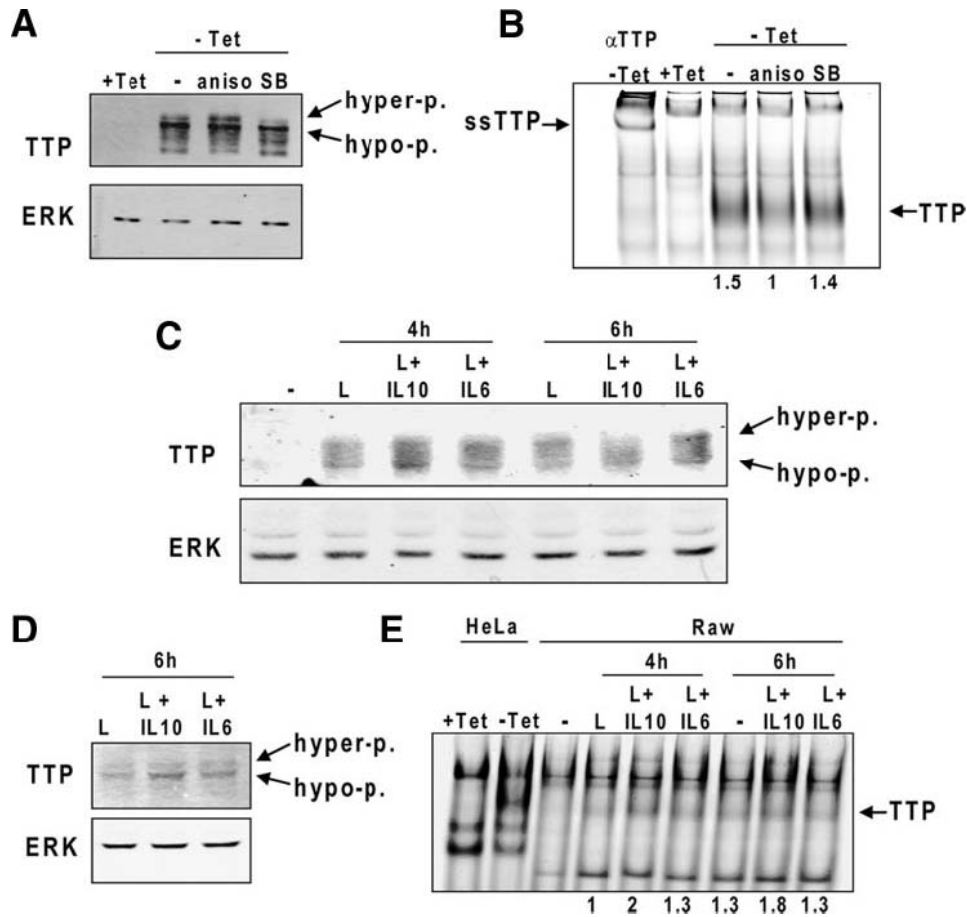
pTRE-TTPfl and equally split into four 6-cm dishes. In three dishes, the expression of TTP was allowed overnight in medium without tetracycline (-Tet), whereas in one dish the TTP expression was blocked by tetracycline (+Tet). The (-Tet) cells were treated for 60 min with anisomycin (aniso) or SB. Whole cell extracts were prepared and split into one part for Western blot analysis (*A*) and a second part for RNA EMSA (*B*). The position of hyperphosphorylated (hyper-p.) and hypophosphorylated (hypo-p.) TTP is marked in *A*. *B*, The TTP-ARE complexes (TTP) were identified by a supershift (ssTTP) using a TTP Ab (aTTP). The relative intensity of the TTP-ARE complexes (as indicated be the numbers 1.5, 1, and 1.4) was quantitated using the LI-COR Odyssey software (supplementary Fig. 4*A*). *C*, Whole cell extracts of BMDMs treated for 4 and 6 h with LPS alone or cotreated with IL-10 or IL-6 were analyzed for TTP expression and SDS-PAGE mobility by Western blotting using Ab to TTP. Equal protein loading was controlled by reprobing with an anti-ERK Ab. The position of hyperphosphorylated (hyper-p.) and hypophosphorylated (hypo-p.) TTP is marked. *D*, Whole cell extracts of RAW 264.7 treated for 6 h with LPS alone or cotreated with IL-10 or IL-6 were analyzed as in *C*. *E*, Whole cell extracts of RAW 264.7 cells treated for 4 or 6 h with LPS alone or cotreated with IL-10 or IL-6 were assayed for in vitro binding of TTP to TNF-a ARE using RNA EMSA. The relative intensity of the TTP-ARE complexes (as indicated by the numbers 1, 2, 1.3, 1.3, 1.8, and 1.3) was quantitated using the LI-COR Odyssey software (supplementary Fig. 4*B*). To control the position of the TTP-ARE complexes extracts from HeLa-Tet-off cells expressing TTP (-Tet) or without TTP expression (+Tet) were used. The data are representative of three independent experiments.

the same extracts in a RNA EMSA experiment revealed that anisomycin reduced binding of TTP to the TNF-a ARE by 50% (Fig. 5*B*), whereas inhibition of p38 MAPK resulted in a similar amount of ARE-bound TTP as in untreated cells (Fig. 5*B*) despite a reduced TTP protein level present in that sample (compare SB-labeled lanes in Fig. 5*A* and 5*B*). Consistent with the IL-10-mediated p38 MAPK inhibition, the treatment of BMDMs with LPS plus IL-10 resulted in a shift to less phosphorylated TTP bands in SDSPAGE if compared with cells treated with LPS alone or with LPS plus IL-6 (Fig. 5*C*). This shift to faster migrating TTP bands was more pronounced after6hof treatment. To address the IL-10 effect on TTP binding to AREs, we used the murine macrophage cell line RAW 264.7 since we were not able to detect TTP-ARE complexes in RNA EMSA experiments if BMDMs were used. LPS-stimulated RAW 264.7 cells express at least 3- to 5-fold more TTP than BMDMs (data not shown). Similar to BMDMs, LPS plus IL-10 treatment resulted in a more pronounced appearance of the hypophosphorylated TTP if compared with treatment with LPS alone or LPS plus IL-6 (Fig. 5*D*). Consistently, LPS plus IL-10 treatment caused an 50–80% increase in the formation of TTPARE complexes in RNA EMSA experiments compared with LPS alone or LPS plus IL-6 treatments (Fig. 5*E*). These data show that IL-10 decreases the phosphorylation of TTP and enhances the in vitro binding of TTP to TNF-a ARE in a manner similar to the pharmacological inhibition of p38 MAPK. These findings are in agreement with an increased TTP activity under conditions of reduced p38 MAPK activation as is the case in IL-10-treated cells. Interestingly, despite the reduced p38 MAPK activity and hence increased proteasome-mediated TTP degradation in IL-10-treated cells, the TTP protein levels were not diminished compared with LPS plus IL-6-treated cells (Fig. 5, *C* and *D*). We explain this observation by the sustained Stat3 activation and, hence, a strong Stat3-driven transcription of the TTP gene in IL-10-treated cells (supplemental Fig. 3*C*).

To test whether p38 MAPK activity protects mRNA from TTPmediated decay, we examined the stability of TNF-a and IL-1a

A

TNFa mRNA decay

Legend:
- ● WT
- ○ WT; SB
- ▲ TTP(-/-)
- △ TTP(-/-); SB

y-axis: % remaining TNFa mRNA (100, 10, 1)
x-axis: time (min after act. D) (0, 15, 30, 45)

B

IL-1a mRNA decay

Legend:
- ● WT
- ○ WT; SB
- ▲ TTP-/-
- △ TTP-/-; SB

y-axis: % remaining IL-1 mRNA (100, 10, 1)
x-axis: time (min after act. D) (0, 45, 90)
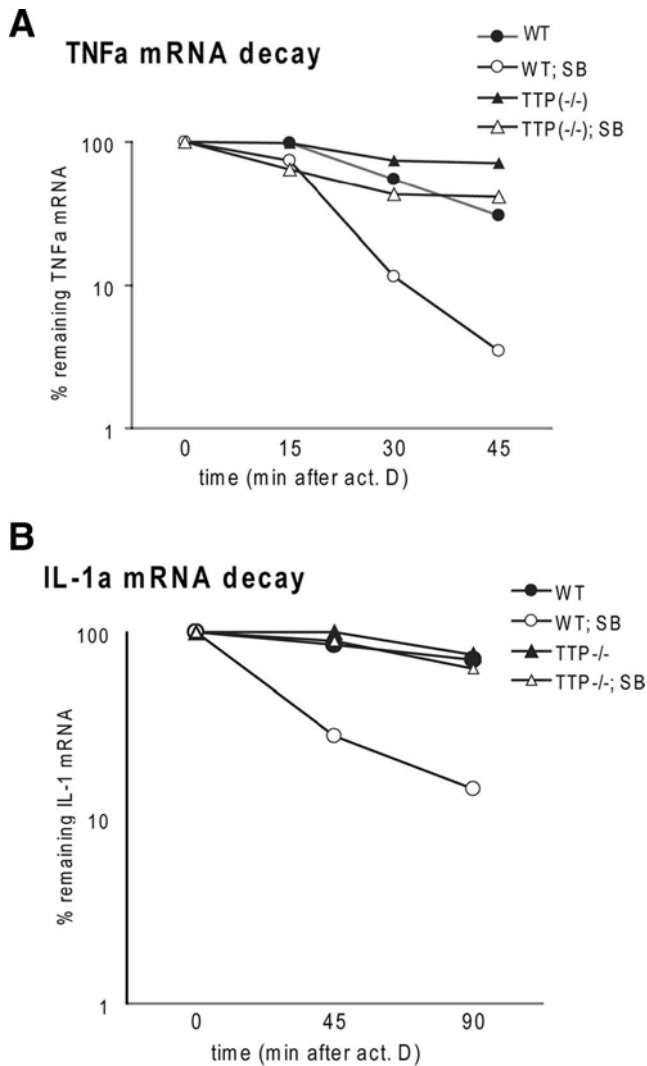
FIGURE 6. Effects of p38 MAPK inhibition on TTP-dependent re

duction of mRNA for TNF-a and IL-1a. *A* and *B*, WT and TTP BMDMs were treated with LPS for 2 h, followed by treatment with SB or solvent control. Actinomycin D was added simultaneously with SB. The decay rates of TNF-a (*A*) and IL-1a (*B*) were monitored by qRT-PCR for the times indicated. Remnant TNF-a or IL-1a mRNA in percentage of the amount at the time point 0 of actinomycin D treatment is depicted.

mRNAs in the presence of the p38 MAPK inhibitor SB in TTP and control WT BMDMs. Two hours after LPS stimulation, SB was added in combination with actinomycin D. p38 MAPK inhibition caused a 4-fold decrease of mRNA stability of TNF-a (TNF-a without SB: $t_{1/2}$=31 min; TNF-a with SB: $t_{1/2}$=8 min) and an 8-to 10-fold decrease in IL-1a mRNA stability (IL-1a without SB: $t_{1/2}$>2 h; IL-1a with SB: $t_{1/2}$=14 min; Fig. 6). In TTP cells, the inhibition of p38 MAPK caused only a modest (2-fold) decrease in mRNA stability of TNF-a mRNA (TNF-a without SB: $t_{1/2}$=80 min; TNF-a with SB: $t_{1/2}$=37 min with SB) and no detectable decrease of IL-1a mRNA stability (IL-1a without SB: $t_{1/2}$=>2 h; IL-1a with SB: $t_{1/2}$=>2 h). These data indicate that the augmentation of mRNA decay by inhibition of p38 MAPK is to a large part TTP dependent. The contribution of TTP to the effects of p38 MAPK inhibition depends on the nature of the target mRNA.

We conclude that the IL-10-mediated reduction of p38 MAPK activity increases TTP-dependent mRNA decay. The combined ef-
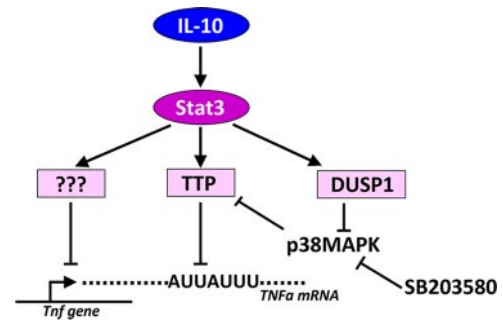
FIGURE 7. Model of IL-10-mediated anti-inflammatory effects. IL-10 activates the transcription factor Stat3 that drives the expression of at least three effector genes. The still unidentified repressors of transcription are depicted by question marks. The other effector is TTP that requires the activity of a third effector, the DUSP1 phosphatase, that reduces the activity of p38 MAPK, thereby increasing the TTP-destabilizing activity toward specific ARE-containing mRNAs. The activity of DUSP1 can be mimicked by, for example, the p38 MAPK inhibitor SB.

fect of IL-10 on p38 MAPK activity and TTP expression contributes to the anti-inflammatory properties of IL-10.

Discussion

This study provides evidence that the mRNA-destabilizing factor TTP plays an important role in anti-inflammatory effects of IL-10. BMDMs deficient in TTP show a strongly reduced antiinflammatory response to IL-10. Two cytokines, TNF-a and IL1a, were here demonstrated to be inhibited by IL-10 in a TTP-dependent manner. IL-10 appears to regulate TTP function in two ways (Fig. 7). First, IL-10 increases TTP expression in LPS-treated BMDMs. This augmented expression depends on Stat3, the key immediate effector of IL-10 effects. Second, IL-10 reduces at later time points the activity of p38 MAPK in LPS-treated BMDMs, hereby releasing TTP from the p38 MAPK-mediated inhibition. Since the increased expression of TTP is not sufficient to initiate an anti-inflammatory response (as demonstrated by IL-6-mediated up-regulation of TTP), we conclude that the TTP-dependent IL-10 effects can be best explained by the combination of higher TTP expression and reduction of p38 MAPK activity.

TTP is known for its mRNA-destabilizing activity most notably, but not exclusively, toward TNF-a mRNA via AREs in 3'UTR. Thus, the IL-10-mediated rise in TNF-a decay rate is consistent with the elevated TTP levels and activity. In addition to TNF-a, our data suggest that IL-1a is also a TTP target. The 3'UTR of the murine IL-1a (GenBank accession no. NM_010554; http://www. ncbi.nlm.nih.gov/GenBank/) contains three elements (UAUUUA UA, AUAUUUAU, and UAUUAUUUAU) with similar sequences as the nonameric canonical sequence (UUAUUUAUU) recognized by TTP (45, 46). IL-1a has so far not been described as TTP target despite of several recently published global screens for novel TTP targets (36, 47). However, these searches revealed that in such global screens important targets might be missed (e.g., TNF-a in the study of Stoecklin et al. (36)). In addition, the finding that TTP regulates also mRNAs with no obvious AREs in 3'UTR adds another degree of complexity to searches for TTP targets (47). The role of TTP in IL-10 responses is also in agreement with a study reporting IL-10-mediated ARE-dependent destabilization of CXCL1 mRNA (16). Importantly, in that study, the IL-10-induced mRNA decay was not detectable before 2 h of LPS/IL-10 treatment. This time point correlates well with the appearance of TTP

51

expression (42) and with our data showing that IL-10-mediated decay of TNF-a mRNA is not apparent before2hofLPS treatment.

TTP-deficient cells are known to produce 2-to 3-fold more TNF-a (both mRNA and cytokine) than WT cells (26, 48). At the same time, IL-10 mRNA was shown to be targeted by TTP for degradation (36) and we found that the TTP-deficient BMDMs produce more IL-10 cytokine (supplemental Fig. S1). Thus, TTP cells produce more of both the proinflammatory TNF-a and the anti-inflammatory IL-10. Yet, the TTP cells still respond to IL-10 treatment (by e.g., Stat3 activation) and LPS treatment (by e.g., p38 MAPK activation) similarly as the WT cells (Fig. 4). We conclude that despite the 2-to 3-fold higher production of pro-and anti-inflammatory cytokines the TTP-deficient cells display comparable immediate-early response to pro-(LPS) or antiinflammatory (IL-10) stimuli as WT cells.

We were not able to detect any differences in the TTP expression or p38 MAPK activity, the two key factors influencing the TTP function, when we compared the two protocols for IL-10 treatment. Thus, the higher absolute contribution of TTP to IL-10 responses in the pretreatment protocol suggests that IL-10 induces a cofactor of TTP during the pretreatment period. TTP serves as an adaptor protein linking mRNA to the mRNA processing and degradation machinery located in stress granules and processing bodies (21, 22). Some of the components of these complexes may be up-regulated by IL-10 during the pretreatment phase to enhance TTP function. Alternatively, IL-10-activated Stat3 may increase transcription of micro-RNAs such as micro-R16 that was shown to assist TTP in degradation of ARE-containing mRNAs (49). The influence of the experimental protocol on the IL-10 effects may also partially explain the discrepancy between our study and the study of Kontoyiannis et al. (14) who found no evidence for a role of TTP in IL-10 responses in the simultaneous treatment protocol. Instead, they proposed a rapid (within 15 min of IL-10 treatment) inhibition of p38 MAPK as the main mechanism of IL-10 action. We did not detect any inhibition of p38 MAPK activity by IL-10 at early time points regardless of applied protocol for IL-10 treatment (supplemental Fig. S2, *A* and *B*). These data are in agreement with several other studies showing no effect of IL-10 on p38 MAPK activity at early time points (2, 12, 50, 51). In a kinetics analysis of p38 MAPK activity, IL-10 was found t

o exhibit a modest inhibitory effect on p38 MAPK activity at later time points (after3hofLPS plus IL-10 treatment) (18). The IL-10-mediated inhibition of p38 MAPK correlated with the induction of the dualspecificity phosphatase DUSP1, a MAPK phosphatase (18). We observed a similar reduction in p38 MAPK phosphorylation in terms of both, the magnitude and kinetics, and found that DUSP1 was required for this effect. The inhibition of p38 MAPK was caused specifically by IL-10 but not by IL-6 and correlated with the ability of IL-10 (but not IL-6) to induce sustained Stat3 activation. Consistently, IL-10 but not IL-6 was reported to increase expression of DUSP1 in LPS-treated macrophages (18). DUSP1 function as a critical p38 MAPK-inactivating enzyme provides the most likely explanation for the susceptibility of DUSP1^{-/-} mice to LPS-mediated toxic shock (52, 53). We speculate that the inhibition of the proinflammatory p38 MAPK by IL-10 at the later stages of macrophage stimulation is a key factor in immune homeostasis since p38 MAPK influences inflammation-related transcription, RNA stability, translation, as well as secretion. To mimic the inhibition of p38 MAPK by IL-10 at the late phase of stimulation, we used the p38 MAPK inhibitor SB and examined the effect of p38 MAPK on the TTP-dependent decrease of target mRNA molecules. Interestingly, whereas in the case of TNF-a a different decay rate (i.e., different decay rate in TTP^{+/+} and TTP^{-/-} cells) was observed also without p38 MAPK inhibition, for IL-1a mRNA the TTP-dependent decay was detectable only if p38 MAPK was inhibited (Fig. 5). A similar

requirement for p38 MAPK inhibition has been recently described also for the TTP target CXCL1 (KC) mRNA (54). These findings indicate that the p38 MAPK-mediated control of TTP activity has a differential impact on target mRNAs. Although the TTP-dependent decay of some mRNAs (e.g., TNF-a) proceeds in the presence of p38 MAPK activity, the degradation of other mRNAs (e.g., IL-1a and CXCL1) is strongly dependent on the kinase inhibition. This mechanism may play an important role in the specificity of TTPmediated RNA decay: depending on the activation status of p38 MAPK or other kinases implicated in regulation of TTP activity (e.g., ERK of MK2), TTP would discriminate between various targets. The critical role that p38 MAPK plays in TTP-mediated RNA decay also suggests that the time point that is taken to determine RNA stability has a decisive effect on the outcome of the assay. The activation/inactivation profile of p38 MAPK is likely to vary between different experimental settings (e.g., amount and quality of LPS, the use of primary or immortalized cells, the origin of primary cells such as bone marrow or peritoneum) so that this aspect may also contribute to the variability of published data. For example, we did not observe an IL-10-mediated increase in TNF-a mRNA decay in peritoneal-derived macrophages.

Suppression of inflammatory responses by IL-10 is one of the key features in immune homeostasis. Despite many years of research, the question of how a single cytokine can specifically inhibit various inflammatory reactions with such a high efficiency remains unresolved. Recent studies suggest that known as well as yet unknown IL-10 effectors interfere on different levels and by different mechanisms with the intracellular inflammatory net-works. This multitasking system employed by IL-10 is likely to be essential for the efficiency and specificity of the anti-inflammatory properties of IL-10. For example, the efficient and dominant inhibition of *Tnf* gene transcription by IL-10 still requires the remaining TNF-a mRNA to be removed from the system, i.e., by TTP. Although the primary IL-10-elicited signaling events that involve the IL-10 receptor, Jak1 and Tyk2 kinases, as well as the transcription factor Stat3, are to a large part common to all cell types, the more complex effects downstream of Stat3 may be cell type dependent. Thus, the function and activity of the Stat3-induced IL-10 effectors may be regulated by the environment within the particular cell type, hereby helping to explain the still incoherent and sometimes contradictory studies of the anti-inflammatory effects of IL-10.

Acknowledgments

Disclosures

The authors have no financial conflict of interest.

References

1. Fiorentino, D. F., M. W. Bond, and T. R. Mosmann. 1989. Two types of mouse T helper cell: IV. Th2 clones secrete a factor that inhibits cytokine production by Th1 clones. *J. Exp. Med.* 170: 2081–2095.
2. Williams, L. M., G. Ricchetti, U. Sarma, T. Smallie, and B. M. Foxwell. 2004. Interleukin-10 suppression of myeloid cell activation–a continuing puzzle. *Immunology* 113: 281–292.
3. Kuhn, R., J. Lohler, D. Rennick, K. Rajewsky, and W. Muller. 1993. Interleukin-10-deficient mice develop chronic enterocolitis. *Cell* 75: 263–274.
4. Berg, D. J., R. Kuhn, K. Rajewsky, W. Muller, S. Menon, N. Davidson, G. Grunig, and D. Rennick. 1995. Interleukin-10 is a central regulator of the response to LPS in murine models of endotoxic shock and the Shwartzman reaction but not endotoxin tolerance. *J. Clin. Invest.* 96: 2339–2347.
5. Roers, A., L. Siewe, E. Strittmatter, M. Deckert, D. Schluter, W. Stenzel, A. D. Gruber, T. Krieg, K. Rajewsky, and W. Muller. 2004. T cell-specific inactivation of the interleukin 10 gene in mice results in enhanced T cell responses but normal innate responses to lipopolysaccharide or skin irritation. *J. Exp. Med.* 200: 1289–1297.

6. Siewe, L., M. Bollati-Fogolin, C. Wickenhauser, T. Krieg, W. Muller, and A. Roers. 2006. Interleukin-10 derived from macrophages and/or neutrophils regulates the inflammatory response to LPS but not the response to CpG DNA. *Eur. J. Immunol.* 36: 3248–3255.

7. Takeda, K., B. E. Clausen, T. Kaisho, T. Tsujimura, N. Terada, I. Forster, and S. Akira. 1999. Enhanced Th1 activity and development of chronic enterocolitis in mice devoid of Stat3 in macrophages and neutrophils. *Immunity* 10: 39 – 49.

8. Lang, R., D. Patel, J. J. Morris, R. L. Rutschman, and P. J. Murray. 2002. Shaping gene expression in activated and resting primary macrophages by IL-10. *J. Immunol.* 169: 2253–2263.

9. Williams, L., L. Bradley, A. Smith, and B. Foxwell. 2004. Signal transducer and activator of transcription 3 is the dominant mediator of the anti-inflammatory effects of IL-10 in human macrophages. *J. Immunol.* 172: 567–576.

10. Maritano, D., M. L. Sugrue, S. Tininini, S. Dewilde, B. Strobl, X. Fu, V. Murray-Tait, R. Chiarle, and V. Poli. 2004. The STAT3 isoforms a and ß have unique and specific functions. *Nat. Immunol.* 5: 401–409.

11. Williams, L. M., U. Sarma, K. Willets, T. Smallie, F. Brennan, and B. M. Foxwell. 2007. Expression of constitutively active STAT3 can replicate the cytokine-suppressive activity of interleukin-10 in human primary macrophages. *J. Biol. Chem.* 282: 6965–6975.

12. Denys, A., I. A. Udalova, C. Smith, L. M. Williams, C. J. Ciesielski, J. Campbell, C. Andrews, D. Kwaitkowski, and B. M. Foxwell. 2002. Evidence for a dual mechanism for IL-10 suppression of TNF-a production that does not involve inhibition of p38 mitogen-activated protein kinase or NF-KB in primary human macrophages. *J. Immunol.* 168: 4837–4845.

13. Murray, P. J. 2005. The primary mechanism of the IL-10-regulated antiinflammatory response is to selectively inhibit transcription. *Proc. Natl. Acad. Sci. USA* 102: 8686 –8691.

14. Kontoyiannis, D., A. Kotlyarov, E. Carballo, L. Alexopoulou, P. J. Blackshear, M. Gaestel, R. Davis, R. Flavell, and G. Kollias. 2001. Interleukin-10 targets p38 MAPK to modulate ARE-dependent TNF mRNA translation and limit intestinal pathology. *EMBO J.* 20: 3760–3770.

15. Rajasingh, J., E. Bord, C. Luedemann, J. Asai, H. Hamada, T. Thorne, G. Qin, D. Goukassian, Y. Zhu, D. W. Losordo, and R. Kishore. 2006. IL-10-induced TNF-a mRNA destabilization is mediated via IL-10 suppression of p38 MAP kinase activation and inhibition of HuR expression. *FASEB J.* 20: 2112–2114.

16. Biswas, R., S. Datta, J. D. Gupta, M. Novotny, J. Tebo, and T. A. Hamilton. 2003. Regulation of chemokine mRNA stability by lipopolysaccharide and IL-10. *J. Immunol.* 170: 6202–6208.

17. Kuwata, H., Y. Watanabe, H. Miyoshi, M. Yamamoto, T. Kaisho, K. Takeda, and S. Akira. 2003. IL-10-inducible Bcl-3 negatively regulates LPS-induced TNF-aa production in macrophages. *Blood* 102: 4123–4129.

18. Hammer, M., J. Mages, H. Dietrich, F. Schmitz, F. Striebel, P. J. Murray, H. Wagner, and R. Lang. 2005. Control of dual-specificity phosphatase-1 expression in activated macrophages by IL-10. *Eur. J. Immunol.* 35: 2991–3001.

19. El Kasmi, K. C., A. M. Smith, L. Williams, G. Neale, A. Panopolous, S. S. Watowich, H. Hacker, B. M. Foxwell, and P. J. Murray. 2007. Cutting edge: a transcriptional repressor and corepressor Induced by the STAT3-regulated antiinflammatory signaling pathway. *J. Immunol.* 179: 7215–7219.

20. Carrick, D. M., W. S. Lai, and P. J. Blackshear. 2004. The tandem CCCH zinc finger protein tristetraprolin and its relevance to cytokine mRNA turnover and arthritis. *Arthritis Res. Ther.* 6: 248–264.

21. Kedersha, N., G. Stoecklin, M. Ayodele, P. Yacono, J. Lykke-Andersen, M. J. Fritzler, D. Scheuner, R. J. Kaufman, D. E. Golan, and P. Anderson. 2005. Stress granules and processing bodies are dynamically linked sites of mRNP remodeling. *J. Cell Biol.* 169: 871–884.

22. Franks, T. M., and J. Lykke-Andersen. 2007. TTP and BRF proteins nucleate processing body formation to silence mRNAs with AU-rich elements. *Genes Dev.* 21: 719–735.

23. Stoecklin, G., T. Stubbs, N. Kedersha, S. Wax, W. F. Rigby, T. K. Blackwell, and P. Anderson. 2004. MK2-induced tristetraprolin:14-3-3 complexes prevent stress granule association and ARE-mRNA decay. *EMBO J.* 23: 1313–1324.

24. Brook, M., C. R. Tchen, T. Santalucia, J. McIlrath, J. S. Arthur, J. Saklatvala, and A. R. Clark. 2006. Posttranslational regulation of tristetraprolin subcellular localization and protein stability by p38 mitogen-activated protein kinase and ex-tracellular signal-regulated kinase pathways. *Mol. Cell. Biol.* 26: 2408–2418.

25. Hitti, E., T. Iakovleva, M. Brook, S. Deppenmeier, A. D. Gruber, D. Radzioch, A. R. Clark, P. J. Blackshear, A. Kotlyarov, and M. Gaestel. 2006. Mitogenactivated protein kinase-activated protein kinase 2 regulates tumor necrosis factor mRNA stability and translation mainly by altering tristetraprolin expression, stability, and binding to adenine/uridine-rich element. *Mol. Cell. Biol.* 26: 2399–2407.

26. Taylor, G. A., E. Carballo, D. M. Lee, W. S. Lai, M. J. Thompson, D. D. Patel, D. I. Schenkman, G. S. Gilkeson, H. E. Broxmeyer, B. F. Haynes, and P. J. Blackshear. 1996. A pathogenetic role for TNFa in the syndrome of cachexia, arthritis, and autoimmunity resulting from tristetraprolin (TTP) deficiency. *Immunity* 4: 445–454.

27. Sauer, I., B. Schaljo, C. Vogl, I. Gattermeier, T. Kolbe, M. Muller, P. J. Blackshear, and P. Kovarik. 2006. Interferons limit inflammatory responses by induction of tristetraprolin. *Blood* 107: 4790 –4797.

28. Alonzi, T., D. Maritano, B. Gorgoni, G. Rizzuto, C. Libert, and V. Poli. 2001. Essential role of STAT3 in the control of the acute-phase response as revealed by inducible gene activation in the liver. *Mol. Cell. Biol.* 21: 1621–1632.

29. Kovarik, P., D. Stoiber, M. Novy, and T. Decker. 1998. Stat1 combines signals derived from IFN-y and LPS receptors during macrophage activation. [Published erratum appears in *1998 EMBO J.* 17: 4210]. *EMBO J.* 17: 3660–3668.

30. Morrison, T. B., J. J. Weis, and C. T. Wittwer. 1998. Quantification of low-copy transcripts by continuous SYBR Green I monitoring during amplification. *Bio-Techniques* 24: 954–958, 960, 962.

31. Suzuki, K., H. Nakajima, K. Ikeda, Y. Maezawa, A. Suto, H. Takatori, Y. Saito, and I. Iwamoto. 2003. IL-4-Stat6 signaling induces tristetraprolin expression and inhibits TNF-a production in mast cells. *J. Exp. Med.* 198: 1717–1727.

32. Ramsauer, K., I. Sadzak, A. Porras, A. Pilz, A. R. Nebreda, T. Decker, and P. Kovarik. 2002. p38 MAPK enhances STAT1-dependent transcription independently of Ser-727 phosphorylation. *Proc. Natl. Acad. Sci. USA* 99: 12859–12864.

33. Pesu, M., S. Aittomaki, K. Takaluoma, A. Lagerstedt, and O. Silvennoinen. 2002. p38 Mitogen-activated protein kinase regulates interleukin-4-induced gene expression by stimulating STAT6-mediated transcription. *J. Biol. Chem.* 277: 38254–38261.

34. Li, Y., A. Sassano, B. Majchrzak, D. K. Deb, D. E. Levy, M. Gaestel, A. R. Nebreda, E. N. Fish, and L. C. Platanias. 2004. Role of p38a Map kinase in type I interferon signaling. *J. Biol. Chem.* 279: 970–979.

35. Carballo, E., W. S. Lai, and P. J. Blackshear. 1998. Feedback inhibition of macrophage tumor necrosis factor-a production by tristetraprolin. *Science* 281: 1001–1005.

36. Stoecklin, G., S. A. Tenenbaum, T. Mayo, S. V. Chittur, A. D. George, T. E. Baroni, P. J. Blackshear, and P. Anderson. 2008. Genome-wide analysis identifies interleukin-10 mRNA as target of tristetraprolin. *J. Biol. Chem.* 283: 11689–11699.

37. Sutterwala, F. S., Y. Ogura, M. Szczepanik, M. Lara-Tejero, G. S. Lichtenberger, E. P. Grant, J. Bertin, A. J. Coyle, J. E. Galan, P. W. Askenase, and R. A. Flavell. 2006. Critical role for NALP3/CIAS1/cryopyrin in innate and adaptive immunity through its regulation of caspase-1. *Immunity* 24: 317–327.

38. Yasukawa, H., M. Ohishi, H. Mori, M. Murakami, T. Chinen, D. Aki, T. Hanada,

K. Takeda, S. Akira, M. Hoshijima, et al. 2003. IL-6 induces an antiinflammatory response in the absence of SOCS3 in macrophages. *Nat. Immunol.* 4: 551–556.

39. Lang, R., A. L. Pauleau, E. Parganas, Y. Takahashi, J. Mages, J. N. Ihle, R. Rutschman, and P. J. Murray. 2003. SOCS3 regulates the plasticity of gp130 signaling. *Nat. Immunol.* 4: 546–550.

40. Croker, B. A., D. L. Krebs, J. G. Zhang, S. Wormald, T. A. Willson, E. G. Stanley, L. Robb, C. J. Greenhalgh, I. Forster, B. E. Clausen, et al. 2003. SOCS3 negatively regulates IL-6 signaling in vivo. *Nat. Immunol.* 4: 540–545.

41. Sandler, H., and G. Stoecklin. 2008. Control of mRNA decay by phosphorylation of tristetraprolin. *Biochem. Soc. Trans.* 36: 491–496.

42. Mahtani, K. R., M. Brook, J. L. Dean, G. Sully, J. Saklatvala, and A. R. Clark. 2001. Mitogen-activated protein kinase p38 controls the expression and post-translational modification of tristetraprolin, a regulator of tumor necrosis factor a mRNA stability. *Mol. Cell. Biol.* 21: 6461–6469.

43. Johnson, B. A., J. R. Stehn, M. B. Yaffe, and T. K. Blackwell. 2002. Cytoplasmic localization of tristetraprolin involves 14-3-3-dependent and -independent mechanisms. *J. Biol. Chem.* 277: 18029–18036.

44. Fukunaga, R., and T. Hunter. 1997. MNK1, a new MAP kinase-activated protein kinase, isolated by a novel expression screening method for identifying protein kinase substrates. *EMBO J.* 16: 1921–1933.

45. Worthington, M. T., J. W. Pelo, M. A. Sachedina, J. L. Applegate, K. O. Arseneau, and T. T. Pizarro. 2002. RNA binding properties of the AU-rich element-binding recombinant Nup475/TIS11/tristetraprolin protein. *J. Biol. Chem.* 277: 48558 –48564.

46. Blackshear, P. J., W. S. Lai, E. A. Kennington, G. Brewer, G. M. Wilson, X. Guan, and P. Zhou. 2003. Characteristics of the interaction of a synthetic human tristetraprolin tandem zinc finger peptide with AU-rich element-containing RNA substrates. *J. Biol. Chem.* 278: 19947–19955.

47. Emmons, J., W. H. Townley-Tilson, K. M. Deleault, S. J. Skinner, R. H. Gross, M. L. Whitfield, and S. A. Brooks. 2008. Identification of TTP mRNA targets in human dendritic cells reveals TTP as a critical regulator of dendritic cell maturation. *RNA* 14: 888–902.

48. Lai, W. S., E. Carballo, J. R. Strum, E. A. Kennington, R. S. Phillips, and P. J. Blackshear. 1999. Evidence that tristetraprolin binds to AU-rich elements and promotes the deadenylation and destabilization of tumor necrosis factor a mRNA. *Mol. Cell. Biol.* 19: 4311–4323.

49. Jing, Q., S. Huang, S. Guth, T. Zarubin, A. Motoyama, J. Chen, F. Di Padova, S. C. Lin, H. Gram, and J. Han. 2005. Involvement of microRNA in AU-rich element-mediated mRNA instability. *Cell* 120: 623–634.

50. Donnelly, R. P., H. Dickensheets, and D. S. Finbloom. 1999. The interleukin-10 signal transduction pathway and regulation of gene expression in mononuclear phagocytes. *J. Interferon Cytokine Res.* 19: 563–573.

51. Murray, P. J. 2006. STAT3-mediated anti-inflammatory signalling. *Biochem. Soc. Trans.* 34: 1028–1031.

52. Abraham, S. M., T. Lawrence, A. Kleiman, P. Warden, M. Medghalchi, J. Tuckermann, J. Saklatvala, and A. R. Clark. 2006. Antiinflammatory effects of dexamethasone are partly dependent on induction of dual specificity phosphatase 1. *J. Exp. Med.* 203: 1883–1889.

53. Hammer, M., J. Mages, H. Dietrich, A. Servatius, N. Howells, A. C. Cato, and R. Lang. 2006. Dual specificity phosphatase 1 (DUSP1) regulates a subset of LPS-induced genes and protects mice from lethal endotoxin shock. *J. Exp. Med.* 203: 15–20.

54. Datta, S., R. Biswas, M. Novotny, P. G. Pavicic, Jr., T. Herjan, P. Mandal, and T. A. Hamilton. 2008. Tristetraprolin regulates CXCL1 (KC) mRNA stability. *J. Immunol.* 180: 2545–2552.

6.2 Manuscript: Qualitative and Temporal Control of mRNA Decay During Inflammatory Response is Governed by Tristetraprolin and p38 MAP Kinase

Manuscript submitted

Qualitative and temporal control of mRNA decay during inflammatory response is governed by tristetraprolin and p38 MAP kinase

Franz Kratochvill[a], Christian Machacek[a], Claus Vogl[b], Andreas R. Gruber[c], Harald Hartweger[a], Ivo Hofacker[c], Roland Lang[d], Pavel Kovarik[a1]

[a] Max F. Perutz Laboratories, Department of Microbiology, Immunobiology and Genetics, University of Vienna, A-1030 Vienna, Austria

[b] Institute of Animal Breeding and Genetics, University of Veterinary Medicine Vienna, A-1210 Vienna, Austria

[c] Department of Theoretical Chemistry, University of Vienna, A-1090 Vienna, Austria

[d] Institute of Clinical Microbiology, Immunology and Hygiene, University Hospital Erlangen, 91054 Erlangen, Germany

[1]To whom correspondence should be addressed: Pavel Kovarik, Max F. Perutz Laboratories, Department of Microbiology and Immunobiology, University of Vienna, Dr. Bohr-Gasse 9, A-1030 Vienna, Austria, phone +43 1 427754608, fax +43 1 42779546, E-mail: pavel.kovarik@univie.ac.at

Classification: Immunology

Abstract

Inflammatory diseases can result from uncontrolled immune responses that are, at the level of gene expression, significantly restrained by mRNA decay. However, the circuits regulating inflammation at the level of global mRNA decay, and how the specificity and timing of the elimination of different mRNAs is achieved are not known. Here we describe a relay of regulatory steps that orchestrate the timely removal of a large proportion of unstable inflammation-induced mRNAs in macrophages. Initially, the inflammation-activated p38 MAP kinase (MAPK) inhibits the mRNA-destabilizing function of the RNA-binding protein tristetraprolin (TTP). In this phase, mRNAs of only few genes are targeted by TTP for degradation. In contrast, at a low p38 MAPK activity that prevails during the resolution phase of inflammation TTP destabilized one third of inflammation-induced unstable mRNAs as illustrated by a genome-wide microarray-based analysis of mRNA decay. TTP itself is eliminated by the complete drop of p38 MAPK activity at the end of the inflammatory response. These findings reveal a self-regulatory mechanism that maintains the immune homeostasis by a temporally and qualitatively controlled mRNA decay.

Introduction

Inflammation is a rather stereotypical process that can be in most situations described by recruitment of innate immune cells to the site of inflammation and establishment of an inflammatory gene expression profile. A systematic comparison of reported high throughput gene expression studies revealed that the inflammatory expression profiles acquired upon stimulation of Toll-like receptors (TLRs) by pathogens or pathogens-derived products contain one large cluster of genes induced regardless of the TLR involved and the cell type used [152]. This common expression pattern represents a general inflammatory response signature. Several smaller clusters that are induced in addition to the common cluster are restricted to particular cell types and/or TLRs [152]. Sterile inflammation that is caused by e.g. tissue injury results from the release of inflammatory mediators, such as TNF and IL-1. These mediators establish a gene expression pattern that resembles the TLR-elicited general inflammatory response signature [2]. The inflammatory genes can be categorized by the kinetics of their induction into three groups [2]. The rate of mRNA decay was shown to play a critical role in the fast appearance and disappearance of the early inflammatory genes that also contain the highest number of AU-rich elements (AREs) in their 3′ untranslated regions (UTRs)[2]. This is in agreement with the prominent role of AREs in the recruitment of mRNA-stabilizing or -destabilizing proteins [15, 20, 153, 154]. One of the best studied mRNA-destabilizing proteins is tristetraprolin (TTP). TTP, encoded by the *Zfp36* gene (TTP, as a more common name, is used synonymously for both gene and protein throughout) was initially characterized as a key inflammation-inducible *Tnf* mRNA-destabilizing factor whose deficiency resulted in multiple chronic inflammatory syndromes in mice [76]. After binding to AREs, preferentially but not exclusively to a UUAUUUAUU nonamer, TTP initiates the assembly of the mRNA degradation machinery thereby causing elimination of the bound mRNAs [21, 27, 155-157].

Because of their functions as sensors and effectors of inflammation, macrophages are often used to study inflammatory gene expression patterns. Macrophages stimulated with TLR

ligands exhibit highly dynamic gene expression profiles in terms of both the magnitude and timing. At the level of gene transcription, this dynamic behavior is brought about by a network of positive and negative feedback mechanisms [5, 158]. The transcription factors NF-κB, C/EBPδ and ATF3 were shown to act as critical components of a regulatory circuit that determines the timing and duration of global expression changes. Another important broad range mechanism of controlling the inflammatory response employs mRNA stability [2]. The circuit regulating this key process is as yet unknown. The requirement for TTP in the IL-10-mediated inhibition of Tnf production [30] raised the question whether TTP is more generally involved in the removal of mRNAs encoding inflammation mediators, and if yes, how the specificity and timing of the elimination of different mRNAs is achieved. In this study we identify TTP as a non-redundant component of a negative regulatory loop that targets one third of intrinsically unstable inflammation-induced mRNAs for degradation. This negative feedback is driven by the dual function of p38 MAPK in the regulation of TTP activity. p38 MAPK is needed for TTP expression but it restrains the mRNA-destabilizing activity of TTP thereby preventing a premature degradation of many inflammatory mRNAs until the onset of the resolution phase of the inflammatory response.

Results

Genome-wide analysis of mRNA stability in LPS-stimulated WT and TTP$^{-/-}$ macrophages.

To address the regulatory mechanisms that govern the specificity and timing of the removal of inflammation-induced mRNAs, we examined the global effect of TTP on mRNA decay rates in LPS-stimulated macrophages. In addition to its function as a critical *Tnf* mRNA-destabilizing protein, TTP was found to destabilize several other mRNAs encoding e.g. GM-CSF (Csf2), IL-3, IL-2, Ier3, IL-1β, E47, IL-10, Cxcl1, Plk3 and IFN-γ in various cell systems [24-28, 31, 83, 159-162]. These findings suggested that TTP might be a more general mRNA-destabilizing factor than previously anticipated. However, three different large scale

screens did not support a more fundamental involvement of TTP in mRNA decay since only a limited number of previously unknown TTP targets were identified [23, 24, 27]. Importantly, these screens were not successful in the identification of one or more of the few already known TTP targets such as *Tnf*, the best characterized TTP target. To address the global role of TTP in mRNA decay, we decided to measure mRNA decay rates in LPS-treated bone marrow-derived macrophages (BMDMs) isolated from WT and TTP$^{-/-}$ mice. To increase the sensitivity of the mRNA decay profiling we pharmacologically inhibited the LPS-activated p38 MAPK (using SB203580, a specific p38 MAPK inhibitor [163]) at the time of transcriptional blockage by actinomycin D (act D). Although p38 MAPK is required for TTP expression and TTP protein stability, it simultaneously blocks the mRNA-destabilizing activity of TTP [72]. We therefore inhibited p38 MAPK that the differences in mRNA decay between WT and TTP$^{-/-}$ BMDMs would become more apparent. The pharmacological inhibition of p38 MAPK mimics an intrinsic inhibitory pathway that is driven by IL-10. IL-10 that starts to be produced by BMDMs after ~2-3 h of LPS treatment induces the expression of the phosphatase *Dusp1* that inactivates p38 MAPK [64]. The pharmacological inhibition of p38 MAPK has been successfully used by us and others to reveal an otherwise only poorly detectable TTP-mediated decay of several mRNAs ([28, 30, 164]). We employed this approach in a microarray-based analysis of mRNA decay. After 3 h of stimulation with LPS, BMDMs from WT and TTP$^{-/-}$ animals were treated with act D and SB203580, and the remnant mRNA levels were measured at 45 and 90 min thereafter. TTP protein was induced after 3 h of LPS treatment (Fig. S1*A*), and remained detectable at 90 min after the transcriptional block despite of a considerable degradation caused by the inhibition of p38 MAPK (Fig. S1*B*). After normalization, filtering, and statistical analysis of the microarray data, the probe set IDs of the remaining genes (9847 from total 28853 present on the chip) were classified according to two criteria: 1) mRNA decay significantly ($P < 0.05$) increased above the overall average of the dataset in WT cells, and 2) additionally, a significantly ($P < 0.05$) slower decay in TTP$^{-/-}$ compared to WT cells. Using these criteria mRNAs with P values below the 0.05 limit were selected (Table S1). In addition to P values, we also show the approximate half-lives of the

mRNAs (Tables 1 and S1). Nevertheless, it should be noted that the only criterion for classification of an mRNA as unstable or TTP-destabilized was the P value, but not the half-life. In addition, we analyzed the 3′ UTRs for the occurrence and frequency of the sequence AUUUA, which represents the most basic ARE [15]. For the 3′ UTR analysis, we took sequences downstream of the stop codon using the coding sequence (CDS) annotation from the GenBank (http://www.ncbi.nlm.nih.gov/GenBank/). Among the 9847 genes 1090 (10%) were found to be significantly unstable (Fig. S2 and Table S1), with the 25 most significantly unstable genes listed in the Table 1*A*. Out of these 1090 unstable mRNAs 309 (28%) displayed significantly decreased decay rates in TTP$^{-/-}$ cells (Fig. S2). The mRNAs that were destabilized by TTP contained most of the so far known TTP targets (Tables 1*B* and S1). The reported and well characterized targets that were not found in our screen are known to be expressed in other cell types than BMDMs, i.e. in T cells (*Il2*, *Ifng*), B cells (*E47*) or mast cells (*Il3*). Consistently, the expression of these genes was below the threshold (see Methods) in BMDMs. Several of the known TTP targets did not rank among the top 25 unstable mRNAs though they all displayed TTP-dependent decays with P values < 0.05 (Table 1*B*).

Out of 309 TTP-destabilized mRNAs 116 transcripts (38%) had no AREs in their 3′ UTRs (Fig. S2) confirming also other reports on ARE-free TTP targets [23, 24, 27]. In the analysis we defined the AREs as AUUUA pentamers present in the 3′ UTR. By such a low-stringency definition of an ARE, we aimed at finding an estimate for the number of mRNAs that are degraded in a fully ARE-independent way. This type of analysis revealed that an unexpectedly high percentage (55%) of ARE-free mRNAs could be classified as unstable.

Analysis of TTP-mediated decay of *Cxcl2*, *Il6*, and *IL1a* mRNAs.

The increased mRNA stability in TTP$^{-/-}$ BMDMs could be also explained by an indirect involvement of TTP, e.g. by an mRNA-stabilizing protein that may be more abundant in TTP$^{-/-}$ cells. Thus, several criteria beyond the TTP-dependent decay must be met for an mRNA to be classified as a TTP target [24, 27]. We selected the mRNAs of *Il1a*, *Il6*, and *Cxcl2*

(GenBank IDs: NM_010554, NM_031168 and NM_009140, respectively) to examine the direct role of TTP in their decay. The P values for TTP-mediated decays and the half-lives of these mRNAs ranged from being strongly (*Cxcl2*) to modestly (*IL1a* and *IL6*) dependent on TTP (Table 1*B*). The 3´ UTRs of all three mRNAs contained several AUUUA pentamers and at least one UAUUUAU heptamer (Fig. S3*A*), the core TTP binding site [24]. Only in *Cxcl2* the ideal TTP binding nonamers UUAUUUAUU were found. Accordingly, all three mRNAs were able to bind to TTP in BMDMs as shown by RNA immunoprecipitations (Fig. 1*A*). To prove that TTP conferred instability through the 3´ UTRs, and to exclude secondary effects of the general transcriptional block by act D (by e.g. inhibition of transcription of genes encoding labile RNases), we fused the 3´ UTRs of the chosen mRNAs to a tetracycline-regulated beta-globin reporter [25]. Hela Tet-Off cells were co-transfected with a TTP expression construct and the 3´ UTR reporters. After transcriptional stop by tetracycline, TTP accelerated the decay of all three targets but not that of the control reporter (3´ UTR of *Hprt*) (Fig. 1*B*). To address the ability of TTP to bind to the AREs of the selected targets, the conserved AREs in the 3´ UTRs of the chosen mRNAs were determined by alignment of several mammalian 3´ UTRs (Fig. S3*B*). *Cxcl2* contained two and *Il1a* and *IL6* contained one TTP binding UAUUUAU heptamers. RNA oligonucleotides comprising the conserved murine AREs were analyzed for their ability to compete with the optimal ARE of *Tnf* [21, 156] for TTP binding in RNA EMSA experiments (Fig. 1*C*). These experiments revealed that all three selected AREs successfully competed the *Tnf* ARE for binding to TTP. Finally, we validated the microarray data by measuring the decay rates of *Il1a*, *Il6* and *Cxcl2* in WT and TTP$^{-/-}$ BMDMs using qRT-PCR. These experiments confirmed that all three mRNAs were degraded in a TTP-dependent way (Fig. 1*D*). Importantly, the TTP-mediated decay was detectable only if the cells were treated with the p38 MAPK inhibitor SB203580 at the time of the transcription inhibition. Without p38 MAPK inhibition, all mRNAs were stable during the time of measurement. Cumulatively, our data that were collected in several independent assays for the first time demonstrate that *Cxcl2*, *Il6* and *Il1a* are TTP targets in BMDMs.

mRNA decay in the LPS-induced transcriptome.

LPS-induced transcripts displaying the most dynamic expression profile, i.e. those showing a rapid and transient induction were recently shown to be particularly robustly regulated at the level of mRNA stability [2]. To examine the role of TTP in the stability of these mRNAs we used our recently published dataset of the LPS-induced transcriptome [165]. Transcripts which were induced at least 3-fold after stimulation with LPS for 3 h were investigated for stability using our mRNA decay dataset. Out of 548 LPS-induced transcripts 138 transcripts (25%) were classified as significantly unstable. Thus, unstable transcripts were enriched in the LPS-induced transcriptome compared to the whole transcriptome (25% compared to 10%) (Fig. 2 and Fig. S2). Out of 138 unstable LPS-induced transcripts, 116 (84%) contained AUUUA type AREs demonstrating that they were overrepresented in the LPS-induced fraction compared to the whole transcriptome (45%). Transcripts displaying TTP-dependent decay represented 33% of the unstable LPS-induced mRNAs (Fig. 2, Tables 2 and S2). Importantly, all immunologically relevant and known TTP targets (i.e. *Tnf*, *Il10*, *Cxcl1*, *Il1b*) as well as those identified in this study (*Il1a*, *Il6* and *Cxcl2*) were among the mRNAs destabilized by TTP. Several other important inflammatory mediators including *Ccl2*, *Ccl3*, *Ccl4*, and *Il23* were also found among the TTP-destabilized transcripts (Table 2). The results indicate that 1/3 of unstable mRNAs induced during the acute phase of the innate immune response is removed by TTP-dependent degradation, and hence they are putative TTP targets.

Although the LPS-induced transcriptome was enriched in unstable and ARE-containing mRNAs, many (64%) of the ARE-containing transcripts were stable. The broad definition that we used for an ARE (i.e. AUUUA) could not solely account for this finding since the 3´ UTRs of e.g. *Cxcl3* (NM_203320) or *Ccl12* (NM_011331) (Fig. 2) contained UAUUUAU heptamers that constitute functional AREs [24].

Several unstable mRNAs (e.g. *Dusp1* and *Dusp2*) containing putative core TTP-binding sites of the UAUUUAU type were not degraded in a TTP-dependent way (Fig. 2 and Fig. S4). On the other hand, three unstable mRNAs (*Bcl3*, *Nfil3*, *Phldb1*) displaying destabilization by TTP

were lacking even the simple ARE, i.e. the AUUUA sequence in the 3′ UTR (Fig. 2). These data confirm that although AREs have a prominent role in the mRNA decay in general, and in the TTP-dependent decay in particular, the presence of an ARE is neither sufficient nor necessary for an mRNA to be destabilized by TTP.

Timing and specificity of mRNA decay in the LPS-induced transcriptome is controlled by a negative feedback loop.

The analysis of the LPS-induced transcriptome revealed a so far underestimated extent of TTP-mediated removal of inflammatory mRNAs. In fact, *Socs3* mRNA has been reported in one study not to be an exclusive TTP target [166]. That study showed that co-transfected (overexpressed) TTP destabilized *Socs3* mRNA, yet the *Socs3* mRNA was not stabilized in TTP$^{-/-}$ BMDMs and fibroblasts compared to WT cells. In contrast, our work revealed a non-redundant role of TTP in *Socs3* mRNA destabilization (Fig. 2 and Table 2), which we explain to result from the pharmacological p38 MAPK inhibition. Normally, this inactivation occurs gradually due to the endogenous IL-10 production that is needed for a sustained expression of *Dusp1* in LPS-treated BMDMs [30, 64, 66]. Consequently, the TTP-dependent mRNA decay should become more pronounced during the resolution phase of inflammation when the p38 MAPK-mediated inhibition of TTP activity is already strongly diminished. To substantiate this hypothesis examined the expression profile of TTP and activation kinetics of p38 MAPK during the stimulation of BMDMs with LPS (Fig. 3*A*). TTP was induced after 3 h of LPS treatment and remained high until 8 h. Thereafter, TTP gradually disappeared and after 25 h the TTP levels were comparable to those in unstimulated cells. Consistently, p38 MAPK activity was high until 6 h, thus supporting TTP expression (Fig. 3*A*). After 6 h p38 MAPK was declining thereby initiating the phase of TTP disappearance. The comparison of TTP expression and p38 MAPK activity suggested that after about 6 – 8 h the TTP activity should become more apparent since the protein was still present yet the inhibitory effect of p38 MAPK activity on the mRNA-destabilizing function of TTP gradually diminished. We tested this model by assaying the decay of *Cxcl2* mRNA at later time points after LPS

stimulation. At the 3 h time point only the use of the p38 MAPK inhibitor revealed an increased decay in WT compared to TTP$^{-/-}$ cells (Fig. 1D). However, after 6 h and 8 h of LPS treatment *Cxcl2* mRNA was more unstable in WT compared to TTP$^{-/-}$ cells even without the inhibition of p38 MAPK (Fig. 3). Importantly, the half-life of *Cxcl2* mRNA in WT cells decreased with time of LPS treatment (at 6 h $t_{1/2}$ was 75 min; at 8 h $t_{1/2}$ was 36 min) which is in agreement with the concomitant decrease in mRNA stability and p38 MAPK activity in the later phase of inflammation. These results confirmed that the pharmacological inhibition of p38 MAPK merely synchronized intrinsic regulatory events. Importantly, all stable LPS-induced mRNAs recently reported and analyzed in more detail by Hao and Baltimore [2] were found stable also in our study (*Mmp13*, *Ccl5*, and *Saa3*, Table S2) indicating that the pharmacological p38 MAPK inhibition did not introduce an artificial TTP-mediated mRNA degradation.

We conclude that the microarray-based mRNA decay dataset resulting from TTP- and p38 MAPK-controlled negative feedback mechanistically explains the reported profound role of mRNA stability in the establishment of inflammatory gene expression profiles [2].

Discussion

Cessation of transcription does not immediately result in the termination of expression unless the already generated mRNAs are degraded. This has been demonstrated by studies describing lethal consequences of uncontrolled *Tnf* expression caused by the removal of AREs from its 3´ UTR [167, 168]. On the other hand, immune cells must be able to robustly stimulate the expression of inflammatory genes in the early phase of the inflammatory response. Thus, a mechanism must be in place that actuates the inflammatory mRNA degradation with some delay after the initial inflammatory stimulus has been sensed. This study describes a negative feedback system that executes a delayed yet robust elimination of a large number of inflammation-induced mRNAs. The downstream effector of the system is the mRNA-destabilizing protein TTP whose expression is strongly up-regulated during the

initial phase of inflammation yet its mRNA-destabilizing function is in this phase blocked by a high p38 MAPK activity.

The differential mRNA decay profiling uncovered a previously unanticipated large number of TTP-destabilized mRNAs. For the following reasons we believe that the majority of mRNAs stabilized in TTP$^{-/-}$ cells are direct TTP targets: 1) consistent with the prominent binding of TTP to ARE sequences, ARE-containing mRNAs were enriched in the TTP-dependent group (Fig. 2), 2) the most stringent criterion namely a slower decay in TTP$^{-/-}$ compared to WT cells was used to identify putative TTP targets, and 3) three selected mRNAs were confirmed by detailed studies as TTP targets. Consistently, most of the best-characterized TTP targets were found in our profile. The large number of TTP targets results from the increased sensitivity due to the inhibition of p38 MAPK. This inhibition does not introduce an artificial TTP-dependent decay since no inhibition of the kinase is needed for detection of differential decay of *Cxcl2* mRNA in WT and TTP$^{-/-}$ cells at 6 h or 8 h of LPS treatment, when p38 MAPK activity is already diminished by endogenous processes (Fig. 3). In addition, all stable LPS-induced mRNAs analyzed in more detail recently (*Mmp13*, *Ccl5* and *Saa3* [2]) were found stable also in our study (Table S2).

Our study indicates that the TTP-mediated mRNA destabilization process discriminates between the different targets depending on the p38 MAPK activity. This allows for a fine-tuning of the control of the inflammatory response in both kinetics and strength. Whereas some targets can be degraded at a high p38 MAPK activity (e.g. *Tnf*), for the decay of other targets a low p38 MAPK activity i.e. a high TTP activity is needed. This is illustrated by the high stability of the herein described three novel TTP targets, *Il1a*, *Il6* and *Cxcl2* (Fig. 1), after 3 h of LPS treatment when only the pharmacological inhibition of p38 MAPK reveals these targets to be unstable. After 6 and 8 h of LPS treatment *Cxcl2* becomes spontaneously unstable and the inhibition of p38 MAPK is no longer needed to detect TTP-dependent decay (Fig. 3). How does p38 MAPK enable TTP to discriminate between different targets is an important topic for future studies. The sequence of ARE alone cannot account for the observed differences since both *Tnf* and *Cxcl2* possess comparable AREs

yet only *Tnf* is destabilized by TTP at a high p38 MAPK activity. Thus, so far unknown regulatory elements in the 3′ UTRs or proteins controlling mRNA stability are likely to be involved. Our study confirms that AREs play a dominant though not exclusive role in the TTP binding.

It is becoming increasingly clear how several regulatory circuits control the activation and subsequent attenuation of inflammatory responses. In this study we propose how a so far not appreciated negative feedback loop controls the removal of inflammatory mRNAs, thereby contributing to the self-limiting principle of inflammation. This regulatory mechanism employs a small number of successive events (Figure 4): 1) p38 MAPK-mediated expression of TTP with a low mRNA-destabilizing activity, 2) inflammation-induced IL-10 production, 3) IL-10-induced reduction of p38 MAPK activity, and 4) increase in TTP activity due to gradual inactivation of p38 MAPK (Figure 3). This regulatory system is adjusted by the concurrent p38 MAPK activity such that only a subset of TTP targets is destabilized at a time ensuring that pro-inflammatory mRNAs (e.g. *Tnf*) and anti-inflammatory mRNAs (such as *Il10* [27]) are not simultaneously eliminated. Due to the less efficient *Il10* mRNA removal at high p38 MAPK activity [164], the *Il10* transcript is efficiently degraded only during the resolution phase of inflammation when the IL-10 function is no longer needed. Finally, the complete drop of p38 MAPK activity at the end of the resolution phase causes degradation of the TTP protein (Fig. 3*A*). The profound role of TTP in the removal of pro-inflammatory mRNAs followed by the elimination of the anti-inflammatory *Il10* mRNA and the concomitant disappearance of the TTP protein indicates TTP to be a key factor regulating the immune homeostasis.

Materials and Methods

Reagents. Rabbit antibody to TTP was used as described [30]. LPS from *Escherichia coli* 055:B5 was used at a concentration of 10 ng/ml, actinomycin D (act D) and SB203580 (all Sigma) were used at a concentration of 5 μg/ml and 4 μM, respectively.

Cell culture. Primary macrophages were grown in L cell-derived CSF-1 as described [39]. TTP$^{-/-}$ (*Zfp36$^{-/-}$*) mice [76] were on C57Bl/6 background. Mice, 8 to 12 weeks old at the time of bone marrow collection, were housed under specific pathogen-free conditions. Mouse experiments were carried out in compliance with national laws. HeLa Tet-Off cells (Clontech) were grown in DMEM supplemented with 10 % FCS.

Microarray analysis. BMDMs from WT and TTP$^{-/-}$ mice were treated with LPS for 3 h. Medium was then replaced by fresh medium containing act D and SB203580 for 0, 45 and 90 min before RNA extraction. BMDMs from three different mice were used for each time point, i.e. in total 18 independent biological samples were collected (9 for WT and 9 for TTP$^{-/-}$ cells). Total RNA was then used for genome-wide expression analysis using Affymetrix Mouse Gene ST 1.0 microarrays containing 28853 genes. Standard protocols for labeling and hybridization were used (supporting Materials and Methods). Biotinylated DNA was hybridized to Mouse Gene ST 1.0 GeneChips and scanned following Affymetrix protocols. For generation of probe set expression values, CEL files containing probe level data were normalized using the RMA algorithm implemented in the Affymetrix Expression Console. Microarray data have been deposited in Gene Expression Omnibus (GEO, http://www.ncbi.nlm.nih.gov/geo/) and will be publicly accessible after acceptance of the paper. Subsequently the data were log transformed, after subtraction of a constant of 1.41 to account for the background, to achieve approximate normality and standardized to zero mean and unit variance. A linear model with genotype (WT and TTP$^{-/-}$), treatment (0 min, 45 min, and 90 min), and their interaction as independent variables was fitted. Residual variances were adjusted using an empirical bayes method [169] to obtain approximately t-distributed differences in gene expression values. It turned out that the resulting distribution of log 2 transformed signal intensities was slightly bi-modal, with a sharp peak at low values. We interpreted this peak as resulting from spurious background fluorescence of unexpressed genes. We thus filtered out genes expressed at an absolute level of less than 11.3, which falls into the valley between the two peaks. In addition, much less genes could be classified as unstable at the 45 min decay time point than at 90 min so that only the

results for the 90 min time point are presented. The most extremely regulated genes were then selected according to the following criteria: i) genes where the decay of mRNAs after 90 min was outside the one-sided α = 0.05 limit (=one *; or $P < 0.05$) (t-value > 1.86); ii) genes where additionally the decay of mRNAs in TTP$^{-/-}$ compared to WT cells after 90 min was outside the one-sided α = 0.05 limit.

The half-lives determined using the microarray dataset. First, the average difference between the time point 0 (= transcription blockage) and 90 min (end of the decay assay) in the three biological replicates was calculated for each mRNA. These average decay values were then used to calculate the half-lives. For half-lives higher than 600 min the value was set as "stable".

Analysis of mRNA decay in the LPS-induced transcriptome . LPS-induced genes were retrieved from our recently published microarray dataset (GEO accession number GSE8621, [165]) obtained by stimulation of BMDMs for 3 h with LPS. Transcripts that were induced at least 3-fold in comparison with unstimulated cells were examined with regard to their decay rates using the mRNA decay dataset from this study.

3´ UTR analysis. Sequence files were retrieved from the GenBank using the Refseq accession numbers. A Perl script was implemented that uses regular expressions to find the core ARE motifs (i.e. the AUUUA sequence) in the nucleotide sequences and to annotate these hits in the GenBank files. Annotation of ARE motifs also included the assignment to the location classes (5´ UTR, CDS, 3´ UTR, NA) based on the annotation available in the GenBank files. Only AREs located in the 3´ UTRs were included in the final analysis.

Measurements of RNA stability. $5x10^6$ HeLa Tet-Off cells were transfected by nucleofection with 4 µg pCMV-TTP or 4 µg pCMV-TTP together with 1 µg pTetBBB/IL1α, pTetBBB/IL6, pTetBBB/Cxcl2 or pTet/HPRT, respectively. 24 h later 200 ng/ml tetracycline was added to stop transcription from the pTetBBB plasmids. Total RNA was prepared and analyzed by qRT-PCR as described. To assay mRNA stability in BMDMs, $5x10^6$ cells were treated with LPS for 3 h or 6 h. Medium was then removed and fresh medium containing act

D or act D and SB203580 was added for the times indicated before preparing total RNA. RNA was analyzed by qRT-PCR as described before or used for microarray hybridization.

Statistical analysis. For microarray data a linear model analysis with genotype (WT versus TTP$^{-/-}$), treatment (0 min, 45 min, 90 min), their interaction, and individual as independent variables was fitted. Residuals were plotted, visually inspected, and tested for normality. Design matrices were specified such that the coefficients for the relevant comparisons could be calculated, e.g., between the baseline and induced states and between genotypes. Only the significance levels are reported. For the qRT-PCR data, normalized copy numbers were log-transformed, and mean values and standard deviations (SDs) were calculated (for n as described in the figure legends).

Acknowledgements

References

1. Jenner RG & Young RA (2005) Insights into host responses against pathogens from transcriptional profiling. (Translated from eng) *Nat Rev Microbiol* 3(4):281-294 (in eng).
2. Hao S & Baltimore D (2009) The stability of mRNA influences the temporal order of the induction of genes encoding inflammatory molecules. (Translated from eng) *Nat Immunol* 10(3):281-288 (in eng).
3. Barreau C, Paillard L, & Osborne HB (2005) AU-rich elements and associated factors: are there unifying principles? (Translated from eng) *Nucleic Acids Res* 33(22):7138-7150 (in eng).
4. Khabar KS (2005) The AU-rich transcriptome: more than interferons and cytokines, and its role in disease. (Translated from eng) *J Interferon Cytokine Res* 25(1):1-10 (in eng).

5.   Stoecklin G & Anderson P (2007) In a tight spot: ARE-mRNAs at processing bodies. (Translated from eng) *Genes Dev* 21(6):627-631 (in eng).

6.   Franks TM & Lykke-Andersen J (2008) The control of mRNA decapping and P-body formation. (Translated from eng) *Mol Cell* 32(5):605-615 (in eng).

7.   Taylor GA*, et al.* (1996) A pathogenetic role for TNF alpha in the syndrome of cachexia, arthritis, and autoimmunity resulting from tristetraprolin (TTP) deficiency. *Immunity* 4(5):445-454.

8.   Carballo E, Lai WS, & Blackshear PJ (1998) Feedback inhibition of macrophage tumor necrosis factor-alpha production by tristetraprolin. *Science* 281(5379):1001-1005.

9.   Worthington MT*, et al.* (2002) RNA binding properties of the AU-rich element-binding recombinant Nup475/TIS11/tristetraprolin protein. *J Biol Chem* 277(50):48558-48564.

10.   Blackshear PJ*, et al.* (2003) Characteristics of the interaction of a synthetic human tristetraprolin tandem zinc finger peptide with AU-rich element-containing RNA substrates. *J Biol Chem* 278(22):19947-19955.

11.   Stoecklin G*, et al.* (2004) MK2-induced tristetraprolin:14-3-3 complexes prevent stress granule association and ARE-mRNA decay. *Embo J* 23(6):1313-1324.

12.   Stoecklin G*, et al.* (2008) Genome-wide analysis identifies interleukin-10 mRNA as target of tristetraprolin. (Translated from eng) *J Biol Chem* 283(17):11689-11699 (in eng).

13.   Gilchrist M*, et al.* (2006) Systems biology approaches identify ATF3 as a negative regulator of Toll-like receptor 4. (Translated from eng) *Nature* 441(7090):173-178 (in eng).

14.   Litvak V*, et al.* (2009) Function of C/EBPdelta in a regulatory circuit that discriminates between transient and persistent TLR4-induced signals. (Translated from eng) *Nat Immunol* 10(4):437-443 (in eng).

15.   Schaljo B*, et al.* (2009) Tristetraprolin is required for full anti-inflammatory response of murine macrophages to IL-10. (Translated from eng) *J Immunol* 183(2):1197-1206 (in eng).

16.   Carballo E, Lai WS, & Blackshear PJ (2000) Evidence that tristetraprolin is a physiological regulator of granulocyte-macrophage colony-stimulating factor messenger RNA deadenylation and stability. *Blood* 95(6):1891-1899.

17.   Stoecklin G, Gross B, Ming XF, & Moroni C (2003) A novel mechanism of tumor suppression by destabilizing AU-rich growth factor mRNA. *Oncogene* 22(23):3554-3561.

18.   Tchen CR, Brook M, Saklatvala J, & Clark AR (2004) The stability of tristetraprolin mRNA is regulated by mitogen activated protein kinase p38 and by tristetraprolin itself. *J Biol Chem*.

19.   Ogilvie RL*, et al.* (2005) Tristetraprolin Down-Regulates IL-2 Gene Expression through AU-Rich Element-Mediated mRNA Decay. *J Immunol* 174(2):953-961.

20.   Lai WS, Parker JS, Grissom SF, Stumpo DJ, & Blackshear PJ (2006) Novel mRNA targets for tristetraprolin (TTP) identified by global analysis of stabilized transcripts in TTP-deficient fibroblasts. (Translated from eng) *Mol Cell Biol* 26(24):9196-9208 (in eng).

21.   Chen YL*, et al.* (2006) Differential regulation of ARE-mediated TNFalpha and IL-1beta mRNA stability by lipopolysaccharide in RAW264.7 cells. *Biochemical and biophysical research communications* 346(1):160-168.

22.   Frasca D*, et al.* (2007) Tristetraprolin, a negative regulator of mRNA stability, is increased in old B cells and is involved in the degradation of E47 mRNA. (Translated from eng) *J Immunol* 179(2):918-927 (in eng).

23.   Datta S*, et al.* (2008) Tristetraprolin regulates CXCL1 (KC) mRNA stability. (Translated from eng) *J Immunol* 180(4):2545-2552 (in eng).

24.   Horner TJ, Lai WS, Stumpo DJ, & Blackshear PJ (2009) Stimulation of polo-like kinase 3 mRNA decay by tristetraprolin. (Translated from eng) *Mol Cell Biol* 29(8):1999-2010 (in eng).

25. Ogilvie RL*, et al.* (2009) Tristetraprolin mediates interferon-gamma mRNA decay. (Translated from eng) *J Biol Chem* 284(17):11216-11223 (in eng).

26. Emmons J*, et al.* (2008) Identification of TTP mRNA targets in human dendritic cells reveals TTP as a critical regulator of dendritic cell maturation. (Translated from eng) *RNA (New York, N.Y* 14(5):888-902 (in eng).

27. Eyers PA, van den IP, Quinlan RA, Goedert M, & Cohen P (1999) Use of a drug-resistant mutant of stress-activated protein kinase 2a/p38 to validate the in vivo specificity of SB 203580. *FEBS letters* 451(2):191-196.

28. Sandler H & Stoecklin G (2008) Control of mRNA decay by phosphorylation of tristetraprolin. (Translated from eng) *Biochemical Society transactions* 36(Pt 3):491-496 (in eng).

29. Hammer M*, et al.* (2005) Control of dual-specificity phosphatase-1 expression in activated macrophages by IL-10. *European journal of immunology* 35(10):2991-3001.

30. Tudor C*, et al.* (2009) The p38 MAPK pathway inhibits tristetraprolin-directed decay of interleukin-10 and pro-inflammatory mediator mRNAs in murine macrophages. (Translated from Eng) *FEBS letters* (in Eng).

31. Mages J, Dietrich H, & Lang R (2007) A genome-wide analysis of LPS tolerance in macrophages. (Translated from eng) *Immunobiology* 212(9-10):723-737 (in eng).

32. Ehlting C*, et al.* (2007) Regulation of suppressor of cytokine signaling 3 (SOCS3) mRNA stability by TNF-alpha involves activation of the MKK6/p38MAPK/MK2 cascade. (Translated from eng) *J Immunol* 178(5):2813-2826 (in eng).

33. Hammer M*, et al.* (2006) Dual specificity phosphatase 1 (DUSP1) regulates a subset of LPS-induced genes and protects mice from lethal endotoxin shock. *J Exp Med* 203(1):15-20.

34. Kontoyiannis D, Pasparakis M, Pizarro TT, Cominelli F, & Kollias G (1999) Impaired on/off regulation of TNF biosynthesis in mice lacking TNF AU-rich elements: implications for joint and gut-associated immunopathologies. *Immunity* 10(3):387-398.

35. Murray PJ (2005) The primary mechanism of the IL-10-regulated antiinflammatory response is to selectively inhibit transcription. *Proc Natl Acad Sci U S A* 102(24):8686-8691.

36. Sauer I*, et al.* (2006) Interferons limit inflammatory responses by induction of tristetraprolin. *Blood* 107(12):4790-4797.

37. Smyth GK (2004) Linear models and empirical bayes methods for assessing differential expression in microarray experiments. (Translated from eng) *Statistical applications in genetics and molecular biology* 3:Article3 (in eng).

Figure and table legends

Fig. 1. Detailed characterization of *Il1a, Il6* and *Cxcl2* mRNAs as TTP targets. (A) TTP

interacts with *Il1a, Il6, Cxcl2* and *Tnf* but not *Hprt* mRNA. WT or TTP^{-/-} BMDMs were treated

with LPS for 4 h and then used for RNA immunoprecipitation using anti-TTP antibody (AB) or preimmune serum control (SC). Isolated RNA was reverse transcribed and analyzed by RT-PCR using primers for *Il1a*, *Il6*, *Cxcl2*, *Tnf* and *Hprt*. The data are representative of 3 independent experiments. (B) 3′ UTRs of *Il1a*, *Il6* or *Cxcl2* confer TTP-dependent instability. HeLa Tet-Off cells were transfected with reporter plasmids containing tetracycline-regulated β-globin fused to 3′ UTRs of *Il1a* (pTetBBB/IL1α), *Il6* (pTetBBB/IL6), *Cxcl2* (pTetBBB/Cxcl2) and the control *Hprt* (pTetBBB/HPRT) together with pCMV-TTP or empty pCMV vector. 24 h after transfection, tetracycline was added to stop the reporter gene transcription from the pTetBBB constructs and RNA was isolated at the times indicated. Remnant mRNA, as determined by qRT-PCR, is shown in % of the amount at the time point of transcription stop. The values at each time point represent the mean and SDs of independent experiments (n=3). (C) TTP binds to conserved AREs within the 3′ UTR of *Il1a*, *Il6* and *Cxcl2*. Extracts of HeLa Tet-Off cells expressing Flag-TTP (-tetracycline) or without Flag-TTP expression (+tetracycline) were assayed by RNA-EMSA for binding to Cy5.5 labeled *Tnf* ARE in the presence of competing 1x, 10x or 100x excess of unlabeled *Tnf* ARE, a random RNA sequence, *Il1a* ARE, *Il6* ARE or *Cxcl2* ARE. The identity of TTP-containing complexes was confirmed by supershift (ssTTP) using Flag antibody. (D) WT (TTP$^{+/+}$) and TTP$^{-/-}$ BMDMs were stimulated for 3 h with LPS followed by transcriptional blockage with act D in the presence or absence of the p38 MAPK inhibitor SB203580 (SB). Decay rates of *Il1a*, *Il6* and *Cxcl2* were monitored by qRT-PCR at the indicated time points. Remnant *Il1a*, *Il6* or *Cxcl2* mRNA in % of the amount at the time point of act D treatment is depicted. SDs are shown (n=3).

Fig. 2. Venn diagram showing the decay properties of the LPS-induced transcriptome. Unstable mRNAs represent 25% of LPS-induced transcripts (138 out of 548). One third (45 out of 138) of unstable mRNAs are destabilized by TTP. Ninety five % (42 out of 45) of TTP-destabilized mRNAs contain AREs in their 3′ UTR. Examples of mRNAs in each category

are displayed. The Venn diagram is a graphical representation of the dataset shown in the Table S2.

Fig. 3. *Cxcl2* mRNA is destabilized by TTP at later phase of LPS treatment when p38 MAPK is declining and TTP is still expressed. (A) BMDMs were treated for indicated times with LPS and the expression of TTP (upper panel) and p38 MAPK activity (lower panel) was examined by Western blotting using antibodies to TTP and phosphorylated p38 MAPK (pp38 MAPK). For loading control, the blots were reprobed with antibodies to total p38 MAPK. (B) BMDMs were stimulated with LPS for 6 h (upper panel) or 8 h (lower panel) followed by act D treatment. *Cxcl2* mRNA decay was monitored for 90 min after the addition of act D. Note, no p38 MAPK inhibitor was used in this experiment. Error bars display SDs (n=3).

Fig. 4. Scheme of the qualitative and temporal control of mRNA decay by negative feedback in inflammatory response. Inflammatory stimulus activates the stress-regulated p38 MAPK that in turn induces the expression of TTP. At this phase, TTP mRNA-destabilizing activity is kept low by high p38 MAPK resulting of the destabilization of only few mRNAs (e.g. *Tnf*). p38 MAPK is gradually inactivated by the intrinsic negative feedback loop that is predominantly initiated by the endogenous IL-10 production and up-regulation of DUSP1, the p38 MAPK phosphatase. TTP activity unfolds as p38 MAPK decreases resulting in the removal of additional mRNAs targeted by TTP (e.g. *Cxcl2*).

Table 1. Decay of most unstable transcripts is TTP-dependent. (A) Top 25 transcripts displaying most significant instability values. P values for stability in WT cells and for TTP-dependent decay are shown. Half-lives that were calculated on the basis of mRNA decay within 90 min after transcriptional stop serve for visualization of the P values. The number of AREs (of the AUUUA type) in the 3´ UTR is depicted. Among these 25 mRNAs, 22 are degraded in a TTP-dependent decay (highlighted in gray), whereas only three transcripts

(*Clec2d*, *Hist1h1b* and *Cebpd*) are destabilized independently of TTP. (B) Reported TTP targets. Data as in (A) and references for reported targets are shown. (C) Three new TTP targets (i.e. *Cxcl2*, *Il1a* and *Il6*) characterized in this study.

Table 2. LPS-induced transcripts destabilized by TTP. Forty five LPS-induced unstable transcripts are shown that display TTP-dependent decay as judged by P values < 0.05 for decay differences in WT and TTP$^{-/-}$ cells (i.e. P value for TTP-dependent decay). The transcripts are ordered according to their P values for decay in WT cells. Calculated half-lives support the visualization of the P values. Number of AREs (of the AUUUA type) in the 3´ UTR and fold-induction by LPS are depicted. Reported TTP targets are shown with references.

Cxcl3, Ccl12

Dusp1, Dusp2, Dusp16

unstable mRNAs
138

22

ARE-containing mRNAs
408

TTP-destabilized mRNAs
45

3

Ier2, Socs1

Bcl3, Nfil3, Phldb1

LPS-induced mRNAs
548

TNFa, Il1a, Il1b, Cxcl1, Cxcl2, Il6, Ccl3, Ccl4, Socs3, Il10

Irf7, Ccl5, Fas

A

LPS (h):   0   0.5   3   6   8   10   15   25

TTP ⟶

p38 ⟶

pp38 ⟶

p38 ⟶

B

6 h LPS

Cxcl2 mRNA decay

8 h LPS

Cxcl2 mRNA decay
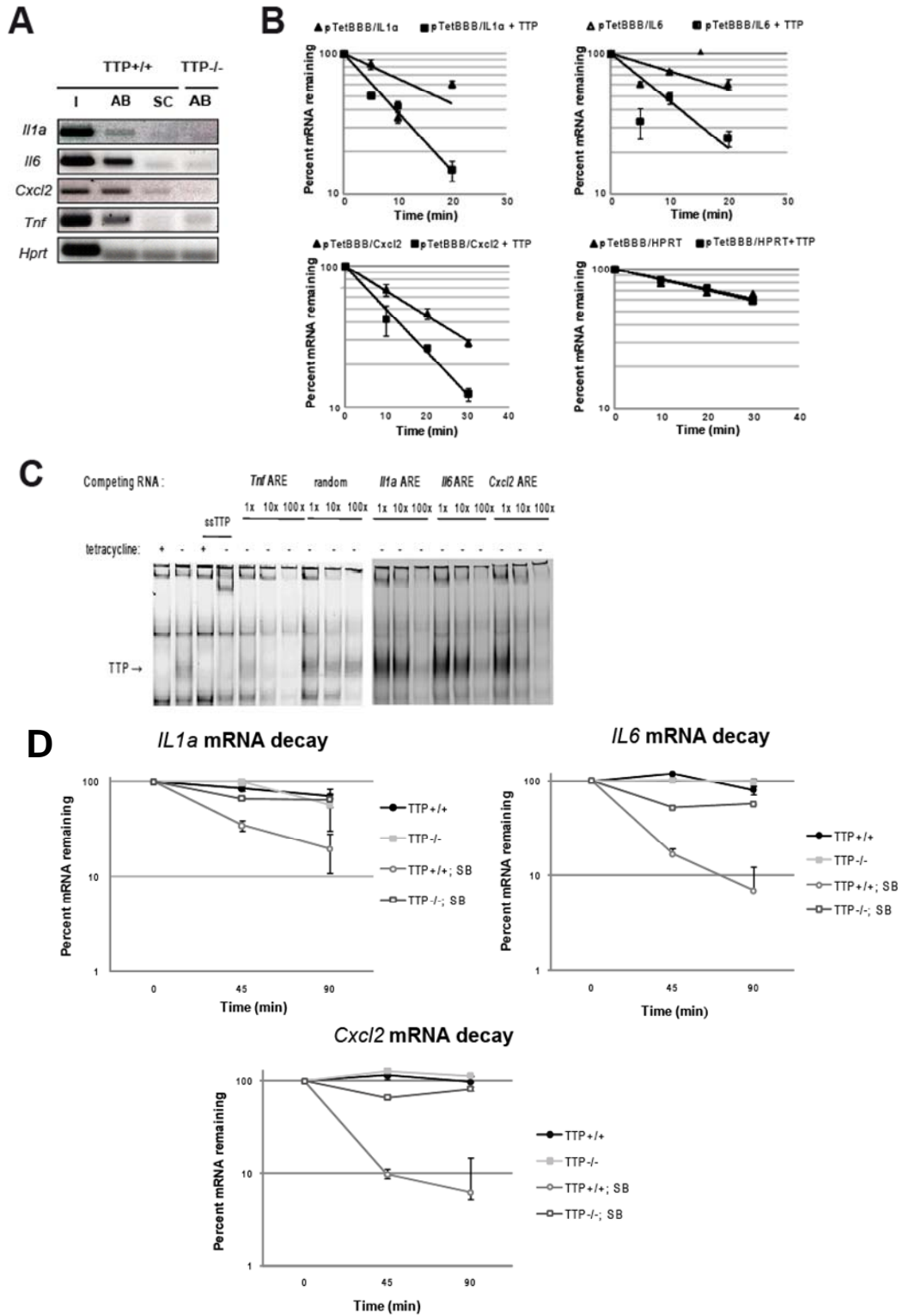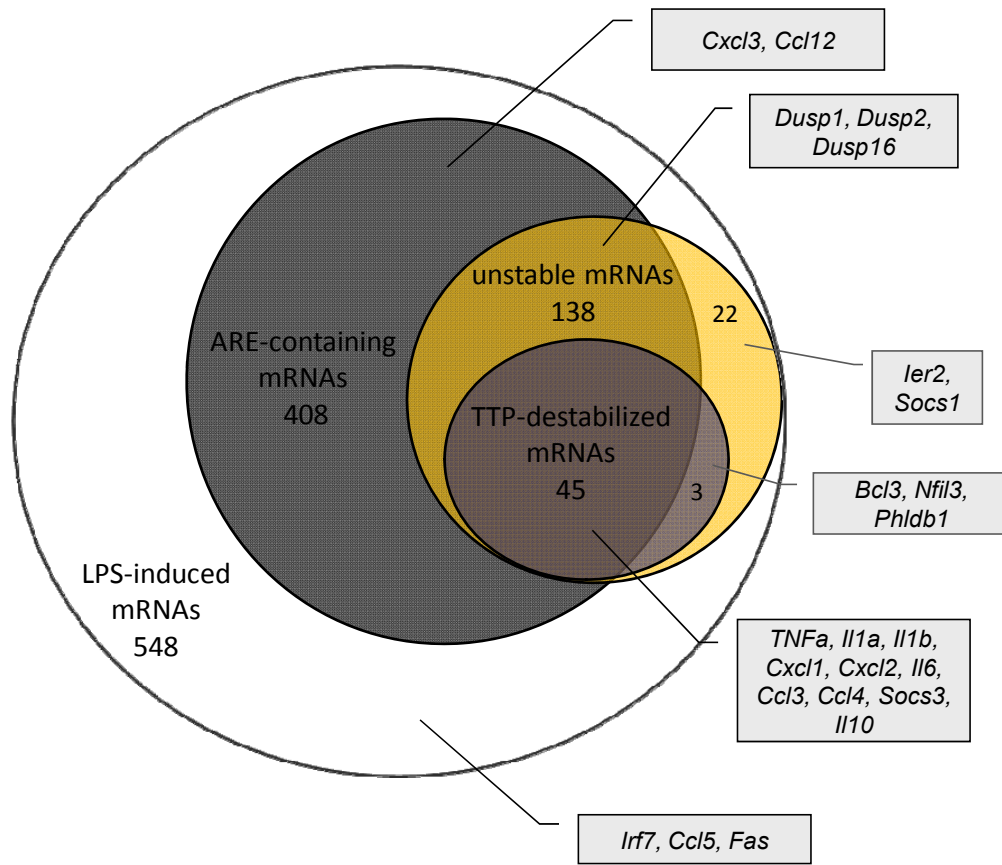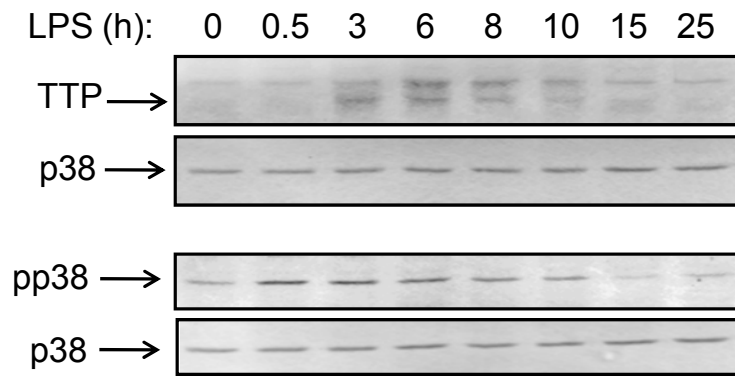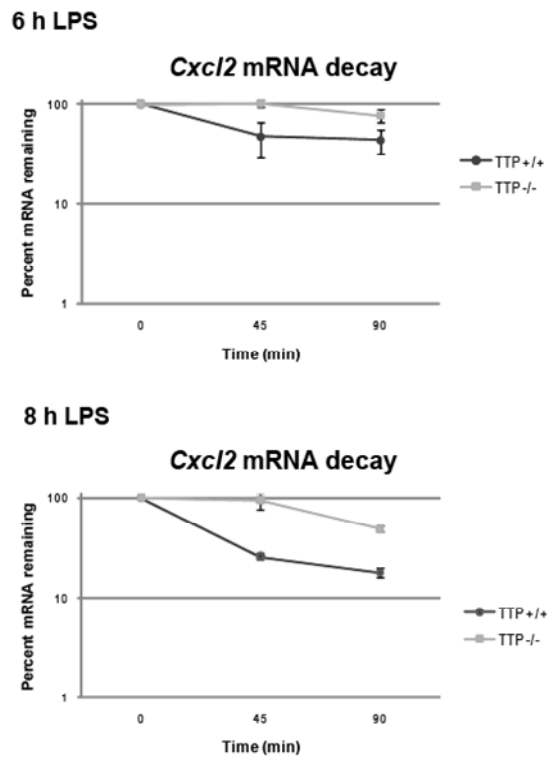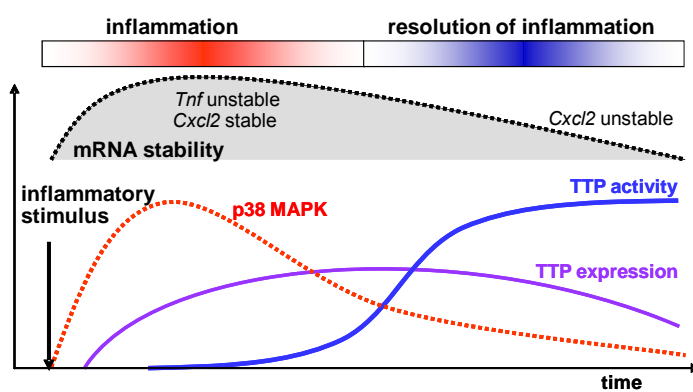
Supporting Information

Materials and Methods

Labeling and hybridization to microarrays. Standard protocols for labeling and hybridization were followed. In brief, 200 ng of total RNA were reverse transcribed introducing by random priming a T7-binding site into the cDNA for subsequent *in vitro* transcription. The resulting cRNA was subjected to a second round of random primed cDNA synthesis in the presence of dUTP, that allows fragmentation of the cDNA with uracil DNA glycosylase and apurinic/apyrimidinic endonuclease 1. Fragmented cDNA was biotinylated by incubation with Terminal Deoxynucleotidyltransferase (TdT), and 5.5 µg of biotinylated DNA were hybridized to Mouse Gene ST 1.0 GeneChips overnight, washed, stained and scanned following Affymetrix protocols.

RNA immunoprecipitation. Isolation of TTP associated mRNAs under native conditions was performed essentially as described previously [170] with modifications. Briefly, the precleared extract of 1×10^7 TTP$^{-/-}$ or WT primary macrophages was immunoprecipitated using TTP antiserum or preimmune serum control for 1 h at 4°C. Immune complexes were precipitated using protein A sepharose beads (GE Healthcare) coated with tRNA and RNAse free bovine serum albumin (Ambion) by rotating for 1 h at 4°C. After 3 washing steps with lysis buffer, bound complexes were eluted using TES buffer (10 mmol/l Tris pH 8.0, 0.5 mmol/l EDTA, 0.5% SDS) at 65°C for 15 min. RNA was isolated and reverse transcribed as mentioned before. Samples were analyzed by RT-PCR performing 35 cycles using the primers as described for qRT-PCR.

RNA electrophoretic mobility shift assay (RNA-EMSA). To prepare TTP-containing extracts, HeLa-Tet-Off cells were transfected with pTRE-TTPfl plasmid as described [30]. 24 h after transfection the cells were washed with cold PBS and lysed in buffer containing 10 mM Tris-HCl (pH 7.5), 50 mM NaCl, 30 mM NaPP$_i$, 50 mM NaF, 2 mM EDTA, 1 % Triton X-100 and protease inhibitor cocktail (Roche). Extracts were cleared by centrifugation at 15.000 rpm. 5 µl cell extract (15 µg protein) were incubated with 0.5 µl Poly-U RNA (100

ng/µl)(Microsynth), 0.5 µl Cy5.5 5'-labeled Tnf ARE (1 pmol/µl), 1 µL RiboLock RNase Inhibitor (Fermentas) and 2.5 µL 5x gel shift buffer (200 mM KCl, 5 mM $MgCl_2$, 0.5 mM EGTA, 2.5 mM DTT, 100 mM Hepes-KOH pH 7.9, Glycerin 50% (v/v)) for 20 min at room temperature. For supershift assays, 0.5 µl anti-Flag M2 antibody (Sigma) was added. For competition experiments, 0.5 µl competing RNA oligonucleotides were added at a concentration of 0, 1, 10 or 100 pmol/µl for further 20 min. Samples were then separated on a 6 % polyacrylamide gel. The Cy5.5 signal was detected and quantified using the infrared imaging system Odyssey (LI-COR Biosciences). RNA oligonucleotides and the *Tnf* RNA Cy5.5 5'-labeled oligonucleotide were purchased from Microsynth. The RNA sequence was as follows: for Cy5.5 5'-labeled or unlabeled *Tnf* ARE, Cy5-TNFα-ARE 5'-AUUAUUUAUUAUUUAUUUAUUAUUUA-3'; as random sequence, random 5'-AGCUUAGGAAUAUCAAUGUUAAGUAG-3'; for the *Il1a* ARE, *Il1a*-ARE 5'-UAUUUAUAAAUAUAUUUAUGAUAAUUAUAUUAUUUAU-3'; for the *IL6* ARE, IL6-ARE 5'-UAUUUUUAAUUUAUUGAUAAUUUAAAUAA-3'; for the *Cxcl2* ARE, Cxcl2-ARE 5'-UUAUUUAUUUAUCUAUGUAUUUAUUUAUUUAUU-3'.

Plasmids. pTetBBB/IL1α, pTetBBB/IL6, pTetBBB/Cxcl2 and pTetBBB/HPRT were created by insertion of the full-length 3´ UTRs of *Il1a*, *Il6*, *Cxcl2* and *Hprt* into the *Bgl*II and *Bam*HI site located in the β-globin 3´UTR of pTetBBB plasmid also containing a TRE in the promoter. The 3´ UTRs were PCR-cloned using the following primers (restriction sites and flanking nucleotides for efficient restriction digests are included):

for *Il1a*,

fwd 5´- TTTTTTGGATCCGCAGCCTTATTTCGGGAGTCTA -3´

rev 5´- TTTTTTAGATCTGTTGATAGTTACATGACACTGTGG -3´

 for *Il6*,

fwd 5´- TTTTTTGGATCCGCGTTATGCCTAAGCATATCAG -3´

rev 5´- TTTTTTAGATCTTTTGTTTGAAGACAGTCTAAACAT -3'

for *Cxcl2*,

fwd 5´- TTTTTTGGATCCGAAAGGAGGAGCCTGGGCTG -3´

rev 5´- TTTTTTAGATCTCATGAATAAATAAATGTGTCCACTTC -3´

for *Hprt*,

fwd 5´- TTTTTTGGATCCTGAGCGCAAGTTGAATCTGCA -3´

rev 5´- TTTTTTAGATCTATTTAAAAGGAACTGTTGACAACG -3´.

For constitutive expression of TTP, murine TTP was expressed from the CMV promoter in the plasmid pCMV-TTP.

Quantitation of gene expression by quantitative RT-PCR (qRT-PCR). Total RNA was isolated using Trizol-Reagent (Invitrogen) and reverse transcribed by Mu-MLV reverse transcriptase (Fermentas). Amplification of DNA was monitored by SYBR Green (Molecular Probes) as described [171]. Following primers were used: for murine *Hprt*, the housekeeping gene used for normalization., HPRT-fwd 5´-GGATTTGAATCACGTTTGTGTCAT-3´, and HPRT-rev 5´-ACACCTGCTAATTTTACTGGCAA-3´; for human *Hprt*, hHPRT-fwd 5´-TGTGTGCTCAAGGGGGGGC-3´ and hHPRT-rev 5´-CGTGGGGTCCTTTTCACC-3´; for rabbit β-globin, RbGl-fwd 5´-TCCTAAGGTGAAGGCTCATGGCAA-3´ and RbGl-rev GTGGTATTTGTGAGCCAGGGCATT; for *IL6*, IL6-fwd 5´-ATGGATGCTACCAAACTGGAT-3´ and IL6-rev 5´-TGAAGGACTCTGGCTTTGTCT-3´; for *Il1a* and *Cxcl2* the primer sets QT00113253 and QT00113505 (Qiagen), respectively.

References

1. Gama-Carvalho M, Barbosa-Morais NL, Brodsky AS, Silver PA, & Carmo-Fonseca M (2006) Genome-wide identification of functionally distinct subsets of cellular mRNAs associated with two nucleocytoplasmic-shuttling mammalian splicing factors. (Translated from eng) *Genome biology* 7(11):R113 (in eng).
2. Schaljo B*, et al.* (2009) Tristetraprolin is required for full anti-inflammatory response of murine macrophages to IL-10. (Translated from eng) *J Immunol* 183(2):1197-1206 (in eng).
3. Morrison TB, Weis JJ, & Wittwer CT (1998) Quantification of low-copy transcripts by continuous SYBR Green I monitoring during amplification. *Biotechniques* 24(6):954-958, 960, 962.

A

LPS(h):   0   2   4

TTP

panERK

B

SB203580

actinomycin D(min):   0   30   60   90   30   60   90

TTP

panERK
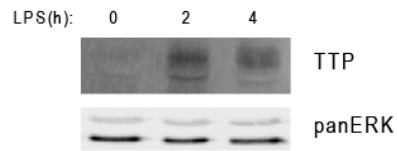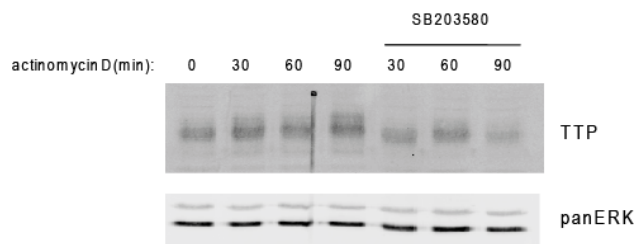
Figure S1 TTP protein levels in LPS-treated BMDMs and the effect of p38 MAPK inhibition on TTP stability.

(A) BMDMs were treated with LPS for the times indicated.

(B) BMDMs were treated for 3 h with LPS followed by treatment with act D with or without SB203580 for the depicted times. TTP protein levels were examined by Western blotting with antibody to TTP. The blots were reprobed with antibody to ERK to control for loading.
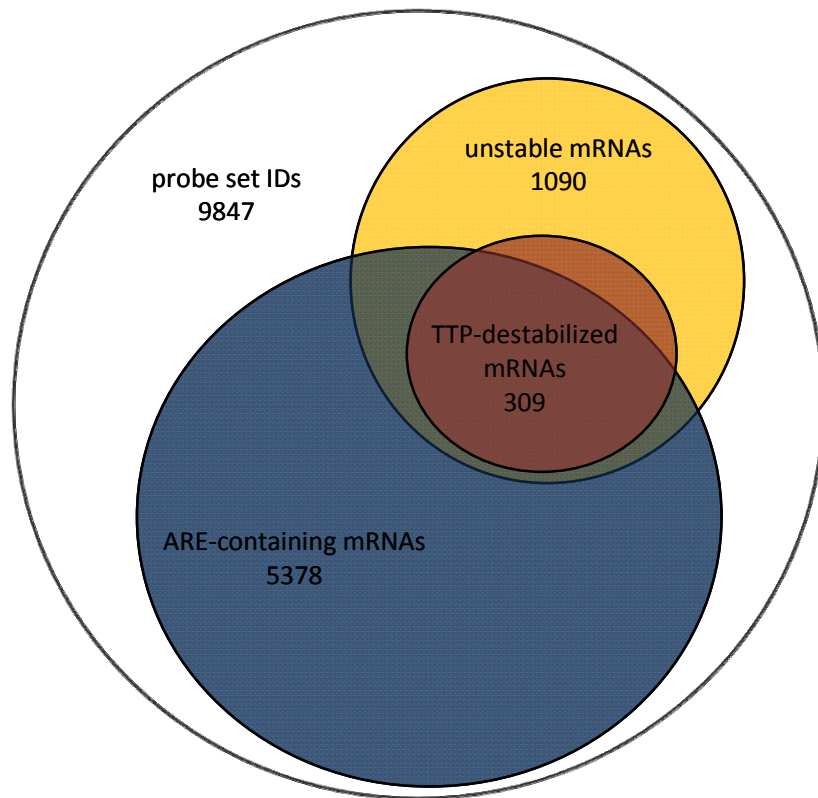
Figure S2 Venn diagram showing the global distribution of unstable transcripts. Within 9847 transcripts 1090 (10%) were found unstable. Out of the 1090 unstable transcripts 309 (28%) mRNAs displayed TTP-dependent decay. 475 (45%) unstable transcripts contained AREs, 582 (55%) unstable transcripts were ARE-free. Unstable mRNAs that were destabilized by TTP were enriched for ARE-containing 3´ UTRs: 185 out of 309 (= 61%) unstable TTP-destabilized mRNAs contained at least one ARE, 116 (39%) mRNAs were ARE-free. The Venn diagram is a graphical representation of the dataset shown in the Table S1.

A

Il1a 3' UTR

```
AAGCAGCCUUAUUUCGGGAGUCUAUUCACUUGGGAAGUGCUGACAGUCUGUAUGUACCAUGUACAGGAACCUUCCUCACCC
UGAGUCACUUGCACAGCAUGUGCUGAGUCUCUGUAAUUCUAAAUGAAUGUUUACCCUCUUUGUAAGAGAAGAGCAAACCCU
AGUGGAGCCACCCCGACAUAUGAUACUAUCUGUUAUUUUAAAGAGUACCCUAUAGUUUGCUCAGUACUAAUCAUUUUAAUU
ACUAUUCUGCAUGGCAUUCUUAGGAGGAUCAAAAAGACUCUACACAUAUUACAGAUGGGGUUAACAAAGGGAUAAAACAACU
GAAAAGCACACUCAAUGCAUUUGGAAUAUAAAUUCACAGACCAAUCUCACUGUGCACCUUCGGCUUCAAAAUGCCAGUUGA
GUAGGAUAAAGGUAUAAGAACUUAAUGCUGUCAUUUUCAAAAGGAAGGGGACAAUAGCUACAUCUUUCCUACCUCAGUGGG
UUUUACUCCAGUGAGAUCAUUUGGAUGAAAUCCUCCUGUAACAGACCUCAAGAAGGAGACAGACUGUUGAAUGUUAUUUUU
AAGUUAUUUUAUCUAUGUAUUUAUAAAAUAUAUUUAUGAUAAUUAUAUUUAUUUAUGGAACAUCCUUAAAUCCUCUGAG
CUUGACGGCGUUCCUCGCAGCAGGGUUUUCUAGGUGGUCAGUUAGAUGUAGUCUCCCUCUAGAGCUCCAUGCUACAGACUUUU
ACACUUUUUCCACAGCCACGAAGCUCUCCGUACAUUCCUGCACUUGGGAGCCCUUUCAUCAUGAUCUUUAAUCUGUGCUGUU
UACUUUGUGCAUCUAAAAUGAUAAUUGAGUCAGUCUUUCUCCCUCCCGUCCUUAAAGCUGUCUGGGUAUUCUUACAUCAUU
CAGUCUCACCUGUAACUAACACCAACCAUCUAAAGAUGGAAAGAGCUUAACUGUGACAACCACAUCACUGAUACCUGAAGU
UUCUUUUCUAGAAUGUAAUCAGUGUUUCCCCUGGAUUCCAAUUUUUUUUCAAACCACAGUGUCAUGUAACUAUCAACAAU
AACAAUCAACUCAUUAUUAUUAAUCAUAAUUAAAAUAAAACAGGUUUGAGCUG
```

Il6 3' UTR

```
UGCGUUAUGCCUAAGCAUAUCAGUUUGUGGACAUUCCUCACUGUGGUCAGAAAAUAUAUCCUGUUGUCAGGUAUCUGAC
UUAUGUUGUUCUCUACGAAGAACUGACAAUAUGAAUGUUGGGACACUAUUUAAUUAUUUUUAAUUUAUUGAUAAUU
UAAAUAAGUAAACUUUAAGUUAAUUUAUGAUUGAUGAUUAUUUUUAUGAAGUGUCACUUGAAAUGUUAUAUGU
UAUAGUUUUGAAAUGAUAACCUAAAAAUCUAUUUGAUAUAAAUAUUCUGUUACCUAGCCAGAUGGUUUCUUGGAAUGUA
UAAGUUUACCUCAAUGAAUUGCUAAUUUAAAUAUGUUUUUAAAGAAAUCUUUGUGAUGUAUUUUUAUAAUGUUUAGAC
UGUCUUCAAACAAAUAAAUUAUAUUAUAUUU
```

Cxcl2 3' UTR

```
CCUGGAAAGGAGGAGCCUGGGCUGCUGUCCCUCAACGGAAGAACCAAAGAGAAAGAAAAAAACAAACAGCACCCGGGAAG
CCUGGAUCGUACCUGAUGUGCCUCGCUGUCUGAGAGUUCACUUAUUUAUUUAUCUAUGUAUUUAUUUAUUUAUUAA
UUCCAUUGCCCAGAUGUUGUUAUGUUUAUUUUGAUAUUUAAGAUAUGCAUUCGCUAAUUCACUGUAAUAUCUUAAAAGG
UCAUUUUAAUAUGUUAAAGUUUAUUUUAAUAAUGUUUAAUGUGUUCAAUUAAAGUAUAUUUAACUUAUAUAGUUGGAAG
GUGAUAAAUUUUUAAACCUAUUUAUUCAUUAGUUUCUGGGGAGAGGGUGAGUUGGGAACUAGCUACAUCCCACCCACAC
AGUGAAAGAGACUGGGGAUAAGGGGUGGGGGUGGGGACAAAUAGAUGCAGUCGGAUGGCUUUCAUGGAAGGAGUGUGCAU
GUUCACAUCAUUUUUUUGUAAGCACCGAGGAGAGUAGAACAGCUGUUAUUUAGGUUUCAGUGUUUGUAAACUGUAUGUA
CAACAUUUUUGAUGCUGGAUUUCAAUGUAAUGUUGUGAGUAACCCUUGGACAUUUUAUGUCUUCCUCGUAAGGCACAGUG
CCUUGCUUAGCAAUUGUUUUGUCAUGCCUUUUCGUGUCUUGAAGUGGACACAUUUAUUUAUUCAUGUAUUUUU
```

B

Il1a ARE

Mus musculus	UAUUUAUAAAUA-UAUUUAUGAUAAUUAU----------AU--UAUUUAU
Homo sapiens	UAUUUAUAAAUA-UAUUUAAGAUAAUUAUAAAUAUAC--UA---UAUUUAU
Rattus norvegicus	UAUUUAUAAAUA-UAUUUAUGAUAAUUAU----------AU--UAUUUAU
Sus scrofa	UAUUUAUAUAA-UAUUUAUUUCUAAUAUAAGUAGAACAUAUUAUUAUAUUUAU
Bos taurus	UAUUUAUAAGCAUUAUUAUUUCUAAGAUUUAU---------UAU--UAUUUAU
Consensus	UAUUUAUAUAA-YA-UAUUUMWRAKAWWWRU--------------UAUUUAU

Il6 ARE

Mus musculus	UAUUUUUAAUUUAUUGAUAAUUUAAAUAA
Homo sapiens	UAUUUUUAAUUUAUUAAU-AUUUAAAUAU
Rattus norvegicus	UAUUUUUAAUUUAUUGAU-AUUUAAAUAA
Sus scrofa	UAU-UUUAAUUUAUUGAU-AUUUAAAUAU
Bos taurus	UAUCUUUAAUUUAUUGA-AUUUAAAUAU
Consensus	UAU-UUUAAUUUAUURAU-AUUUAAAUAW

Cxcl2 ARE

Mus musculus	UUAUUUAUUUAUCUAUGUAUUUAUUUAUUUAUU
Homo sapiens	UUAUUUAUUUAUUUAUUUAUUUAUUUGUUUGUU
Rattus norvegicus	UUAUUUAUUUAUAUAUGUAUUUAUUUAUUUAUU
Sus scrofa	UUAUUUAUUUAUAUGUGUAUUUAUUUAUUUAUU
Bos taurus	UUAUUUAUUUAUAUACGUAUUUAUUUUUUCAAAG
Consensus	UUAUUUAUUUAUHURYKUAUUUAUUUDUYWRWK

Figure S3 3′ UTRs of *Il1*, *Il6* and *Cxcl2* contain conserved AREs. (*A*) *Il1a*, *Il6* and *Cxcl2* sequences of murine 3′ UTRs of *Il1a*, *Il6* and *Cxcl2* are shown. The minimal ARE sequence AUUUA is highlighted in bold, UAUUUAU sequences representing the core TTP binding site are underlined, ideal TTP binding consensus sequences UUAUUUAUU are in boxes. (*B*) ARE-containing regions of murine *Il1a*, *Il6* and *Cxcl2* were aligned with the corresponding 3′ UTRs of 4 other species, and consensus sequences were derived.

Dusp1
3' UTR

AGUUGUAUGUUUGUUUAUUUAUGAUCUGAAGUAAUAUAUUUCUUCUUCUGAGAAGACAUUUUGUUACUGGGAUGACUUUUUUUAUACAACA
GAAUAAAUUAUGACGUUUCGGGCAAGGGGAGGUGUGGGAGUUUCACUUGCCACCGGGUCGCCACUCCUCCUGUGGGAGGAGCAAUGCAAUAAC
UCUGGGAGAGGCUCAUGGGAGCUGGUCCUUAUUUAUUUAAACACCCCCCUCACCCCCCAACUCCUCCUGAGUUCCACUGAGUUCCUAAGCA
GUCACAACAAUGACUUGACCGCAAGACAUUUGCUGAACUCGGCACAUUCGGGACCAAUAUAUUGUGGGUACAUCAAGUCCCUCUGACAAAAC
AGGGCAGAAGAGAAAGGACUCUGUUUGAGGCAGUUUCUUCGCUUGCCUGUUUUUUUUUUUCUAGAAACUUCAUGCUUGACACACCCACCAGU
AUUAACCAUUCCCGAUGACAUGCGCGUAUGAGAGUUUUUACCUUUAUUUAUUUUUGUGUAGGUCGGUGGUCUGCCUUCACAAAUGUCAUUG
UCUACUCAUAGAAGAACCAAAUACCUCAAUUUUGUGUUUGCGUACUGUACUAUCUUGUAAAUAGACCCAGAGCAGGUUUGCUUUCGGCACUG
ACAGACAAAGCCAGUGUAGGUUUGUAGCUUUCAGUUAUCGACA

Dusp2
3' UTR

GGCAAAGCCCAGCCUGGCCCCACCCACAGCUCUGGCUUUGACUGACUCCUGGGGGAAGCUGCUGUGGCCCAGCUCCUCCCUCCUCAUCUUGCC
GUCCCACUGGGGGUGCUAGGAAAUCCAGGAUGACGGCUGCUCUCGAUAUGGUGCUCUUCUGAGGUGGCAUAAGGGCUGGCCCUUAUUUGCUCUCC
CUCCUUCGACUUGCAGAAAUUAAUUUAAUUAAUUAAUUAAUUAACUAUAUUAAAGCCCUUGGUCACCCAAGGGCUCAGAAAACAAGCUGUGACAA
GCAGAAACCAUGUCUAGGGGUGUGCAGCCCUUGACCCAAAGCUUAAGCCUUGUGCUCCCAGGGGAGCCAGGAAGUGACGUGUGUGUCAUGUUA
CGGACAUCUGACUUUUGUGUGUGUGUGUGUGGGGCAUCUCGCUGUAAUUGGUGCUGAAAAGUUAUUUGUGUUCAACUGAC AUUUAACGCUCUC
UCCCCAACUUCCUCCCGGCCCUGUGGGCCAGGGAGGGGCGUUGGAAACAGCACUUUAUAUUUAUAUAGAACAUUGAGGUUGUGUCAAUAAAA
ACAGUGUUUUGUUU

Figure S4 3´ UTRs of *Dusp1* and *Dusp2* contain core TTP binding heptamers but are not destabilized by TTP. The mRNAs of *Dusp1* and *Dusp2* are unstable but not TTP-destabilized. The minimal ARE sequence AUUUA is highlighted in bold, UAUUUAU sequences representing the core TTP binding site are underlined, ideal TTP binding consensus sequences UUAUUUAUU are in boxes.

Table S1. Complete list of unstable mRNAs (total 1090) containing 309 (28%) mRNAs which display TTP-dependent decay

Nr.	mRNA accession nr.	Gene name	P value for decay in WT	P value for TTP-dependent decay	Half-life in WT	Half-life in TTP-/-	number of AREs in 3'UTR
1	NM_013693	*Tnf*	0	0	21.20946	207.5789	8
2	NM_008176	*Cxcl1*	0	0.0000002	31.07276	567.1402	7
3	NM_009140	*Cxcl2*	0	0.0000004	47.29714	stable	11
4	NM_009404	*Tnfsf9*	0	0.000013	28.70494	65.04472	2
5	NM_008348	*Il10ra*	0	0.0000224	40.38975	129.8841	3
6	NM_011756	*Zfp36*	0	0.0000521	24.46368	60.25917	3
7	NM_175666	*Hist2h2bb*	0	0.0003104	41.63198	89.00077	0
8	NM_010104	*Edn1*	0	0.0005397	31.2201	54.49831	3
9	NM_017373	*Nfil3*	0	0.0012455	38.09607	75.15834	0
10	NM_152804	*Plk2*	0	0.002859	24.67139	43.03888	2
11	NM_008416	*Junb*	0	0.0035771	36.13899	65.6606	2
12	NM_010500	*Ier5*	0	0.0038812	40.37415	86.18643	2
13	NM_010907	*Nfkbia*	0	0.0047751	26.25408	44.57574	2
14	NM_018820	*Sertad1*	0	0.0050462	40.79785	82.93476	0
15	NM_007707	*Socs3*	0	0.0071504	24.42704	37.86671	4
16	NM_019873	*Fkbpl*	0	0.007719	48.22481	80.79188	0
17	NM_007746	*Map3k8*	0	0.0093796	36.49274	57.6634	4
18	NM_178199	*Hist1h2bl*	0	0.0247592	44.42711	70.24036	0
19	BC011440	*LOC665622*	0	0.0370359	45.39825	67.83972	0
20	NM_178201	*Hist1h2bn*	0	0.0372713	46.37479	70.85897	0
21	NM_009397	*Tnfaip3*	0	0.0409466	27.56316	39.03424	5
22	NM_030609	*Hist1h1a*	0	0.043499	46.7165	64.72092	0
23	NM_053109	*Clec2d*	0	0.0611456	32.90272	43.60137	2
24	NM_007679	*Cebpd*	0	0.0959877	44.16169	59.76528	5
25	NM_020034	*Hist1h1b*	0	0.1940511	37.32267	47.86972	0
26	NM_013642	*Dusp1*	0.0000001	0.2650471	25.02538	27.60435	4
27	NM_010090	*Dusp2*	0.0000001	0.2834996	26.30208	30.07205	4
28	NM_147155	*Tagap1*	0.0000001	0.0184291	30.23063	48.70641	1
29	NM_145968	*Tagap*	0.0000001	0.0199915	30.59076	51.16997	1
30	NM_009895	*Cish*	0.0000001	0.0003343	34.40339	129.21	3
31	NM_133662	*Ier3*	0.0000001	0.0081914	38.94605	62.66906	5
32	NM_175660	*Hist1h2ab*	0.0000001	0.0175598	39.46088	63.71486	0
33	NM_007413	*Adora2b*	0.0000001	0.0686846	43.45355	60.57669	3
34	NM_178195	*Hist1h2bf*	0.0000001	0.0425455	47.16311	70.10726	0
35	NM_146118	*Slc25a25*	0.0000001	0.00264	47.26885	100.4739	3
36	NM_008321	*Id3*	0.0000001	0.0002816	47.79365	152.2342	0
37	NM_008654	*Myd116*	0.0000001	0.0012735	48.36718	117.2872	4
38	NM_011227	*Rab20*	0.0000001	0.0014769	49.06124	120.4097	0
39	NM_008965	*Ptger4*	0.0000001	0.0291617	49.32638	75.69801	5
40	NM_007548	*Prdm1*	0.0000001	0.0273941	49.42345	75.54951	6

41	NM_172142	Nfkbid	0.0000001	0.0005073	51.51403	132.7398	1
42	NM_013562	Ifrd1	0.0000001	0.0897321	51.98328	72.51007	1
43	NM_001097979	RP23-38E20.1	0.0000001	0.0279283	52.03329	81.72102	0
44	NM_178216	Hist2h3c1	0.0000001	0.070857	52.03679	80.3983	0
45	NM_145073	Hist1h3g	0.0000001	0.0751702	52.56248	81.74907	0
46	NM_053074	Nup62	0.0000001	0.0101932	52.97086	90.29656	1
47	NM_033596	Hist2h4	0.0000001	0.0118277	55.87829	98.9998	0
48	NM_175662	Hist2h2ac	0.0000001	0.3180427	55.97639	65.61534	0
49	NM_178200	Hist1h2bm	0.0000001	0.0024485	56.0315	115.9365	0
50	NM_178212	Hist2h2aa2	0.0000001	0.40988	56.12068	63.12482	0
51	NM_013549	Hist2h2aa1	0.0000001	0.4075366	57.14079	64.25436	0
52	NM_178184	Hist1h2an	0.0000001	0.326447	58.23676	68.50827	0
53	BC052902	Gdap10	0.0000002	0.5700381	33.34789	40.06458	3
54	NM_178892	Tiparp	0.0000002	0.415153	41.42411	52.47923	9
55	NM_178215	Hist2h3b	0.0000002	0.0881301	52.97477	81.70949	0
56	NM_013550	Hist1h3a	0.0000002	0.0784766	52.99493	84.19713	1
57	NM_009969	Csf2	0.0000003	0.001545	35.72238	81.79367	9
58	XR_032641	LOC668786	0.0000003	0.0473939	43.78877	72.29813	0
59	NM_175657	Hist1h4m	0.0000003	0.0518978	54.41408	88.28547	0
60	NM_175661	Hist1h2af	0.0000003	0.5219671	63.59633	69.20645	0
61	NM_178185	Hist1h2ao	0.0000003	0.4500718	63.65899	71.19939	0
62	NM_008390	Irf1	0.0000004	0.0739166	34.85353	62.6254	3
63	NM_153287	Axud1	0.0000004	0.0167641	38.37771	77.97565	5
64	NM_175934	Ppp1r10	0.0000004	0.0352756	40.2941	78.69479	1
65	NM_133228	Zfp87	0.0000004	0.2882798	43.99162	53.32952	1
66	NM_133840	Clp1	0.0000004	0.322674	46.52348	57.74703	2
67	NM_178193	Hist1h4b	0.0000004	0.045012	56.15911	94.19868	0
68	NM_172911	D8Ertd82e	0.0000004	.0137223	57.09145	87.40008	1
69	NM_178183	Hist1h2ak	0.0000004	0.0621625	58.93389	92.54414	0
70	NM_007930	Enc1	0.0000004	0.0004381	62.21797	232.0883	10
71	NM_026407	Tmem39a	0.0000004	0.000474	68.22743	252.0579	1
72	NM_145839	Rasgef1b	0.0000005	0.0312997	42.89136	92.18893	2
73	NM_011057	Pdgfb	0.0000005	0.0004302	47.33222	162.8042	3
74	NM_013923	Rnf19a	0.0000005	0.1260749	50.55379	68.92483	3
75	NM_133819	Ppp1r15b	0.0000006	0.051471	63.26241	99.99386	1
76	NM_178218	Hist3h2a	0.0000007	0.1462923	55.80485	72.58689	8
77	NM_148924	Zfp263	0.0000008	0.0393433	60.60091	102.7487	3
78	NM_008842	Pim1	0.0000009	0.0004057	73.08955	380.7073	1
79	NM_030064	Phf23	0.000001	0.1248099	61.68012	83.68379	0
80	BC020005	1200011M11Rik	0.0000011	0.0178721	68.46593	131.2366	1
81	NM_023233	Trim13	0.0000012	0.3589248	40.41363	48.32103	0
82	NM_010118	Egr2	0.0000013	0.001656	65.02383	192.3418	3
83	NM_020579	B4galt3	0.0000015	0.0000155	67.91434	Stable	2
84	NM_144549	Trib1	1.6E-06	0.2614963	54.25024	62.07845	0
85	BC044749	2310057M21Rik	0.0000018	0.4339355	61.28806	67.35324	3
86	ENSMUST00000101675	OTTMUSG00000017540	1.9E-06	0.6412799	35.26682	41.43305	0

87	NM_010548	*Il10*	0.0000022	0.0005031	28.48885	151.3574	6
88	NM_178197	*Hist1h2bh*	0.0000024	0.4349102	69.63239	76.25005	0
89	NM_175664	*Hist1h2bb*	0.0000029	0.5723425	42.00737	50.35726	0
90	NM_007634	*Ccnf*	0.0000029	0.0328424	63.17174	114.6005	0
91	NM_133210	*Sertad3*	0.000003	0.3888468	61.87747	75.70344	1
92	BC057309	*6430706D22Rik*	0.000003	0.0232259	63.47725	150.7914	2
93	NM_009896	*Socs1*	0.0000031	0.0892753	59.86748	89.78243	0
94	NM_172683	*Pogz*	0.0000032	0.0663501	70.08822	121.2578	1
95	NR_002840	*Gas5*	0.000004	0.066432	42.22211	78.14149	0
96	NM_144913	*Mepce*	0.0000042	0.0096295	64.35172	150.3181	0
97	NM_028778	*Nuak2*	0.0000042	0.1414955	71.65578	97.28803	2
98	NM_010499	*Ier2*	0.0000044	0.4567824	65.30931	69.59225	0
99	NM_015811	*Rgs1*	0.0000046	0.0718006	41.41418	50.35538	4
100	NM_175654	*Hist1h4d*	0.0000046	0.0387486	68.78784	128.0309	0
101	NM_008655	*Gadd45b*	0.0000046	0.4442298	72.60359	78.75101	0
102	NM_011361	*Sgk1*	0.0000048	0.0316435	52.58946	115.9604	3
103	NM_010938	*Nrf1*	0.0000051	0.0087758	81.39296	187.7963	2
104	NM_133753	*Errfi1*	0.0000052	0.0860016	46.10209	62.62744	4
105	NM_153159	*Zc3h12a*	0.0000052	0.0166611	61.9993	108.4246	3
106	NM_145958	*Kbtbd2*	0.00000545	0.2323126	72.91182	103.0283	3
107	NM_197993	*Tut1*	0.0000059	0.0962438	73.32871	113.3501	0
108	NM_008562	*Mcl1*	0.000006	0.2501675	80.87278	104.3098	8
109	NM_019840	*Pde4b*	0.0000062	0.313077	64.10926	82.99424	3
110	ENSMUST00000110674	*Lcmt2*	0.0000064	0.1547163	70.63992	102.7819	4
111	NM_028810	*Rnd3*	0.0000066	0.786317	65.03631	61.10496	4
112	NM_007483	*Rhob*	0.0000071	0.0624429	55.93983	114.8131	3
113	NM_008873	*Plau*	0.0000073	0.0013336	81.01594	437.729	2
114	NM_175655	*Hist1h4f*	0.000008	0.2227861	61.04208	82.77347	0
115	BC031781	*BC031781*	0.0000083	0.1070299	68.95588	98.12597	2
116	NM_175045	*Bcor*	0.0000084	0.0045317	81.71792	223.7878	3
117	NR_003508	*Mx2*	0.0000086	0.3860922	52.00646	54.07889	0
118	NM_029571	*Kti12*	0.0000086	0.0149454	77.10979	174.0718	0
119	NM_001012236	*Trex1*	0.000009299	0.0169041	83.36407	201.0275	0
120	NM_009372	*Tgif1*	0.0000096	0.2418402	74.87886	105.8934	0
121	NM_001033299	*Zfp217*	0.0000102	0.94269498	66.24146	50.83258	1
122	NM_031172	*Trim17*	0.0000104	0.3271127	76.56865	91.64894	0
123	AK051045	*Snhg1*	0.0000113	0.0720629	48.9048	116.3409	0
124	NM_031403	*Dbr1*	0.0000121	0.0518658	75.32602	141.4493	2
125	NM_001013769	*Rsl1*	0.0000136	0.94432965	67.33081	55.82862	2
126	NM_153789	*Mylip*	0.0000136	0.1744088	67.51724	90.11933	1
127	NM_197992	*Pcgf1*	0.0000169	0.0171259	62.99447	163.8532	1
128	NM_134048	*Cbll1*	0.000018	0.0081741	79.75485	254.7972	0
129	NM_010554	*Il1a*	0.0000182	0.0044801	73.3755	354.8769	3
130	NM_024199	*Cstf1*	0.0000202	0.0050042	84.1717	325.3229	0
131	NM_028862	*Rnf145*	0.0000211	0.0901283	91.30077	159.3653	5
132	NM_145610	*Ppan*	0.0000252	0.0347599	77.54692	151.4984	0

133	NM_010496	*Id2*	0.000026	0.0099571	95.30773	315.3409	3
134	NM_008250	*Hlx*	0.0000271	0.0790647	69.34659	99.08736	0
135	NM_173399	*Zbtb5*	0.0000304	0.2469218	68.45349	90.26299	2
136	NM_019937	*Ccnl1*	0.0000307	0.5719629	70.99635	81.81878	2
137	NM_021419	*Rnf8*	0.0000314	0.0647366	83.8056	159.4749	0
138	NM_001081175	*Itpkb*	0.0000339	0.0114582	74.5215	165.0719	0
139	NM_153566	*Yrdc*	0.0000342	7.78E-05	96.29956	stable	7
140	NM_001039939	*Asxl1*	0.0000359	0.2982634	86.72262	109.5009	4
141	NM_145857	*Nod2*	0.0000386	0.0451037	75.24799	146.9582	4
142	AF357390	*Rpl27a*	0.0000396	0.590539	70.9312	74.96649	0
143	NM_030612	*Nfkbiz*	0.0000414	0.7170741	95.02451	98.54103	4
144	NM_009281	*Zfp143*	0.0000427	0.533091	84.27438	96.16221	4
145	NM_001113460	*Tec*	0.000043	0.6080858	82.47814	89.58366	1
146	NM_009716	*Atf4*	0.0000435	0.0291161	91.07642	202.5213	0
147	NM_009733	*Axin1*	0.0000438	0.0048987	92.56337	343.3646	0
148	NM_174989	*Ticam1*	0.0000443	0.162546	86.27498	125.3563	0
149	NM_001042634	*Clk1*	0.0000452	0.94734097	75.80821	63.42952	1
150	NM_026772	*Cdc42ep2*	0.0000483	0.0898276	85.29161	140.3009	0
151	NM_175530	*Fbxo46*	0.0000484	0.2878145	75.93861	102.2323	1
152	NM_015759	*Fgd3*	0.0000503	0.4470993	97.08098	110.1666	0
153	NM_001081214	*Pprc1*	0.0000528	0.0096125	79.83682	302.5386	0
154	AK164247	*Nfxl1*	0.0000561	0.4049874	64.52218	73.04768	0
155	NM_010902	*Nfe2l2*	0.0000582	0.0626975	79.77501	178.8517	1
156	NM_001024726	*Zfp607*	0.0000619	0.179446	79.51246	113.3518	3
157	NM_011497	*Aurka*	0.0000623	0.0918944	91.10654	165.5125	1
158	NM_175652	*Hist4h4*	0.0000636	0.0180393	85.55882	245.1856	0
159	NM_028005	*2310047M10Rik*	0.0000637	0.0290036	88.86797	209.0606	0
160	NM_008297	*Hsf2*	0.000064	93.60	93.60798	288.9954	4
161	NM_031168	*Il6*	0.0000653	0.0047999	76.9014	269.3892	5
162	NM_015790	*Icosl*	0.0000653	0.0136124	91.67319	411.1724	1
163	NM_027496	*5730557B15Rik*	0.0000659	0.0278175	97.39371	232.3369	2
164	NM_176933	*Dusp4*	0.000066	0.0111659	85.07239	299.8753	2
165	NM_025649	*Mad2l1bp*	0.0000671	0.1226232	81.61582	119.7792	0
166	NM_145148	*Frmd4b*	0.0000687	0.2357251	96.4132	146.7675	1
167	XM_905850	*LOC382523*	0.000069	0.0552914	100.2242	203.3098	0
168	NM_007935	*Epc1*	0.0000693	0.342332	94.43004	116.0002	1
169	NM_007569	*Btg1*	0.0000701	0.1392832	101.5094	159.2372	11
170	NM_145576	*Zfp212*	0.0000752	0.2821981	85.68939	110.6892	2
171	NM_146253	*Zbtb6*	0.0000762	0.2547525	77.28714	108.7488	8
172	NM_011333	*Ccl2*	0.0000776	0.0048941	85.29748	409.1243	1
173	NM_178623	*2010005J08Rik*	0.0000791	0.0141547	76.85228	339.9703	1
174	NM_170756	*Spata2*	0.0000806	0.0990813	87.52095	150.0288	4
175	NM_001081229	*Tsc22d2*	0.0000839	0.1657929	104.9323	160.46	17
176	NM_015787	*Hist1h1e*	0.0000844	0.1357618	92.03555	135.7393	1
177	NM_010755	*Maff*	0.0000846	0.0013232	94.76328	Stable	4
178	NM_007464	*Birc3*	0.0000881	0.2215159	106.7708	155.1429	4

179	NM_011813	Fiz1	0.0000886	0.057459	82.58043	180.077	0
180	NM_001045514	Akna	0.0000899	0.0970136	90.94035	156.5171	1
181	NM_001039967	1200003I07Rik	0.0000946	0.3179906	98.06242	126.8721	3
182	NM_009422	Traf2	0.0000948	0.2927149	98.19867	138.9176	1
183	NM_030715	Polh	0.0001019	0.0217162	101.64	286.8874	0
184	NM_025699	3230401D17Rik	0.0001041	0.3675968	90.91136	117.8448	1
185	NM_023598	Arid5b	0.0001058	0.587234	84.73553	93.54601	1
186	AY036118	AY036118	0.0001082	0.012419	54.60362	150.2074	0
187	NM_011893	Sh3bp2	0.0001132	0.1522846	90.98366	163.9408	0
188	NM_018808	Dnajb1	0.0001149	0.1242093	95.71044	152.2759	0
189	NM_145827	Nlrp3	0.0001196	0.1091044	101.6229	172.1766	5
190	NM_153800	Arhgap22	0.0001246	0.0403633	93.06388	278.6566	0
191	NM_178729	Fbxl5	0.0001256	0.1367113	73.65052	118.3019	5
192	NM_021556	Mrps30	0.0001297	0.0073716	103.6673	528.8957	3
193	BC046791	D530033C11Rik	0.0001304	0.4156937	102.5073	127.6878	0
194	NM_009740	Bcl10	0.0001311	0.1112692	112.4779	203.0198	2
195	NM_144797	Metrnl	0.0001337	0.0483161	106.9434	257.0127	3
196	NM_178707	Zfp592	0.0001387	0.0174332	103.7756	323.1831	1
197	NM_027514	Pvr	0.0001394	0.0689445	119.9497	249.2952	5
198	NM_013652	Ccl4	0.0001399	0.0050759	106.2439	stable	2
199	NM_177643	Zfp281	0.0001414	0.818766	70.8731	72.40865	2
200	NM_027404	Bag5	0.0001436	0.0403323	100.7644	233.7367	2
201	NM_183263	Rnmtl1	0.0001462	0.0297792	105.9154	264.12	0
202	NM_030178	Brpf1	0.0001465	0.2071171	95.87987	128.0692	1
203	NM_026040	Srfbp1	0.0001523	0.2138732	71.77872	115.8815	1
204	ENSMUST00000085177	Msl2l1	0.0001525	0.7688691	95.78151	86.57158	9
205	NM_033601	Bcl3	0.0001525	0.0132693	106.1592	421.5771	0
206	NM_010278	Gfi1	0.000161	0.0650334	93.53847	184.2812	2
207	NM_001115153	Uspl1	0.0001666	0.4664354	100.3201	118.8914	0
208	NM_153119	Plekho2	0.0001667	0.0738975	109.5935	214.7007	1
209	NM_031252	Il23a	0.0001671	0.0028789	108.708	stable	6
210	NM_007713	Clk3	0.0001696	0.022045	119.3717	378.8346	1
211	BC013092	A830007P12Rik	0.0001728	0.0192311	102.1929	316.6174	2
212	NM_178668	E430028B21Rik	0.0001745	0.0887326	102.0869	196.6615	6
213	NM_198169	Gmeb2	0.0001748	0.1173792	95.84213	193.4571	4
214	NM_008361	Il1b	0.0001762	0.0113839	101.8997	stable	4
215	NM_013822	Jag1	0.0001777	0.0063803	114.3891	stable	10
216	NM_028023	Cdca4	0.0001893	0.2049229	112.364	178.9679	4
217	NM_022981	Zfp110	0.0002012	0.2553002	85.82894	129.5554	2
218	NM_019914	Mllt11	0.0002083	0.0029921	97.47539	stable	10
219	NM_026758	Mphosph6	0.000211	0.0053825	120.25	stable	2
220	NM_024467	Zfp319	0.0002112	0.1411859	83.6661	164.0794	0
221	NM_145996	Arid5a	0.0002158	0.1412889	88.67761	176.1851	2
222	NM_009044	Rel	0.0002186	0.7998143	101.0554	95.56135	2
223	ENSMUST00000082411	ND3	0.0002257	0.4532691	114.3241	139.9843	0
224	NM_029749	Usp42	0.0002325	0.529691	72.20015	91.04434	5

225	NM_027871	Arhgef3	0.0002329	0.2662817	100.1195	162.7741	3
226	NM_172555	Papolg	0.0002334	0.0172615	85.59707	390.6789	3
227	NM_172593	Mier3	0.0002373	0.1718187	101.6027	164.2684	13
228	NM_133906	Zkscan1	0.0002391	0.6699961	98.5411	107.9961	9
229	NM_026193	Ap4b1	0.0002436	0.4690591	110.3216	132.9846	1
230	NM_026350	Ccdc130	0.0002462	0.0219701	115.9486	385.3613	1
231	NM_026689	Mul1	0.0002584	0.0783594	115.465	243.4337	0
232	BC056964	Josd3	0.0002658	0.1127224	83.4345	169.2556	0
233	BC028641	2010109K11Rik	0.0002808	0.4051918	121.521	158.6563	0
234	NM_173423	Fem1c	0.0002842	0.80384	97.35305	93.5715	0
235	NM_025945	Polr3d	0.0002868	0.0062517	111.0472	stable	2
236	NM_009743	Bcl2l1	0.0002942	0.0303611	105.821	354.2126	1
237	ENSMUST00000052168	Otud1	0.0003068	0.1484392	53.35249	107.1038	3
238	NM_018807	Plagl2	0.0003075	0.3777822	109.415	129.8803	5
239	NM_026277	Nob1	0.0003149	0.0664285	114.3251	276.9167	0
240	NM_008453	Klf3	0.0003204	0.6271218	117.569	118.539	2
241	NM_172598	Wdhd1	0.0003238	0.069538	111.131	257.919	0
242	NM_177684	Zfp637	0.0003252	0.6711591	104.8644	-08.7896	0
243	BC004040	Cnot8	0.0003322	0.0002385	113.1419	stable	3
244	NM_007772	Hivep1	0.0003348	0.0605405	111.1305	262.8044	1
245	NM_013684	Tbp	0.0003469	0.0650171	119.008	287.1577	4
246	NM_134139	Wdr74	0.0003475	0.0257198	127.8059	431.4594	0
247	NM_001081298	Lphn2	0.0003477	0.0003298	80.84893	stable	3
248	NM_146000	Bud13	0.0003543	0.0456656	115.0802	283.7594	1
249	NM_010577	Itga5	0.000361	0.0132158	107.2288	465.5728	2
250	NM_011378	Sin3a	0.0003667	0.062822	96.15673	189.1017	2
251	NM_172518	Fbxo42	0.0003848	0.0181999	111.0115	stable	5
252	NM_001033463	Tatdn2	0.0004106	0.0676229	125.5614	298.5259	0
253	NM_023750	Zfp84	0.0004166	0.6838565	74.92527	92.04053	10
254	NM_001110159	Nxt1	0.0004307	0.188458	110.546	172.8881	0
255	NM_025884	Zfp830	0.0004329	0.8074997	108.9646	98.44964	6
256	NM_029846	Atg16l1	0.0004365	0.0637691	122.8265	331.4264	2
257	NM_009628	Adnp	0.0004401	0.1452652	123.0882	221.1213	2
258	NM_025825	Appbp2	0.0004468	0.4466022	119.5683	147.0667	1
259	XR_032694	LOC675799	0.0004482	0.0535779	103.0326	278.358	0
260	NM_145546	Gtf2b	0.0004559	0.1741231	141.7247	213.3881	2
261	NM_013745	Nufip1	0.0004679	0.696931	100.8099	115.1341	12
262	NM_178872	Trim36	0.0004752	0.3397578	122.6696	171.185	6
263	NM_178918	Utp15	0.0004786	0.3318751	109.0351	163.9723	6
264	NR_002900	Snora69	0.000479	0.0363566	93.36411	253.9381	0
265	NM_174850	Micall2	0.0004828	0.0015207	106.6406	stable	0
266	NM_144523	Zfp622	0.0004984	0.3583436	126.5201	145.6503	3
267	NM_009054	Trim27	0.0005045	0.2336442	111.9438	147.6454	0
268	NM_172860	Cbfa2t2	0.0005279	0.0041676	109.3274	stable	6
269	NM_019653	Wsb1	0.0005427	0.4292457	138.1236	164.9791	5
270	NM_029682	Stambpl1	0.0005646	0.0883077	109.3231	259.4203	2

271	NM_009551	*Zfand5*	0.0005656	0.1346127	99.01123	179.1798	4
272	NM_008882	*Plxna2*	0.0005734	0.003583	122.6367	stable	7
273	NM_001025597	*Ikzf1*	0.0005795	0.0989966	122.2146	stable	4
274	NM_001081379	*Ankrd11*	0.0006059	0.1370491	122.1577	206.091	1
275	NM_011633	*Traf5*	0.0006074	0.0361629	124.1481	380.4496	1
276	NM_011113	*Plaur*	0.0006103	0.0080586	136.3904	stable	2
277	NM_009883	*Cebpb*	0.0006134	0.0757638	109.8739	206.0642	0
278	NM_026453	*Rbm13*	0.0006183	0.0680904	105.5855	320.1295	2
279	NM_198162	*Morc2a*	0.0006189	0.0541732	130.6895	346.5298	1
280	NM_181593	*Itpkc*	0.0006214	0.089121	121.4487	258.2995	1
281	NM_138747	*Nol1*	0.0006273	0.38724	123.2204	149.5828	1
282	NM_025934	*Riok2*	0.0006386	0.5362139	118.4677	129.6803	2
283	NM_172162	*Mizf*	0.0006451	0.1413603	115.1295	217.8915	1
284	NM_145569	*Mat2a*	0.000649	0.3950824	142.6725	181.5682	3
285	XR_031582	*LOC546077*	0.0006595	0.0046606	115.0041	stable	0
286	NM_009595	*Abl2*	0.0006637	0.0213515	120.2916	stable	8
287	NM_181403	*Vps37c*	0.0006649	0.0062617	117.1571	stable	1
288	NM_153537	*Phldb1*	0.0006709	0.0297879	126.8146	414.7206	0
289	NM_172876	*Gpatch3*	0.0006892	0.0320545	116.2632	465.1292	0
290	NM_010828	*Cited2*	0.0006895	0.104852	76.71955	253.0344	1
291	NM_145589	*Prr14*	0.0006936	0.0369452	134.5005	430.3081	0
292	NM_001033271	*Tmem55b*	0.0006941	0.0025332	130.5533	stable	1
293	NM_011615	*Dedd*	0.0007019	0.3486343	124.8467	173.8428	1
294	AK089165	*Dpep2*	0.0007037	0.3903677	79.12793	124.6369	0
295	NM_011574	*Cirh1a*	0.0007079	0.1454449	144.5073	267.8345	0
296	M13967	*Hspa8*	0.0007101	0.0164364	97.94553	516.6369	0
297	NM_175092	*Rhof*	0.0007265	0.1718921	119.0312	190.5497	1
298	NM_148933	*Slco4a1*	0.000744	0.5225831	126.5516	140.2681	1
299	NM_011408	*Slfn2*	0.0007462	0.7050187	159.8424	145.8909	0
300	NM_028881	*Crtc2*	0.0007565	0.0053346	133.0205	stable	0
301	XM_001480385	*LOC433036*	0.0007677	0.96867568	90.58028	72.12375	0
302	NM_015747	*Slc20a1*	0.0007736	0.048614	133.807	446.4174	2
303	NM_194334	*Tbc1d2b*	0.000779	0.1567234	114.4574	199.2912	4
304	NM_009890	*Ch25h*	0.000792	0.0685088	117.794	306.4119	3
305	NM_019921	*Akap10*	0.0007957	0.1812812	80.11519	141.7569	4
306	NM_009410	*Top3a*	0.0008072	0.0527088	97.95759	307.1658	0
307	NM_023502	*Elf2*	0.0008174	0.5001145	102.1038	121.5551	0
308	ENSMUST00000030584	*Rnf19b*	0.0008329	0.0762434	145.3386	402.7923	0
309	NM_008057	*Fzd7*	0.0008446	0.0173227	116.6451	stable	3
310	NM_175930	*Rapgef5*	0.000855	0.045012	92.52231	272.3725	0
311	BC085269	*Rps13*	0.0008564	0.1236072	89.02569	140.8792	0
312	NM_013654	*Ccl7*	0.00086	0.0314306	116.6052	453.9574	2
313	NM_011337	*Ccl3*	0.0008641	0.0107849	183.5935	stable	5
314	NM_001085440	*Smcr8*	0.0008716	0.2401219	130.372	228.7247	6
315	ENSMUST00000029662	*Alpk1*	0.000874	0.8352189	93.77643	88.6948	0
316	NM_001083318	*Etv3*	0.0008965	0.7389497	116.1498	104.9399	8

317	BC117501	*F630043A04Rik*	0.0009014	0.289726	121.3855	171.4509	0
318	NM_207680	*Bcl2l11*	0.0009072	0.2950965	144.1961	185.8269	6
319	NM_177003	*9630033F20Rik*	0.0009354	0.0373271	136.1025	526.5473	4
320	NM_023140	*Glrx3*	0.0009356	0.0252038	114.8954	505.194	1
321	NM_178277	*A630042L21Rik*	0.0009576	0.0233988	126.1234	stable	3
322	NM_145376	*Lpcat1*	0.0009586	0.3679611	139.742	177.9579	0
323	NM_029623	*3110002H16Rik*	0.0009831	0.0592439	149.0687	stable	1
324	NM_001098237	*Zbtb3*	0.0009939	0.3976168	126.9471	161.5493	0
325	NM_133744	*Ccdc71*	0.0009948	0.2764493	134.3211	194.5093	3
326	NM_178891	*Prmt6*	0.000999	0.1973957	125.3894	199.8086	2
327	NM_199199	*Tmem199*	0.0010363	0.0263855	138.1015	stable	2
328	NM_025298	*Polr3e*	0.0010374	0.0239438	127.8366	383.4102	1
329	NM_001036293	*Nrbf2*	0.0010396	0.2827254	128.2122	188.628	2
330	NM_001013376	*Rpp38*	0.0010426	0.8254939	89.34579	87.00753	0
331	NM_010786	*Mdm2*	0.0010514	0.6065172	120.6445	137.1598	8
332	NM_001081417	*Chd7*	0.0010595	0.1785486	120.1246	181.8281	0
333	NM_027134	*Mtfmt*	0.001081	0.90181569	126.0417	101.1939	3
334	BC145719	*AA673488*	0.0011215	0.072639	133.3686	308.3654	0
335	NM_172734	*Stk38l*	0.0011285	0.0707798	124.6435	309.2709	2
336	NM_009462	*Usp10*	0.0011299	0.0762302	137.7803	337.9641	0
337	NM_025878	*Mrps18b*	0.0011306	0.0906064	152.3026	376.488	1
338	NM_030245	*Tada1l*	0.0011393	0.6735002	137.0845	133.3574	1
339	BC125631	*2310037I24Rik*	0.0011592	0.0702356	136.5603	398.6995	1
340	NM_027485	*Med26*	0.0011634	0.1493709	123.9213	221.4001	1
341	NM_010359	*Gstm3*	0.0011791	0.00056	110.9319	stable	0
342	NM_145706	*Nup43*	0.0011905	0.0382662	120.4956	533.2433	0
343	NM_145471	*Lrrc14*	0.0011919	0.0255774	128.0093	stable	1
344	NM_020006	*Cdc42ep4*	0.0012037	0.3075121	119.2527	166.3377	0
345	NM_027968	*Fbxo30*	0.0012075	0.97842938	80.19443	62.87601	3
346	NM_172584	*Itpk1*	0.0012177	0.035961	132.0104	491.1043	1
347	NM_009630	*Adora2a*	0.0012438	0.1574697	129.2348	258.7674	0
348	NM_009344	*Phlda1*	0.0012459	0.3176665	116.3841	163.9144	3
349	NM_023906	*Asb3*	0.0012464	0.0099289	137.31	stable	4
350	NM_198600	*Pols*	0.0012851	0.0077397	106.0294	stable	8
351	NM_153419	*Grwd1*	0.0012861	0.1382152	140.2543	245.2407	1
352	NM_181590	*Shq1*	0.0013038	0.0398789	128.2598	443.8558	1
353	NM_133966	*Taf5l*	0.0013051	0.0006444	104.3666	stable	2
354	NM_028727	*Nol9*	0.0013051	0.3610076	148.801	192.2323	0
355	NM_026779	*Mocos*	0.0013115	0.0060661	139.2315	stable	0
356	NR_002899	*Snora70*	0.0013222	0.121751	104.856	351.4576	0
357	NM_009424	*Traf6*	0.0013312	0.632484	127.6044	139.3634	8
358	BC116778	*1810013L24Rik*	0.0013482	0.4891308	139.7151	164.9648	0
359	NM_009862	*Cdc45l*	0.0013678	0.5551589	133.5258	148.3444	1
360	NM_007714	*Clk4*	0.0013736	0.7067274	91.99779	103.8237	0
361	NM_025926	*Dnajb4*	0.0013858	0.6740533	114.1145	128.0522	3
362	NM_133787	*Nmd3*	0.0014101	0.8218172	104.6224	104.7557	0

363	NM_010566	*Inpp5d*	0.0014117	0.0645992	137.1528	279.4161	0
364	NM_029498	*Zmym2*	0.00145	0.5308103	84.85286	119.2031	1
365	BC027368	*5930416I19Rik*	0.0014524	0.0384655	128.1461	465.0142	1
366	NM_130447	*Dusp16*	0.0014579	0.7016994	109.2798	106.3011	3
367	NM_177663	*Isg20l2*	0.0014796	0.0079972	132.3487	stable	1
368	NM_172699	*Foxj3*	0.0014883	0.6112388	124.1939	138.6764	8
369	NM_022015	*Taf8*	0.001531	0.1360911	127.4205	275.8892	2
370	NR_004414	*Rnu2*	0.0015414	0.0153132	71.63824	stable	0
371	NM_027091	*Nup35*	0.0015456	0.0035968	117.7347	stable	2
372	NM_001001187	*3830402I07Rik*	0.0015506	0.0259529	116.2942	582.86	0
373	NM_172612	*Rnd1*	0.0015549	0.2121812	84.61005	124.4145	1
374	NM_010093	*E2f3*	0.001556	0.2263012	131.231	212.357	6
375	NM_175028	*Adnp2*	0.0015586	0.6329905	129.8594	130.8903	1
376	NR_002842	*Rnu3a*	0.0015633	0.0016501	68.36265	stable	0
377	NM_173002	*Zxdc*	0.0015727	0.5660813	132.0905	152.5618	0
378	NM_011753	*Zfp26*	0.001584	0.8000233	96.0105	99.06173	16
379	NM_145604	*D230025D16Rik*	0.0016019	0.0214221	142.6981	stable	1
380	NM_133976	*Imp3*	0.0016264	0.0482142	134.2286	366.052	1
381	BC120889	*8030462N17Rik*	0.001631	0.0543039	115.7498	398.7204	5
382	NM_017407	*Spag5*	0.0016366	0.0137749	107.0899	stable	2
383	NM_008856	*Prkch*	0.0016455	0.0181898	139.103	stable	2
384	NM_011809	*Ets2*	0.0016679	0.0226189	147.1954	stable	6
385	NM_172402	*Slc25a32*	0.0017115	0.0099155	126.4432	stable	9
386	NM_175384	*Cdca2*	0.001715	0.0757277	129.1264	401.1519	1
387	NM_001113198	*Mitf*	0.0017206	0.0049164	94.64675	stable	7
388	ENSMUST00000101381	*C530030P08Rik*	0.0017321	0.992611597	121.7465	59.63765	0
389	NM_133978	*Cmtm7*	0.0017471	0.0054991	153.966	stable	1
390	NM_009085	*Rpo1-1*	0.001756	0.5974236	145.6372	153.7437	0
391	NM_013924	*Abt1*	0.0017812	0.3540049	139.8163	194.6453	3
392	NM_009875	*Cdkn1b*	0.0018001	0.3767134	122.0063	145.8552	5
393	NM_009834	*Ccrn4l*	0.0018073	0.1016081	151.3905	291.4825	4
394	NM_021788	*Sap30*	0.0018105	0.4365891	147.2355	197.2247	1
395	BC016463	*9430023L20Rik*	0.0018622	0.0087365	125.4546	stable	0
396	NM_001025387	*Brd2*	0.0018696	0.0991699	156.2477	400.8565	2
397	NM_139064	*Tnip2*	0.0018892	0.2869435	134.9719	178.5393	1
398	BC099925	*BC037112*	0.0018899	0.053546	124.9932	364.5614	0
399	BC014729	*8430410K20Rik*	0.0018911	0.7561559	131.3167	119.6314	2
400	NM_001081240	*AI931714*	0.0019291	0.2503755	141.8611	239.1996	0
401	NM_025518	*Dus2l*	0.0019553	0.0107634	150.3137	stable	0
402	NM_020587	*Sfrs4*	0.0020047	0.3245282	161.5658	220.2521	0
403	NM_138590	*Zcchc7*	0.0020106	0.2117511	104.1268	192.8042	0
404	NM_177374	*6720458F09Rik*	0.0020113	0.0192621	138.3322	stable	0
405	NM_010878	*Nck1*	0.002023	0.95293642	135.8066	92.26473	0
406	NM_011757	*Zscan21*	0.0020754	0.521313	134.171	158.9475	0
407	NM_026014	*Cdt1*	0.0021226	0.0124229	125.2222	stable	1
408	NM_019662	*Rrad*	0.0021459	0.5466951	138.8709	145.6839	0

409	BC052148	A430005L14Rik	0.0022721	0.4486273	131.0641	171.182	0
410	NM_146239	Pctk2	0.0023081	0.1795146	137.552	257.883	6
411	NM_016681	Chek2	0.0023246	0.4676268	131.4965	171.6289	0
412	NM_178208	Hist1h4c	0.0023306	0.0734498	114.9557	394.1127	0
413	NM_017397	Ddx20	0.0023434	0.131485	122.9687	332.1859	0
414	NM_001013368	E2f8	0.0023645	0.2250459	130.1446	264.1472	3
415	NM_133817	Zfp451	0.0023963	0.8375983	104.5619	101.67	0
416	NM_001081549	Rcan1	0.0024107	0.6631423	152.886	151.0258	0
417	NR_004432	Rnu12	0.0024552	0.0804566	114.2137	247.4516	0
418	NM_174852	Phf12	0.0024559	0.0588646	145.8208	382.8692	1
419	NM_011980	Zfp146	0.0024584	0.95168714	118.9436	94.17349	3
420	NM_175268	A930008G19Rik	0.00246	0.0362264	120.3607	stable	1
421	NR_004417	Rnu73a	0.0024957	0.167421	94.52005	145.3321	0
422	NM_172422	Fastkd2	0.0024965	0.5686457	150.8162	162.1365	3
423	NM_026949	Cnot8	0.0025096	0.0931686	162.6577	501.9902	3
424	NM_026267	Necap1	0.0025188	0.1091477	149.9447	408.4243	4
425	NM_021343	Spata5	0.0025274	0.6943334	107.832	128.1286	0
426	NM_020625	Zbtb22	0.0025572	0.0048477	148.0212	stable	1
427	NM_178210	Hist1h4j	0.0025766	0.0631537	117.4266	282.4838	0
428	NM_010360	Gstm5	0.0025965	0.0114749	130.9585	stable	0
429	BC076612	3110043O21Rik	0.0026001	0.94828217	162.1971	103.2676	5
430	NM_181650	Prdm4	0.0026175	0.0654203	157.4882	554.1864	3
431	NM_145636	Il27	0.0026237	0.0030587	114.7755	stable	0
432	NM_030701	Gpr109a	0.0026526	0.1264854	159.7179	367.9499	1
433	NM_010193	Fem1b	0.0027126	0.98212901	137.9291	86.29417	4
434	NM_001110832	Nfya	0.0027197	0.1411946	149.8982	311.8471	4
435	NM_025447	Dimt1	0.0027381	0.2034649	107.5557	224.8724	9
436	NM_001024919	2310022M17Rik	0.0028063	0.1040678	129.9792	300.7735	0
437	NM_007498	Atf3	0.0028484	0.3992037	93.56328	121.2412	3
438	XR_032128	LOC668990	0.002876	0.0742303	127.112	339.1498	0
439	NM_133706	Tmem97	0.0028774	0.0029688	126.483	stable	0
440	NM_145430	BC017647	0.0029017	0.6315117	141.0088	136.3642	2
441	NM_172269	Vps18	0.0029268	0.0411424	145.7146	stable	0
442	NM_021720	Donson	0.0030253	0.0032819	137.3796	stable	0
443	NM_178593	Rcsd1	0.0030278	0.1424987	150.5888	404.5024	3
444	NM_010436	H2afx	0.0030371	0.0724334	128.9033	344.3749	1
445	NM_146103	Tmem185b	0.0030388	0.0063322	150.1213	stable	1
446	NM_001039493	Plekhm3	0.00307	0.2870422	142.5932	229.8547	9
447	NM_178719	Smcr7l	0.0030901	0.1108239	139.1584	303.0548	10
448	NM_199322	Dot1l	0.0031028	0.0153945	144.9819	stable	3
449	NM_138660	Casc3	0.0031092	0.1326817	141.5932	302.0366	2
450	NM_001033198	Ankrd50	0.0031097	0.8072827	135.3994	105.0456	2
451	NM_001122676	Zcchc2	0.0031521	0.2609472	123.5624	258.2056	2
452	NM_001044386	Zfx	0.0031769	0.511565	111.5696	150.1239	13
453	NM_008715	Ints6	0.0032057	0.6063098	112.6302	146.2079	4
454	NM_011267	Rgs16	0.0032244	0.3667741	88.00611	137.0093	4

455	NM_172747	Kctd13	0.0032264	0.0010489	133.8763	stable	1
456	NM_177798	Frs2	0.0032503	0.7773505	137.2223	133.137	7
457	NM_028900	Gcc1	0.0032562	0.0980387	135.9178	382.0659	1
458	NM_172814	Lrp12	0.0033745	0.032466	121.1084	stable	7
459	NM_146154	Ppp1r8	0.0034194	0.0743889	149.1534	472.4854	2
460	NM_001081382	Zfp777	0.0034957	0.0663474	146.3644	509.5031	1
461	NM_019925	Gpr132	0.0034984	0.0686697	171.3333	stable	1
462	NM_016670	Pknox1	0.0035155	0.1147139	154.5495	354.4472	2
463	NM_001040400	Tet2	0.0035165	0.3613409	122.494	186.8832	7
464	NM_001081211	Ptafr	0.0035384	0.4980734	174.9081	180.9016	0
465	NM_007465	Birc2	0.0035404	0.3776557	133.0386	185.7116	1
466	NM_008197	H1f0	0.0035589	0.0351537	157.5332	stable	0
467	NM_130796	Snx18	0.0036069	0.5079227	144.5634	163.5552	7
468	NM_175175	Plekhf2	0.0036184	0.6941439	127.0406	116.0065	7
469	NR_004410	Rnu87	0.0036252	0.5778144	99.28949	80.25439	0
470	NM_153799	Edc3	0.0037228	0.5115759	154.9712	178.4878	0
471	NM_173001	Jmjd1a	0.0037782	0.2381193	104.6886	185.6355	2
472	NM_008872	Plat	0.0037898	0.134152	167.9118	383.0525	2
473	NM_178632	Ints7	0.0038167	0.1055277	145.8538	465.7157	1
474	NM_153416	Aaas	0.0038617	0.0165749	152.1561	stable	0
475	NM_030240	2900092E17Rik	0.0039241	0.2325154	151.5222	280.18	0
476	NM_175127	Fbxo28	0.0039309	0.3353479	137.4174	210.3253	4
477	NM_181854	Zfp828	0.0039414	0.2774225	123.1871	161.7749	1
478	NM_029578	Tgds	0.0039686	0.0153012	140.8455	stable	1
479	NM_172288	Nup133	0.003981	0.1696719	162.5262	395.9311	0
480	NM_008021	Foxm1	0.0040206	0.0623473	133.1162	stable	1
481	NM_010070	Dok1	0.004046	0.3238648	138.8138	230.8089	1
482	NM_021878	Jarid2	0.0040497	0.7991243	161.6046	146.5501	0
483	NM_011198	Ptgs2	0.0041577	0.0380289	139.2352	stable	12
484	NM_009856	Cd83	0.0042133	0.1934395	151.784	313.2239	2
485	NM_011231	Rabggtb	0.0042189	0.464674	178.5747	195.1663	1
486	NM_021513	Thap11	0.0042871	0.3101798	150.1682	186.8043	1
487	NM_019639	Ubc	0.0043168	0.2300285	198.1164	343.9516	0
488	NM_001045486	Zfp180	0.0043546	0.1698147	154.2241	341.4958	2
489	NM_029094	Pik3cb	0.0043673	0.2195043	177.4586	350.8449	5
490	XR_034114	LOC676530	0.0044186	0.1142956	126.0993	324.5138	0
491	NM_134097	Topors	0.0044468	0.97666961	133.956	95.20716	2
492	NM_025654	Rdm1	0.0044677	0.1918908	132.7002	270.0411	0
493	NM_030887	Jdp2	0.0044745	0.1770236	152.9108	318.1193	0
494	NM_175428	Zfp295	0.004551	0.7964	160.6561	140.2331	4
495	NM_019704	Tmem115	0.0047171	0.0532198	170.4053	stable	0
496	NM_024184	Asf1b	0.0047904	0.2878575	178.3142	310.3265	0
497	NM_011914	Whsc2	0.0048183	0.1038801	165.7143	451.1544	1
498	NM_144800	Mtss1	0.0048582	0.5437729	168.2778	174.6059	0
499	NM_010591	Jun	0.0048926	0.5117754	133.9433	162.3953	4
500	NM_182782	Klhl25	0.0049055	0.4219402	135.0214	187.5355	1

501	NM_148928	Gtf3c5	0.0049063	0.0025493	142.1698	stable	0
502	NM_133735	Ptcd1	0.0049083	0.3412903	144.8239	231.2193	0
503	NM_029274	Wbp7	0.0049453	0.0592621	146.2306	stable	1
504	NM_009396	Tnfaip2	0.0050232	0.0943573	220.1598	stable	2
505	NM_029585	Det1	0.0050462	0.0075516	147.2744	stable	1
506	NM_029581	Mtif3	0.0050604	0.3003564	155.2782	246.9551	1
507	NM_001033525	Kcnk6	0.0050732	0.0104294	165.6535	stable	2
508	BC020112	0610011L14Rik	0.005107	0.1817233	160.795	335.1445	1
509	NM_001099624	Rapgef2	0.0051429	0.7734397	153.299	135.7419	4
510	NM_028696	Obfc2a	0.0051918	0.7092458	146.8051	131.8883	4
511	NM_010303	Gna13	0.0052112	0.4740168	156.2078	201.9331	9
512	NM_022012	Map3k11	0.0052328	0.0727161	164.771	stable	0
513	NM_023054	Utp3	0.0052486	0.5745721	138.7468	152.7315	0
514	NM_178603	Mrpl50	0.0053066	0.1449263	130.7093	315.419	1
515	NM_001009935	Txnip	0.0053373	0.6766989	159.6034	159.2544	0
516	NM_172958	Mtmr12	0.0053677	0.2533099	136.6309	210.0556	3
517	NM_175433	Zfp710	0.0053874	0.2055959	134.7173	296.6813	2
518	NM_022323	Moap1	0.0053911	0.0816552	135.3615	stable	3
519	NM_011509	Supt4h2	0.0054612	0.0048609	183.9798	stable	0
520	NM_172839	Ccnj	0.0054958	0.5384996	121.9159	138.1631	5
521	NM_146083	Sfrs7	0.0055088	0.312888	178.2433	272.1753	3
522	NM_133761	Dcp1a	0.0055806	0.3293261	148.0223	239.8573	6
523	NM_001007465	Rffl	0.0056328	0.3500748	137.8817	197.6678	2
524	NM_145588	Kif22	0.0056366	0.0081252	155.3393	stable	0
525	NM_153547	Gnl3	0.0056452	0.8441686	104.0006	98.5866	0
526	ENSMUST00000054960	Irf2bp2	0.0056645	0.2405552	146.9909	262.6367	0
527	NM_011885	Mrps12	0.0057345	0.00824	140.1865	stable	0
528	NM_033604	Rnf111	0.0057611	0.0795914	165.1153	507.7773	7
529	NM_007658	Cdc25a	0.0057729	0.415055	160.017	205.5063	2
530	NM_029035	Spsb1	0.005781	0.0648092	161.2262	stable	4
531	XR_032234	LOC675534	0.0058715	0.1476672	155.9288	365.8708	0
532	NM_010731	Zbtb7a	0.0058894	0.0452536	149.9581	stable	2
533	NM_007672	Cdr2	0.0059103	0.1128903	149.9144	477.0067	2
534	NM_178446	Rbm47	0.0059362	0.0477534	186.8697	stable	8
535	NM_001017426	Jmjd3	0.00596	0.089602	156.0723	447.8215	3
536	NM_178782	Bcorl1	0.0059647	0.0092729	139.0386	stable	2
537	NM_013880	Plcl2	0.0060125	0.4163029	157.8039	199.1495	2
538	NM_001083810	2600010E01Rik	0.0060487	0.059208	137.8688	stable	6
539	NM_172663	Epc2	0.0061051	0.6742962	118.8514	140.6776	5
540	ENSMUST00000022566	Spata13	0.00613	0.1615795	140.7652	240.2306	6
541	NM_173453	Tmem11	0.0061832	0.436644	182.0114	220.9099	0
542	NM_001013392	Rreb1	0.0062658	0.7884696	137.3485	116.8855	7
543	BC057552	BC057552	0.0063959	0.0037034	156.2108	stable	2
544	NM_144798	Slc30a6	0.0064053	0.0282926	185.5565	stable	4
545	NM_181423	Supv3l1	0.0064257	0.1129537	148.3874	408.7246	0
546	NM_026054	2810474O19Rik	0.0064682	0.7999792	137.0946	98.52487	2

547	NM_010437	Hivep2	0.0065048	0.0533823	121.5931	378.3657	3
548	BC026926	C87436	0.0065051	0.4107509	160.0963	205.3871	0
549	NM_015769	Ercc4	0.0065339	0.0414862	151.1427	stable	1
550	NM_025991	Kbtbd4	0.0066004	0.2274792	174.3687	315.6504	0
551	NM_011636	Plscr1	0.006603	0.3118355	205.6788	305.7458	7
552	NM_023739	Nfx1	0.0066059	0.3280782	172.6731	245.9663	1
553	NM_026524	Mid1ip1	0.0066313	0.0610553	168.9097	stable	2
554	NM_134152	Lpxn	0.0066343	0.5105044	190.9715	232.7232	2
555	NM_146164	Lrch4	0.0066411	0.0036222	181.109	stable	1
556	NM_009298	Surf6	0.0066815	0.0647309	138.6377	stable	1
557	BC118934	2310022K01Rik	0.006704	0.0044348	155.3473	stable	0
558	NM_019996	Rnuxa	0.0067262	0.95382629	136.7392	102.1001	0
559	NM_145600	Zfp330	0.0067766	0.96347584	122.3414	91.81708	1
560	NM_026981	Dtwd1	0.0067946	0.5717667	179.5698	205.9891	1
561	ENSMUST00000098501	BC023892	0.0068225	0.6853006	139.0784	115.0535	0
562	NM_029896	Wdr82	0.0068253	0.0986982	194.0605	stable	5
563	NM_024187	U2af1	0.0068277	0.4592113	174.1055	238.3118	0
564	NM_172277	Snx8	0.0068558	0.0596074	183.1689	stable	0
565	NM_172268	Nup214	0.0068998	0.0026842	165.2772	stable	1
566	ENSMUST00000105502	Foxo3a	0.0070136	0.0238068	153.6327	stable	6
567	NM_008564	Mcm2	0.007079	0.0639414	179.4359	stable	1
568	NM_133665	Mef2d	0.0071066	0.0058038	164.8412	stable	0
569	NM_001033225	Pnrc1	0.0071186	0.2752927	192.3167	287.1516	1
570	NM_008652	Mybl2	0.0071534	0.0021537	161.0876	stable	0
571	NM_172511	Abhd10	0.0071604	0.0596411	153.7355	stable	4
572	NM_025716	Spryd4	0.0071941	0.5755174	162.8983	170.709	1
573	NM_026175	Sf3a1	0.0072859	0.0034389	183.2287	stable	1
574	NM_025391	Nip7	0.0072927	0.0253445	144.995	stable	2
575	NM_009911	Cxcr4	0.0073247	0.6293433	125.0466	129.2639	1
576	NM_022331	Herpud1	0.0074204	0.1827271	143.0308	215.0011	0
577	NM_153142	Slc35e4	0.0075375	0.1295201	177.0316	395.7738	0
578	NM_026157	Papd1	0.0075544	0.2360308	165.7943	356.5512	0
579	NM_144792	Sgms1	0.0075677	0.4851689	168.1705	213.253	5
580	NM_027445	Rnf167	0.0075779	0.0104565	154.7361	stable	0
581	NM_175656	Hist1h4i	0.0075996	0.7783022	138.4235	108.3647	0
582	NM_027347	Med23	0.0076059	0.0380673	176.191	stable	0
583	NM_001111141	Gm505	0.0077111	0.7086304	125.1766	124.6757	0
584	NM_008928	Map2k3	0.0077257	0.0358645	193.1349	stable	0
585	ENSMUST00000108430	Rps19	0.0077284	0.0219033	196.3585	stable	0
586	NM_133931	Pot1a	0.0077675	0.1960948	139.2138	287.8244	3
587	NM_001013792	BC087945	0.0077888	0.0489614	185.5775	stable	0
588	NM_008668	Nab2	0.0078078	0.1540548	161.3298	292.1609	3
589	BC052855	BC055324	0.0078794	0.0867458	169.659	stable	0
590	NM_027030	Dcps	0.0079405	0.4496288	140.8605	212.19	0
591	NM_020575	March7	0.007964	0.5821292	90.97554	125.9431	2
592	AK047224	Mafg	0.0079743	0.0384702	164.137	stable	2

593	NM_176860	*Ubash3b*	0.0080207	0.2089265	167.208	402.5649	3
594	NM_198644	*Zfat*	0.0081269	0.3498113	159.133	233.027	0
595	NM_019835	*B4galt5*	0.0081316	0.0417357	195.5514	stable	1
596	NM_001033274	*Brd1*	0.0082181	0.2550315	172.2748	278.591	6
597	NM_001081013	*Rlf*	0.0082892	0.8507272	88.29131	91.91973	0
598	NM_175112	*Rae1*	0.0083086	0.0894316	189.4817	stable	0
599	NM_033398	*Jmjd6*	0.0083242	0.1914114	163.9561	352.3583	1
600	NM_178732	*Zfp324*	0.008386	0.1969931	136.6002	246.408	2
601	NM_021511	*Rrs1*	0.0084535	0.8262566	131.832	102.782	1
602	NM_001029876	*AK122209*	0.0084608	0.3810186	139.6689	198.366	1
603	NM_146037	*Kcnk13*	0.0086341	0.1419153	174.8647	436.7464	2
604	NM_021891	*Fignl1*	0.0086471	0.70683	142.8437	136.9078	1
605	NM_010511	*Ifngr1*	0.008665	0.333283	206.7147	339.0862	0
606	AK007434	*1810011H11Rik*	0.0087582	0.8269218	141.5814	85.78826	0
607	ENSMUST00000050248	*Zbtb11*	0.0087624	0.7623333	89.83973	101.0144	0
608	NM_025426	*Med7*	0.0087748	0.991104605	149.2572	83.0195	4
609	BC023403	*4632415L05Rik*	0.0087751	0.2228755	166.8894	354.6492	1
610	NM_194344	*Sh3tc1*	0.0088065	0.0824825	201.1628	stable	0
611	NM_133227	*Nup155*	0.0088886	0.4068635	186.9619	274.0952	6
612	NM_028015	*Lass5*	0.0089993	0.0336118	02.8528	stable	2
613	NM_023605	*Fbxo9*	0.0090855	0.3615893	169.2073	258.7243	1
614	NM_009878	*Cdkn2d*	0.0091006	0.1925387	180.1146	364.4415	1
615	NM_008255	*Hmgcr*	0.0091651	0.1831081	198.998	491.4236	5
616	NM_009471	*Umps*	0.0091998	0.0356226	185.236	stable	2
617	BC075621	*Rbm16*	0.0092543	0.8025997	147.0697	141.5145	0
618	NM_153144	*Ggnbp2*	0.0092562	0.8547205	141.7877	122.0869	5
619	NM_172280	*2210018M11Rik*	0.0092565	0.1035428	167.0765	556.8443	0
620	NM_010657	*Hivep3*	0.0092722	0.1622706	184.8457	410.815	0
621	NM_010234	*Fos*	0.0094939	0.96211623	140.4223	94.23565	4
622	NM_145480	*Rfc4*	0.0095086	0.6454089	173.9566	180.1888	0
623	BC025577	*BC002230*	0.009573	0.5098973	178.1348	189.1457	0
624	NM_019812	*Sirt1*	0.0095835	0.7247316	146.7124	128.7978	7
625	NM_172572	*Rhbdf2*	0.0096571	0.0266272	188.5124	stable	1
626	BC048957	*Dgkd*	0.009691	0.0107528	198.729	stable	3
627	NM_029512	*5830472M02Rik*	0.0097659	0.0511641	180.2708	stable	5
628	NM_026403	*2610027L16Rik*	0.0097725	0.4037166	174.9355	249.8522	0
629	NM_026365	*Jagn1*	0.0098881	0.0121267	196.1191	stable	2
630	NM_133215	*Mtmr4*	0.0100099	0.1546995	171.6029	422.0875	3
631	NM_009667	*Ampd3*	0.0101069	0.2199189	195.3967	438.8719	1
632	NM_011762	*Zfp59*	0.0101744	0.7021457	156.2864	148.9264	2
633	BC056931	*4732496O08Rik*	0.0101793	0.97271342	155.1838	89.70296	2
634	NM_001085390	*Dusp5*	0.0101953	0.333536	186.6656	272.0575	0
635	NM_177620	*Rin3*	0.0102538	0.0063556	210.4746	stable	0
636	NM_019805	*Anapc7*	0.0103992	0.0893285	190.6291	stable	0
637	NM_008979	*Ptpn22*	0.0104046	0.3965205	149.442	266.6159	1
638	NM_021313	*Rnf25*	0.0104624	0.4312979	161.4507	206.281	0

639	NM_028245	Zfp131	0.0105619	0.7000216	123.1207	136.3141	4
640	NM_027891	Lrwd1	0.0106369	0.0663447	187.0677	stable	0
641	NM_018879	Tusc4	0.0106543	0.0049724	179.1774	stable	0
642	NM_010479	Hspa1a	0.0107709	0.4244631	128.4756	194.8547	0
643	NM_009480	Usf1	0.0108657	0.2285568	179.2227	341.3613	0
644	NM_146165	Jtv1	0.0109666	0.1079616	201.5923	stable	0
645	ENSMUST00000020315	Cand1	0.0109996	0.1001082	217.5563	stable	1
646	NM_032000	Trps1	0.0110057	0.8668998	108.2185	101.9858	11
647	ENSMUST00000101536	1810058I24Rik	0.0110071	0.0108851	209.5926	stable	3
648	NM_026538	Ddx56	0.0110373	0.0606816	199.9722	stable	0
649	NM_029546	Pwp2	0.0110568	0.0553988	178.7287	stable	1
650	NM_009871	Cdk5r1	0.0110822	0.1529785	171.0945	455.8361	4
651	NM_080554	Psmd5	0.011085	0.0342135	191.219	stable	1
652	NM_008580	Map3k5	0.0110858	0.5066601	169.3342	214.4294	1
653	NM_008922	Prim2	0.0110871	0.0847063	179.4969	stable	1
654	NM_007988	Fasn	0.0112656	0.0143474	211.0482	stable	2
655	NM_172924	C230081A13Rik	0.0113575	0.6025273	153.2602	183.8797	7
656	NM_144871	Suv420h1	0.0115052	0.6129974	155.0903	179.3396	2
657	NM_146116	Tubb2c	0.0115161	0.0253437	223.4062	stable	0
658	NM_001081005	1500012F01Rik	0.0115237	0.8152678	161.7837	113.8824	1
659	NM_207652	Tsc22d1	0.0115622	0.2043638	188.1518	439.6216	1
660	NM_001013366	Wdr91	0.0116052	0.136399	198.5439	577.4009	1
661	BC062166	4631422O05Rik	0.0116332	0.6340552	196.402	205.4538	2
662	ENSMUST00000080817	Rnf169	0.0116374	0.0363876	199.4198	stable	6
663	NM_172735	Zc3hc1	0.0117651	0.0885635	189.9477	stable	0
664	NM_175311	Zfp513	0.0119092	0.4128313	174.1111	270.3669	0
665	NM_026549	Pdcd2l	0.0120071	0.0845629	198.8569	stable	1
666	NM_011262	Dpf2	0.0120893	0.1651058	180.3533	stable	1
667	NM_144933	Med17	0.0120941	0.55247	181.7044	244.5864	1
668	NM_016877	Cnot4	0.0122592	0.3939915	178.7269	267.4062	3
669	NM_001112729	BC019943	0.0122646	0.1233032	186.654	567.1633	4
670	NM_145582	Atpbd3	0.0122796	0.8934419	160.5926	115.7217	1
671	NM_001042655	Tbc1d17	0.012326	0.0144737	188.2608	stable	0
672	NM_009046	Relb	0.0123332	0.0850602	209.7997	stable	0
673	NM_175334	Maml1	0.0123938	0.1350182	177.8573	565.6642	2
674	NM_146001	Hip1	0.01242	0.1754752	181.3615	337.3442	3
675	NM_146045	B4galt7	0.0124252	0.1600301	194.9985	463.2557	1
676	NM_010066	Dnmt1	0.0125564	0.1284414	195.7354	stable	0
677	NM_009828	Ccna2	0.0125759	0.2826343	193.5161	415.9895	1
678	NM_146171	Ncapd2	0.0125844	0.0755447	139.2734	stable	0
679	NM_023292	Pus3	0.0127184	0.6735228	125.2024	149.9303	0
680	NM_016714	Nup50	0.0127872	0.5013781	193.5003	206.6834	2
681	NM_001114609	A430093A21Rik	0.0127995	0.1823553	190.1696	477.4777	33
682	ENSMUST00000038926	Baz1a	0.0128622	0.5507386	102.282	141.4458	8
683	NM_021789	Trappc4	0.0128906	0.0475693	213.5499	stable	2
684	NM_178113	Ncapd3	0.0130103	0.62555	154.1246	207.319	3

685	NM_011597	Tjp2	0.0130119	0.1401013	228.3916	597.2181	2
686	NM_080562	Ubox5	0.0131211	0.7092875	169.0944	175.9976	0
687	NM_177619	Myst2	0.0132676	0.5285634	208.0414	184.2825	1
688	BC004022	N4bp1	0.0133301	0.856387	220.2711	162.2866	1
689	NM_020483	Sap30bp	0.0133777	0.0898759	208.2789	stable	0
690	NM_009174	Siah2	0.0133797	0.3934309	208.4925	262.9532	2
691	NM_053100	Trim8	0.0134396	0.0138762	174.0027	stable	1
692	NM_009874	Cdk7	0.013492	0.5713571	165.9151	206.4245	7
693	NM_026483	Mphosph10	0.0135925	0.8297658	123.8864	124.294	1
694	NM_011803	Klf6	0.0136153	0.7627761	176.3939	178.7919	7
695	NM_010493	Icam1	0.0138196	0.0140545	247.4043	stable	4
696	NM_146069	Lrrc33	0.0139207	0.1382117	154.3523	409.9819	2
697	NM_007678	Cebpa	0.0139262	0.0348645	167.2311	stable	0
698	NM_183426	Sbno2	0.0139299	0.017203	257.5363	stable	1
699	NM_024193	Nol5a	0.0140122	0.4820367	210.4943	268.9338	0
700	NM_007712	Clk2	0.0140308	0.2028014	207.8159	503.5824	0
701	NM_001110148	Mgat1	0.014101	0.0774834	192.721	stable	0
702	NM_172503	Zswim4	0.0141187	0.3994191	193.4098		1
703	NM_138315	Mical1	0.0142174	0.0625954	192.3388	stable	0
704	NM_026505	Bambi	0.0142497	0.6673147	170.3133	151.9948	4
705	NM_019750	Nat6	0.0144167	0.0107437	169.1813	stable	0
706	BC027193	Fbrs	0.0144345	0.0161637	225.886	stable	1
707	NM_016692	Incenp	0.014521	0.0432098	188.6238	stable	0
708	NM_001001559	Dub2a	0.014637	0.1275941	38.66544	217.7069	0
709	NM_026156	Xab2	0.0148052	0.0978311	222.4894	stable	0
710	NM_008893	Pola2	0.0148467	0.0666391	186.8825	stable	0
711	NM_008358	Il15ra	0.0150355	0.1666399	143.157	389.4082	0
712	NM_008394	Irf9	0.0151008	0.2024864	209.4445	stable	1
713	NM_183146	A530054K11Rik	0.0151027	0.996841606	139.697	71.77071	3
714	NM_029564	Tax1bp3	0.0151054	0.0533648	207.8668	stable	1
715	NM_028083	Chaf1b	0.0151686	0.2078594	196.9132	503.5841	0
716	NM_027554	Usp38	0.0151752	0.3090346	153.6602	300.5277	3
717	ENSMUST00000098860	Ddhd2	0.0151765	0.0414239	186.213	stable	0
718	NM_178923	Sfrs15	0.0153204	0.0215398	184.0114	stable	1
719	NM_177464	D19Ertd386e	0.0154202	0.6805941	139.4624	151.11	0
720	NM_175749	Nup153	0.0154362	0.5139924	162.4159	241.4397	2
721	NM_028150	Supt7l	0.0156915	0.3827324	187.9153	311.9914	1
722	NM_020616	D930014E17Rik	0.0158052	0.0260347	221.5502	stable	0
723	NM_026890	Ngdn	0.0158116	0.3607863	155.0474	249.639	0
724	NM_030886	Ankrd17	0.0158361	0.7244204	168.8897	185.2667	6
725	NM_008832	Phka1	0.0159834	0.1333698	190.671	518.3852	4
726	NM_010892	Nek2	0.0161074	0.0566897	189.3237	stable	5
727	NM_027353	Cd2bp2	0.0164745	0.2386322	200.0038	415.7239	2
728	NM_010509	Ifnar2	0.0166659	0.1060416	228.2473	stable	0
729	NM_010213	Fhl3	0.0167352	0.0362959	215.3194	stable	0
730	NM_008679	Ncoa3	0.0167537	0.1807878	198.3162	585.8958	5

731	NM_011299	*Rps6ka2*	0.0168793	0.0095684	205.7781	stable	1
732	NM_019825	*Ncoa6*	0.0169178	0.3476368	164.3964	255.4257	0
733	XM_910980	*LOC635812*	0.0169852	0.8426147	191.0527	153.7233	0
734	NM_026068	*Med31*	0.0170529	0.1128237	190.5045	523.7179	1
735	NM_021876	*Eed*	0.0170747	0.7694042	135.4001	126.799	2
736	NM_144918	*Smyd5*	0.0171165	0.004046	200.4347	stable	1
737	NM_183168	*P2ry6*	0.0171885	0.1193829	233.1595	stable	0
738	NM_007890	*Dyrk1a*	0.017214	0.6427213	189.5555	182.979	5
739	NM_021525	*Rcl1*	0.0172314	0.248888	178.3545	330.591	0
740	NM_026936	*Oxa1l*	0.0173303	0.1488568	200.8642	stable	1
741	NM_011121	*Plk1*	0.0173812	0.089687	158.8378	stable	0
742	NM_207302	*Zranb1*	0.0176784	0.8576716	122.1927	110.701	0
743	NM_145128	*Mgat5*	0.0176895	0.2030335	209.0309	535.5136	0
744	NM_172161	*Irak2*	0.0177712	0.0795097	231.5426	stable	4
745	NM_010276	*Gem*	0.017976	0.215806	192.832	395.7792	4
746	NM_001110197	*Rnf146*	0.0180671	0.5686713	172.4193	216.3437	12
747	NM_173382	*2810046L04Rik*	0.0181804	0.0422218	200.8893	stable	4
748	NM_001005223	*Znhit3*	0.0181888	0.2447156	199.3189	394.9408	3
749	NM_021327	*Tnip1*	0.0182404	0.2729027	236.4086	334.6022	0
750	NM_172458	*9030612M13Rik*	0.0182663	0.8722313	119.3589	113.1374	18
751	BC080661	*2410042D21Rik*	0.0183585	0.2789726	128.3203	298.7995	3
752	NM_027141	*Spsb3*	0.0185107	0.0418263	195.8535	stable	0
753	NM_010811	*Ndst2*	0.0185273	0.0127418	164.16	stable	0
754	NM_018788	*Extl3*	0.0185727	0.0244222	206.1303	stable	3
755	NM_027494	*Zcchc8*	0.0186006	0.4016439	194.5342	349.8618	5
756	NM_080848	*Wdr5*	0.018838	0.021278	208.4157	stable	1
757	NM_019679	*Fmnl1*	0.0190574	0.0323251	267.1769	stable	0
758	NM_016764	*Prdx4*	0.0190751	0.1036669	231.4132	stable	0
759	NM_011278	*Rnf4*	0.0190824	0.3706733	238.5751	375.6173	1
760	NM_026331	*Slc25a37*	0.0191636	0.3155792	192.1988	392.0137	5
761	NM_025399	*Nudt14*	0.0192962	0.0010153	188.9183	stable	0
762	NM_008037	*Fosl2*	0.0193174	0.5078065	143.4983	134.0104	8
763	NM_172498	*Ptk2b*	0.0193452	0.0521223	251.2151	stable	3
764	NM_172301	*Ccnb1*	0.0194048	0.3817835	185.8331	243.9821	4
765	NM_153408	*Lincr*	0.0194222	0.0703856	233.0234	stable	1
766	NM_138669	*Eif4a3*	0.0195022	0.0742941	245.1765	stable	1
767	NM_133249	*Ppargc1b*	0.0196027	0.128689	186.738	stable	0
768	NM_010831	*Snf1lk*	0.0196242	0.1876558	198.2108	476.9938	3
769	NR_002902	*Snora62*	0.0196839	0.3156578	173.6767	265.5934	0
770	NM_133968	*Snapc2*	0.0197085	0.520257	197.9944	219.2449	0
771	NM_145133	*Tifa*	0.0201275	0.708908	239.4387	229.9671	6
772	NM_010560	*Il6st*	0.0202256	0.2521104	188.5175	326.0772	6
773	NM_153583	*Atg4d*	0.0203413	0.0105228	190.0713	stable	2
774	NM_009387	*Tk1*	0.020348	0.1118591	219.7214	stable	1
775	NM_028599	*Wdr75*	0.0203747	0.5360635	174.8209	235.2727	0
776	NM_145928	*Tspan14*	0.0203941	0.0066532	192.2581	stable	1

777	NM_175272	*Nav2*	0.0204392	0.0450986	183.2268	stable	3
778	NM_180588	*Reep4*	0.0205197	0.0073814	198.3183	stable	1
779	NM_028753	*Pop7*	0.020554	0.0728636	210.832	stable	0
780	BC065058	*BC048403*	0.0205689	0.0188473	182.4515	stable	4
781	NM_173394	*Ticam2*	0.0205963	0.5842847	200.7597	219.5438	1
782	NM_025301	*Mrpl17*	0.0206375	0.0582645	167.6512	stable	6
783	NM_177688	*H2afj*	0.0206422	0.1668002	205.2947	595.4846	3
784	NM_133346	*Asb6*	0.0206672	0.2884692	212.0462	296.8409	2
785	NM_026396	*Bxdc2*	0.0206824	0.8347517	144.4742	140.2532	3
786	NM_028385	*Setd5*	0.0206998	0.866546	187.3395	152.7284	1
787	NM_021565	*Midn*	0.0208186	0.4153301	151.9584	128.8474	2
788	NM_001114119	*Qrich1*	0.0208616	0.5139579	210.874	266.9175	0
789	NM_177364	Sh3pxd2b	0.020896	0.0173156	297.8471	stable	4
790	NM_130860	*Cdk9*	0.0210661	0.34184	222.4721	377.6137	3
791	NM_175095	*Commd2*	0.0211446	0.5233448	195.3248	230.9277	6
792	NM_001033238	*Cblb*	0.0212106	0.4186112	188.8576	282.542	5
793	NM_026824	*Dus1l*	0.0212732	0.0716339	232.0954	stable	0
794	NM_023794	*Etv5*	0.0212851	0.022323	199.5304	stable	5
795	NM_001024205	*Nufip2*	0.0212933	0.8070726	99.84515	123.3935	26
796	NM_130862	*Baiap2*	0.0213722	0.0108868	221.0277	stable	2
797	NM_175224	*Metap1*	0.021504	0.4435953	241.3819	334.2203	2
798	NM_025415	*Cks2*	0.0215739	0.0583565	155.1742	stable	2
799	NM_009015	*Rad54l*	0.0216539	0.4002818	196.8757	275.7255	1
800	NM_183034	*Plekhm1*	0.0219555	0.1111399	219.5888	stable	0
801	ENSMUST00000097505	*AI848100*	0.0219564	0.3444712	120.8399	235.3144	6
802	BC115576	*5430427O19Rik*	0.0220796	0.992776274	181.8398	93.55766	0
803	NM_011905	Tlr2	0.022306	0.5433992	279.6711	321.3804	0
804	NM_019663	*Pias1*	0.0223453	0.91031814	186.8752	145.8832	1
805	NM_009094	Rps4x	0.0223702	0.1817805	281.7869	stable	0
806	NM_025907	*Mettl6*	0.0225741	0.92026119	170.7021	124.9407	1
807	NM_008568	*Mcm7*	0.022716	0.1382405	186.7003	stable	0
808	NM_001045513	*Raph1*	0.0228569	0.6334905	157.3625	162.2345	0
809	NM_031165	Hspa8	0.0229275	0.231771	315.5063	stable	1
810	NM_173757	*Mrps27*	0.0229825	0.1573667	190.3033	stable	0
811	NM_027149	*Wdr20a*	0.023083	0.7955693	189.4413	165.4397	4
812	NM_019717	*Arl6ip2*	0.0231618	0.5162921	198.5686	259.0944	5
813	NM_029976	*Cdkn2aipnl*	0.0232857	0.1959039	250.6969	stable	4
814	ENSMUST00000038822	*Zc3h12c*	0.0233863	0.8003073	225.5794	173.5448	0
815	NM_001007581	*2810408M09Rik*	0.023454	0.0631011	170.5347	stable	0
816	NM_010442	*Hmox1*	0.0234689	0.1734206	222.7451	stable	1
817	NM_013733	*Chaf1a*	0.0236838	0.2208796	206.0664	475.5624	0
818	NM_145429	*Arrb2*	0.0237227	0.0909215	258.0066	stable	0
819	NM_001033331	*Gas2l3*	0.0237809	0.2694083	166.3982	449.6898	13
820	NM_178056	*Tm2d3*	0.0240507	0.1244918	208.1835	stable	1
821	ENSMUST00000082392	ND1	0.0241208	0.686455	327.7151	249.4363	0
822	NM_026375	*Ahctf1*	0.0241237	0.6055299	145.594	173.373	6

823	NM_153515	Ammecr1l	0.0241451	0.0886428	216.6808	stable	2
824	NM_001080813	Rab11fip1	0.0241472	0.2660912	219.0824	385.5782	4
825	AF357367	Rpl23a	0.0242516	0.1288989	160.5231	510.5525	0
826	NM_026238	Narfl	0.0242852	0.1381361	217.929	stable	0
827	NM_198246	Yars2	0.0243254	0.0627039	204.488	stable	0
828	BC061220	Cdc40	0.0243707	0.3386707	188.276	373.7382	0
829	NM_153085	Wac	0.0245052	0.4129604	173.936	330.1929	3
830	NM_010478	Hspa1b	0.0246145	0.5143573	174.7168	219.5027	2
831	NM_027213	Med6	0.0246603	0.2408896	216.6445	514.7598	0
832	NM_178644	Oaf	0.0247839	0.0107945	221.995	stable	3
833	NM_172644	Dars2	0.0248322	0.1413491	192.8511	stable	3
834	NM_009296	Supt4h1	0.0248437	0.0429781	260.7506	stable	0
835	XM_910030	LOC635086	0.0248989	0.0147552	218.9938	stable	1
836	ENSMUST00000034802	BC023892	0.0249765	0.98810658	185.1574	95.59816	0
837	NM_001001295	Dis3l	0.025029	0.1250372	205.2637	stable	0
838	BC028637	2900009I07Rik	0.0251215	0.055729	200.9229	stable	5
839	NM_172304	Tex10	0.0251438	0.8861568	164.2337	131.2345	0
840	NM_033573	Prcc	0.0251892	0.0225735	225.8389	stable	0
841	NM_134136	Fbxo38	0.0252348	0.8110387	194.3252	177.3004	4
842	NM_144873	Uhrf2	0.0252399	0.8110646	197.3398	170.0027	3
843	NM_029746	Cog2	0.025258	0.1714453	235.8697	stable	0
844	NM_001081119	Abhd13	0.0254087	0.379491	209.2913	351.043	10
845	NM_026454	Ube2f	0.0255256	0.6248001	224.0159	233.1685	2
846	NM_030557	Mynn	0.0255885	0.8827817	120.0019	129.1595	6
847	NM_198423	Bahcc1	0.02561	0.0355947	222.8208	stable	1
848	NM_146073	Zdhhc14	0.0256114	0.6384626	209.1771	203.0862	0
849	NM_024472	Gltpd1	0.0257755	0.1331423	160.0834	stable	0
850	NM_031251	Ctns	0.0258214	0.107569	206.9808	stable	0
851	NM_145066	Gpr85	0.0258599	0.8489978	211.7193	160.6421	0
852	NM_026360	Ddx47	0.0259116	0.0445915	239.2083	stable	0
853	NM_001025606	Tmem171	0.0259707	0.1090015	188.7057	stable	1
854	NM_017466	Ccrl2	0.0259922	0.3107222	190.4524	325.059	2
855	NM_177381	Cog3	0.0260446	0.4770107	169.6803	246.5613	2
856	NM_013842	Xbp1	0.0261722	0.2943849	246.9403	374.3335	3
857	NR_002889	EG545056	0.0263334	0.3575463	236.4835	354.1628	0
858	NR_001460	Rmrp	0.0265302	0.0138458	205.3317	stable	0
859	ENSMUST00000049917	Zfp407	0.0266246	0.8493569	158.9186	125.2531	1
860	NM_027996	2310021P13Rik	0.0267566	0.0006396	211.3231	stable	3
861	NM_001114088	Pdlim7	0.0268913	0.174472	231.9158	stable	0
862	NM_009128	Scd2	0.0272233	0.0458466	185.8149	stable	6
863	ENSMUST00000099160	BC029722	0.0272564	0.0216124	205.5457	stable	0
864	NM_009833	Ccnt1	0.0275115	0.2434309	182.6673	538.5009	0
865	NM_019716	Orc6l	0.0277809	0.500623	198.392	262.6328	0
866	NM_028079	2010111I01Rik	0.0278439	0.1408626	208.1991	stable	3
867	NM_013889	Zfp292	0.0278814	0.9033929	133.9249	112.1404	8
868	NM_030565	BC004044	0.0278885	0.090286	278.5179	stable	0

869	NM_009193	*Slbp*	0.0280831	0.0901038	184.1168	stable	2
870	BC003993	*BC003993*	0.0280929	0.97057063	146.929	95.29214	1
871	NM_148932	*Pom121*	0.0281838	0.1060926	204.3835	stable	3
872	NM_026071	*Slc25a19*	0.028233	0.0505015	243.5616	stable	1
873	NM_013664	*Sh3gl1*	0.0283171	0.1256964	237.412	stable	0
874	ENSMUST00000093336	*2610318N02Rik*	0.0283768	0.0142369	184.694	stable	0
875	NM_013506	*Eif4a2*	0.0285469	0.582381	205.1995	269.6123	6
876	NM_011341	*Sdf4*	0.0285674	0.0874726	264.5043	stable	1
877	NM_148930	*Rbm5*	0.0286087	0.405782	223.6419	328.2776	1
878	NM_172807	*Ppwd1*	0.0286372	0.7047159	164.0667	181.9475	0
879	NM_178890	*Abtb2*	0.0289155	0.0928376	189.1274	stable	1
880	NM_028860	*Mtmr3*	0.0289185	0.117815	229.8689	stable	0
881	NM_026698	*Tmem129*	0.028919	0.0593693	205.8443	stable	2
882	NM_011678	Usp4	0.0290665	0.0913978	270.9487	stable	0
883	NM_144833	*Zfp410*	0.0292681	0.718482	223.053	205.2758	0
884	BC052328	*BC052328*	0.0294085	0.2349385	150.7786	398.3621	2
885	NM_144801	*Tmem143*	0.0295587	0.0198689	183.0082	stable	1
886	NM_026845	*Ppil1*	0.0295635	0.303243	219.8266	444.7043	0
887	BC003730	*Ncf2*	0.0296682	0.049008	226.7499	stable	0
888	NM_008566	*Mcm5*	0.0297179	0.170197	227.3797	stable	4
889	NM_001033448	*Gm962*	0.0297494	0.278048	172.7616	374.7478	0
890	NM_010931	*Uhrf1*	0.0299329	0.0356228	198.5073	stable	2
891	BC057071	*1810026J23Rik*	0.030087	0.0885827	217.4233	stable	0
892	NM_207207	*Mrps26*	0.0301183	0.0760616	210.129	able	0
893	NM_001080798	*Aff1*	0.0301856	0.1045256	199.7065	stable	9
894	NM_001014390	*Dyrk2*	0.0304575	0.2783361	158.6408	422.7628	0
895	NM_001110100	*Banp*	0.0304715	0.3014533	208.1228	399.9062	4
896	NM_019426	*Atf7ip*	0.0305067	0.2912252	150.2575	308.7325	2
897	NM_011752	*Zfp259*	0.0305464	0.3679741	231.6293	412.4801	2
898	NM_001080930	*Atxn1l*	0.0305491	0.6111907	203.668	219.6297	4
899	BC053067	*2610036D13Rik*	0.0307699	0.2269224	221.7521	466.496	1
900	NM_011303	*Dhrs3*	0.0310148	0.0641328	245.8129	stable	0
901	ENSMUST00000093902	*LOC672511*	0.0311117	0.0506093	185.0812	stable	1
902	NM_011588	*Trim28*	0.0311164	0.012749	256.166	stable	1
903	NM_007396	*Acvr2a*	0.0312793	0.8737397	131.1008	98.97175	10
904	NM_133865	*Dclre1b*	0.0312935	0.1041287	200.5465	stable	4
905	BC048169	*1700020O03Rik*	0.0313891	0.5532179	215.0003	269.4076	7
906	NM_178069	*Lsg1*	0.031547	0.4943091	252.968	333.9537	0
907	NM_009773	*Bub1b*	0.0316134	0.808369	211.3598	161.7905	0
908	ENSMUST00000084013	*ND4L*	0.0316959	0.4826877	262.7467	387.5467	0
909	NM_134471	*Kif2c*	0.0317132	0.2814895	199.752	447.227	1
910	NM_153065	*Ddx27*	0.0318595	0.2244423	234.6585	stable	0
911	NM_172990	*Pank4*	0.0319048	0.1505471	226.3871	stable	2
912	NM_024245	*Kif23*	0.0320599	0.6347763	179.2614	221.5535	1
913	NM_008307	*Htf9c*	0.0321809	0.0623446	231.7075	stable	0
914	NM_010124	*Eif4ebp2*	0.0321897	0.0039683	199.3573	stable	0

915	NM_172669	Ambra1	0.0323675	0.046615	224.7448	stable	1
916	NM_030249	Cttnbp2nl	0.0324524	0.117948	175.0905	stable	2
917	NM_025555	2410004B18Rik	0.0325753	0.4388947	231.7108	301.2267	3
918	NM_133947	Numa1	0.0326496	0.2233118	234.0023	stable	0
919	NM_019721	Mettl3	0.0326577	0.0820456	246.0651	stable	0
920	NM_025454	Ing5	0.0327084	0.3274082	199.8971	310.2863	6
921	NM_008079	Galc	0.032785	0.0381665	229.2578	stable	5
922	NM_134024	Tubg1	0.0328497	0.0054271	235.9597	stable	1
923	NM_023324	Peli1	0.0329826	0.6023922	280.7627	309.4366	5
924	NM_009949	Cpt2	0.0330328	0.0082069	214.0875	stable	1
925	NR_002898	Snora65	0.0330384	0.0510693	158.6129	stable	0
926	AF357383	Ipo7	0.0330876	0.1793648	131.8272	stable	0
927	NM_001113362	Tbc1d14	0.0332583	0.1393784	236.6124	stable	0
928	NM_053214	Myo1f	0.0333184	0.0896635	284.439	stable	0
929	NM_001039710	Coq10b	0.0334078	0.2519055	177.2767	465.5954	3
930	NR_004445	Snord22	0.0335727	0.0160128	165.7211	stable	0
931	NM_001045523	Bahd1	0.0335772	0.1182725	220.853	stable	1
932	NM_010192	Fem1a	0.033715	0.5298343	181.5475	210.9473	5
933	ENSMUST00000037810	4921511H13Rik	0.0339379	0.5515224	196.3095	213.8144	1
934	NM_012025	Racgap1	0.0339595	0.0940874	202.7715	stable	1
935	NM_024284	Hagh	0.0340052	0.0048781	241.2031	stable	2
936	NM_030215	Wrnip1	0.0340638	0.0027358	226.447	stable	2
937	ENSMUST00000054963	Fdft1	0.0340729	0.1225383	180.1459	stable	2
938	NM_001014976	Espl1	0.0340896	0.037097	180.9046	stable	1
939	BC115985	Mocs3	0.0340897	0.0757495	237.2846	stable	0
940	NM_008563	Mcm3	0.0341085	0.4021282	201.9495	476.4474	0
941	NM_011181	Pscd2	0.034146	0.0635356	223.1627	stable	5
942	NM_145393	Ythdf2	0.0341967	0.5832284	213.1292	265.3462	0
943	NM_133928	Chchd4	0.0342119	0.0904716	209.0373	stable	0
944	NM_144818	Ncaph	0.0343304	0.1915797	192.7223	stable	2
945	NM_010700	Ldlr	0.0346084	0.023486	281.8911	stable	3
946	NM_024168	Tsen34	0.0346276	0.0416928	229.9868	stable	0
947	BC051473	Rbx1	0.0347115	0.0265247	273.3809	stable	0
948	NM_178627	Poldip3	0.0347573	0.2294381	263.2536	stable	0
949	NM_001081354	Mamld1	0.0348102	0.1648614	240.6289	stable	0
950	NM_175318	Spty2d1	0.034855	0.8834874	152.7092	133.534	5
951	NM_011603	Tbpl1	0.0350474	0.1766096	220.917	stable	3
952	NM_019975	Hacl1	0.0350514	0.2483025	212.5375	504.3096	4
953	NM_027493	Actr8	0.0350988	0.2583049	224.6637	529.4242	0
954	NM_145371	Eif2b1	0.0353126	0.0424991	239.8777	stable	1
955	NM_021535	Smu1	0.0353942	0.1571943	286.0439	stable	0
956	NM_207669	Gabpb1	0.0355388	0.0763847	271.7361	stable	2
957	BC024401	8430410A17Rik	0.0355433	0.2342655	215.0951	432.656	0
958	NM_133232	Pfkfb3	0.0355716	0.3164032	152.4027	196.4128	7
959	NR_004415	Rnu3b1	0.0357787	0.0110601	241.4258	stable	0
960	NM_025788	Btbd14b	0.0358315	0.0520242	270.1885	stable	0

961	NM_133895	*Slc15a4*	0.035832	0.0527625	224.9978	stable	0
962	NM_177778	*Armc7*	0.0360195	0.2921801	226.9702	492.0576	0
963	NR_003966	*Atp10d*	0.0362783	0.7529525	205.7503	206.5155	0
964	NM_145634	*Cd300lf*	0.036285	0.1744233	193.2597	stable	1
965	NM_134149	*AI837181*	0.0363831	0.0486684	166.4165	stable	0
966	BC118516	Stx11	0.0364024	0.5337785	273.4128	329.1913	1
967	BC070402	*BC024868*	0.0364089	0.0420416	236.2495	stable	1
968	NM_177185	D130059P03Rik	0.036435	0.3566402	177.687	345.4529	14
969	NM_001081058	*Cdc2l5*	0.0365865	0.3947779	206.1186	316.0662	6
970	NM_008690	*Nfkbie*	0.0366325	0.1683221	249.4967	stable	0
971	NM_175375	*Ankhd1*	0.0367199	0.8996195	142.2025	124.5365	1
972	NM_172739	*Grlf1*	0.0367935	0.96625195	212.5189	117.105	0
973	NM_008795	*Pctk3*	0.0369464	0.0300496	262.1066	stable	1
974	XM_887553	*EG623114*	0.0369809	0.0164785	208.6155	stable	0
975	NM_001081345	*Chd2*	0.0371279	0.98312269	114.259	78.39267	1
976	NM_029036	*S100pbp*	0.0373483	0.2417723	171.0654	300.6678	1
977	NM_015792	*Fbxo18*	0.0374178	0.0983761	237.7007	stable	1
978	BC071241	*9430016H08Rik*	0.0375955	0.4877004	207.7925	265.4078	2
979	NM_009541	*Zbtb17*	0.0376511	0.2692629	222.6285	518.0564	2
980	NM_018742	*Bet1l*	0.0376881	0.4318925	230.107	345.0804	0
981	NM_021493	*4933428G20Rik*	0.0381778	0.078105	213.8545	stable	2
982	NM_012057	*Irf5*	0.0381936	0.0945743	213.6133		2
983	NM_009421	Traf1	0.0383028	0.4707379	279.071	396.1431	1
984	NM_001081057	*4930573I19Rik*	0.0383045	0.0053479	216.9191	stable	4
985	NM_028868	*Cxxc1*	0.0386695	0.039576	225.7726	stable	0
986	NM_008692	*Nfyc*	0.0389103	0.4991903	228.9896	304.5518	1
987	NM_001033156	*Fbxo33*	0.0390113	0.8328598	227.0147	182.9997	7
988	NM_028199	*Plxdc1*	0.0392397	0.0147409	253.2145	stable	2
989	NM_031198	*Tcfec*	0.0393062	0.94751135	259.6388	145.481	2
990	NM_022328	*Mllt1*	0.0393065	0.3354642	237.9519	360.0018	0
991	NM_009881	*Cdyl*	0.0393577	0.503953	202.9164	247.6715	4
992	NM_016748	*Ctps*	0.039533	0.0502395	238.2018	stable	1
993	ENSMUST00000031839	*2410003K15Rik*	0.0396343	0.0050304	226.647	stable	0
994	NM_028127	*Frmd6*	0.0396555	0.990905126	222.3158	97.64561	3
995	NM_016910	*Ppm1d*	0.0396686	0.4925198	206.8413	245.3771	3
996	NM_146081	*Ppp4r1*	0.0396801	0.2844113	263.1501	364.1736	3
997	NM_010655	Kpna2	0.0398082	0.7350097	275.0689	236.8403	1
998	NM_019570	*Rev1*	0.0398232	0.8969288	165.2429	127.0198	1
999	ENSMUST00000093450	*Tmem16h*	0.0398274	0.0188624	225.3881	stable	0
1000	NM_026644	Agpat4	0.0399481	0.0096254	293.041	stable	0
1001	NM_021288	Tyms	0.0399808	0.0648055	286.2016	stable	3
1002	NM_007435	Abcd1	0.0400601	0.0179279	292.8954	stable	1
1003	NM_198017	*C430003P19Rik*	0.0401127	0.8814703	216.3323	162.947	6
1004	NM_009419	*Tpst2*	0.0403768	0.2545706	234.5859	stable	1
1005	NM_026472	*Mki67ip*	0.0404184	0.6656523	198.0806	219.2565	0
1006	NM_178029	*Setd1a*	0.0404271	0.1300248	259.8871	stable	1

1007	NM_023331	Mrpl46	0.0404975	0.2177391	249.0425	stable	1
1008	NM_023536	Mrto4	0.0406362	0.2573239	254.6586	575.495	1
1009	BC029025	1110031B06Rik	0.0407619	0.0869835	271.0254	stable	0
1010	NM_007763	Crip1	0.0410717	0.1397597	254.3969	stable	0
1011	NM_007633	Ccne1	0.0413082	0.189862	205.4109	stable	0
1012	NM_028751	Tjap1	0.0413169	0.1354135	213.8044	stable	1
1013	NM_011186	Psmb5	0.0415605	0.067394	258.9869	stable	0
1014	NM_012039	Zw10	0.0416066	0.7635918	232.4435	209.293	1
1015	NM_011655	Tubb5	0.0416133	0.0872644	367.6275	stable	2
1016	NM_175306	Phactr4	0.0418715	0.0168694	206.3851	stable	0
1017	NM_025400	Nat9	0.041896	0.1954204	207.3663	stable	0
1018	NM_016849	Irf3	0.0419176	0.4175195	243.0387	446.1521	0
1019	NM_001079901	Repin1	0.0419657	0.2225624	223.9771	546.4524	2
1020	NM_133816	Sh3bp4	0.0419686	0.3907664	244.6096	337.8634	2
1021	NM_133666	Ndufv1	0.0420401	0.0955074	256.0245	stable	0
1022	NM_028209	Ttc4	0.0421802	0.3098346	232.7604	stable	0
1023	NM_178907	Mapkapk3	0.0423227	0.0803543	315.052	stable	1
1024	NM_134138	Psmg2	0.0423719	0.2007923	241.4918	stable	0
1025	NM_001113533	Wtap	0.0424084	0.6783237	207.815	215.1203	2
1026	NM_001081034	Fbxo11	0.0425087	0.868248	227.6353	167.5413	1
1027	NM_177001	9130023H24Rik	0.0426108	0.3479343	220.4295	392.2062	1
1028	NM_133724	Cno	0.0426123	0.2161036	200.1251	stable	4
1029	NM_019715	Kcmf1	0.0429961	0.386294	289.9788	473.8646	6
1030	NM_133347	Dhx30	0.0430224	0.0548867	235.4937	stable	2
1031	NM_176843	Ints5	0.0432748	0.2492144	224.2346	stable	0
1032	NM_011630	Nr2c2	0.0432885	0.5576175	164.7926	205.4515	0
1033	NM_001033439	Lrch1	0.0432935	0.1338204	230.2697	stable	6
1034	NM_027470	Pak4	0.0433791	0.095504	219.4747	stable	1
1035	NM_010757	Mafk	0.0434731	0.2544603	139.0376	536.4708	5
1036	BC051044	AU042671	0.0436638	0.004695	219.1156	stable	3
1037	NM_001025432	Crebbp	0.0437611	0.044283	231.7011	stable	0
1038	NM_027203	Leng1	0.0437687	0.4905772	219.1072	294.5242	1
1039	NM_001007589	2700059D21Rik	0.0437809	0.5765993	267.8617	303.9152	3
1040	NM_028009	Rpusd1	0.0442821	0.0245193	222.5731	stable	0
1041	NM_011514	Suv39h1	0.0443746	0.1168379	214.5537	stable	0
1042	NM_001081109	Lmtk2	0.0445105	0.0604869	262.2048	stable	5
1043	NM_007783	Csk	0.0446202	0.0224031	274.5236	stable	0
1044	NM_007408	Adfp	0.0446853	0.2170571	331.4963	stable	0
1045	NM_053163	Mrpl36	0.0447173	0.0043499	242.3217	stable	1
1046	NM_001037757	ORF19	0.0447339	0.0150108	206.0748	stable	0
1047	NM_175658	Hist1h2aa	0.0448224	0.8286067	217.4313	170.9309	0
1048	NM_001126047	Sema4c	0.0448979	0.2334777	226.6348	388.8852	2
1049	NM_027927	Ints12	0.0449001	0.9273191	279.1642	161.7864	7
1050	NM_144908	Galnt11	0.0452238	0.0874849	245.8107	stable	4
1051	NM_145355	Rnf185	0.045382	0.6836817	199.0288	188.5532	2
1052	NM_178785	A430107D22Rik	0.0454226	0.1129569	210.4329	stable	0

1053	NM_198103	Exoc8	0.0454618	0.0770704	222.0746	stable	8
1054	BC019457	4930471M23Rik	0.0455779	0.2936488	283.339	308.5809	0
1055	NM_011379	Sipa1	0.0456087	0.0206509	240.5723	stable	0
1056	ENSMUST00000084563	Srcap	0.0458658	0.0336833	251.6964	stable	0
1057	NM_153053	Sf3b4	0.0458848	0.0512362	191.9363	stable	1
1058	NM_172726	E130309D02Rik	0.0458963	0.2279922	243.4759	stable	0
1059	NM_133349	Zfand2a	0.045933	0.2209311	256.3948	stable	1
1060	NM_138306	Dgkz	0.0459814	0.2659401	283.4415	526.3098	0
1061	NM_172297	Ccdc9	0.046252	0.4936392	227.2753	346.8773	0
1062	NM_026410	Cdca5	0.0463875	0.5982672	220.9905	222.1141	0
1063	NM_021549	Pnkp	0.0464273	0.0321789	252.7457	stable	0
1064	NM_028850	Chic2	0.0468044	0.0721485	307.4576	stable	1
1065	NM_145428	Dhrs7b	0.0468746	0.2937204	257.3656	579.9327	0
1066	NM_027521	Hmha1	0.0469886	0.1672716	287.0078	stable	0
1067	NM_009089	Polr2a	0.0470501	0.0235539	358.4842	stable	0
1068	BC017158	BC017158	0.0471003	0.0113717	210.9814	stable	0
1069	XM_001472875	LOC664870	0.0471045	0.1170553	238.3981	stable	3
1070	NM_022408	Es2el	0.0471452	0.2026956	268.8593	stable	0
1071	NM_007659	Cdc2a	0.0472741	0.3272396	237.9157	419.8172	4
1072	NM_007996	Fdx1	0.0473247	0.0804587	220.3179	stable	0
1073	NM_011981	Zfp260	0.0473644	0.8690871	135.6429	141.4086	3
1074	NM_175121	Slc38a2	0.047489	0.2453198	204.681	578.9392	5
1075	NM_201407	Dennd4b	0.0475281	0.0197547	264.0503	stable	2
1076	NM_009450	Tubb2a	0.0476668	0.2126199	248.1039	stable	0
1077	NM_023260	Mrps34	0.0477395	0.1143206	228.8546	stable	0
1078	NM_027695	Oxsm	0.0477534	0.4229128	207.1051	stable	5
1079	BC034876	1110008L16Rik	0.0480308	0.045385	246.6356	stable	0
1080	NM_009045	Rela	0.0480425	0.0447272	242.0295	stable	0
1081	BC017154	2610024G14Rik	0.0484659	0.7779433	236.7721	208.9422	0
1082	NM_205820	Tlr13	0.04867	0.90756744	192.5267	143.934	0
1083	NM_199027	Zfp335	0.0490603	0.0086982	259.5404	stable	1
1084	NM_028639	Ttc7	0.0491024	0.0120769	316.3157	stable	1
1085	XM_001476259	Dennd4a	0.0494015	0.6851018	189.3688	191.9404	2
1086	NM_001081177	Kif13b	0.0495558	0.1881473	253.4267	stable	0
1087	NM_026409	Ddx55	0.049678	0.1510447	223.0196	stable	1
1088	BC054752	1700081L11Rik	0.049778	0.8359151	229.4857	195.0275	4
1089	NM_133953	Sf3b3	0.0498431	0.1241426	347.5395	stable	1
1090	BC026590	BC026590	0.049903	0.0342599	190.9417	stable	0

Table S1. Complete list of unstable mRNAs (total 1090) containing 309 (28%) mRNAs which display TTP-dependent decay. P values for stability in WT cells and for TTP-dependent decay are shown. The transcripts are ordered according to the P values for decay in WT cells. Transcripts significantly stabilized in TTP$^{-/-}$ cells and therefore putative

TTP-targets are highlighted in grey boxes. Half-lives were calculated on the basis of mRNA decay within 90 min after transcriptional stop. Number of AREs (of the AUUUA type) in the 3´ UTR is depicted.

Table S2. Decay properties of 548 LPS-induced transcripts

Nr.	mRNA accession nr.	Gene name	P value for decay in WT	P value for TTP-dependent decay	Half-life in WT	Half-life in TTP-/-	Number of AREs in 3'UTR	Fold-induction by LPS
1	NM_013693	*Tnf*	0	0	21.20946	207.5789	8	4.52
2	NM_008176	*Cxcl1*	0	0.0000002	31.07276	567.1402	7	5.83
3	NM_009140	*Cxcl2*	0	0.0000004	47.29714	stable	11	24.42
4	NM_009404	*Tnfsf9*	0	0.000013	28.70494	65.04472	2	3.55
5	NM_010104	*Edn1*	0	0.0005397	31.2201	54.49831	3	3.2
6	NM_017373	*Nfil3*	0	0.0012455	38.09607	75.15834	0	15.1
7	NM_008416	*Junb*	0	0.0035771	36.13899	65.6606	2	3.23
8	NM_010907	*Nfkbia*	0	0.0047751	26.25408	44.57574	2	3.65
9	NM_007707	*Socs3*	0	0.0071504	24.42704	37.86671	4	5.37
10	NM_007746	*Map3k8*	0	0.0093796	36.49274	57.6634	4	7.31
11	NM_009397	*Tnfaip3*	0	0.0409466	27.56316	39.03424	5	9.8
12	NM_007679	*Cebpd*	0	0.0959877	44.16169	59.76528	5	16.74
13	NM_013642	*Dusp1*	0.0000001	0.2650471	25.02538	27.60435	4	9.41
14	NM_010090	*Dusp2*	0.0000001	0.2834996	26.30208	30.07205	4	30.81
15	NM_007413	*Adora2b*	0.0000001	0.0686846	43.45355	60.57669	3	5.86
16	NM_133662	*Ier3*	0.0000001	0.0081914	38.94605	62.66906	5	3.51
17	NM_013562	*Ifrd1*	0.0000001	0.0897321	51.98328	72.51007	1	3.65
18	NM_008654	*Myd116*	0.0000001	0.0012735	48.36718	117.2872	4	3.67
19	NM_009895	*Cish*	0.0000001	0.0003343	34.40339	129.21	3	100.62
20	NM_178892	*Tiparp*	0.0000002	0.415153	41.42411	52.47923	9	6.07
21	NM_009969	*Csf2*	0.0000003	0.001545	35.72238	81.79367	9	3.86
22	NM_008390	*Irf1*	0.0000004	0.0739166	34.85353	62.6254	3	4.79
23	NM_153287	*Axud1*	0.0000004	0.0167641	38.37771	77.97565	5	4.81
24	NM_172911	*D8Ertd82e*	0.0000004	0.0137223	57.09145	87.40008	1	7.02
25	NM_013923	*Rnf19a*	0.0000005	0.1260749	50.55379	68.92483	3	3.9
26	NM_133819	*Ppp1r15b*	0.0000006	0.051471	63.26241	99.99386	1	52.1
27	NM_008842	*Pim1*	0.0000009	0.0004057	73.08955	380.7073	1	8.73
28	NM_023233	*Trim13*	0.0000012	0.3589248	40.41363	48.32103	0	5.38
29	NM_010548	*Il10*	0.0000022	0.0005031	28.48885	151.3574	6	3.41
30	NM_009896	*Socs1*	0.0000031	0.0892753	59.86748	89.78243	0	3.82
31	NM_010499	*Ier2*	0.0000044	0.4567824	65.30931	69.59225	0	3.13
32	NM_008655	*Gadd45b*	0.0000046	0.4442298	72.60359	78.75101	0	3.27
33	NM_133753	*Errfi1*	0.0000052	0.0860016	46.10209	62.62744	4	28.19

34	NM_153159	Zc3h12a	0.0000052	0.0166611	61.9993	108.4246	3	3.13
35	NM_019840	Pde4b	0.0000062	0.313077	64.10926	82.99424	3	6.43
36	NM_175045	Bcor	0.0000084	0.0045317	81.71792	223.7878	3	4.83
37	NR_003508	Mx2	0.0000086	0.3860922	52.00646	54.07889	0	10.03
38	NM_010554	Il1a	0.0000182	0.0044801	73.3755	354.8769	3	49.23
39	NM_030612	Nfkbiz	0.0000414	0.7170741	95.02451	98.54103	4	3.37
40	NM_026772	Cdc42ep2	0.0000483	0.0898276	85.29161	140.3009	0	3.14
41	NM_010902	Nfe2l2	0.0000582	0.0626975	79.77501	178.8517	1	7.26
42	NM_031168	Il6	0.0000653	0.0047999	76.9014	269.3892	5	5.83
43	NM_015790	Icosl	0.0000653	0.0136124	91.67319	411.1724	1	.51
44	NM_011333	Ccl2	0.0000776	0.0048941	85.29748	409.1243	1	3.81
45	NM_010755	Maff	0.0000846	0.0013232	94.76328	stable	4	94.21
46	NM_007464	Birc3	0.0000881	0.2215159	106.7708	155.1429	4	47.11
47	NM_145827	Nlrp3	0.0001196	0.1091044	101.6229	172.1766	5	17.31
48	NM_027514	Pvr	0.0001394	0.0689445	119.9497	249.2952	5	5.73
49	NM_013652	Ccl4	0.0001399	0.0050759	106.2439	stable	2	4.54
50	NM_177643	Zfp281	0.0001414	0.818766	70.8731	72.40865	2	8.92
51	NM_033601	Bcl3	0.0001525	0.0132693	106.1592	421.5771	0	4.16
52	NM_010278	Gfi1	0.000161	0.0650334	93.53847	184.2812	2	3.11
53	NM_031252	Il23a	0.0001671	0.0028789	108.708	stable	6	4.92
54	NM_008361	Il1b	0.0001762	0.0113839	101.8997	stable	4	5.54
55	NM_013822	Jag1	0.0001777	0.0063803	114.3891	stable	10	8.78
56	NM_145996	Arid5a	0.0002158	0.1412889	88.67761	176.1851	2	7.7
57	NM_009044	Rel	0.0002186	0.7998143	101.0554	95.56135	2	3.32
58	NM_027871	Arhgef3	0.0002329	0.2662817	100.1195	162.7741	3	3.02
59	NM_026689	Mul1	0.0002584	0.0783594	115.465	243.4337	0	8.9
60	NM_018807	Plagl2	0.0003075	0.3777822	109.415	129.8803	5	49.84
61	NM_001081298	Lphn2	0.0003477	0.0003298	80.84893	stable	3	3.01
62	NM_178872	Trim36	0.0004752	0.3397578	122.6696	171.185	6	7.2
63	NM_009551	Zfand5	0.0005656	0.1346127	99.01123	179.1798	4	22.37
64	NM_011113	Plaur	0.0006103	0.0080586	136.3904	stable	2	167.55
65	NM_153537	Phldb1	0.0006709	0.0297879	126.8146	414.7206	0	52.95
66	NM_011408	Slfn2	0.0007462	0.7050187	159.8424	145.8909	0	3.09
67	NM_009890	Ch25h	0.000792	0.0685088	117.794	306.4119	3	4.09
68	NM_008057	Fzd7	0.0008446	0.0173227	116.6451	stable	3	3.92
69	NM_013654	Ccl7	0.00086	0.0314306	116.6052	453.9574	2	8.85
70	NM_011337	Ccl3	0.0008641	0.0107849	183.5935	stable	5	14.94
71	NM_207680	Bcl2l11	0.0009072	0.2950965	144.1961	185.8269	6	3.51
72	NM_172734	Stk38l	0.0011285	0.0707798	124.6435	309.2709	2	3.18
73	NM_020006	Cdc42ep4	0.0012037	0.3075121	119.2527	166.3377	0	25.03
74	NM_009630	Adora2a	0.0012438	0.1574697	129.2348	258.7674	0	3.27
75	NM_009344	Phlda1	0.0012459	0.3176665	116.3841	163.9144	3	12.18
76	NM_198600	Pol s	0.0012851	0.0077397	106.0294	stable	8	4.12
77	NM_130447	Dusp16	0.0014579	0.7016994	109.2798	106.3011	3	3.41
78	NM_172612	Rnd1	0.0015549	0.2121812	84.61005	124.4145	1	4.63
79	NM_011809	Ets2	0.0016679	0.0226189	147.1954	stable	6	3.04

80	NM_009834	*Ccrn4l*	0.0018073	0.1016081	151.3905	291.4825	4	65.89
81	NM_021788	*Sap30*	0.0018105	0.4365891	147.2355	197.2247	1	3.89
82	NM_010878	*Nck1*	0.002023	0.95293642	135.8066	92.26473	0	3.83
83	NM_172422	*Fastkd2*	0.0024965	0.5686457	150.8162	162.1365	3	3.74
84	NM_011636	*Plscr1*	0.0025655	0.305751	181.6501	255.7817	7	37.92
85	NM_030701	*Gpr109a*	0.0026526	0.1264854	159.7179	367.9499	1	3.56
86	NM_019925	*Gpr132*	0.0034984	0.0686697	171.3333	stable	1	6.9
87	NM_001040400	*Tet2*	0.0035165	0.3613409	122.494	186.8832	7	35.11
88	NM_130796	*Snx18*	0.0036069	0.5079227	144.5634	163.5552	7	3
89	NM_008872	*Plat*	0.0037898	0.134152	167.9118	383.0525	2	71.63
90	NM_011198	*Ptgs2*	0.0041577	0.0380289	139.2352	stable	12	4.15
91	NM_030887	*Jdp2*	0.0044745	0.1770236	152.9108	318.1193	0	6.07
92	NM_009396	*Tnfaip2*	0.0050232	0.0943573	220.1598	stable	2	3.45
93	NM_001099624	*Rapgef2*	0.0051429	0.7734397	153.299	135.7419	4	3.26
94	NM_010303	*Gna13*	0.0052112	0.4740168	156.2078	201.9331	9	25.16
95	NM_001007465	*Rffl*	0.0056328	0.3500748	137.8817	197.6678	2	60.42
96	NM_010731	*Zbtb7a*	0.0058894	0.0452536	149.9581	stable	2	10.13
97	NM_001017426	*Jmjd3*	0.00596	0.089602	156.0723	447.8215	3	8.03
98	NM_001083810	*2600010E01Rik*	0.0060487	0.059208	137.8688	stable	6	19.4
99	ENSMUST00000022566	*Spata13*	0.00613	0.1615795	140.7652	240.2306	6	35.81
100	NM_010437	*Hivep2*	0.0065048	0.0533823	121.5931	378.3657	3	3.16
101	NM_022331	*Herpud1*	0.0074204	0.1827271	143.0308	215.0011	0	9.09
102	NM_144792	*Sgms1*	0.0075677	0.4851689	168.1705	213.253	5	4.39
103	NM_019835	*B4galt5*	0.0081316	0.0417357	195.5514	stable	1	8.21
104	NM_033398	*Jmjd6*	0.0083242	0.1914114	163.9561	352.3583	1	25.03
105	NM_021511	*Rrs1*	0.0084535	0.8262566	131.832	102.782	1	3.93
106	NM_010657	*Hivep3*	0.0092722	0.1622706	184.8457	410.815	0	10.1
107	NM_172572	*Rhbdf2*	0.0096571	0.0266272	188.5124	stable	1	25.03
108	NM_028245	*Zfp131*	0.0105619	0.7000216	123.1207	136.3141	4	3.48
109	NM_009046	*Relb*	0.0123332	0.0850602	209.7997	stable	0	55.32
110	BC004022	*N4bp1*	0.0133301	0.856387	220.2711	162.2866	1	3.36
111	NM_009174	*Siah2*	0.0133797	0.3934309	208.4925	262.9532	2	3.04
112	NM_011803	*Klf6*	0.0136153	0.7627761	176.3939	178.7919	7	3.68
113	NM_010493	*Icam1*	0.0138196	0.0140545	247.4043	stable	4	4.55
114	NM_008358	*Il15ra*	0.0150355	0.1666399	143.157	389.4082	0	8.4
115	NM_021525	*Rcl1*	0.0172314	0.248888	178.3545	330.591	0	21.58
116	NM_010276	*Gem*	0.017976	0.215806	192.832	395.7792	4	6.1
117	NM_021327	*Tnip1*	0.0182404	0.2729027	236.4086	334.6022	0	3.02
118	NM_028599	*Wdr75*	0.0203747	0.5360635	174.8209	235.2727	0	6.59
119	ENSMUST00000038822	*Zc3h12c*	0.0233863	0.8003073	225.5794	173.5448	0	9.92
120	NM_001080813	*Rab11fip1*	0.0241472	0.2660912	219.0824	385.5782	4	3.8
121	NM_178644	*Oaf*	0.0247839	0.0107945	221.995	stable	3	8.4
122	NM_145066	*Gpr85*	0.0258599	0.8489978	211.7193	160.6421	0	3.77
123	NM_017466	*Ccrl2*	0.0259922	0.3107222	190.4524	325.059	2	3.23
124	NM_178890	*Abtb2*	0.0289155	0.0928376	189.1274	stable	1	7.66
125	NM_001080798	*Aff1*	0.0301856	0.1045256	199.7065	stable	9	6.85

126	NM_023324	Peli1	0.0329826	0.6023922	280.7627	309.4366	5	11.76
127	NM_001039710	Coq10b	0.0334078	0.2519055	177.2767	465.5954	3	6.76
128	NM_207669	Gabpb1	0.0355388	0.0763847	271.7361	stable	2	3.39
129	NM_133232	Pfkfb3	0.0355716	0.3164032	152.4027	196.4128	7	12.7
130	BC118516	Stx11	0.0364024	0.5337785	273.4128	329.1913	1	3.27
131	NM_008690	Nfkbie	0.0366325	0.1683221	249.4967	stable	0	6.7
132	BC071241	9430016H08Rik	0.0375955	0.4877004	207.7925	265.4078	2	10.17
133	NM_009421	Traf1	0.0383028	0.4707379	279.071	396.1431	1	30.91
134	NM_031198	Tcfec	0.0393062	0.94751135	259.6388	145.481	2	3.31
135	NM_133816	Sh3bp4	0.0419686	0.3907664	244.6096	337.8634	2	4.38
136	NM_001033439	Lrch1	0.0432935	0.1338204	230.2697	stable	6	4.32
137	NM_001126047	Sema4c	0.0448979	0.2334777	226.6348	388.8852	2	17.83
138	NM_028850	Chic2	0.0468044	0.0721485	307.4576	stable	1	7.03
139	NM_022988	Nif3l1	0.0520625	-	stable	-	1	7.77
140	NM_030720	Gpr84	0.0542015	-	stable	-	1	4.73
141	NM_199449	Zhx2	0.0549828	-	stable	-	1	10.61
142	NM_008359	Il17ra	0.0554184	-	stable	-	1	7.03
143	NM_010696	Lcp2	0.0555468	-	stable	-	2	3.51
144	NM_030266	Inpp4a	0.0563744	-	stable	-	9	3.68
145	NM_145950	Osgin2	0.057658	-	stable	-	9	8.1
146	BC052696	5730528L13Rik	0.0588549	-	stable	-	1	6.6
147	NM_172768	Gramd1b	0.0599562	-	stable	-	0	28.78
148	NM_010119	Ehd1	0.0609508	-	stable	-	0	3.2
149	NM_001080931	Med13	0.0654495	-	stable	-	11	3.11
150	NM_023386	Rtp4	0.068345	-	stable	-	1	3.02
151	NM_010215	Il4i1	0.070361	-	stable	-	0	235.45
152	NM_008773	P2ry2	0.0710631	-	stable	-	2	17.17
153	NM_021893	Cd274	0.0723669	-	stable	-	11	3.01
154	NM_178607	Rnf24	0.0758296	-	stable	-	7	9.72
155	NM_008102	Gch1	0.0771754	-	stable	-	7	10.59
156	BC049091	D1Bwg0212e	0.077254	-	stable	-	6	88.97
157	NM_028800	Stk40	0.0777579	-	stable	-	2	13.34
158	BC127040	AI504432	0.085528	-	stable	-	0	35.03
159	NM_009231	Sos1	0.0881684	-	stable	-	10	4.96
160	NM_033563	Klf7	0.090224	-	stable	-	0	12.7
161	NM_007669	Cdkn1a	0.0924714	-	stable	-	3	3.67
162	NM_138952	Ripk2	0.0941131	-	stable	-	1	5.55
163	NM_001008700	Il4ra	0.1031369	-	stable	-	0	3.94
164	NM_172845	Adamts4	0.1051419	-	stable	-	4	3.49
165	NM_144958	Eif4a1	0.1125681	-	stable	-	1	3.11
166	NM_028381	Ccdc94	0.1136571	-	stable	-	0	9.22
167	NM_007836	Gadd45a	0.1141619	-	stable	-	2	3.22
168	NM_027898	Gramd1a	0.1156471	-	stable	-	1	3.24
169	NM_001081024	Setdb2	0.1156797	-	stable	-	0	4.85
170	NM_013614	Odc1	0.121439	-	stable	-	1	10.5
171	NM_178647	Cggbp1	0.1256659	-	stable	-	13	19.23

172	NM_009058	Ralgds	0.1353768	-	stable	-	1	5.6
173	NM_011400	Slc2a1	0.143413	-	stable	-	1	9
174	NM_023742	Dtx2	0.1446114	-	stable	-	0	9.24
175	NM_019743	Rybp	0.1485718	-	stable	-	15	21.31
176	NM_172656	Als2cr2	0.1487854	-	stable	-	1	15.49
177	NM_008551	Mapkapk2	0.1510386	-	stable	-	1	4.19
178	NM_001112705	Tlk2	0.1513183	-	stable	-	6	18.15
179	NM_007961	Etv6	0.156605	-	stable	-	7	7.03
180	NM_007534	Bcl2a1b	0.1579807	-	stable	-	1	5.22
181	NM_008392	Irg1	0.1595446	-	stable	-	1	3.38
182	NM_028967	Batf2	0.1609481	-	stable	-	0	20.4
183	NM_019453	Mefv	0.1671391	-	stable	-	1	3.23
184	NM_178751	Orai2	0.1681194	-	stable	-	3	3.51
185	NM_009543	Rnf103	0.1687393	-	stable	-	3	7.03
186	NM_030705	Mesdc1	0.1698731	-	stable	-	4	3.78
187	NM_001083927	Tle3	0.1736256	-	stable	-	1	3.23
188	NM_021274	Cxcl10	0.1784777	-	stable	-	2	4.76
189	NM_134133	2010002N04Rik	0.1813338	-	stable	-	4	3.93
190	NM_009137	Ccl22	0.1864503	-	stable	-	2	3.53
191	NM_010846	Mx1	0.1868578	-	stable	-	1	3.58
192	NM_019494	Cxcl11	0.1881973	-	stable	-	1	7.29
193	NM_025564	Magohb	0.1891568	-	stable	-	2	3.72
194	NM_009177	St3gal1	0.1910448	-	stable	-	6	6.89
195	BC037015	6330409N04Rik	0.1995848	-	stable	-	3	3.48
196	NM_008252	Hmgb2	0.204515	-	stable	-	2	14.79
197	NM_133897	Lrrc8c	0.2224986	-	stable	-	1	4.47
198	NM_001033122	Cd69	0.2238139	-	stable	-	2	3.15
199	NM_008732	Slc11a2	0.2248385	-	stable	-	2	5.79
200	NM_019408	Nfkb2	0.2262849	-	stable	-	1	3.21
201	NM_010751	Mxd1	0.2265904	-	stable	-	5	12.85
202	NM_011407	Slfn1	0.2289437	-	stable	-	0	6.55
203	NM_031997	Tmem2	0.2294408	-	stable	-	4	21.01
204	NM_145478	Pim3	0.2348542	-	stable	-	5	3.06
205	NM_145209	Oasl1	0.2414016	-	stable	-	0	4.47
206	NM_011990	Slc7a11	0.2473429	-	stable	-	11	5.9
207	NM_170701	Cd40	0.2497252	-	stable	-	4	3.88
208	NM_027415	Tmem70	0.2533507	-	stable	-	2	12.23
209	NM_011331	Ccl12	0.2544511	-	stable	-	4	25.38
210	NM_026178	Mmd	0.2588106	-	stable	-	2	10.57
211	NM_016888	B3gnt2	0.267408	-	stable	-	2	7.34
212	NM_019983	Rabgef1	0.2707919	-	stable	-	3	3.38
213	BC080290	5033414K04Rik	0.2725727	-	stable	-	3	12.73
214	NM_178382	Flrt3	0.2734672	-	stable	-	5	8.78
215	NM_203320	Cxcl3	0.2739031	-	stable	-	5	5.83
216	XR_033941	LOC666793	0.2766083	-	stable	-	0	6.06
217	NM_173408	Dcun1d3	0.2783687	-	stable	-	7	42.99

218	NM_019949	Ube2l6	0.2789974	-	stable	-	1	3.35
219	NM_001081678	Zfp800	0.2820799	-	stable	-	11	3.2
220	NM_010336	Lpar1	0.2874431	-	stable	-	8	72.68
221	NM_001029841	Sla	0.2917758	-	stable	-	2	7.52
222	NM_207653	Cflar	0.2939943	-	stable	-	13	5.55
223	NM_001042501	5830415L20Rik	0.2957403	-	stable	-	3	4.46
224	NM_008987	Ptx3	0.2961022	-	stable	-	2	3.36
225	NM_145516	Plekhb2	0.2970045	-	stable	-	5	3.62
226	NM_001097644	Ccnyl1	0.300946	-	stable	-	1	9.1
227	NM_053268	Rasa2	0.3057707	0.4408617	265.1644	502.8133	5	21.3
228	NM_144808	Slc39a14	0.3080582	-	stable	-	4	6.77
229	NM_133955	Rhou	0.309297	-	stable	-	5	3.18
230	BC020021	2810439F02Rik	0.317235	-	stable	-	0	5.21
231	NM_009271	Src	0.3190516	-	stable	-	1	15.86
232	NM_010807	Marcksl1	0.3239971	-	stable	-	1	3.05
233	NM_011521	Sdc4	0.326994	-	stable	-	1	41.14
234	NM_178601	Imp4	0.3408987	-	stable	-	1	15.73
235	NM_010344	Gsr	0.3472975	-	stable	-	3	3.04
236	NM_009082	Rpl29	0.3533361	-	stable	-	0	6.85
237	NM_134080	Flnb	0.3544861	-	stable	-	0	6.59
238	NM_153783	Paox	0.3553786	-	stable	-	0	3.22
239	NM_001110826	Ddx6	0.3560468	-	stable	-	7	3.44
240	NM_008418	Kcna3	0.3571191	-	stable	-	1	59.59
241	NM_011579	Tgtp	0.357608	-	stable	-	1	32.28
242	NM_172382	Jmjd2a	0.3620274	-	stable	-	0	4.59
243	NM_011968	Psma6	0.3654876	-	stable	-	0	3.28
244	NM_001081223	Rbbp8	0.3823852	-	stable	-	6	8.52
245	NM_020557	Cmpk2	0.3827572	-	stable	-	7	5.37
246	NM_009048	Reps1	0.3846944	-	stable	-	1	29.48
247	BC028767	3110009E18Rik	0.3848906	-	stable	-	0	29.66
248	NM_001081117	Mki67	0.3862654	-	stable	-	1	16.65
249	NM_008977	Ptpn2	0.3866258	-	stable	-	0	3.93
250	NM_001110824	Foxp4	0.3894786	-	stable	-	1	3.82
251	XR_033701	LOC667592	0.4052824	-	stable	-	0	30.16
252	NM_008506	Mycl1	0.414843	-	stable	-	2	10.52
253	XR_030655	LOC666676	0.4162803	-	stable	-	0	4.79
254	NM_008357	Il15	0.4167258	-	stable	-	2	3.93
255	NM_183392	Nup54	0.4189171	-	stable	-	3	7.29
256	NM_001013371	Dtx3l	0.4190653	-	stable	-	2	11.03
257	NM_011627	Tpbg	0.4194296	-	stable	-	0	5.72
258	NM_016980	Rpl5	0.4254555	-	stable	-	0	11.3
259	NM_016846	Rgl1	0.4289596	-	stable	-	1	3.54
260	NM_199012	Fchsd2	0.4423135	-	stable	-	8	6.17
261	NM_022332	St7	0.4485921	-	stable	-	1	6.43
262	NM_009338	Acat2	0.4508173	-	stable	-	0	48.8
263	NM_028864	Zc3hav1	0.4571493	-	stable	-	3	3.2

264	EF660528	*AW112010*	0.4585857	-	stable	-	1	29.05
265	NM_139311	*Mllt6*	0.4595708	-	stable	-	0	18.46
266	NM_010908	*Nfkbib*	0.4614539	-	stable	-	0	3.4
267	NM_028287	*Zufsp*	0.4690604	-	stable	-	2	16.13
268	NM_001113421	*Schip1*	0.4739509	-	stable	-	2	11.62
269	NM_015818	*Hs6st1*	0.4769448	-	stable	-	5	22.95
270	NM_013671	*Sod2*	0.4787719	-	stable	-	8	7.02
271	BC116791	*5730508B09Rik*	0.4807311	-	stable	-	0	141.25
272	NM_018764	*Pcdh7*	0.481313	-	stable	-	3	5.83
273	NM_021457	*Fzd1*	0.4841183	-	stable	-	7	7.03
274	NM_026102	*Daam1*	0.4923529	-	stable	-	6	3.65
275	NM_030013	*Cyp20a1*	0.4961387	-	stable	-	0	9.52
276	NM_009942	*Cox5b*	0.4982232	-	stable	-	0	6.93
277	NM_019636	*Tbc1d1*	0.4993166	-	stable	-	4	5.83
278	NM_172713	*Sdad1*	0.5048299	-	stable	-	1	19.4
279	NM_026123	*Unc50*	0.5140454	-	stable	-	1	4.55
280	NM_011941	*Mapkbp1*	0.5229208	-	stable	-	4	10.55
281	NM_138648	*Olr1*	0.5229662	-	stable	-	5	48.84
282	NM_008088	*Gas7*	0.5283881	-	stable	-	3	7.91
283	BC016246	*1810029B16Rik*	0.5285181	-	stable	-	4	3.89
284	NM_019702	*Hbs1l*	0.531092	-	stable	-	1	9.81
285	NM_013653	*Ccl5*	0.5320018	-	stable	-	0	3.51
286	NM_008869	*Pla2g4a*	0.5482599	-	stable	-	4	4.13
287	NM_001038653	*Slc16a3*	0.5495113	-	stable	-	1	5.01
288	NM_001039530	*Parp14*	0.5552447	-	stable	-	3	4.79
289	NM_134141	*Ciapin1*	0.5598759	-	stable		2	3.86
290	NM_053257	*Rpl31*	0.560164	-	stable	-	0	7.7
291	NM_021384	*Rsad2*	0.5603833	-	stable	-	2	35.2
292	NM_009977	*Cst7*	0.5606065	-	stable	-	1	9.97
293	NM_011909	*Usp18*	0.5638119	-	stable	-	2	7.03
294	NM_011203	*Ptpn12*	0.5668482	-	stable	-	0	7.03
295	L32836	*Ahcy*	0.576416	-	stable	-	1	15.75
296	NM_010120	*Eif1a*	0.5794396	-	stable	-	3	3.37
297	NM_009195	*Slc12a4*	0.5817344	-	stable	-	3	3.1
298	NM_010579	*Eif6*	0.5839363	-	stable	-	0	4.22
299	ENSMUST00000085632	*EG227054*	0.5892458	-	stable	-	0	15.49
300	NM_026719	*Lmbrd1*	0.5940994	-	stable	-	10	3.75
301	NM_026656	*Mcoln2*	0.5953332	-	stable	-	3	3.02
302	ENSMUST00000029803	*Eif4e*	0.5966588	-	stable	-	3	5.87
303	NM_013885	*Clic4*	0.5974344	-	stable	-	8	12.23
304	NM_008330	*Ifi47*	0.6042324	-	stable	-	1	5.59
305	NM_023143	*C1r*	0.6044072	-	stable	-	2	7.03
306	NM_001039509	*Pnkd*	0.6090919	-	stable	-	1	8.52
307	NM_015766	*Ebi3*	0.6103368	-	stable	-	1	3.1
308	NM_013521	*Fpr1*	0.6128143	-	stable	-	0	7.2
309	NM_015783	*Isg15*	0.6130107	-	stable	-	0	12.8

310	NM_009982	Ctsc	0.6158767	-	stable	-	3	6.01
311	NM_010174	Fabp3	0.6169984	-	stable	-	0	15.21
312	U90926	U90926	0.6219469	-	stable	-	0	7.03
313	NM_009778	C3	0.6254077	-	stable	-	0	4.96
314	NM_025286	Slc31a2	0.626644	-	stable	-	0	6
315	NM_133826	Atp6v1h	0.6367219	-	stable	-	3	5.68
316	NM_153402	Eif2c3	0.6387632	-	stable	-	0	10.63
317	NM_172659	Slc2a6	0.640045	-	stable	-	0	4.7
318	NM_018796	Eef1b2	0.6419935	-	stable	-	0	3.13
319	NM_001114332	Slc16a10	0.6486314	-	stable	-	15	6.1
320	NM_133206	Znrf1	0.6510499	-	stable	-	4	5.38
321	NM_013683	Tap1	0.6536442	-	stable	-	0	17.86
322	NM_025846	Rras2	0.6558459	-	stable	-	2	104.72
323	NM_133196	Cstf2	0.6619437	-	stable	-	5	4.21
324	NM_139308	Stard7	0.6729921	-	stable	-	1	9.69
325	NM_022028	Sav1	0.675861	-	stable	-	1	3.65
326	NM_011673	Ugcg	0.6803404	-	stable	-	6	31.38
327	NM_008809	Pdgfrb	0.6832712	-	stable	-	1	3.11
328	NM_019948	Clec4e	0.6891658	-	stable	-	5	464.12
329	NM_001077403	Nrp2	0.6908642	-	stable	-	5	3.48
330	NM_008385	Inpp5b	0.691485	-	stable	-	2	10.31
331	NM_001002268	Gpr126	0.6937807	-	stable	-	6	4.92
332	NM_001077353	Gsta3	0.6940295	-	stable	-	1	14.18
333	NM_008331	Ifit1	0.6979813	-	stable	-	1	5.56
334	NM_207648	H2-Q6	0.7033391	-	stable	-	0	3.27
335	NM_001037713	Xaf1	0.7033962	-	stable	-	0	10.65
336	NM_027000	Gtpbp4	0.704975	-	stable	-	2	11.09
337	NM_008303	Hspe1	0.7051002	-	stable	-	0	12.77
338	NM_007987	Fas	0.7073284	-	stable	-	0	3.07
339	NM_207176	Tes	0.7076778	-	stable	-	5	3.2
340	NM_008352	Il12b	0.7082865	-	stable	-	6	8.73
341	BC049633	AA467197	0.7101916	-	stable	-	0	14.02
342	NM_183162	BC006779	0.7104348	-	stable	-	0	3.12
343	NM_021433	Stx6	0.7138078	-	stable	-	0	71.22
344	NM_026829	Mthfs	0.7159543	-	stable	-	0	9.3
345	NM_008630	Mt2	0.7176836	-	stable	-	0	35.53
346	NM_015774	Ero1l	0.7193526	-	stable	-	10	3.4
347	NM_009642	Agtrap	0.7254602	-	stable	-	0	3.31
348	NM_021439	Chst11	0.72571	-	stable	-	10	5.24
349	NM_194446	Cdk10	0.7298415	-	stable	-	0	31.6
350	NM_001083938	Rnaset2a	0.732573	-	stable	-	0	4.79
351	NM_033524	Spred1	0.7334409	-	stable	-	5	8.64
352	NM_181545	Slfn8	0.7359334	-	stable	-	2	4.67
353	NM_172507	Sh3bgrl2	0.7361675	-	stable	-	2	6.45
354	NM_009283	Stat1	0.7367697	-	stable	-	5	15.49
355	BC091759	Rpl17	0.7398895	-	stable	-	0	3.05

356	NM_018868	Nol5	0.7455176	-	stable	-	0	3.44
357	NM_172833	Malt1	0.7476653	-	stable	-	4	3.5
358	NM_009647	Ak3l1	0.7504197	-	stable	-	2	6.43
359	NM_175090	Slc31a1	0.7509025	-	stable	-	6	8.75
360	NM_011410	Slfn4	0.7513993	-	stable	-	3	3.43
361	NM_026851	Mrpl52	0.7579867	-	stable	-	0	16.47
362	NM_001081300	Tshz1	0.7589192	-	stable	-	7	3.7
363	NM_023377	Stard5	0.7596653	-	stable	-	4	6.01
364	NM_001033270	Slc4a7	0.7639317	-	stable	-	25	3.17
365	NM_007616	Cav1	0.7646944	-	stable	-	5	6.98
366	NM_153510	Pilra	0.7674274	-	stable	-	0	3.59
367	NM_146066	Gspt1	0.7688086	-	stable	-	8	6.86
368	NM_011488	Stat5a	0.7703629	-	stable	-	1	4.31
369	NM_172445	Wdr37	0.77079	-	stable	-	7	15.2
370	XR_030609	LOC620009	0.7777561	-	stable	-	0	12.59
371	NM_008957	Ptch1	0.7834761	-	stable	-	0	4.54
372	AK144579	ENSMUSG00000073665	0.7860735	-	stable	-	4	4.02
373	NM_011546	Zeb1	0.7863441	-	stable	-	6	4.96
374	NM_007611	Casp7	0.7867708	-	stable	-	3	4.08
375	NM_008982	Ptprj	0.790989	-	stable	-	4	5.48
376	NM_008491	Lcn2	0.7916642	-	stable	-	0	6.62
377	NM_011315	Saa3	0.7916848	-	stable	-	0	96.2
378	NM_007581	Cacnb3	0.7917165	-	stable	-	0	3.13
379	NM_173868	蜃t18	0.7957796	-	stable	-	17	6.91
380	NM_175164	Arhgap26	0.795788	-	stable	-	3	6.23
381	NM_198127	Abi2	0.7975577	-	stable	-	9	9.97
382	NM_009176	St3gal3	0.7985855	-	stable	-	1	4.34
383	NM_023514	Mrps9	0.8027302	-	stable	-	0	7.71
384	XR_032183	LOC665262	0.8081044	-	stable	-	0	34.05
385	BC115559	Nudt17	0.8082128	-	stable	-	0	17.87
386	NM_016737	Stip1	0.8105572	-	stable	-	1	3.02
387	NM_008599	Cxcl9	0.8133085	-	stable	-	3	8.02
388	NM_010818	Cd200	0.815681	-	stable	-	3	5.39
389	NM_011464	Spint2	0.8160221	-	stable	-	1	11.37
390	NM_001081298	Lphn2	0.8214649	-	stable	-	3	18.58
391	NM_010407	Hck	0.8222221	-	stable	-	2	5.16
392	NM_009510	Ezr	0.8247147	-	stable	-	3	9.34
393	NM_010260	Gbp2	0.8260327	-	stable	-	0	3.58
394	ENSMUST00000001113	Samd9l	0.826272	-	stable	-	0	5.68
395	NM_019808	Pdlim5	0.8294286	-	stable	-	4	7.72
396	NM_175026	Pyhin1	0.8305614	-	stable	-	0	30.18
397	NM_027182	Trip13	0.8330164	-	stable	-	0	3.23
398	NM_053202	Foxp1	0.8371289	-	stable	-	0	4.36
399	NM_031167	Il1rn	0.8374451	-	stable	-	0	3.12
400	NM_145523	Gca	0.8377623	-	stable	-	8	10.29
401	NM_133828	Creb1	0.8393968	-	stable	-	17	3.48

402	NM_028523	Dcbld2	0.8448216	-	stable	-	11	4.16
403	NM_022415	Ptges	0.8458673	-	stable	-	0	42.34
404	NM_008696	Map4k4	0.8465312	-	stable	-	4	5.17
405	NM_025315	Med21	0.8477882	-	stable	-	0	7.03
406	BC080777	730494M16Rik	0.8485923	-	stable	-	0	9.41
407	NM_008413	Jak2	0.8498534	-	stable	-	2	14.26
408	NM_145432	Heatr6	0.8514284	-	stable	-	8	18.96
409	NM_026603	Denr	0.8526931	-	stable	-	3	3.37
410	NM_011246	Rasgrp1	0.8572785	-	stable	-	7	3.02
411	NM_182806	Gpr18	0.8658273	-	stable	-	0	3.77
412	NM_025283	Mobkl3	0.8692889	-	stable	-	10	3.37
413	NM_133664	Lad1	0.8704867	-	stable	-	2	3.54
414	NM_011693	Vcam1	0.8717003	-	stable	-	2	3.87
415	NM_009812	Casp8	0.8724617	-	stable	-	3	6.6
416	NM_013658	Sema4a	0.8730394	-	stable	-	1	3.44
417	NM_001033242	Cln5	0.8765409	-	stable	-	3	6.51
418	NM_030253	Parp9	0.8768395	-	stable	-	0	8
419	NM_019736	Acot9	0.8772422	-	stable	-	0	3.71
420	NM_001025439	Camk2d	0.8780997	-	stable	-	7	24.6
421	NM_028679	Irak3	0.8796482	-	stable	-	1	3.81
422	NM_011529	Tank	0.8814956	-	stable	-	3	4.87
423	NM_029508	Pcgf5	0.8841062	-	stable	-	1	7.06
424	NM_027098	Mrpl30	0.8843666	-	stable	-	0	3.15
425	NM_145517	Ormdl1	0.8868121	-	stable	-	3	6.6
426	NM_001033415	Shisa3	0.8888956	-	stable	-	3	5.83
427	NM_001081566	Pik3r6	0.8898669	-	stable	-	1	118.15
428	NM_008591	Met	0.8918269	-	stable	-	5	5.07
429	NM_007646	Cd38	0.8918765	-	stable	-	6	5.83
430	NM_016767	Batf	0.8934579	-	stable	-	0	60.42
431	NM_025597	Ndufb3	0.8956582	-	stable	-	0	7.77
432	NM_001033632	Ifitm6	0.8988123	-	stable	-	1	16.65
433	NM_010723	Lmo4	0.90183549	-	stable	-	3	18.99
434	NM_008230	Hdc	0.90240857	-	stable	-	0	3.12
435	BC132172	C330023M02Rik	0.90364288	-	stable	-	0	3.13
436	NM_133737	Lancl2	0.9049753	-	stable	-	1	7.03
437	ENSMUST00000097783	D1Ertd448e	0.90743339	-	stable	-	0	3.49
438	NM_026221	Ppfibp1	0.90809432	-	stable	-	3	5.48
439	NM_015806	Mapk6	0.90893282	-	stable	-	4	3.69
440	NM_008689	Nfkb1	0.90944285	-	stable	-	4	5.23
441	NM_001114665	Fnbp1l	0.91129021	-	stable	-	6	7.66
442	BC048158	1700047I17Rik1	0.91176499	-	stable	-	8	37.33
443	NM_007904	Ednrb	0.91234002	-	stable	-	3	7.73
444	NM_032396	Kremen1	0.91691897	-	stable	-	2	5.91
445	NM_001037725	Als2cr13	0.91798079	-	stable	-	8	21.34
446	NM_019549	Plek	0.92372275	-	stable	-	8	3.26
447	NM_001042611	Cp	0.92685506	-	stable	-	1	15.71

448	NM_009183	St8sia4	0.93026603	-	stable	-	16	6.76
449	NM_001081029	4930420K17Rik	0.93119276	-	stable	-	2	3.84
450	NM_177960	Idi1	0.93292354	-	stable	-	6	3.14
451	NM_007514	Slc7a2	0.93393756	-	stable	-	12	5.33
452	NM_009728	Atp10a	0.93459655	-	stable	-	2	100.05
453	NM_145360	Idi1	0.93468778	-	stable	-	6	3.99
454	NM_028360	Ttc19	0.93656342	-	stable	-	8	6.67
455	NM_175236	Adhfe1	0.93733079	-	stable	-	5	6.5
456	NM_007981	Acsl1	0.93960762	-	stable	-	2	3
457	NM_134448	Dst	0.94019857	-	stable	-	6	4.74
458	NM_021604	Agrn	0.94040012	-	stable	-	0	3.49
459	NM_008402	Itgav	0.94428844	-	stable	-	19	9.25
460	NM_023380	Samsn1	0.94587173	-	stable	-	2	3.91
461	NM_172579	Sipa1l1	0.94646715	-	stable	-	1	3.29
462	NM_001037917	EG622976	0.94979427	-	stable	-	10	4.9
463	NM_007561	Bmpr2	0.95071767	-	stable	-	2	6.5
464	NM_001102404	Acp5	0.95511454	-	stable	-	0	4.02
465	NM_025972	Naaa	0.95678483	-	stable	-	2	7.03
466	NM_029499	Ms4a4c	0.95680212	-	stable	-	2	13.21
467	NM_194336	Mpa2l	0.95702544	-	stable	-	8	15.57
468	NM_019472	Myo10	0.95749459	-	stable	-	1	5.82
469	NM_008915	Ppp3cc	0.95853974	-	stable	-	4	3.12
470	NM_146112	Gigyf2	0.95883343	-	stable	-	0	3.76
471	NM_018734	Gbp3	0.96287101	-	stable	-	2	10.01
472	NM_019738	Nupr1	0.96364041	-	stable	-	0	3.34
473	NM_013831	Pstpip2	0.96377325	-	stable	-	5	90.55
474	NM_001005605	Aebp2	0.96398803	-	stable	-	15	7.03
475	NM_015743	Nr4a3	0.96476702	-	stable	-	0	14.03
476	BC145673	D14Ertd668e	0.96621615	-	stable	-	0	10.59
477	BC010602	H2-gs10	0.96679887	-	stable	-	0	6.13
478	NM_025824	Bzw1	0.96693031	-	stable	-	3	5.67
479	NM_027835	Ifih1	0.96816018	-	stable	-	0	3.78
480	NM_028179	2200002D01Rik	0.96847617	-	stable	-	0	4.88
481	NM_026002	Mtdh	0.96862464	-	stable	-	8	5.36
482	NM_016923	Ly96	0.96917315	-	stable	-	0	5.08
483	NM_010576	Itga4	0.96919875	-	stable	-	16	7.96
484	NM_010266	Gda	0.9704762	-	stable	-	10	6.73
485	NM_024495	Car13	0.97104047	-	stable	-	2	13.78
486	NM_001077189	Fcgr2b	0.97296937	-	stable	-	0	6.5
487	NM_021394	Zbp1	0.97545664	-	stable	-	1	6.37
488	ENSMUST00000031817	Herc5	0.9754634	-	stable	-	2	7.03
489	NM_009763	Bst1	0.97555151	-	stable	-	4	5.83
490	NM_133832	Rdh10	0.97753623	-	stable	-	1	3.2
491	NM_009418	Tpp2	0.97757153	-	stable	-	2	5.5
492	NM_020583	Isg20	0.97791058	-	stable	-	0	28.93
493	NM_008466	Kpna3	0.97800885	-	stable	-	0	3.12

494	ENSMUST00000042734	*1700066M21Rik*	0.9801035	-	stable	-	0	3.31
495	NM_010228	*Flt1*	0.9806505	-	stable	-	3	3.44
496	NM_023124	*H2-Q8*	0.98213552	-	stable	-	0	16.86
497	NM_027919	*Tha1*	0.98226361	-	stable	-	0	43.2
498	NM_001045481	*Ifi203*	0.98356804	-	stable	-	4	14.44
499	NM_172980	*Slc28a2*	0.98424308	-	stable	-	1	11.28
500	BC072629	*2510009E07Rik*	0.98440868	-	stable	-	5	6.86
501	NM_011854	*Oasl2*	0.98445208	-	stable	-	1	4.47
502	NM_028768	*Armc8*	0.98452376	-	stable	-	1	5.61
503	NM_033560	*Vps37a*	0.98464794	-	stable	-	16	3.74
504	NM_010433	*Hipk2*	0.98483092	-	stable	-	0	3.17
505	NM_010431	*Hif1a*	0.98499855	-	stable	-	7	3.27
506	XR_032810	*LOC100046859*	0.98521352	-	stable	-	0	3.21
507	NM_001038604	*Clec5a*	0.98566385	-	stable	-	2	3.44
508	NM_025789	*Rshl2a*	0.98591419	-	stable	-	2	10.21
509	NM_183029	*Igf2bp2*	0.98656523	-	stable	-	4	197.09
510	NM_009655	*Alcam*	0.98724738	-	stable	-	7	5.85
511	NM_207659	*Hook3*	0.98754442	-	stable	-	37	4.15
512	NM_001077190	*Abi1*	0.9883751	-	stable	-	8	7.83
513	NM_008607	*Mmp13*	0.98843055		stable	-	6	11.8
514	NM_026850	*Pdcl3*	0.98870198	-	stable	-	4	25.25
515	NM_001083312	*Gbp6*	0.98898226	-	stable	-	6	3.02
516	NM_007624	*Cbx3*	0.98987414	-	stable	-	8	3.22
517	NM_016850	*Irf7*	0.98991833	-	stable	-	0	69.22
518	NM_213659	*Stat3*	0.99045799	-	stable	-	2	11.32
519	NM_172648	*Ifi205*	0.99184232	-	stable	-	0	10.78
520	NM_025685	*Col27a1*	0.99197321	-	stable	-	4	14.91
521	BC006931	*AI597479*	0.99231435	-	stable	-	3	22.02
522	NM_010274	*Gpd2*	0.99304301	-	stable	-	0	8.59
523	NM_026493	*Cspp1*	0.99324256	-	stable	-	2	3.13
524	NM_023908	*Slco3a1*	0.99370314	-	stable	-	0	4.11
525	NM_011171	*Procr*	0.99372256	-	stable	-	1	4.34
526	NM_010288	*Gja1*	0.99391844	-	stable	-	4	3.69
527	NM_145221	*Appl1*	0.99404206	-	stable	-	14	4
528	NM_172413	*Rap2c*	0.99434116	-	stable	-	7	59.89
529	NM_018782	*Calcrl*	0.99479834	-	stable	-	6	5.53
530	NM_008608	*Mmp14*	0.99595071	-	stable	-	0	7.67
531	NM_133220	*Sgk3*	0.99602939	-	stable	-	8	4.4
532	NM_028680	*Ift57*	0.99607831	-	stable	-	2	4.36
533	NM_026202	*Ccdc50*	0.99658315	-	stable	-	13	5.96
534	NM_172409	*Fmnl2*	0.99684509	-	stable	-	8	5.6
535	NM_212444	*Gyk*	0.99766511	-	stable	-	7	6.87
536	NM_172952	*Gphn*	0.99781229	-	stable	-	2	4.57
537	NM_008866	*Lypla1*	0.99783147	-	stable	-	8	3.54
538	NM_007609	*Casp4*	0.99814892	-	stable	-	2	8.32
539	NM_023248	*Sbds*	0.99864992	-	stable	-	3	4.01

540	NM_010766	Marco	0.99895754	-	stable	-	0	6.82
541	NM_031195	Msr1	0.99899125	-	stable	-	5	18.11
542	NM_012054	Aoah	0.99904503	-	stable	-	2	3.34
543	NM_198303	Eif5b	0.99907857	-	stable	-	4	3.03
544	NM_025816	Tax1bp1	0.99929023	-	stable	-	1	4.64
545	NM_011541	Tcea1	0.99931233	-	stable	-	0	8.97
546	NM_033322	Lztfl1	0.99942381	-	stable	-	10	7.66
547	ENSMUST00000090792	Hnrpa3	0.99945841	-	stable	-	0	3.06
548	NM_008198	Cfb	0.99976704	-	stable	-	0	11.98

Table S2. Decay properties of 548 LPS-induced transcripts. P values for stability in WT cells and for TTP-dependent decay are shown. The transcripts are ordered according to the P values for decay in WT cells. In total, 138 unstable transcripts (i.e. P value < 0.05 for decay in WT cells) were found. Transcripts significantly stabilized in TTP$^{-/-}$ cells (45 in total) are highlighted in grey boxes. Calculated average half-lives, the number of AREs (of the AUUUA type) in the 3´ UTR and fold-induction by LPS are depicted.

6.3 Additional Data to the Manuscript

In addition to the three new TTP-targets characterized in detail in the manuscript (i.e. *IL-1α*, *IL-6* and *Cxcl2*), the putative mRNA target *Bcl3* was selected for further investigation. This transcript displayed increased stability in TTP-/- cells in the microarray analysis but did not contain any form of ARE (see manuscript, Table S2).

On the other hand we also started to validate the microarray results for *Dusp1* mRNA, which appeared to be unstable in a TTP-independent way, although its mRNA contains several AREs.

6.3.1 Role of AREs in TTP-mediated turnover

In the current view, TTP determines the mRNA stability by direct or indirect binding to AREs [9, 33]. In agreement with this model, AREs were enriched among putative TTP targets identified in our global screen (see manuscript figure S2). However, almost 40 % of TTP-targets detected had no ARE (defined as AUUUA) confirming recent reports that transcripts devoid of any ARE can be regulated by TTP [23, 24, 27]. One example for such an mRNA is *Bcl3* (NM_033601). It was highly expressed after LPS treatment (Manuscript Supplementary Table 2) and appeared to be stabilized in TTP-/- macrophages. Nevertheless, its 3' UTR does not contain even the simplest AUUUA ARE sequence (figure 7A). In preliminary experiments we could confirm by qRT-PCR the increase in mRNA stability in TTP-/- cells. TTP-dependent mRNA decay could only be detected when p38 MAPK was blocked (figure 7B) as shown for the other three validated mRNA targets (i.e. *IL-1α*, *IL-6* and *Cxcl2*, see manuscript figure 1D). We therefore propose that TTP regulates *Bcl3* mRNA decay in a p38 MAPK dependent fashion similar to other TTP-targets. TTP might indirectly affect this target as shown for *iNOS* [172], or directly interact with *Bcl3* by a yet unknown non-ARE binding-sequence or secondary structure. Indirect effects caused by the up-regulation of other factors in the TTP-/- background or by the treatment applied (e.g. SB203580 and act D) have to be excluded by more detailed analysis.

A) GACGGATGGGGGGGCAGACCCGGACTCATGAGGAGGGGCCTCCCTGCCCTGTGGGGACCA
CTCTTCTGGAAACTGTGAGGACCTTGTTCTGCTTCCCCCCGCCCAATCCTCGGGACCAGG
TTTTGCACCAAGGCACATGCACATACTACTGAGCACAGATCCTCCCAATCGCGCCCCTTG
CCCAGGACTCTCAGCCCCCACTTAATCTCAGGCACCCAGGTTCCCTGTCTGGAATCCACC
AGATACTCAATTCTTTGAGTGGAGGAACCAAAGGACAGCCAGCCTCTCCTCTGCCACCCT
CCACCCTGAGGGACCCAGAGAAACAGAGGGGTCTGGGAGGGCATTGATCACAGTGTAAAT
TATTAGGTTTGGGTCAGATTTCTTTTGTAATAAACTATTTTTGTATCATA

B)
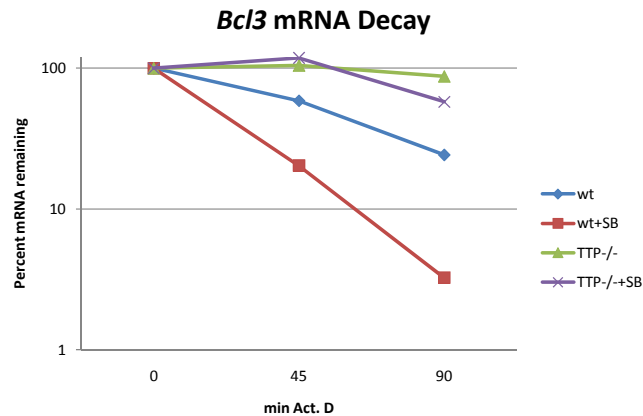
Figure 7: *Bcl3* mRNA, containing no ARE in the 3' UTR, is destabilized by TTP in a p38 MAPK-dependent way. (**A**) The murine 3' UTR of *Bcl3* lacks even the simplest core ARE sequence AUUUA. (**B**) WT and TTP$^{-/-}$ BMDMs were stimulated for 3 h with LPS followed by transcriptional blockage with act D in the presence or absence of the p38 MAPK inhibitor SB203580 (SB). The decay rate of *Bcl3* was monitored by qRT-PCR at the indicated time points. Remnant *Bcl3* mRNA in % of the amount at the time point act D treatment is depicted.

Besides ARE-less TTP targets, our screen revealed a large amount of transcripts containing AREs that appeared to be stable (~ 85 % of all ARE containing transcripts). Therefore an ARE does not necessarily confer instability. Even among those messages that contain AREs and were unstable, not all of them were destabilized in a TTP-dependent manner (~ 60 % of ARE containing unstable messages). One of them, *Dusp1* mRNA, displays several ideal TTP binding sites (figure 8A). However, preliminary experiments measuring mRNA stability of *Dusp1* could again confirm the data acquired by the microarray analysis. This message

was very rapidly degraded independently of p38 MAPK activity or TTP (figure 8B). We therefore suggest that *Dusp1* stability is controlled by a TTP-independent mechanism that overrides any putative TTP-mediated mRNA degradation.

A)
```
AGTTGTATGTTTGTTTATTTATGATCTGAAGTAATATATTTCTTCTTCTGAGAAGACATTTTGTTA
CTGGGATGACTTTTTTTATACAACAGAATAAATTATGACGTTTCGGGCAAGGGGAGGTGTGGAGTT
TCACTTGCCACCGGGTCGCCACTCCTCCTGTGGGAGGAGCAATGCAATAACTCTGGGAGAGGCTCA
TGGGAGCTGGTCCTTATTTATTTAACACCCCCCTCACCCCCCAACTCCTCCTGAGTTCCACTGAG
TTCCTAAGCAGTCACAACAATGACTTGACCGCAAGACATTTGCTGAACTCGGCACATTCGGGACCA
ATATATTGTGGGTACATCAAGTCCCTCTGACAAAACAGGGCAGAAGAGAAAGGACTCTGTTTGAGG
CAGTTTCTTCGCTTGCCTGTTTTTTTTTTTCTAGAAACTTCATGCTTGACACACCCACCAGTATTA
ACCATTCCCGATGACATGCGCGTATGAGAGTTTTTACCTTTATTTATTTTTGTGTAGGTCGGTGGT
CTGCCTTCACAAATGTCATTGTCTACTCATAGAAGAACCAAATACCTCAATTTTGTGTTTGCGTAC
TGTACTATCTTGTAAATAGACCCAGAGCAGGTTTGCTTTCGGCACTGACAGACAAAGCCAGTGTAG
GTTTGTAGCTTTCAGTTATCGACA
```

B)
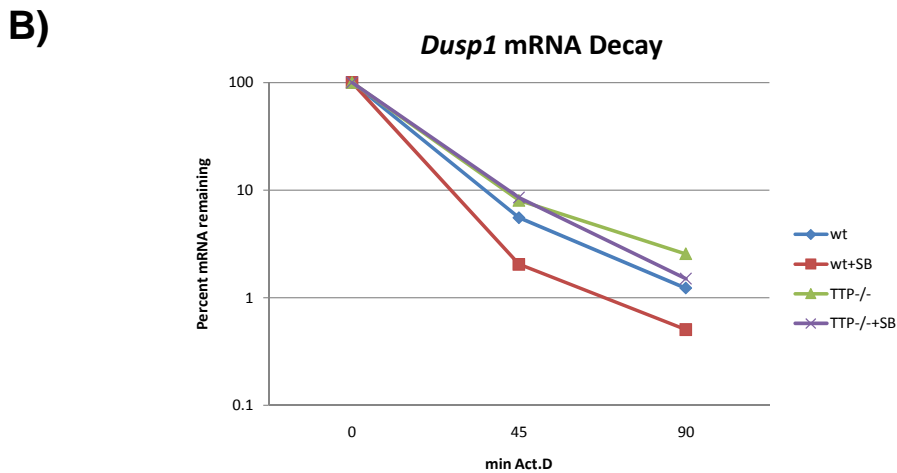
Figure 8: *Dusp1* mRNA, containing ideal TTP binding sites, is destabilized in a TTP-independent way. (**A**) The murine *Dusp1* has several AREs in its 3' UTR. The minimal ARE sequence AUUUA is highlighted in bold, UAUUUAU sequences representing the core TTP binding site are underlined, ideal TTP binding consensus sequences UUAUUUAUU are in boxes. (**B**) Wt and TTP-/- BMDMs were stimulated for 3 h with LPS followed by transcriptional blockage with act D in the presence or absence of the p38 MAPK inhibitor SB203580 (SB). The decay rate of D*usp1* was monitored by qRT-PCR at the indicated time points. Remaining *Dusp1* mRNA in % of the amount at the time point act D treatment is depicted.

6.4   Conditional TTP Ablation

Due to the strong phenotype developed by the conventional TTP knockout mouse, it was so far impossible to study the role of TTP in different tissues and forms of diseases *in vivo [76, 77]*. We hence established a conditional TTP knockout mouse and tested its utility for the study of disease models.

6.4.1 Generation of conditional TTP knockout mice

The murine *zfp36* gene encodes two exons, a very small exon 1 (24 bp) and exon 2 (1710 bp). The targeting vector was designed to replace the second larger exon 2 of *zfp36*, which includes the two zinc finger domains (bases 314-401 and 428-515 of NM_011756.4) by a *LoxP* site flanked exon 2 next to a Neo cassette that is followed by a third *LoxP* site (figure 9 A and B). After electroporation of the targeting construct into 129/OlaHsd ES cells, clones were selected for Neo expression and were tested for correct integration by PCR of genomic DNA using the primer P1, P2 and P3 (figure 9A). To avoid potential adverse effects, the Neo cassette was removed by transiently transfecting a Cre recombinase-expressing construct and resulting clones were checked for correct excision by PCR using the primer P4 and P5 (figure 9C). The targeted allele was subsequently sequenced to avoid possible mutations within the *LoxP* sites during recombination for Neo excision (figure 9C). The resulting allele with exon 2 of *zfp36* flanked by *LoxP* sites is called TTP^{fl} hereafter (figure 9C).

Two ES cell clones were then injected into C57Bl/6 blastocysts to generate chimeric mice. These animals were further crossed with C57Bl/6 mice and heterozygote offspring were interbred or backcrossed into C57Bl/6 strain using speed congenics.

Homozygous TTP^{fl} mice (TTP$^{fl/fl}$) on a mixed background were then crossed to LysMCre mice (C57Bl/6) for myeloid specific TTP ablation [173].
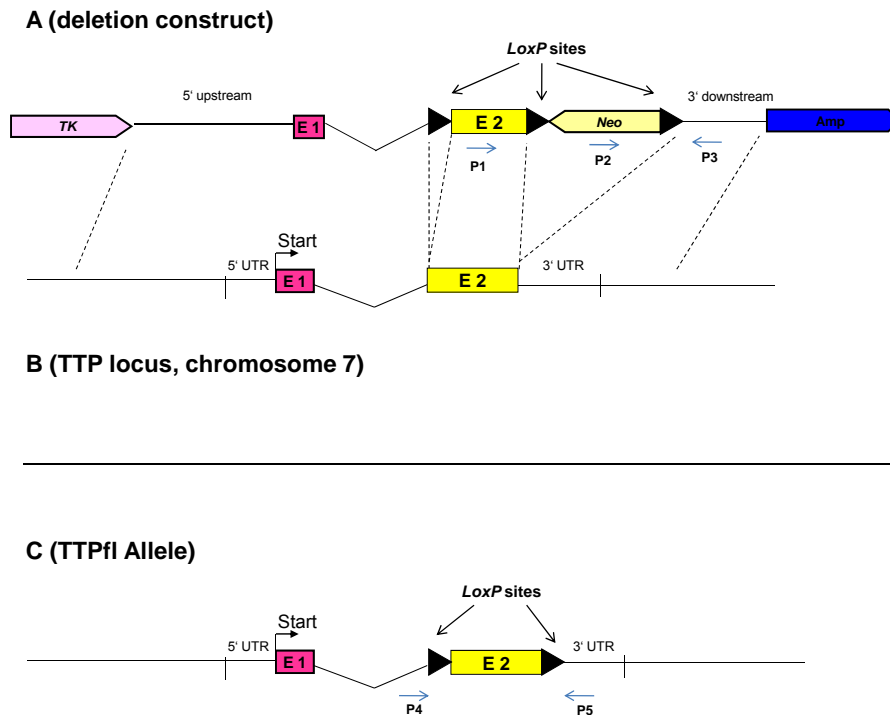
Figure 9: (**A**) Schematic picture of the construct for conditional TTP deletion, (**B**) the genomic locus of TTP on chromosome 7 and (**C**) the TTP^{fl} allele after Neo cassette excision. The corresponding sites between the construct and the chromosomal locus are indicated by dashed lines. Exon 1 and exon 2 of TTP are depicted as E1 and E2 boxes. TK, thymidine kinase; Amp, ampicillin.

6.4.2 Role of TTP during acute inflammation

TTP$^{fl/fl}$ LysMCre mice on a mixed background appeared normal at birth and did not show the decreased gain in weight typical for conventional TTP knockout (TTP-/-) animals on mixed or C57Bl/6 background after a few weeks of age (data not shown). First we tested whether exon 2 of TTP^{fl} LysMCre mice is efficiently excised by doing PCR on chromosomal DNA. As shown in figure 10A, exon 2 was deleted in BMDMs from TTP$^{fl/fl}$ LysMCre but not TTP$^{fl/fl}$ and Wt animals. We then examined TTP protein expression in these cells by Western blotting. TTP is undetectable in macrophages without LPS stimulation. As depicted in figure 10B, after 3 and 6 hours of stimulation, TTP protein was induced in Wt as well as in TTP$^{fl/fl}$, but not in TTP$^{fl/fl}$ LysMCre macrophages. Although the phosphorylation pattern with an increase of higher molecular weight TTP at later time-points was similar in TTP$^{fl/fl}$ and Wt cells, TTP protein expression from the TTP^{fl} allele was slightly lower after 3 and 6 hours of LPS treatment than in Wt cells. We conclude that the established TTP^{fl} allele can be used to

specifically excise exon 2 of *zfp36* and therefore abrogate TTP expression by addition of a Cre recombinase.
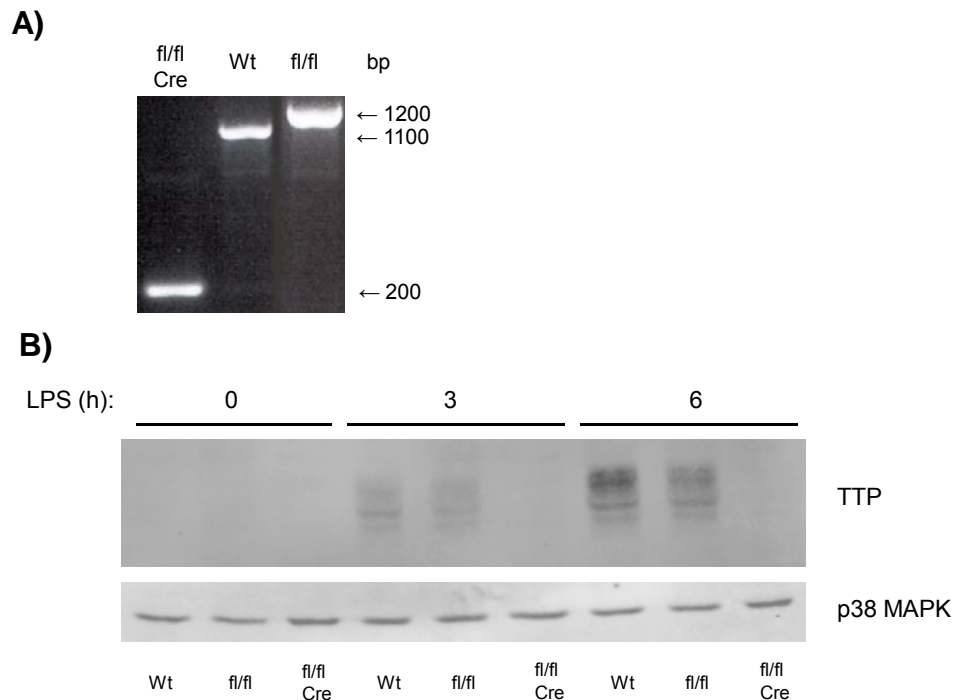
Figure 10: TTP expression in BMDMs of myeloid-specific TTP knockout mice. **(A)** PCR analysis of chromosomal DNA from BMDMs of TTP^fl/fl LysMCre (fl/fl Cre), Wt and TTP^fl/fl (fl/fl) mice using the Primer P4 and P5 as depicted in (figure 9). The Wt allele results in an 1100 bp band, the slightly larger TTP^fl allele in a 1200 bp and the excised exon 2 in a truncated 200 bp fragment. (B) BMDMs from Wt, TTP^fl/fl (fl/fl) or TTP^fl/fl LysMCre mice (fl/fl Cre) were treated with LPS for 3 or 6 hours or left untreated. TTP protein levels were examined by Western blotting with antibody to TTP. The blots were reprobed with antibody to p38 MAPK to control for loading. One out of 3 independent experiments is shown.

TTP was suggested to play a main role during chronic inflammation by regulating TNFα levels as demonstrated by studies using TTP-/- mice. In these animals, predominantly macrophages are supposed to be the main source for elevated TNFα production responsible for the TTP-/- phenotype [76]. However, without stimulation, TTP was almost undetectable in macrophages but could be transiently induced by various inflammatory stimuli like LPS (figure 10). We therefore hypothesized that TTP might also play a role during acute inflammation *in vivo*. The TTP-/- mice are of poor health and the number and degree of

pathologies developed is rather heterogeneous [76]. The availability of the TTP^{fl/fl} LysMCre allowed us to use animals without an obvious health defect for *in vivo* studies. By using TTP^{fl/fl} LysMCre mice, we tested the role of myeloid TTP during endotoxic shock. Upon injection of a lethal dose of LPS, the engagement of the TLR4, the LPS receptor, predominantly on monocytes and macrophages induces the production of an array of pro-inflammatory cytokines [174]. We could show that the development of the subsequent lethal shock is enhanced when TTP is ablated in myeloid cells (figure 11). TTP^{fl/fl} LysMCre mice died significantly earlier than did their Wt and TTP^{fl/fl} littermates pointing out an important role for TTP in limiting the immune response elicited by myeloid cells during acute inflammation. This finding is in accordance with the role of TTP in macrophages, controlling mRNA stability of important pro-inflammatory cytokines as TNFα, IL-1α, IL-1β and IL-6 [31, 76] (see manuscript).
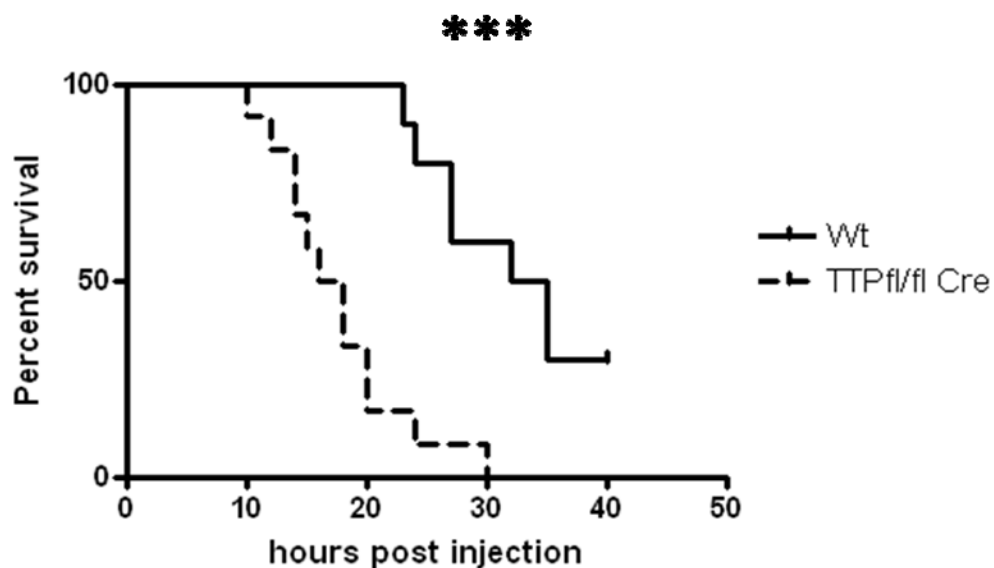
Figure 11: Myeloid-specific TTP knockout mice are more susceptible to LPS driven endotoxic shock. Kaplan-Meier blot of Wt mice (n=10; comprising Wt and TTP^{fl/fl} mice) and TTP^{fl/fl} LysMCre mice (n=12) treated with LPS by intraperitoneal injection. Significance of the difference of the obtained survival curves was calculated using Logrank Test (***: P<0.001).

6.5   Conditional TTP Overexpression

We next asked, as a "proof of principle", whether an increase in TTP expression can be beneficial during different forms of inflammation. Therefore we aimed to establish a mouse-line conditionally overexpressing TTP. This system would allow the investigation of the tissue specific effect of increased TTP levels during infection, inflammation and other pathological conditions.

6.5.1 Generation of mice conditionally overexpressing TTP

The targeting construct (hereafter referred to as UbiC-flSTOPfl-TTP) for the generation of a transgenic TTP mouse-line was designed to integrate by homologous recombination into the collagen type A locus. The TTP transgene (cDNA) is expressed from the construct using a UbiC promoter known to drive ubiquitous expression in transgenic mice [150]. A floxed Neo and transcriptional STOP cassette in between the UbiC promoter and the *TTP* cDNA allows conditional activation of cDNA expression. The transcribed message is bicistronic facilitating the expression of an enhanced cyan fluorescent protein (ECFP) due to an IRES after the *TTP* cDNA (figure 12A). Transient cotransfections of the UbiC-flSTOPfl-TTP targeting construct and a Cre recombinase expressing plasmid into murine embryonic fibroblasts (MEFs) demonstrated the construct to be functionally expressing TTP in a Cre dependent way (figure 12B). ES cells were transfected with the targeting construct, selected for Neo expression and clones were tested for correct integration by PCR (figure 12C). Positive clones were further injected into C57Bl/6 blastocysts to generate chimeric mice. These animals were backcrossed into C57Bl/6 background using speed congenics. The mouse strain harbouring an UbiC-flSTOPfl-TTP allele will be hereafter referred to as TTP^{high}.

A) Targeting Construct

B)

+ Cre   - Cre
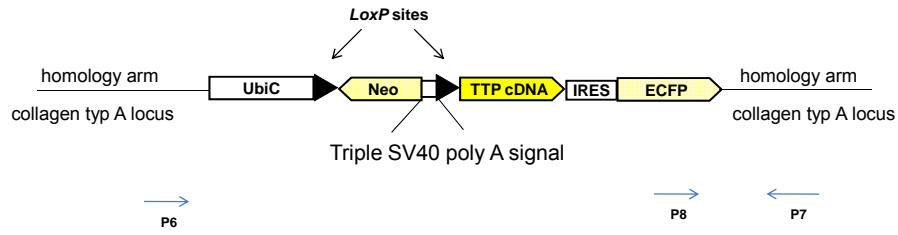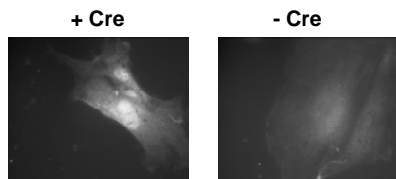
C)
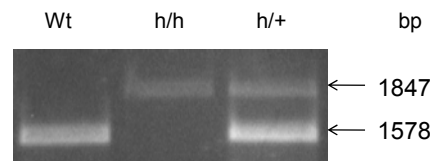
Figure 12. (**A**) Schematic picture of the construct for conditional TTP overexpression. (**B**) Anti-TTP immunofluorescence of MEFs transfected with the Ubi-flSTOPfl-TTP plasmid alone (-Cre) or cotransfected with a Cre recombinase expressing plasmid (+Cre). (**C**) PCR analysis of genomic DNA from Wt, homozygous TTP[high] (h/h) and heterozygous (h/+) mice using the primer P6, P7 and P8.

TTP[high] mice were then crossed to LysMCre mice, also on C57Bl/6 background. BMDMs of these animals were further examined for TTP overproduction. Untreated as well as LPS-treated (4 h) macrophages from TTP[high] LysMCre mice did not produce significantly higher levels of TTP protein (figure 13A). In addition, analysis using a fluorescence-activated cell sorter (FACS) revealed a very limited expression of ECFP from the construct (figure 13B). Therefore a possible TTP overexpression might be too low to be detected by Western blotting of cells that produce high endogenous levels of TTP. Hence we tested whether these cells produce different amounts of TNFα after LPS stimulation. Decreased TNFα protein levels after LPS stimulation due to an increased *Tnf* mRNA degradation could indicate TTP overexpression in TTP[high] LysMCre BMDMs. However, Wt and TTP[high] LysMCre macrophages produced equal TNFα levels as depicted in figure 13C. We therefore conclude that TTP[high] LysMCre BMDMs do not produce detectable higher amounts of TTP nor do BMDMs of these mice show the expected phenotype after LPS stimulation. A

possible explanation is that the UbiC promoter is too weak to drive robust TTP expression in this cell-type or that cells overexpressing TTP are lost due negative selection caused by possible harmful effects of constitutively increased TTP levels.
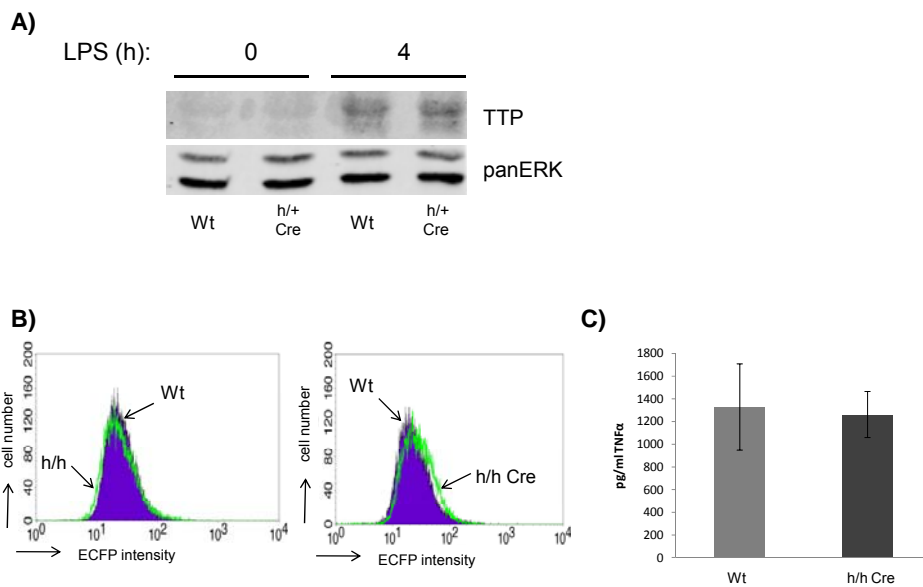
Figure 13. TTP[high] LysMCre macrophages do not display elevated TTP protein levels. (**A**) BMDMs of Wt and heterozygous TTP[high] LysMCre (h/+ Cre) mice were left untreated or were stimulated with LPS for four hours and TTP protein was measured by Western blotting. The blots were reprobed with antibody to panERK to control for loading. One representative example out of three is shown. (**B**) FACS analysis comparing ECFP expression of Wt and homozygous TTP[high] (h/h) BMDMs (left panel), and Wt and homozygous TTP[high] LysMCre (h/h Cre) BMDSs (right panel). One out of three independent experiments is depicted. (**C**) TNFα protein secreted by Wt and homozygous TTP[high] LysMCre (h/h Cre) BMDMs after three hours LPS treatment was measured by ELISA. Data show mean +/- SD of three independent experiments.

6.6 Role of TTP in Abelson-induced Transformation of B-cells

Pathologically stable mRNAs have been proposed to influence cancer development [122, 175-178]. In agreement with this, a recent study demonstrated that TTP can influence tumorigenesis in a mast cell tumor model. The authors could show that introduction of a TTP expressing plasmid into v-H-*ras* transformed PB-3c mast cells leads to decreased IL-3 expression and reduced tumor formation. Tumor formation of PB-3c cells transformed by *v-abl*, which happens in a nonautocrine manner independent of IL-3, was shown to be unaltered upon TTP transfection [83]. However, as TTP influences B-cell function, we investigated the role of TTP in a model of Abelson-induced B-cell lymphoma formation [161, 179]. B-cell progenitors can be easily transformed into tumor cell lines by single exposure to Abelson murine leukemia virus (Ab-MuLV) [180]. The *v-abl* oncogene provided by Ab-MuLV is a hybrid of the viral *gag* gene fused to a part of the *c-abl* gene encoding a nonreceptor tyrosine kinase [181].

We could show that TTP mRNA is readily expressed in spleen and bone marrow of Wt mice. In Abelson-transformed B-cell-lines however, TTP mRNA levels appeared to be diminished, indicating a putative negative selection for TTP expression (figure 14).
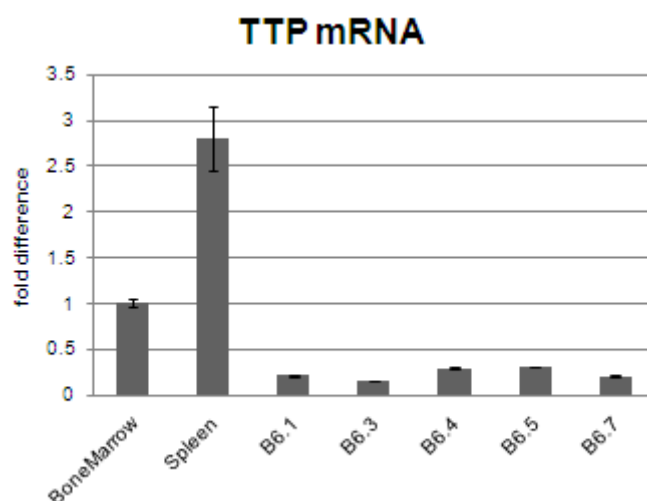
Figure 14. *TTP* mRNA expression in bone marrow, spleen and five Abelson-transformed B-cell lines (B6.1, B6.3, B6.4, B6.5 and B6.7). mRNA levels are normalized to *HPRT* and bone marrow *TTP* levels. Data show mean +/- SD of three experiments.

6.6.1 B-cell development in TTP knockout animals

Previous studies using mixed background TTP-/- mice revealed some abnormalities of the hematopoietic system characterized by an increase in myeloid cells in peripheral blood, spleen and bone marrow and a slight decrease in B and T lymphocytes [76]. We could confirm for TTP-/- mice on C57Bl/6 background an increased number of granulocytes and monocytes in blood and a small decrease for B-cells, especially late B-cell stages in spleen, lymph nodes and blood. However, there were no gross abnormalities detectable in the different B-cell progenitor stages indicating a minor role for TTP in normal B-cell development (see master thesis of Christian Machacek).

6.6.2 TTP in Abelson induced B-cell transformation

We first investigated the influence of TTP on the efficiency of Ab-MuLV-induced transformation of B-cell progenitors which includes the loss of growth factor requirement (i.e. IL-7). Bone marrow from Wt and TTP-/- mice was infected with Ab-MuLV and then cultivated in cytokine-free methylcellulose. As illustrated in figure 15A, the number of clones from B-cell progenitors of TTP-/- animals was increased compared to Wt. The colonies were identified by FACS as pre B-cells (CD19$^+$/CD43$^+$/B220$^+$). As the number of CD43$^+$/B220$^+$ B-cell precursor cells is slightly different in Wt and TTP-/- bone marrow as determined by FACS (43 % and 39 % pre B-cells of CD43+/B220+ Wt and TTP-/- cells, respectively; see master thesis of Christian Machacek), we corrected the number of colonies per 10^6 cells accordingly (figure 15B). We therefore propose that lack of TTP promotes Abelson-induced transformation of B-cell progenitors into cell-lines that grow independently of any growth factor as IL-7 (figure 15A and B). In *v-abl*-induced transformation of B-cells potentially one or more TTP target mRNAs are stabilized by the loss of TTP and alleviate transformation, being in accordance with a role of TTP as tumor suppressor [83].
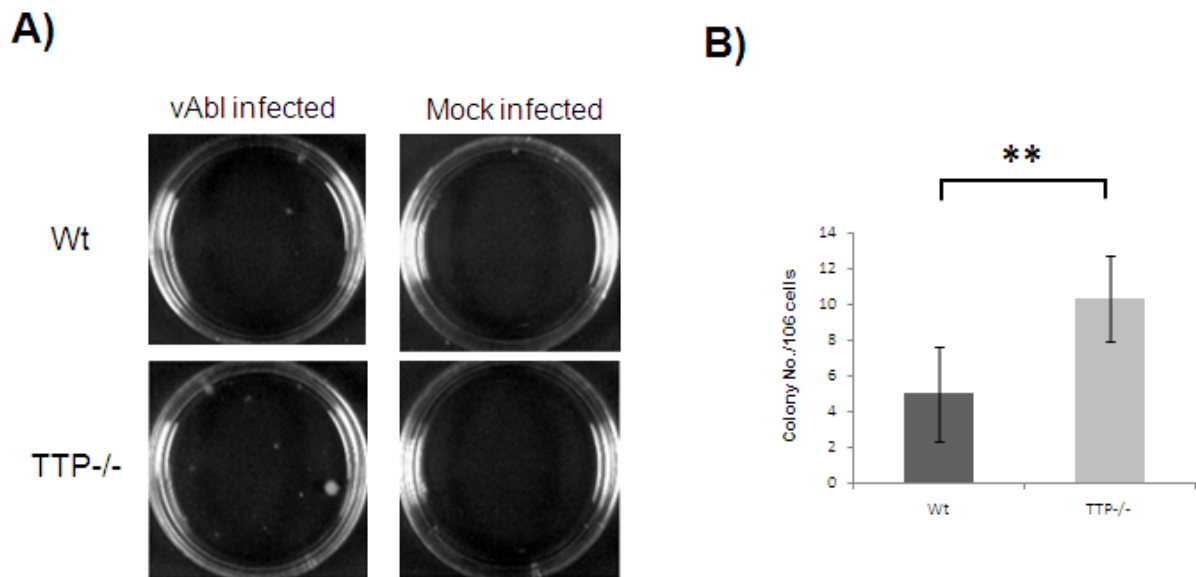
Figure 15. (**A**) Bone marrow of Wt and TTP-/- mice was infected with Abelson virus (*vAbl*) or left uninfected (Mock) and was subsequently grown in growth factor-free methylcellulose. One representative example is shown. (**B**) Colonies from two plates as seen in (**A**) from 3 independent experiments per genotype were counted. The resulting numbers were normalized to the amount of B-cell progenitors of WT and TTP-/- bone marrow determined by FACS. Data show the mean value +/- SD. Statistical significance was determined using students t-test (**: P<0.01)

6.6.3 Role of TTP in B-cell lymphoma formation

In addition to the transformation efficiency, the transformed clones were examined for tumor growth *in vivo* by subcutaneously injecting cells of four TTP-/- and three Wt Abelson-transformed B-cell-lines into Wt mice (C57Bl/6). Each clone was thereby injected into four individual mice. After 10 days TTP-/- clones showed increased average tumor mass, although the tumor size was very heterogeneous between different clones. We therefore conclude that lack of TTP leads on average to increased tumor growth. However, the heterogeneous growth rate of TTP-/- tumors derived from different clones might indicate that additional unknown factors and/or secondary mutations work in concert with TTP. Whether the overall enhanced tumor formation is due to increased proliferation and/or reduced apoptosis has to be elucidated. As *VEGF* mRNA can be targeted by TTP [81], differences in vascularisation might also play a role. However, at the time of tumor-isolation, tumor-size

was too small to address this question. The precise molecular mechanism of the tumor-suppressive function of TTP in this tumor model will be investigated in future studies.
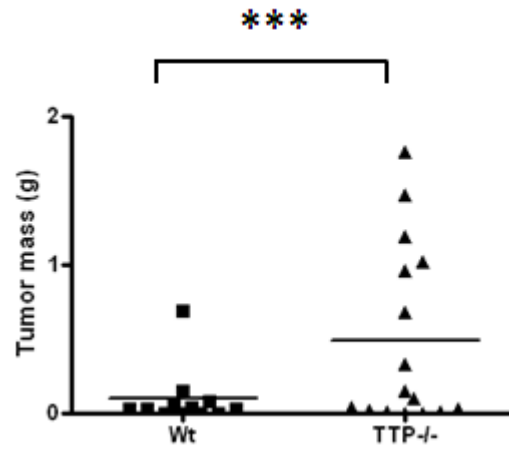
Figure 16. Mean tumor mass in Wt animals injected with 2x10^6 Wt or TTP-/- Abelson transformed B-cells. Four independent TTP-/- and three Wt clones were injected subcutaneously into four Wt mice each. Statistical significance was analyzed using nested anova (*: P<0.001)

7. FINAL DISCUSSION

7.1 Role of TTP-mediated mRNA Decay in LPS-treated Macrophages

After infection or tissue injury, the immune system must be able to induce a robust response. However, a prolonged or uncontrolled immune reaction can be as detrimental as a reduced one that might lead to inefficient pathogen clearing. In this context, mRNA degradation is of supreme importance because simply stopping transcription does not necessarily lead to the termination of expression unless the already generated mRNAs are removed [167]. This has been documented in a knockin mouse model bearing a stabilized version of *Tnf* mRNA (due to the deletion of AREs in the 3´ UTR of *Tnf*). These animals developed chronic inflammatory arthritis and inflammatory bowel disease (IBD) pointing out the importance of mRNA stability in the regulation of gene expression and immune homeostasis [167]. Therefore a mechanism must be provided that can selectively stabilize or degrade certain transcripts during distinct phases of inflammation in order to allow both a strong induction as well as elimination of mRNAs in appropriate times and quantity. We could show that TTP, as a protein controlling mRNA removal, is part of a negative feedback loop that leads to the delayed degradation of a broad set of inflammation induced mRNAs. In this loop, pro-inflammatory stimuli like LPS trigger activation p38 MAPK. This kinase is important for the initiation of the immune response by up-regulating several mediators of inflammation. At the same time p38 MAPK increases expression of TTP as well as other anti-inflammatory proteins like IL-10. Consistently, p38 MAPK has been shown to play an essential role for both pro- and anti-inflammatory mechanisms [39, 61, 65]. In the initial phase of inflammation, high p38 MAPK activity blocks TTP function by phosphorylation and thereby protects certain mRNAs from TTP-mediated degradation as shown for *IL-1α*, *IL-6* and *Cxcl2* (figure 17).

We demonstrated that only some very unstable messages like *Tnf* mRNA can be targeted by TTP for degradation after short LPS stimulation whereas most other TTP targets appear stable in this phase. Simultaneously, TTP expression is highly induced in BMDMs after p38

MAPK activation and TTP protein accumulates because a p38 MAPK-dependent phosphorylation of TTP blocks proteasome-dependent TTP-degradation [45]. After prolonged LPS treatment, the endogenously produced IL-10 gradually inactivates p38 MAPK. This inactivation happens via the IL-10 dependent up-regulation of the p38 MAPK phosphatase DUSP1 [30, 66] (figure 17). In addition, IL-10 signaling, by activating STAT3, further increases TTP expression in LPS treated macrophages [30, 64]. Activation of STAT3 by IL-6 signaling also increases TTP expression in LPS stimulated macrophages but does not lead to p38 MAPK inactivation. Hence, IL-6 does not initiate the TTP-dependent anti-inflammatory response seen for IL-10. Thus, our data indicate that both the IL-10-mediated increase of TTP expression as well as the IL-10-induced dephosphorylation of TTP are essential for the full anti-inflammatory function of this cytokine.
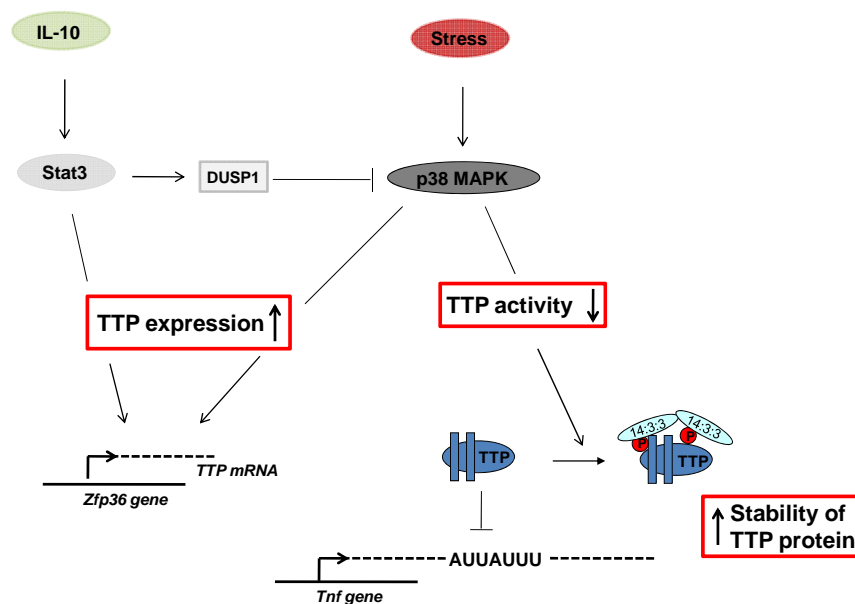
Figure 17. p38 MAPK regulates TTP functions in three ways. First, when p38 MAPK gets activated it increases TTP expression. Second, it rapidly blocks TTP activity by phosphorylation and third, it protects TTP-protein from degradation [39, 182]. IL-10 signaling at later stages additionally increases TTP expression and deactivates p38 MAPK thereby releasing the p38 MAPK imposed block on TTP activity [30].

In the ensuing work we showed that at later stages of inflammation, the reduced activity of p38 MAPK leads to diminished phosphorylation and thereby to increased activity of the accumulated TTP resulting to the TTP-dependent removal of a big proportion of inflammation induced unstable transcripts [72, 73]. By mimicking the gradually reduced p38 MAPK activity through the pharmacological inhibition of p38 MAPK we revealed that 30 % of all unstable LPS-induced mRNAs are degraded in a TTP-dependent way (see manuscript figure 2). TTP-target mRNAs like *Cxcl2* that appear stable in the initial phase of inflammation (e.g. 3 hours after LPS stimulation), become increasingly unstable at later stages, coinciding with an IL-10 dependent decrease in p38 MAPK activity. This finding is in agreement with the *Cxcl2* mRNA stability profile published recently, showing high stability after short LPS stimulation but reduced stability after prolonged LPS stimulation [2]. *IL-10* mRNA, which has been shown to be a TTP-target too, is also protected by high p38 MAPK activity from decay in the first stages after inflammation. This mechanism allows *IL-10* mRNA to accumulate until the IL-10 cytokine has initiated the resolution phase of the inflammation and the final decline of the p38 MAPK signaling [27]. Then IL-10 can be targeted for degradation by activated TTP in order to restore the original state.

Why targets as *Tnf* are degraded in a TTP-dependent way early during inflammation when p38 MAPK activity is high, whereas other messages like *Cxcl2* are stable in this initial phase is still obscure. A simple explanation might be the affinity of TTP to its target sequence. Suboptimal binding sites as the AREs of *IL-1α* and *IL-6* may require higher TTP activity for efficient degradation. However, *Cxcl2* and *Tnf* contain both a similar ARE pattern. Therefore additional factors as other RNA-binding proteins or secondary structures controlling ARE accessibility might play a role. Although AREs in the 3' UTR have been demonstrated to be an important factor in TTP binding, it is still elusive how a TTP-target can be defined. For example, messages devoid of any form of ARE like *Bcl3* mRNA can be degraded in a TTP and p38 MAPK dependent way. Whether this decay happens through direct interaction of TTP with these messages or by more complex scenarios potentially involving other RNA-binding factors as shown for *iNOS* has to be determined [172]. On the other hand, some

mRNAs comprising AREs suggested to be optimal for binding were not targeted by TTP in our screen. These transcripts were either stable or were unstable even in the absence of TTP. Both situations could result from other factors known to stabilize or destabilize mRNAs. miRNAs for instance are a prominent candidate that might either co-operate with TTP or compensate for the lack of TTP. TTP possibly discriminates not only according to mRNA intrinsic factors as sequence and structural properties but also by competing or cooperating with other factors for binding.

7.2 The Role of TTP *In Vivo*

TTP is expressed in several tissues as liver, lung and colon [183-185] and is induced by various stimuli [36, 37, 39, 40]. However, the so far only described physiological TTP targets are *Tnf* and *GM-Csf*. Although TTP-/- mice do not show elevated TNFα serum levels, administration of anti-mouse neutralizing antibodies to TNFα prevented the phenotype almost completely [10, 76]. However, anti-TNFα antibody treatment and the succeeding dominant neutralization of TNFα-signaling might obscure the influence of other factors involved. Accordingly, TTP-/- mice deficient in both TNFα receptors, TNFR1 and TNFR2, did not develop arthritis or cachexia but still displayed after approximately six month of age medullary and extramedullary myeloid hyperplasia typical for TTP-/- mice [186].

Our study could demonstrate that TTP controls an ample spectrum of mRNAs rather than only a small fraction. We therefore anticipate a broader function of TTP than the so far shown physiological role in controlling *Tnf* mRNA stability during different forms of chronic inflammation [76]. Although the conventional TTP knockout mouse has been published more than 10 years ago, only limited data have been obtained about the role of TTP in disease models because of the overall poor health, a heterogeneous phenotype and the short life span of these animals. Therefore many open questions remain unanswered. For instance, mice deleted for the ARE sequence within the *Tnf* 3' UTR as described before produce a stabilized *Tnf* message and higher amounts of TNFα protein. These animals spontaneously

develop IBD, an inflammation of the intestinal epithelium [167]. TTP is also expressed in this epithelium, yet TTP knockout mice do not develop any form of spontaneous IBD although *Tnf* mRNA is known to be stabilized in these animals [76, 82]. It is up to be determined whether TTP plays a minor role in controlling *Tnf* mRNA stability in the cells responsible for the development of TNFα-mediated IBD, or if other factors (e.g. IL-10) that are up-regulated in the TTP-/- mouse ameliorate the effect of higher TNFα expression. All these questions can be addressed only by employing animals that allow studies of TTP function *in vivo*, that is by using a homogenous cohort of mice conditionally deleting TTP. The mouse-line conditionally ablated for *zfp36* (the gene encoding TTP), that we have established, proved in preliminary experiments to be suitable for studies of the TTP function *in vivo*. These animals delete efficiently the floxed TTP allele in macrophages if crossed to LysMcre. Importantly, these macrophage-specific deleters do not show the typical TTP phenotype like reduced growth and body fat. This was unexpected, since these characteristic features of TTP-deficiency have been attributed to TNFα overproduction mainly by macrophages in a previous report [77]. In that study, transplantation of TTP-/- bone marrow into recombination activating gene-2 (-/-) mice reproduced the TTP phenotype after a lag phase of a few months correlating with the slow repopulation by macrophages [77]. As TTP^{fl/fl} LysMCre mice do not display this type of pathology, we suggest that other hematopoietic cells might influence the development of the phenotype. TTP-deficient macrophages may activate other effector-cells that also need to lack TTP expression in order to develop the phenotype seen in TTP-/- mice. However, a detailed analysis of the health status of myeloid-specific TTP knockout mice will be necessary in order to dissect the contribution of myeloid specific TTP expression.

Ex vivo experiments using TTP-/- macrophages from bone marrow, peritoneal cavity or fetal liver demonstrated that these cells produce more TNFα after LPS treatment than Wt cells [77]. In accordance with this finding, TTP^{fl/fl} LysMCre mice are more susceptible to LPS-driven endotoxic shock. We therefore suggest a role for TTP during acute inflammation by controlling mRNA decay of a broad spectrum of transcripts, in particular by actuating the

expression of pro-inflammatory mediators as TNFα, IL-1α, IL-1β and IL-6 produced by myeloid cells [31, 76] (see manuscript). As myeloid-specific TTP knockout mice do not develop the full-blown phenotype seen in the conventional TTP knockouts, we hypothesize that TTP plays a more general role in immune homeostasis potentially involving other cells of the hematopoietic system.

8. REFERENCES

1. Mittal, N., et al., *Dissecting the expression dynamics of RNA-binding proteins in posttranscriptional regulatory networks.* Proc Natl Acad Sci U S A, 2009.
2. Hao, S. and D. Baltimore, *The stability of mRNA influences the temporal order of the induction of genes encoding inflammatory molecules.* Nat Immunol, 2009. **10**(3): p. 281-8.
3. Akira, S., S. Uematsu, and O. Takeuchi, *Pathogen recognition and innate immunity.* Cell, 2006. **124**(4): p. 783-801.
4. Shaw, G. and R. Kamen, *A conserved AU sequence from the 3' untranslated region of GM-CSF mRNA mediates selective mRNA degradation.* Cell, 1986. **46**(5): p. 659-67.
5. Litvak, V., et al., *Function of C/EBPdelta in a regulatory circuit that discriminates between transient and persistent TLR4-induced signals.* Nat Immunol, 2009. **10**(4): p. 437-43.
6. Lai, W.S., D.J. Stumpo, and P.J. Blackshear, *Rapid insulin-stimulated accumulation of an mRNA encoding a proline-rich protein.* J Biol Chem, 1990. **265**(27): p. 16556-63.
7. Varnum, B.C., et al., *Nucleotide sequence of a cDNA encoding TIS11, a message induced in Swiss 3T3 cells by the tumor promoter tetradecanoyl phorbol acetate.* Oncogene, 1989. **4**(1): p. 119-20.
8. DuBois, R.N., et al., *A growth factor-inducible nuclear protein with a novel cysteine/histidine repetitive sequence.* J Biol Chem, 1990. **265**(31): p. 19185-91.
9. Lai, W.S., et al., *Evidence that tristetraprolin binds to AU-rich elements and promotes the deadenylation and destabilization of tumor necrosis factor alpha mRNA.* Mol Cell Biol, 1999. **19**(6): p. 4311-23.
10. Carballo, E., W.S. Lai, and P.J. Blackshear, *Evidence that tristetraprolin is a physiological regulator of granulocyte-macrophage colony-stimulating factor messenger RNA deadenylation and stability.* Blood, 2000. **95**(6): p. 1891-9.
11. Lai, W.S., E.A. Kennington, and P.J. Blackshear, *Interactions of CCCH zinc finger proteins with mRNA: non-binding tristetraprolin mutants exert an inhibitory effect on degradation of AU-rich element-containing mRNAs.* J Biol Chem, 2002. **277**(11): p. 9606-13.
12. Lykke-Andersen, J. and E. Wagner, *Recruitment and activation of mRNA decay enzymes by two ARE-mediated decay activation domains in the proteins TTP and BRF-1.* Genes Dev, 2005. **19**(3): p. 351-61.
13. Johnson, B.A. and T.K. Blackwell, *Multiple tristetraprolin sequence domains required to induce apoptosis and modulate responses to TNFalpha through distinct pathways.* Oncogene, 2002. **21**(27): p. 4237-46.
14. Baou, M., A. Jewell, and J.J. Murphy, *TIS11 family proteins and their roles in posttranscriptional gene regulation.* J Biomed Biotechnol, 2009. **2009**: p. 634520.
15. Barreau, C., L. Paillard, and H.B. Osborne, *AU-rich elements and associated factors: are there unifying principles?* Nucleic Acids Res, 2005. **33**(22): p. 7138-50.
16. Meisner, N.C., et al., *mRNA openers and closers: modulating AU-rich element-controlled mRNA stability by a molecular switch in mRNA secondary structure.* Chembiochem, 2004. **5**(10): p. 1432-47.
17. Bakheet, T., B.R. Williams, and K.S. Khabar, *ARED 3.0: the large and diverse AU-rich transcriptome.* Nucleic Acids Res, 2006. **34**(Database issue): p. D111-4.
18. Bakheet, T., et al., *ARED: human AU-rich element-containing mRNA database reveals an unexpectedly diverse functional repertoire of encoded proteins.* Nucleic Acids Res, 2001. **29**(1): p. 246-54.
19. Halees, A.S., R. El-Badrawi, and K.S. Khabar, *ARED Organism: expansion of ARED reveals AU-rich element cluster variations between human and mouse.* Nucleic Acids Res, 2008. **36**(Database issue): p. D137-40.

20.   Khabar, K.S., *The AU-rich transcriptome: more than interferons and cytokines, and its role in disease.* J Interferon Cytokine Res, 2005. **25**(1): p. 1-10.

21.   Worthington, M.T., et al., *RNA binding properties of the AU-rich element-binding recombinant Nup475/TIS11/tristetraprolin protein.* J Biol Chem, 2002. **277**(50): p. 48558-64.

22.   Brewer, B.Y., et al., *RNA sequence elements required for high affinity binding by the zinc finger domain of tristetraprolin: conformational changes coupled to the bipartite nature of Au-rich MRNA-destabilizing motifs.* J Biol Chem, 2004. **279**(27): p. 27870-7.

23.   Emmons, J., et al., *Identification of TTP mRNA targets in human dendritic cells reveals TTP as a critical regulator of dendritic cell maturation.* Rna, 2008. **14**(5): p. 888-902.

24.   Lai, W.S., et al., *Novel mRNA targets for tristetraprolin (TTP) identified by global analysis of stabilized transcripts in TTP-deficient fibroblasts.* Mol Cell Biol, 2006. **26**(24): p. 9196-208.

25.   Ogilvie, R.L., et al., *Tristetraprolin Down-Regulates IL-2 Gene Expression through AU-Rich Element-Mediated mRNA Decay.* J Immunol, 2005. **174**(2): p. 953-61.

26.   Ogilvie, R.L., et al., *Tristetraprolin mediates interferon-gamma mRNA decay.* J Biol Chem, 2009. **284**(17): p. 11216-23.

27.   Stoecklin, G., et al., *Genome-wide analysis identifies interleukin-10 mRNA as target of tristetraprolin.* J Biol Chem, 2008. **283**(17): p. 11689-99.

28.   Datta, S., et al., *Tristetraprolin regulates CXCL1 (KC) mRNA stability.* J Immunol, 2008. **180**(4): p. 2545-52.

29.   Stoecklin, G., et al., *Somatic mRNA turnover mutants implicate tristetraprolin in the interleukin-3 mRNA degradation pathway.* Mol Cell Biol, 2000. **20**(11): p. 3753-63.

30.   Schaljo, B., et al., *Tristetraprolin is required for full anti-inflammatory response of murine macrophages to IL-10.* J Immunol, 2009. **183**(2): p. 1197-206.

31.   Chen, Y.L., et al., *Differential regulation of ARE-mediated TNFalpha and IL-1beta mRNA stability by lipopolysaccharide in RAW264.7 cells.* Biochem Biophys Res Commun, 2006. **346**(1): p. 160-8.

32.   Brooks, S.A., J.E. Connolly, and W.F. Rigby, *The role of mRNA turnover in the regulation of tristetraprolin expression: evidence for an extracellular signal-regulated kinase-specific, AU-rich element-dependent, autoregulatory pathway.* J Immunol, 2004. **172**(12): p. 7263-71.

33.   Fechir, M., et al., *Tristetraprolin regulates the expression of the human inducible nitric-oxide synthase gene.* Mol Pharmacol, 2005. **67**(6): p. 2148-61.

34.   Jalonen, U., et al., *Down-regulation of tristetraprolin expression results in enhanced IL-12 and MIP-2 production and reduced MIP-3alpha synthesis in activated macrophages.* Mediators Inflamm, 2006. **2006**(6): p. 40691.

35.   Stoecklin, G., et al., *Cellular mutants define a common mRNA degradation pathway targeting cytokine AU-rich elements.* RNA, 2001. **7**(11): p. 1578-88.

36.   Ogawa, K., et al., *Transcriptional regulation of tristetraprolin by transforming growth factor-beta in human T cells.* J Biol Chem, 2003. **278**(32): p. 30373-81.

37.   Carballo, E., W.S. Lai, and P.J. Blackshear, *Feedback inhibition of macrophage tumor necrosis factor-alpha production by tristetraprolin.* Science, 1998. **281**(5379): p. 1001-5.

38.   Mahtani, K.R., et al., *Mitogen-activated protein kinase p38 controls the expression and posttranslational modification of tristetraprolin, a regulator of tumor necrosis factor alpha mRNA stability.* Mol Cell Biol, 2001. **21**(19): p. 6461-9.

39.   Sauer, I., et al., *Interferons limit inflammatory responses by induction of tristetraprolin.* Blood, 2006. **107**(12): p. 4790-7.

40.   Suzuki, K., et al., *IL-4-Stat6 signaling induces tristetraprolin expression and inhibits TNF-alpha production in mast cells.* J Exp Med, 2003. **198**(11): p. 1717-27.

41.   Smoak, K. and J.A. Cidlowski, *Glucocorticoids regulate tristetraprolin synthesis and posttranscriptionally regulate tumor necrosis factor alpha inflammatory signaling.* Mol Cell Biol, 2006. **26**(23): p. 9126-35.

42.   Lai, W.S., E.A. Kennington, and P.J. Blackshear, *Tristetraprolin and its family members can promote the cell-free deadenylation of AU-rich element-containing mRNAs by poly(A) ribonuclease.* Mol Cell Biol, 2003. **23**(11): p. 3798-812.

43.   Hau, H.H., et al., *Tristetraprolin recruits functional mRNA decay complexes to ARE sequences.* J Cell Biochem, 2007. **100**(6): p. 1477-92.

44.   Blackshear, P.J., *Tristetraprolin and other CCCH tandem zinc-finger proteins in the regulation of mRNA turnover.* Biochem Soc Trans, 2002. **30**(Pt 6): p. 945-52.

45.   Deleault, K.M., S.J. Skinner, and S.A. Brooks, *Tristetraprolin regulates TNF TNF-alpha mRNA stability via a proteasome dependent mechanism involving the combined action of the ERK and p38 pathways.* Mol Immunol, 2008. **45**(1): p. 13-24.

46.   Stoecklin, G., et al., *MK2-induced tristetraprolin:14-3-3 complexes prevent stress granule association and ARE-mRNA decay.* EMBO J, 2004. **23**(6): p. 1313-24.

47.   Kedersha, N.L., et al., *RNA-binding proteins TIA-1 and TIAR link the phosphorylation of eIF-2 alpha to the assembly of mammalian stress granules.* J Cell Biol, 1999. **147**(7): p. 1431-42.

48.   Sheth, U. and R. Parker, *Decapping and decay of messenger RNA occur in cytoplasmic processing bodies.* Science, 2003. **300**(5620): p. 805-8.

49.   Kedersha, N., et al., *Stress granules and processing bodies are dynamically linked sites of mRNP remodeling.* J Cell Biol, 2005. **169**(6): p. 871-84.

50.   Behm-Ansmant, I., J. Rehwinkel, and E. Izaurralde, *MicroRNAs silence gene expression by repressing protein expression and/or by promoting mRNA decay.* Cold Spring Harb Symp Quant Biol, 2006. **71**: p. 523-30.

51.   Hannon, G.J., et al., *The expanding universe of noncoding RNAs.* Cold Spring Harb Symp Quant Biol, 2006. **71**: p. 551-64.

52.   Jing, Q., et al., *Involvement of microRNA in AU-rich element-mediated mRNA instability.* Cell, 2005. **120**(5): p. 623-34.

53.   Schichl, Y.M., et al., *Tristetraprolin impairs NF-kappaB/p65 nuclear translocation.* J Biol Chem, 2009. **284**(43): p. 29571-81.

54.   Liang, J., et al., *RNA-destabilizing factor tristetraprolin negatively regulates NF-kappaB signaling.* J Biol Chem, 2009. **284**(43): p. 29383-90.

55.   Wagner, E.F. and A.R. Nebreda, *Signal integration by JNK and p38 MAPK pathways in cancer development.* Nat Rev Cancer, 2009. **9**(8): p. 537-49.

56.   Chang, L. and M. Karin, *Mammalian MAP kinase signalling cascades.* Nature, 2001. **410**(6824): p. 37-40.

57.   Rincon, M. and R.J. Davis, *Regulation of the immune response by stress-activated protein kinases.* Immunol Rev, 2009. **228**(1): p. 212-24.

58.   Ono, K. and J. Han, *The p38 signal transduction pathway: activation and function.* Cell Signal, 2000. **12**(1): p. 1-13.

59.   Zarubin, T. and J. Han, *Activation and signaling of the p38 MAP kinase pathway.* Cell Res, 2005. **15**(1): p. 11-8.

60.   Roux, P.P. and J. Blenis, *ERK and p38 MAPK-activated protein kinases: a family of protein kinases with diverse biological functions.* Microbiol Mol Biol Rev, 2004. **68**(2): p. 320-44.

61.   Kim, C., et al., *The kinase p38 alpha serves cell type-specific inflammatory functions in skin injury and coordinates pro- and anti-inflammatory gene expression.* Nat Immunol, 2008. **9**(9): p. 1019-27.

62.   Winzen, R., et al., *The p38 MAP kinase pathway signals for cytokine-induced mRNA stabilization via MAP kinase-activated protein kinase 2 and an AU-rich region-targeted mechanism.* EMBO J, 1999. **18**(18): p. 4969-80.

63.   Ming, X.F., et al., *Parallel and independent regulation of interleukin-3 mRNA turnover by phosphatidylinositol 3-kinase and p38 mitogen-activated protein kinase.* Mol Cell Biol, 2001. **21**(17): p. 5778-89.

64.   Hammer, M., et al., *Control of dual-specificity phosphatase-1 expression in activated macrophages by IL-10.* Eur J Immunol, 2005. **35**(10): p. 2991-3001.

65.   Ananieva, O., et al., *The kinases MSK1 and MSK2 act as negative regulators of Toll-like receptor signaling.* Nat Immunol, 2008. **9**(9): p. 1028-36.

66.   Hammer, M., et al., *Dual specificity phosphatase 1 (DUSP1) regulates a subset of LPS-induced genes and protects mice from lethal endotoxin shock.* J Exp Med, 2006. **203**(1): p. 15-20.

67.   Lai, W.S., et al., *Promoter analysis of Zfp-36, the mitogen-inducible gene encoding the zinc finger protein tristetraprolin.* J Biol Chem, 1995. **270**(42): p. 25266-72.

68.   Cao, H., J.S. Tuttle, and P.J. Blackshear, *Immunological characterization of tristetraprolin as a low abundance, inducible, stable cytosolic protein.* J Biol Chem, 2004. **279**(20): p. 21489-99.

69.   Cao, H., et al., *Identification of the anti-inflammatory protein tristetraprolin as a hyperphosphorylated protein by mass spectrometry and site-directed mutagenesis.* Biochem J, 2006. **394**(Pt 1): p. 285-97.

70.   Brook, M., et al., *Posttranslational regulation of tristetraprolin subcellular localization and protein stability by p38 mitogen-activated protein kinase and extracellular signal-regulated kinase pathways.* Mol Cell Biol, 2006. **26**(6): p. 2408-18.

71.   Zhu, W., et al., *Gene suppression by tristetraprolin and release by the p38 pathway.* Am J Physiol Lung Cell Mol Physiol, 2001. **281**(2): p. L499-508.

72.   Sandler, H. and G. Stoecklin, *Control of mRNA decay by phosphorylation of tristetraprolin.* Biochem Soc Trans, 2008. **36**(Pt 3): p. 491-6.

73.   Sun, L., et al., *Tristetraprolin (TTP)-14-3-3 complex formation protects TTP from dephosphorylation by protein phosphatase 2a and stabilizes tumor necrosis factor-alpha mRNA.* J Biol Chem, 2007. **282**(6): p. 3766-77.

74.   Eyers, P.A., et al., *Use of a drug-resistant mutant of stress-activated protein kinase 2a/p38 to validate the in vivo specificity of SB 203580.* FEBS Lett, 1999. **451**(2): p. 191-6.

75.   Anderson, P., et al., *Post-transcriptional regulation of proinflammatory proteins.* J Leukoc Biol, 2004. **76**(1): p. 42-7.

76.   Taylor, G.A., et al., *A pathogenetic role for TNF alpha in the syndrome of cachexia, arthritis, and autoimmunity resulting from tristetraprolin (TTP) deficiency.* Immunity, 1996. **4**(5): p. 445-54.

77.   Carballo, E., G.S. Gilkeson, and P.J. Blackshear, *Bone marrow transplantation reproduces the tristetraprolin-deficiency syndrome in recombination activating gene-2 (-/-) mice. Evidence that monocyte/macrophage progenitors may be responsible for TNFalpha overproduction.* J Clin Invest, 1997. **100**(5): p. 986-95.

78.   Suzuki, T., et al., *Tristetraprolin (TTP) gene polymorphisms in patients with rheumatoid arthritis and healthy individuals.* Mod Rheumatol, 2008. **18**(5): p. 472-9.

79.   Carrick, D.M., W.S. Lai, and P.J. Blackshear, *The tandem CCCH zinc finger protein tristetraprolin and its relevance to cytokine mRNA turnover and arthritis.* Arthritis Res Ther, 2004. **6**(6): p. 248-64.

80.   Suswam, E., et al., *Tristetraprolin down-regulates interleukin-8 and vascular endothelial growth factor in malignant glioma cells.* Cancer Res, 2008. **68**(3): p. 674-82.

81.   Lee, H.H., et al., *Tristetraprolin regulates expression of VEGF and tumorigenesis in human colon cancer.* Int J Cancer, 2009.

82.   Young, L.E., et al., *The mRNA binding proteins HuR and tristetraprolin regulate cyclooxygenase 2 expression during colon carcinogenesis.* Gastroenterology, 2009. **136**(5): p. 1669-79.

83.   Stoecklin, G., et al., *A novel mechanism of tumor suppression by destabilizing AU-rich growth factor mRNA.* Oncogene, 2003. **22**(23): p. 3554-61.

84.   Lu, J.Y., N. Sadri, and R.J. Schneider, *Endotoxic shock in AUF1 knockout mice mediated by failure to degrade proinflammatory cytokine mRNAs.* Genes Dev, 2006. **20**(22): p. 3174-84.

85.   Mosser, D.M. and X. Zhang, *Interleukin-10: new perspectives on an old cytokine.* Immunol Rev, 2008. **226**: p. 205-18.

86.   Commins, S., J.W. Steinke, and L. Borish, *The extended IL-10 superfamily: IL-10, IL-19, IL-20, IL-22, IL-24, IL-26, IL-28, and IL-29.* J Allergy Clin Immunol, 2008. **121**(5): p. 1108-11.

87.   O'Garra, A. and P. Vieira, *T(H)1 cells control themselves by producing interleukin-10.* Nat Rev Immunol, 2007. **7**(6): p. 425-8.

88.   Fillatreau, S., D. Gray, and S.M. Anderton, *Not always the bad guys: B cells as regulators of autoimmune pathology.* Nat Rev Immunol, 2008. **8**(5): p. 391-7.

89.   Ryan, J.J., et al., *Mast cell homeostasis: a fundamental aspect of allergic disease.* Crit Rev Immunol, 2007. **27**(1): p. 15-32.

90.   Moore, K.W., et al., *Interleukin-10 and the interleukin-10 receptor.* Annu Rev Immunol, 2001. **19**: p. 683-765.

91.   Williams, L.M., et al., *Interleukin-10 suppression of myeloid cell activation--a continuing puzzle.* Immunology, 2004. **113**(3): p. 281-92.

92.   Donnelly, R.P., H. Dickensheets, and D.S. Finbloom, *The interleukin-10 signal transduction pathway and regulation of gene expression in mononuclear phagocytes.* J Interferon Cytokine Res, 1999. **19**(6): p. 563-73.

93.   Croker, B.A., et al., *SOCS3 negatively regulates IL-6 signaling in vivo.* Nat Immunol, 2003. **4**(6): p. 540-5.

94.   Lang, R., et al., *SOCS3 regulates the plasticity of gp130 signaling.* Nat Immunol, 2003. **4**(6): p. 546-50.

95.   Yasukawa, H., et al., *IL-6 induces an anti-inflammatory response in the absence of SOCS3 in macrophages.* Nat Immunol, 2003. **4**(6): p. 551-6.

96.   Keene, J.D., *RNA regulons: coordination of post-transcriptional events.* Nat Rev Genet, 2007. **8**(7): p. 533-43.

97.   Blackshear, P.J., et al., *Zfp36l3, a rodent X chromosome gene encoding a placenta-specific member of the Tristetraprolin family of CCCH tandem zinc finger proteins.* Biol Reprod, 2005. **73**(2): p. 297-307.

98.   Carrick, D.M. and P.J. Blackshear, *Comparative expression of tristetraprolin (TTP) family member transcripts in normal human tissues and cancer cell lines.* Arch Biochem Biophys, 2007. **462**(2): p. 278-85.

99.   Ma, Q., et al., *The Drosophila TIS11 homologue encodes a developmentally controlled gene.* Oncogene, 1994. **9**(11): p. 3329-34.

100.   Thompson, M.J., et al., *Cloning and characterization of two yeast genes encoding members of the CCCH class of zinc finger proteins: zinc finger-mediated impairment of cell growth.* Gene, 1996. **174**(2): p. 225-33.

101.   Puig, S., S.V. Vergara, and D.J. Thiele, *Cooperation of two mRNA-binding proteins drives metabolic adaptation to iron deficiency.* Cell Metab, 2008. **7**(6): p. 555-64.

102.   Puig, S., E. Askeland, and D.J. Thiele, *Coordinated remodeling of cellular metabolism during iron deficiency through targeted mRNA degradation.* Cell, 2005. **120**(1): p. 99-110.

103.   Amann, B.T., M.T. Worthington, and J.M. Berg, *A Cys3His zinc-binding domain from Nup475/tristetraprolin: a novel fold with a disklike structure.* Biochemistry, 2003. **42**(1): p. 217-21.

104.   Stumpo, D.J., et al., *Targeted disruption of Zfp36l2, encoding a CCCH tandem zinc finger RNA-binding protein, results in defective hematopoiesis.* Blood, 2009. **114**(12): p. 2401-10.

105.   Stumpo, D.J., et al., *Chorioallantoic fusion defects and embryonic lethality resulting from disruption of Zfp36L1, a gene encoding a CCCH tandem zinc finger protein of the Tristetraprolin family.* Mol Cell Biol, 2004. **24**(14): p. 6445-55.

106.   Wagner, B.J., et al., *Structure and genomic organization of the human AUF1 gene: alternative pre-mRNA splicing generates four protein isoforms.* Genomics, 1998. **48**(2): p. 195-202.

107. Xu, N., C.Y. Chen, and A.B. Shyu, *Versatile role for hnRNP D isoforms in the differential regulation of cytoplasmic mRNA turnover.* Mol Cell Biol, 2001. **21**(20): p. 6960-71.

108. Zhang, W., et al., *Purification, characterization, and cDNA cloning of an AU-rich element RNA-binding protein, AUF1.* Mol Cell Biol, 1993. **13**(12): p. 7652-65.

109. Sela-Brown, A., et al., *Identification of AUF1 as a parathyroid hormone mRNA 3'-untranslated region-binding protein that determines parathyroid hormone mRNA stability.* J Biol Chem, 2000. **275**(10): p. 7424-9.

110. Liao, B., Y. Hu, and G. Brewer, *Competitive binding of AUF1 and TIAR to MYC mRNA controls its translation.* Nat Struct Mol Biol, 2007. **14**(6): p. 511-8.

111. Lin, S., et al., *Down-regulation of cyclin D1 expression by prostaglandin A(2) is mediated by enhanced cyclin D1 mRNA turnover.* Mol Cell Biol, 2000. **20**(21): p. 7903-13.

112. Paschoud, S., et al., *Destabilization of interleukin-6 mRNA requires a putative RNA stem-loop structure, an AU-rich element, and the RNA-binding protein AUF1.* Mol Cell Biol, 2006. **26**(22): p. 8228-41.

113. Cok, S.J., et al., *Identification of RNA-binding proteins in RAW 264.7 cells that recognize a lipopolysaccharide-responsive element in the 3-untranslated region of the murine cyclooxygenase-2 mRNA.* J Biol Chem, 2004. **279**(9): p. 8196-205.

114. Dean, J.L., et al., *Identification of a novel AU-rich-element-binding protein which is related to AUF1.* Biochem J, 2002. **366**(Pt 3): p. 709-19.

115. Yao, K.M., et al., *Gene elav of Drosophila melanogaster: a prototype for neuronal-specific RNA binding protein gene family that is conserved in flies and humans.* J Neurobiol, 1993. **24**(6): p. 723-39.

116. Graus, F., et al., *Anti-Hu antibodies in patients with small-cell lung cancer: association with complete response to therapy and improved survival.* J Clin Oncol, 1997. **15**(8): p. 2866-72.

117. Hinman, M.N. and H. Lou, *Diverse molecular functions of Hu proteins.* Cell Mol Life Sci, 2008. **65**(20): p. 3168-81.

118. Manley, G.T., et al., *Hu antigens: reactivity with Hu antibodies, tumor expression, and major immunogenic sites.* Ann Neurol, 1995. **38**(1): p. 102-10.

119. Verschuuren, J.J., et al., *Paraneoplastic anti-Hu serum: studies on human tumor cell lines.* J Neuroimmunol, 1997. **79**(2): p. 202-10.

120. Fan, X.C. and J.A. Steitz, *Overexpression of HuR, a nuclear-cytoplasmic shuttling protein, increases the in vivo stability of ARE-containing mRNAs.* EMBO J, 1998. **17**(12): p. 3448-60.

121. Lopez de Silanes, I., et al., *Identification of a target RNA motif for RNA-binding protein HuR.* Proc Natl Acad Sci U S A, 2004. **101**(9): p. 2987-92.

122. Wang, W., et al., *HuR regulates cyclin A and cyclin B1 mRNA stability during cell proliferation.* EMBO J, 2000. **19**(10): p. 2340-50.

123. Wang, W., et al., *Loss of HuR is linked to reduced expression of proliferative genes during replicative senescence.* Mol Cell Biol, 2001. **21**(17): p. 5889-98.

124. Nabors, L.B., et al., *HuR, a RNA stability factor, is expressed in malignant brain tumors and binds to adenine- and uridine-rich elements within the 3' untranslated regions of cytokine and angiogenic factor mRNAs.* Cancer Res, 2001. **61**(5): p. 2154-61.

125. Anant, S. and C.W. Houchen, *HuR and TTP: two RNA binding proteins that deliver message from the 3' end.* Gastroenterology, 2009. **136**(5): p. 1495-8.

126. Brennan, S.E., et al., *The mRNA-destabilizing protein tristetraprolin is suppressed in many cancers, altering tumorigenic phenotypes and patient prognosis.* Cancer Res, 2009. **69**(12): p. 5168-76.

127. Katsanou, V., et al., *The RNA-binding protein Elavl1/HuR is essential for placental branching morphogenesis and embryonic development.* Mol Cell Biol, 2009. **29**(10): p. 2762-76.

128. Ghosh, M., et al., *Essential role of the RNA-binding protein HuR in progenitor cell survival in mice.* J Clin Invest, 2009.

129. Gherzi, R., et al., *A KH domain RNA binding protein, KSRP, promotes ARE-directed mRNA turnover by recruiting the degradation machinery.* Mol Cell, 2004. **14**(5): p. 571-83.

130. Chen, C.Y., N. Xu, and A.B. Shyu, *Highly selective actions of HuR in antagonizing AU-rich element-mediated mRNA destabilization.* Mol Cell Biol, 2002. **22**(20): p. 7268-78.

131. Gherzi, R., et al., *The RNA-binding protein KSRP promotes decay of beta-catenin mRNA and is inactivated by PI3K-AKT signaling.* PLoS Biol, 2006. **5**(1): p. e5.

132. Nechama, M., et al., *The mRNA decay promoting factor K-homology splicing regulator protein post-transcriptionally determines parathyroid hormone mRNA levels.* FASEB J, 2008. **22**(10): p. 3458-68.

133. Winzen, R., et al., *Functional analysis of KSRP interaction with the AU-rich element of interleukin-8 and identification of inflammatory mRNA targets.* Mol Cell Biol, 2007. **27**(23): p. 8388-400.

134. Briata, P., et al., *p38-dependent phosphorylation of the mRNA decay-promoting factor KSRP controls the stability of select myogenic transcripts.* Mol Cell, 2005. **20**(6): p. 891-903.

135. Trabucchi, M., et al., *The RNA-binding protein KSRP promotes the biogenesis of a subset of microRNAs.* Nature, 2009. **459**(7249): p. 1010-4.

136. Ruggiero, T., et al., *LPS induces KH-type splicing regulatory protein-dependent processing of microRNA-155 precursors in macrophages.* FASEB J, 2009. **23**(9): p. 2898-908.

137. Dember, L.M., et al., *Individual RNA recognition motifs of TIA-1 and TIAR have different RNA binding specificities.* J Biol Chem, 1996. **271**(5): p. 2783-8.

138. Piecyk, M., et al., *TIA-1 is a translational silencer that selectively regulates the expression of TNF-alpha.* EMBO J, 2000. **19**(15): p. 4154-63.

139. Le Guiner, C., et al., *TIA-1 and TIAR activate splicing of alternative exons with weak 5' splice sites followed by a U-rich stretch on their own pre-mRNAs.* J Biol Chem, 2001. **276**(44): p. 40638-46.

140. Izquierdo, J.M. and J. Valcarcel, *Fas-activated serine/threonine kinase (FAST K) synergizes with TIA-1/TIAR proteins to regulate Fas alternative splicing.* J Biol Chem, 2007. **282**(3): p. 1539-43.

141. Kuwano, Y., et al., *NF90 selectively represses the translation of target mRNAs bearing an AU-rich signature motif.* Nucleic Acids Res, 2009.

142. Kuwano, Y., et al., *MKP-1 mRNA stabilization and translational control by RNA-binding proteins HuR and NF90.* Mol Cell Biol, 2008. **28**(14): p. 4562-75.

143. Parrott, A.M., et al., *RNA binding and phosphorylation determine the intracellular distribution of nuclear factors 90 and 110.* J Mol Biol, 2005. **348**(2): p. 281-93.

144. Shi, L., et al., *NF90 regulates inducible IL-2 gene expression in T cells.* J Exp Med, 2007. **204**(5): p. 971-7.

145. Agbottah, E.T., et al., *Nuclear Factor 90(NF90) targeted to TAR RNA inhibits transcriptional activation of HIV-1.* Retrovirology, 2007. **4**: p. 41.

146. Shi, L., et al., *Dynamic binding of Ku80, Ku70 and NF90 to the IL-2 promoter in vivo in activated T-cells.* Nucleic Acids Res, 2007. **35**(7): p. 2302-10.

147. Liao, H.J., R. Kobayashi, and M.B. Mathews, *Activities of adenovirus virus-associated RNAs: purification and characterization of RNA binding proteins.* Proc Natl Acad Sci U S A, 1998. **95**(15): p. 8514-9.

148. Baccarini, M., F. Bistoni, and M.L. Lohmann-Matthes, *In vitro natural cell-mediated cytotoxicity against Candida albicans: macrophage precursors as effector cells.* J Immunol, 1985. **134**(4): p. 2658-65.

149. Sexl, V., et al., *Stat5a/b contribute to interleukin 7-induced B-cell precursor expansion, but abl- and bcr/abl-induced transformation are independent of stat5.* Blood, 2000. **96**(6): p. 2277-83.

150. Schorpp, M., et al., *The human ubiquitin C promoter directs high ubiquitous expression of transgenes in mice.* Nucleic Acids Res, 1996. **24**(9): p. 1787-8.

151. Kovarik, P., et al., *Stat1 combines signals derived from IFN-gamma and LPS receptors during macrophage activation.* EMBO J, 1998. **17**(13): p. 3660-8.

152. Jenner, R.G. and R.A. Young, *Insights into host responses against pathogens from transcriptional profiling.* Nat Rev Microbiol, 2005. **3**(4): p. 281-94.

153. Stoecklin, G. and P. Anderson, *In a tight spot: ARE-mRNAs at processing bodies.* Genes Dev, 2007. **21**(6): p. 627-31.

154. Franks, T.M. and J. Lykke-Andersen, *The control of mRNA decapping and P-body formation.* Mol Cell, 2008. **32**(5): p. 605-15.

155. Carballo, E., W.S. Lai, and P.J. Blackshear, *Feedback inhibition of macrophage tumor necrosis factor-alpha production by tristetraprolin.* Science, 1998. **281**(5379): p. 1001-5.

156. Blackshear, P.J., et al., *Characteristics of the interaction of a synthetic human tristetraprolin tandem zinc finger peptide with AU-rich element-containing RNA substrates.* J Biol Chem, 2003. **278**(22): p. 19947-55.

157. Stoecklin, G., et al., *MK2-induced tristetraprolin:14-3-3 complexes prevent stress granule association and ARE-mRNA decay.* Embo J, 2004. **23**(6): p. 1313-1324.

158. Gilchrist, M., et al., *Systems biology approaches identify ATF3 as a negative regulator of Toll-like receptor 4.* Nature, 2006. **441**(7090): p. 173-8.

159. Carballo, E., W.S. Lai, and P.J. Blackshear, *Evidence that tristetraprolin is a physiological regulator of granulocyte-macrophage colony-stimulating factor messenger RNA deadenylation and stability.* Blood, 2000. **95**(6): p. 1891-9.

160. Tchen, C.R., et al., *The stability of tristetraprolin mRNA is regulated by mitogen activated protein kinase p38 and by tristetraprolin itself.* J Biol Chem, 2004.

161. Frasca, D., et al., *Tristetraprolin, a negative regulator of mRNA stability, is increased in old B cells and is involved in the degradation of E47 mRNA.* J Immunol, 2007. **179**(2): p. 918-27.

162. Horner, T.J., et al., *Stimulation of polo-like kinase 3 mRNA decay by tristetraprolin.* Mol Cell Biol, 2009. **29**(8): p. 1999-2010.

163. Eyers, P.A., et al., *Use of a drug-resistant mutant of stress-activated protein kinase 2a/p38 to validate the in vivo specificity of SB 203580.* FEBS Lett, 1999. **451**(2): p. 191-6.

164. Tudor, C., et al., *The p38 MAPK pathway inhibits tristetraprolin-directed decay of interleukin-10 and pro-inflammatory mediator mRNAs in murine macrophages.* FEBS Lett, 2009.

165. Mages, J., H. Dietrich, and R. Lang, *A genome-wide analysis of LPS tolerance in macrophages.* Immunobiology, 2007. **212**(9-10): p. 723-37.

166. Ehlting, C., et al., *Regulation of suppressor of cytokine signaling 3 (SOCS3) mRNA stability by TNF-alpha involves activation of the MKK6/p38MAPK/MK2 cascade.* J Immunol, 2007. **178**(5): p. 2813-26.

167. Kontoyiannis, D., et al., *Impaired on/off regulation of TNF biosynthesis in mice lacking TNF AU-rich elements: implications for joint and gut-associated immunopathologies.* Immunity, 1999. **10**(3): p. 387-98.

168. Murray, P.J., *The primary mechanism of the IL-10-regulated antiinflammatory response is to selectively inhibit transcription.* Proc Natl Acad Sci U S A, 2005. **102**(24): p. 8686-91.

169. Smyth, G.K., *Linear models and empirical bayes methods for assessing differential expression in microarray experiments.* Stat Appl Genet Mol Biol, 2004. **3**: p. Article3.

170. Gama-Carvalho, M., et al., *Genome-wide identification of functionally distinct subsets of cellular mRNAs associated with two nucleocytoplasmic-shuttling mammalian splicing factors.* Genome Biol, 2006. **7**(11): p. R113.

171. Morrison, T.B., J.J. Weis, and C.T. Wittwer, *Quantification of low-copy transcripts by continuous SYBR Green I monitoring during amplification.* Biotechniques, 1998. **24**(6): p. 954-8, 960, 962.

172. Linker, K., et al., *Involvement of KSRP in the post-transcriptional regulation of human iNOS expression-complex interplay of KSRP with TTP and HuR.* Nucleic Acids Res, 2005. **33**(15): p. 4813-27.

173. Clausen, B.E., et al., *Conditional gene targeting in macrophages and granulocytes using LysMcre mice.* Transgenic Res, 1999. **8**(4): p. 265-77.

174. Lin, W.J. and W.C. Yeh, *Implication of Toll-like receptor and tumor necrosis factor alpha signaling in septic shock.* Shock, 2005. **24**(3): p. 206-9.

175. Raymond, V., J.A. Atwater, and I.M. Verma, *Removal of an mRNA destabilizing element correlates with the increased oncogenicity of proto-oncogene fos.* Oncogene Res, 1989. **5**(1): p. 1-12.

176. Lee, W.M., C. Lin, and T. Curran, *Activation of the transforming potential of the human fos proto-oncogene requires message stabilization and results in increased amounts of partially modified fos protein.* Mol Cell Biol, 1988. **8**(12): p. 5521-7.

177. Meijlink, F., et al., *Removal of a 67-base-pair sequence in the noncoding region of protooncogene fos converts it to a transforming gene.* Proc Natl Acad Sci U S A, 1985. **82**(15): p. 4987-91.

178. Ruther, U., et al., *c-fos expression induces bone tumors in transgenic mice.* Oncogene, 1989. **4**(7): p. 861-5.

179. Nakajima, K. and R. Wall, *Interleukin-6 signals activating junB and TIS11 gene transcription in a B-cell hybridoma.* Mol Cell Biol, 1991. **11**(3): p. 1409-18.

180. Whitlock, C.A., et al., *Differentiation of cloned populations of immature B cells after transformation with Abelson murine leukemia virus.* Cell, 1983. **32**(3): p. 903-11.

181. Stoiber, D., et al., *TYK2 is a key regulator of the surveillance of B lymphoid tumors.* J Clin Invest, 2004. **114**(11): p. 1650-8.

182. Hitti, E., et al., *Mitogen-activated protein kinase-activated protein kinase 2 regulates tumor necrosis factor mRNA stability and translation mainly by altering tristetraprolin expression, stability, and binding to adenine/uridine-rich element.* Mol Cell Biol, 2006. **26**(6): p. 2399-407.

183. Lu, J.Y. and R.J. Schneider, *Tissue distribution of AU-rich mRNA-binding proteins involved in regulation of mRNA decay.* J Biol Chem, 2004. **279**(13): p. 12974-9.

184. DuBois, R.N., et al., *Transforming growth factor alpha regulation of two zinc finger-containing immediate early response genes in intestine.* Cell Growth Differ, 1995. **6**(5): p. 523-9.

185. Balakathiresan, N.S., et al., *Tristetraprolin regulates IL-8 mRNA stability in cystic fibrosis lung epithelial cells.* Am J Physiol Lung Cell Mol Physiol, 2009. **296**(6): p. L1012-8.

186. Carballo, E. and P.J. Blackshear, *Roles of tumor necrosis factor-alpha receptor subtypes in the pathogenesis of the tristetraprolin-deficiency syndrome.* Blood, 2001. **98**(8): p. 2389-95.

9. ACKNOWLEDGEMENTS

10. LEBENSLAUF

Daten:

Name	**Franz Kratochvill**
Geburtsdatum	**27.04.1982**
Geburtsort	**Allentsteig, Austria**

Wissenschaftlicher Werdegang:

seit Juli 2006	Doktoratsstudium an der Universität Wien mit dem Titel "The Role of Tristetraprolin in inflammation and disease" in der Gruppe von Prof. Pavel Kovarik
Mai 2005 – April 2006	Diplomarbeit mit dem Titel "Cell density-dependent regulatory systems controlling virulence of *Streptococcus pyogenes*" in der Gruppe von Dr. Emmanuelle Charpentier

Ausbildung:

Oktober 2001-2006	Studium der Molekularen Biologie an der Universität Wien
2000	Matura am Bundesrealgymnasium Waidhofen/Thaya

Konferenzen und Workshops:

Oktober 2009	RNA Club, Brno, Czech Republic
August 2009	"Eukaryotic mRNA Processing", Cold Spring Harbor, New York
September 2008	"Post-Transcriptional Control of Gene Expression: Mechanisms of mRNA Decay", FASEB Summer Research Conference, Lucca, Italy
August 2008	Workshop on Structure and Function of mRNP, University of Aarhus, Denmark

Präsentationen:

Oktober 2009   Short Talk, RNA Club, Brno, Czech Republic

September 2008   Short Talk, FASEB Summer Research Conference, Lucca, Italy

Tutorien:

SS und WS 2009   Einführungsübungen in die Bioinformatik

SS 2006   Einführungsübungen in die Biologie (Abschnitt Mikrobiologie und Genetik I)

Auslandsaufenthalte:

August 2007   Labor von Prof. Carmo-Fonseca, Universidade de Lisboa, Lisbon, Portugal

August 2004-Jänner 2005   Universidad Complutense de Madrid, Madrid, Spain (Erasmus)

Publikationen:

Schaljo B*, Kratochvill F*, Gratz N, Sadzak I, Sauer I, Hammer M, Vogl C, Strobl B, Müller M, Blackshear PJ, Poli V, Lang R, Murray PJ, Kovarik P., "Tristetraprolin is required for full anti-inflammatory response of murine macrophages to IL-10", J Immunol. 2009 Jul 15;183(2):1197-206.

Holnthoner W, Kerenyi M, Gröger M, Kratochvill F, Petzelbauer P., "Regulation of matrilysin expression in endothelium by fibroblast growth factor-2",Biochem Biophys Res Commun. 2006 Apr 14;342(3):725-33

Authors labeled with * contributed equally to the publication

11. CURRICULUM VITAE

Personal Data:

Name	**Franz Kratochvill**
Date of birth	**27.04.1982**
Place of birth	**Allentsteig, Austria**

Scientific Career:

since July 2006	Ph.D. student at the Max F. Perutz Laboratories at the University of Vienna with the title "The Role of Tristetraprolin in inflammation and disease" in the group of Prof. Pavel Kovarik
May 2005 – April 2006	Diploma thesis with the title "Cell density-dependent regulatory systems controlling virulence of *Streptococcus pyogenes*" in the group of Dr. Emmanuelle Charpentier

Education:

October 2001-2006	Study of molecular biology at the University of Vienna
2000	Grammar school graduated, completed with the formal exam "Matura"

Scientific Meetings and Workshops:

October 2009	RNA club, Brno, Czech Republic
August 2009	"Eukaryotic mRNA Processing", Cold Spring Harbor, New York
September 2008	"Post-Transcriptional Control of Gene Expression: Mechanisms of mRNA Decay", FASEB Summer Research Conference, Lucca, Italy
August 2008	Workshop on Structure and Function of mRNP, University of Aarhus, Denmark

Talks:

October 2009   Short Talk, RNA Club, Brno, Czech Republic

September 2008   Short Talk, FASEB Summer Research Conference, Lucca, Italy

Tutoring:

Summer and winter term 2009   Introductory tutorial into bioinformatics

Summer term 2006   Introductory tutorial into microbiology and genetics

Temporary Employment Abroad:

August 2007   Lab of Prof. Carmo-Fonseca, Universidade de Lisboa, Lisbon, Portugal

August 2004-January 2005   Universidad Complutense de Madrid, Madrid, Spain (Erasmus)

Publications:

Schaljo B*, Kratochvill F*, Gratz N, Sadzak I, Sauer I, Hammer M, Vogl C, Strobl B, Müller M, Blackshear PJ, Poli V, Lang R, Murray PJ, Kovarik P., "Tristetraprolin is required for full anti-inflammatory response of murine macrophages to IL-10", J Immunol. 2009 Jul 15;183(2):1197-206.

Holnthoner W, Kerenyi M, Gröger M, Kratochvill F, Petzelbauer P., "Regulation of matrilysin expression in endothelium by fibroblast growth factor-2",Biochem Biophys Res Commun. 2006 Apr 14;342(3):725-33

Authors labeled with * contributed equally to the publication